Control of Arabidopsis vein-network formation by auxin transport

by

Megan Grace Sawchuk

A thesis submitted in partial fulfillment of the requirements for the degree of

Doctor of Philosophy

in

Plant Biology

Department of Biological Sciences
University of Alberta

ABSTRACT

Most multicellular organisms form tissue networks for transport function. What controls the formation of tissue networks is thus a central question in biology. In animals, the formation of these networks often involves extensive cell movements—movements that are instead prevented in plants by a wall that holds cells in place; thus plants are a simplified system in which to address the question of tissue network formation.

The vein networks of plant leaves are among the most spectacular examples of tissue networks, and as such the principles controlling their formation have inspired artists and scientists since time immemorial. From a developmental standpoint, this interest seems justified, as vein networks are formed progressively during leaf development by the iteration of initiation, continuation and termination of vein formation.

An additional, equally intriguing feature of vein networks is that they are both reproducible and variable. Consider, for example, the vein networks in leaves of *Arabidopsis thaliana*: lateral veins branch off from a central midvein and join distal veins to form closed loops, and minor veins branch off from midvein and loops to end freely in the leaf or join other veins. Whereas these pattern features of vein networks are reproducible, other features of vein networks, such as the number of veins and the extent of their interconnectedness, are variable. Such coexisting reproducibility and variability argue against a tight specification of vein networks and instead suggest an iterative, self-organizing vein-formation mechanism that functionally integrates vein network formation with leaf growth.

Varied evidence implicates the plant signalling molecule auxin and its polar transport through plant tissues in the control of vein network formation:

(i) Expression of the PIN-FORMED1 (PIN1) auxin effluxer of Arabidopsis is iteratively initiated in broad domains of leaf inner cells that become gradually restricted to files of vascular precursor cells in contact with pre-existing, narrow PIN1 expression domains. Within broad expression domains, PIN1 is localized isotropically—or nearly so—at the plasma membrane of leaf inner cells. As expression of PIN1 becomes gradually restricted to files of vascular precursor cells, PIN1 localization becomes polarized to the side of the plasma membrane facing the pre-existing, narrow PIN1 expression domains with which the narrowing domains are in contact.

(ii) Auxin application to developing leaves induces formation of broad expression domains of isotropically localized PIN1; such domains become restricted to the sites of auxin-induced vein formation, and PIN1 localization becomes polarized toward the pre-existing vasculature.

(iii) Both the restriction of PIN1 expression and the polarization of PIN1 localization that occur during normal leaf development are slowed down by chemical inhibition of auxin transport.

(iv) Auxin transport inhibitors induce characteristic and reproducible vein-pattern defects, similar to—though stronger than—those of *pin1* mutants.

Thus available evidence suggests that auxin induces the polar formation of vein networks, and that such inductive and orienting property of auxin strictly depends on the function of *PIN1* and possibly of the other seven *PIN* genes.

Here I tested this hypothesis. My results suggest that:

(i) *PIN1* is the only *PIN* gene with non-redundant functions in vein patterning; *PIN3*, *PIN4* and *PIN7* act redundantly with *PIN1* in vein patterning; and *PIN6* and *PIN8* inhibit the negative function of *PIN5* in *PIN1*-dependent vein patterning. Further, *PIN1* non-redundantly inhibits vein network formation; *PIN6* acts redundantly with *PIN1* in inhibition of vein network formation; *PIN8* acts redundantly with *PIN6* in *PIN1*-dependent inhibition of vein network

formation; and *PIN6* and *PIN8* redundantly inhibit—independently of *PIN1*—the positive function of *PIN5* in vein network formation.

(ii) Auxin-induced polar vein formation occurs in the absence of the function of PIN proteins or of any known intercellular auxin transporter.

(iii) The vein-forming and -patterning activity independent of carrier-mediated auxin transport relies, at least in part, on the auxin signal transduction mediated by the TRANSPORT INHIBITOR RESPONSE1/AUXIN SIGNALLING F-BOX (TIR1/AFB) auxin receptors and the MONOPTEROS (MP) auxin-responsive transcription factor.

(iv) A polarizing signal that depends on the function of the GNOM guanine-nucleotide exchange factor for ADP-rybosilation-factor GTPases acts upstream of carrier-mediated auxin transport and TIR1/AFB/MP-mediated auxin signalling in vein formation and patterning.

My results define genetic interaction networks controlling vein patterning and network formation.

PREFACE

Parts of my Ph.D. thesis are published.

Chapter 1 was published as MG Sawchuk and E Scarpella, "Polarity, Continuity, and Alignment in Plant Vascular Strands," *Journal of Integrative Plant Biology*, volume 55, issue 9, 824-834. I equally shared with my supervisor, Dr. Enrico Scarpella, the responsibility for conceiving, designing and writing the paper.

Chapter 2 was published as MG Sawchuk, A Edgar and E Scarpella, "Patterning of Leaf Vein Networks by Convergent Auxin Transport Pathways," *PLoS Genetics*, volume 9, issue 2, e1003294. I equally shared with my supervisor the responsibility for conceiving and designing the experiments, analyzing the data and writing the paper. I performed 85% of the experiments, while Dr. Enrico Scarpella and Alexander Edgar performed 10% and 5% of the experiments, respectively.

Chapter 4 was published as O Odat, J Gardiner, MG Sawchuk, C Verna, TJ Donner and E Scarpella, "Characterization of an allelic series in the *MONOPTEROS* gene of Arabidopsis," *genesis*, volume 52, issue 2, 127-133. All authors equally shared the responsibility for conceiving and designing the experiments, analyzing the data and writing the paper. I performed 20% of the experiments, while the first authors, O Odat and J Gardiner, collectively performed 55% of the experiments, and C Verna and TJ Donner performed 15% and 10% of the experiments, respectively.

All the authors and publishers have given their permission for the inclusion of these publications in my thesis.

ACKNOWLEDGEMENTS

The work I present in my Ph.D. thesis would have been impossible without the generous contributions of many other people.

For kindly providing plasmids and seeds, I thank the Arabidopsis Biological Resource Center (ABRC), Jose Alonso, Malcolm Bennett, Thomas Berleth, Ikram Blilou, Sean Cutler, Taku Demura, Tyler Donner, Mark Estelle, Jiří Friml, Hidehiro Fukaki, Hiroo Fukuda, Markus Geisler, Ken-ichiro Hayashi, Gerd Jürgens, Harry Klee, Cris Kuhlemeier, Elliot Meyerowitz, Miyo Morita, Satoshi Naramoto, Sandra Richter, Ben Scheres, Benoît Schoefs, Edgar Spalding, Ranjan Swarup, Masao Tasaka, Petr Valosek, Guosheng Wu, Jian Xu and Jeonga Yun.

For providing technical advice, I thank Renze Heidstra, Dolf Weijers and Viola Willemsen.

For critically reading parts of this thesis, I thank Thomas Berleth, Tyler Donner, Giorgio Morelli and Osama Odat.

For Canada Graduate Scholarships from the Master's and Doctoral programs, I thank the Natural Sciences and Engineering Research Council of Canada.

I thank the members of my supervisory committee, Dr. Michael Deyholos and Dr. Nat Kav, for their support and advice throughout my Ph.D. studies.

I thank the other students in the Scarpella lab for creating a fun and supportive lab environment. To Tyler Donner, Jason Gardiner, Osama Odat and Carla Verna, thank you for your contributions to Chapter 4. To Carla Verna, thank you for your contributions to Chapters 3 and 5. To the undergraduate students I trained, Alexander Edgar, Nawras El-Bekai and Linh Nguyen Manh, thank you for your contributions to my thesis.

Finally, I thank Dr. Enrico Scarpella for giving me the wonderful opportunity to pursue my Ph.D. in his lab. Thank you for your dedication to scientific training. With this training, I feel that I can tackle the many challenges I will encounter in my future career.

TABLE OF CONTENTS

LIST OF TABLES

CHAPTER 2

CHAPTER 3

CHAPTER 4

CHAPTER 5

LIST OF FIGURES

CHAPTER 1

Chapter 2

CHAPTER 3

CHAPTER 4

CHAPTER 5

CHAPTER 6

LIST OF ABBREVIATIONS AND NOTATIONS

ABCB	ATP-BINDING CASSETTE B
AD	activation domain
AFB	AUXIN SIGNALLING F-BOX
ARF	AUXIN RESPONSE FACTOR
ARF GEF	ADP-ribosylation factor guanine-nucleotide exchange factor
AUX	AUXIN RESISTANT
AUX/IAA	INDOLE-3-ACETIC ACID INDUCIBLE
CFP	cyan fluorescent protein
Col	Columbia
CTD	carboxyl-terminal domain
DBD	DNA-binding domain
EIR1	ETHYLENE INSENSITIVE ROOT1
EMB30	EMBRYO DEFECTIVE30
ER	endoplasmic reticulum
er	endoplasmic-reticulum-localization signal
GFP	green fluorescent protein
GN	GNOM
hv	higher vein
IAA	indole-3-acetic acid
l1	first loop
l2	second loop
LAX	LIKE AUX1
LUT	look-up-table
MDR	MULTI-DRUG RESISTANT
MP	MONOPTEROS
mv	midvein
NE	nuclear envelope
NPA	1-N-naphthylphthalamic acid

nuc	nuclear localization signal
PGP	P-GLYCOPROTEIN
PILS	PIN-LIKES
PIN	PIN-FORMED
PM	plasma membrane
pm	plasma-membrane-localization signal
RBR1	RETINOBLASTOMA-RELATED1
RPS5A	RIBOSOMAL PROTEIN S5A
TIR1	TRANSPORT INHIBITOR RESPONSE1
TWD1	TWISTED DWARF1
UCU2	ULTRACURVATA2
YFP	yellow fluorescent protein

Gene and protein notation

PIN	Wild-type protein
pin	Mutant protein
PIN	Wild-type gene
pin	Mutant gene

Gene fusion notation

Doubled colons (::) are used to indicate transcriptional fusions, and single colons (:) are used to indicate translational fusions.

CHAPTER 1: GENERAL INTRODUCTION

1.1 Introduction

In its most basic form, the body of a seed plant can be viewed as a shoot-root axis that grows at both the shoot pole and the root pole; the shoot-root axis is thus a bipolar structure (Groff and Kaplan 1988) (Figure 1.1). The shoot pole forms lateral organs, which arise from external layers of the shoot pole. The root pole forms no lateral organs; instead, lateral roots arise far from the root pole from internal layers of the root. Shoot organs are connected with roots by vascular strands (Figure 1.1): bundles of vascular cell files that mainly transport photosynthesis products from shoot organs to roots, and water and minerals from roots to shoot organs.

The specialized transport function of vascular strands is supported by their relation with the parts of the plant and by the relations between the parts of the strand (Figure 1.1). First, vascular strands primarily connect shoot organs with roots; vascular strands do connect shoot organs with one another and roots with one another, but they do so indirectly, by making contact with vascular strands that ultimately connect with roots or shoot organs (Dengler 2006). It follows that vascular strands are unequal at their ends—one end connects to shoot tissues, the other to root tissues—and are thus polar. Second, vascular strands are continuous. Third, within vascular strands cells are aligned with one another (Esau 1942); put differently, vascular cells have an axis that continues from one cell to another and that coincides with the axis of the strand.

1.2 Induction of vascular strand formation in mature tissue

Evidence of a mechanism that controls the formation of polar, continuous and aligned vascular strands was first provided by experiments in which auxin had been locally applied to mature tissue (Kraus et al. 1936; Jost 1942; Jacobs 1952; Sachs 1968a). Not only did the applied auxin promote the differentiation of vascular cells, but it aligned such differentiation along continuous lines to form vascular strands, a complex response with unique properties (Sachs 1981; Berleth

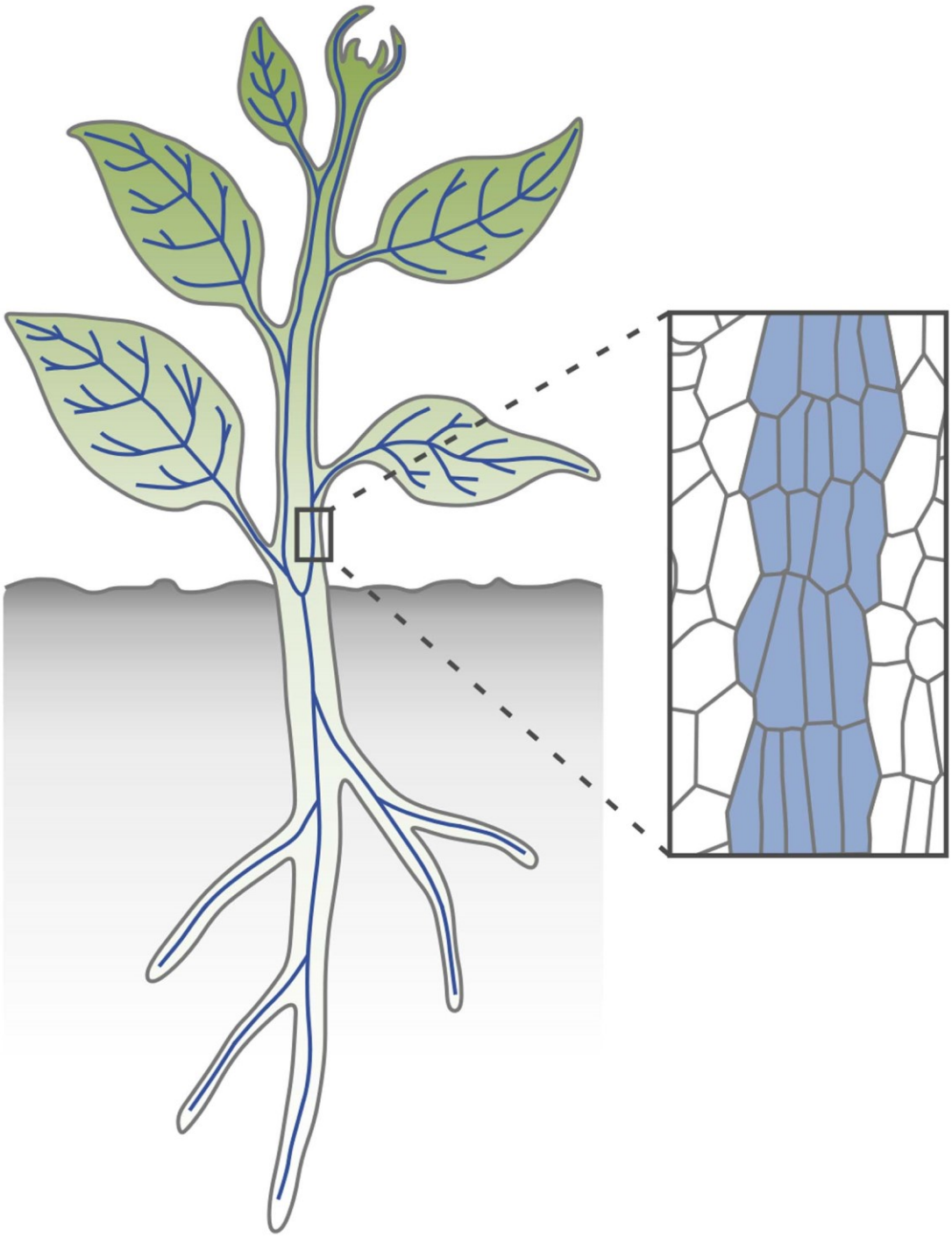

Figure 1.1. Vascular strands: relations between their parts and to the parts of the plant. The plant body is a bipolar axis with shoot pole (green) and root pole (white). Shoot organs are connected with roots by vascular strands (blue lines): continuous files of vascular cells (blue fill) whose axis is aligned along the axis of the strand. Because one end of the strand contacts shoot tissue and the other end contacts root tissue, vascular strands are polar.

et al. 2000) (Figure 1.2A). First, the response is local, as it occurs at the site of auxin application. Second, the response is polar, as it is oriented toward the pre-existing vasculature basal to the site of auxin application—in other words, toward the roots. Third, the response is continuous, as it generates uninterrupted vascular strands. Fourth, the response is spatially constrained, as vascular differentiation is restricted to strips of cells. The axis of these cells is not along the axis of the strand, as in normal development (Esau 1942) (Figure 1.1), but along the shoot-root axis of the tissue (Jost 1942) (Figure 1.2A). And though divisions parallel to the axis of the developing strand are among the defining features of vascular cells formed in normal development (Esau 1942) (Figure 1.1), the auxin-induced vascular differentiation does not require cell division (Roberts and Baba 1968). Auxin application can induce and orient vascular cell division but only in tissue that has retained the capability to divide (Kirschner et al. 1971) (Figure 1.2B), suggesting that other factors in addition to auxin are required in normal vascular development. Fifth, the auxin-induced vascular-differentiation response depends on polar auxin transport, as it requires polarly transported auxins (Dalessandro and Roberts 1971) and is obstructed by inhibitors of polar auxin transport (Gersani 1987), suggesting that the underlying mechanism recruits the machinery that polarly transports auxin.

Auxin is produced in large amounts in immature shoot-organs (Thimann and Skoog 1934; Avery 1935) and is transported to the roots through vascular strands (Went 1928; Wangermann 1974) (Figure 1.2C). Because immature shoot-organs can replace auxin in inducing vascular strand formation (Simon 1930), auxin is at least one of the signals by which shoot organs control formation of the vascular strands that connect them with roots. Roots, on the other hand, orient formation of vascular strands toward themselves by acting as preferred sinks of the auxin that originates in the shoot (Sachs 1968b; Kerk et al. 2000). The formation of polar vascular strands could thus be accounted for by the unequal action of shoot organs and roots on auxin production and consumption, and by the shoot-to-root, apical-basal polarity of auxin transport.

The apical-basal polarity of auxin transport is thought to derive from the localization of auxin efflux proteins at the basal end of auxin-transporting cells (Rubery and Sheldrake 1974; Raven 1975) (Figure 1.2C). As a weak acid, in fact, auxin is negatively charged at the neutral intracellular pH and can only leave the cell through specialized efflux proteins (Figure 1.2C). This picture is certainly an oversimplification, but calculations based on known parameters

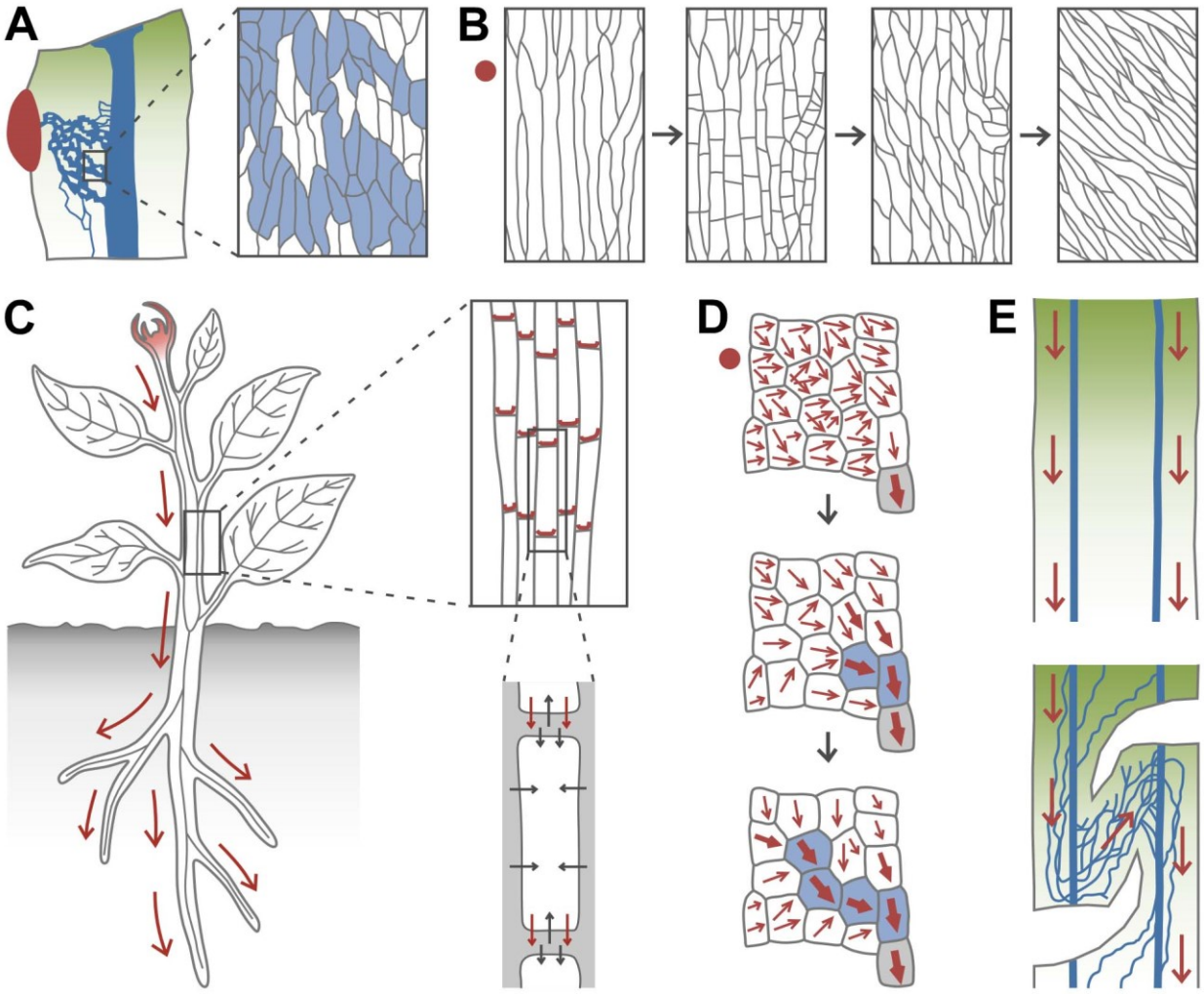

Figure 1.2. Induction of vascular strand formation by auxin and polar auxin transport. (A) Lateral application of auxin (brown) to mature tissue induces differentiation of vascular cells in continuous lines to form vascular strands (blue lines) that connect the applied auxin to the pre-existing vasculature basal to the application site. In the auxin-induced vascular strands, cells are not aligned along the axis of the strand as in Figure 1.1, but along the shoot-root axis of the tissue (green-to-white gradient). After (Sachs 1968a, 1991b). (B) Lateral application of auxin (brown circle) to vascular cells that have retained the capability to divide induces divisions perpendicular to the original axis of the tissue; daughter cells elongate by intrusion along the new axis. Arrows connect successive stages. After (Neeff 1914). (C) Left: auxin (brown fill) is produced in large amounts in immature shoot-organs and transported (brown arrows) to the roots by vascular strands. Top-right: the shoot-to-root, apical-basal polarity of auxin transport derives from the polar localization of efflux carriers of the PIN-FORMED family (brown) at the basal plasma-membrane of vascular cells. Bottom-right: specialized efflux carriers are required for auxin to leave the cell (brown arrows) as auxin is negatively charged at intracellular pH; by contrast, auxin is electrically neutral at extracellular pH and can thus diffuse into the cell (grey arrows). (D) Successive stages (connected by grey arrows) of vascular strand formation in

response to lateral application of auxin (brown circle) according to the "auxin canalization hypothesis". Positive feedback between cellular auxin efflux (brown arrows) and localization of efflux carriers to the cellular site of auxin exit gradually polarize auxin transport (increasingly thicker brown-arrows); this occurs first in cells in contact with the pre-existing vasculature (grey fill), which transports auxin along the original, apical-basal polarity of the tissue and thus orients auxin transport toward itself. Large polar-auxin-transport capacity in selected cells leads to vascular differentiation (blue fill) and drains auxin away from neighbouring cells, thus inhibiting their differentiation. Iteration of the process forms a continuous vascular strand that connects the applied auxin to the pre-existing vasculature basal to the site of auxin application. Figure inspired by (Sachs 1991a). (E) Top: through the auxin transport polarity of the tissue (brown arrows), the polarity of vascular strands (blue lines) is normally aligned with the shoot-to-root polarity of the tissue (green-to-white gradient). Bottom: disruption of the existing auxin-transport polarity allows induction of a new auxin-transport polarity, which can be different from—even opposite to—the original shoot-to-root polarity of the tissue; it is along this new auxin-transport polarity that new vascular strands will form. In these new vascular strands, cells will not be aligned along the axis of the strand as in Figure 1.1, but along the shoot-root axis of the tissue as in (A). After (Sachs 1981).

suggest that it can account for the observed polar transport (Mitchison 1980a); can it also account for the unique properties of the auxin-induced vascular-differentiation response? The "auxin canalization hypothesis" proposes that it can, provided positive feedback between auxin movement through a cell and localization of auxin efflux proteins to the site where auxin leaves the cell (Sachs 1991a; Sachs 2000) (Figure 1.2D). The applied auxin would initially move by diffusion with no preferred orientation, and auxin efflux proteins would be randomly distributed. By efficiently transporting auxin along the original, apical-basal auxin-transport polarity of the tissue, the pre-existing vasculature would act as an auxin sink and orient auxin movement in neighbouring cells, polarizing the localization of auxin efflux proteins in these cells. The initiation of polar auxin transport in these cells would be gradually enhanced by positive feedback between auxin transport and efflux protein localization. By draining auxin in an increasingly more efficient and polar manner, these cells would in turn induce polar auxin transport and polarization of efflux protein localization in the cells above them, and inhibit the same processes in their lateral neighbours. Iteration of these events would result in preferential transport of auxin through limited cell files, which would eventually differentiate into vascular strands. During this process, chance localization of efflux proteins would be stabilized by positive feedback between auxin transport and efflux protein localization, resulting in random elements in the course of the selected cell files and deviations from the shortest routes for auxin transport.

The positive feedback between auxin transport and efflux protein localization can thus account for the unique properties of the auxin-induced vascular-differentiation response. But it can also account for the seemingly conflicting coexistence of stability and flexibility in the alignment between vascular strand polarity and the shoot-to-root polarity of the tissue. Shoot-to-root polarity and auxin transport polarity are normally aligned with each another (Went 1928; Wangermann 1974) (Figure 1.2C). According to the auxin canalization hypothesis, vascular strands would normally form along the existing auxin-transport polarity of the tissue—and thus along the shoot-to-root polarity of the tissue (Figure 1.2E). Induction of a new auxin-transport polarity would require auxin diffusion, but auxin diffusion would be limited, or dominated, by the existing auxin-transport polarity. If, however, the existing auxin-transport polarity were disrupted—for example by wounding—auxin diffusion would no longer be limited, and a new

auxin-transport polarity could be gradually induced. New vascular strands would form along the new auxin-transport polarity, which may even be opposite to the original shoot-to-root polarity of the tissue (Figure 1.2E). Perturbations of the alignment between vascular strand polarity and the shoot-to-root polarity of the tissue are not limited to abnormal growth conditions [e.g., (Sachs 1981)] but also occur in normal development [e.g., (Sachs 1970)]. Though not all the predictions of the auxin canalization hypothesis are necessarily intuitive, they have been rigorously tested and are supported by computer simulation of mathematical models (Mitchison 1980b, 1981; Rolland-Lagan and Prusinkiewicz 2005).

The localization of the five plasma-membrane-localized members of the PIN-FORMED (PIN) family of auxin efflux proteins of *Arabidopsis thaliana* marks the presumed auxin-efflux side of cells (Petrasek et al. 2006; Wisniewska et al. 2006). Thus the polarity of auxin transport can be inferred from the localization of PIN proteins at the plasma membrane. Local application of auxin to mature tissue induces PIN1 expression in broad domains that connect the applied auxin to the pre-existing vasculature (Sauer et al. 2006). In these domains, PIN1 localization is initially apolar but over time becomes polarized to suggest auxin transport away from the site of auxin application and toward the pre-existing vasculature basal to the site of auxin application—observations that are all consistent with predictions of the auxin canalization hypothesis. But these studies have also captured aspects of the auxin-induced vascular differentiation not necessarily implied by the original hypothesis, such as the gradual increase in PIN1 expression in the cells selected for vascular differentiation, and the decline and eventual termination of expression in the cells not selected for vascular differentiation; the underlying mechanism is unknown, but responsiveness of *PIN* gene expression to auxin levels (Heisler et al. 2005; Vieten et al. 2005) could be at its basis.

1.3 Vascular differentiation in callus

Interruption of vascular strand continuity by wounding presumably interrupts polar auxin transport and concentrates auxin in mature tissue near the wound. The disruption of auxin distribution induced by wounding can be imitated in tissue culture—where auxin is continuously

supplied through the culture medium (Gautheret 1939; Nobécourt 1939; White 1939)—or in tumors—where auxin is continuously produced by the tissue itself (Henderson and Bonner 1952). Whether because of wounding, tissue culture or tumor, the resulting disruption of auxin distribution can induce division of vascular-strand-associated cells to give rise to a shapeless mass of cells known as callus (Simon 1908; Sugimoto et al. 2010).

It is often assumed that callus consists of a homogeneous population of undifferentiated cells; instead, differentiation of vascular cells is very common in callus (Simon 1908). In sections, these vascular cells may appear disconnected, an observation in apparent conflict with a control mechanism that requires continuous cell-to-cell transport of an inductive signal; however, in whole-mount preparations of callus tissue, vascular cells are clearly arranged in continuous strands (Aloni et al. 1995), suggesting that the objection is unjustified.

A more serious objection seems to be whether these vascular strands can still be considered expression of a polar control mechanism. Available evidence suggests that they can: when callus forms on both sides of a wound that interrupts the connection of shoot with root, the structure of the callus formed on one side of the wound is different from the structure of the callus formed on the opposite side of the wound (Simon 1908) (Figure 1.3). The callus that is connected with the shoot includes roots and vascular strands with meandering axes, which is the vascular organization that is expected when there is excess auxin that has no uniform polar outlet. On the other hand, the callus that is connected with the root includes shoots and vascular strands oriented along the shoot-root axis, suggesting that this callus is a source of auxin that is readily drained toward the root. By acting as partial replacement of either shoot or root, callus formation can thus be considered an attempt to re-establish the polarity of the vascular strands that connect the different parts of the wounded plant.

1.4 Formation of the first vascular strand

Most of the body of the seedling of a seed plant can be formalized as a cylinder with a vascular strand in its center (Figure 1.4A). The formation of this body axis in the globular embryo is associated with the formation of the first vascular cells, whose axes are aligned along the embryo

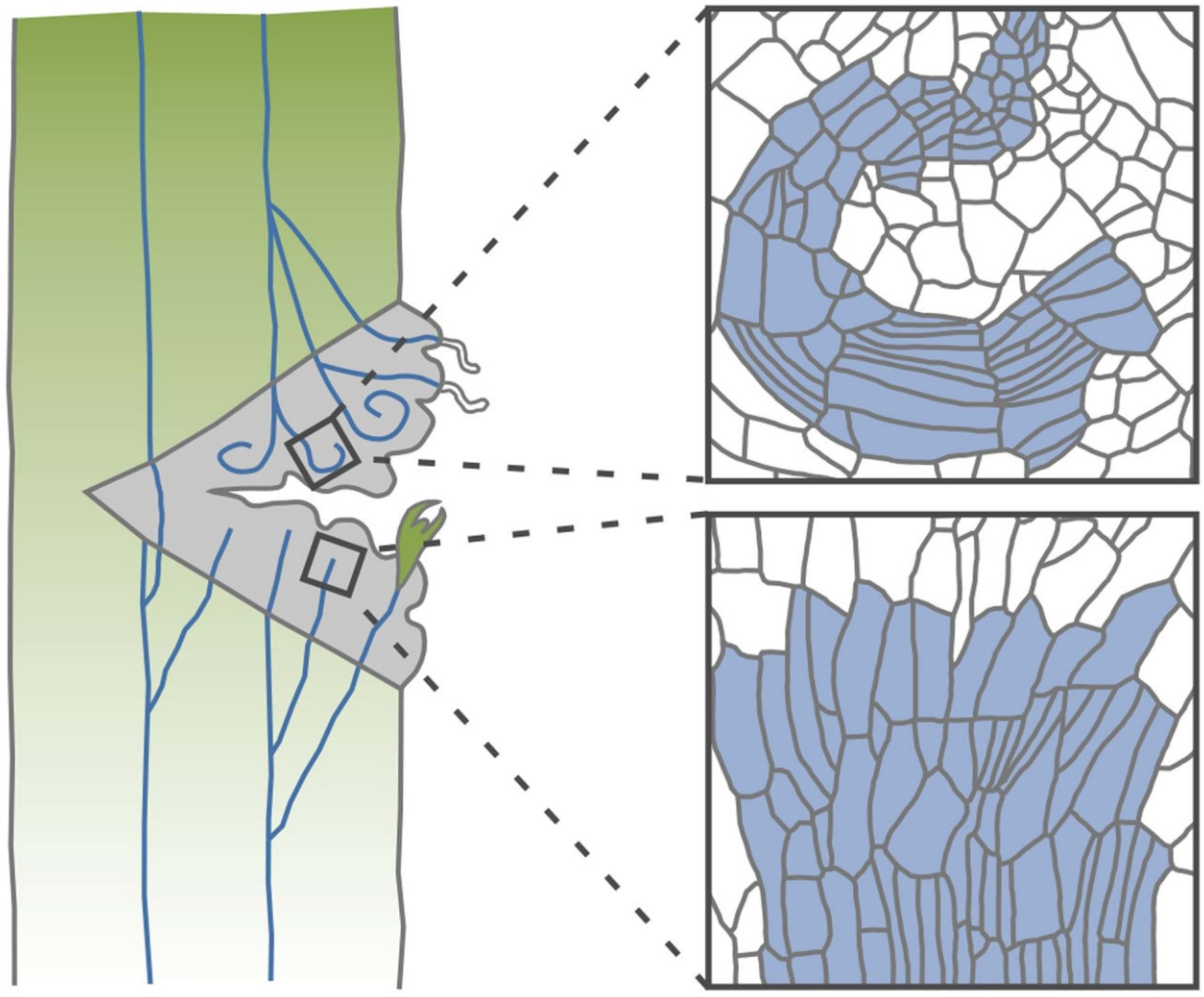

Figure 1.3. Polarity of callus vascular strands. As expressed in the axes of the vascular strands (blue) and in the formation of roots (white) and shoots (green fill), the callus (grey) that forms on the side of the wound that contacts shoot tissue partially replaces the root, while the callus that forms on the side of the wound that contacts root tissue partially replaces the shoot. Callus tissue thus re-establishes the polarity of vascular strands and the connection of shoot organs with roots. After (Sachs 1991a, b).

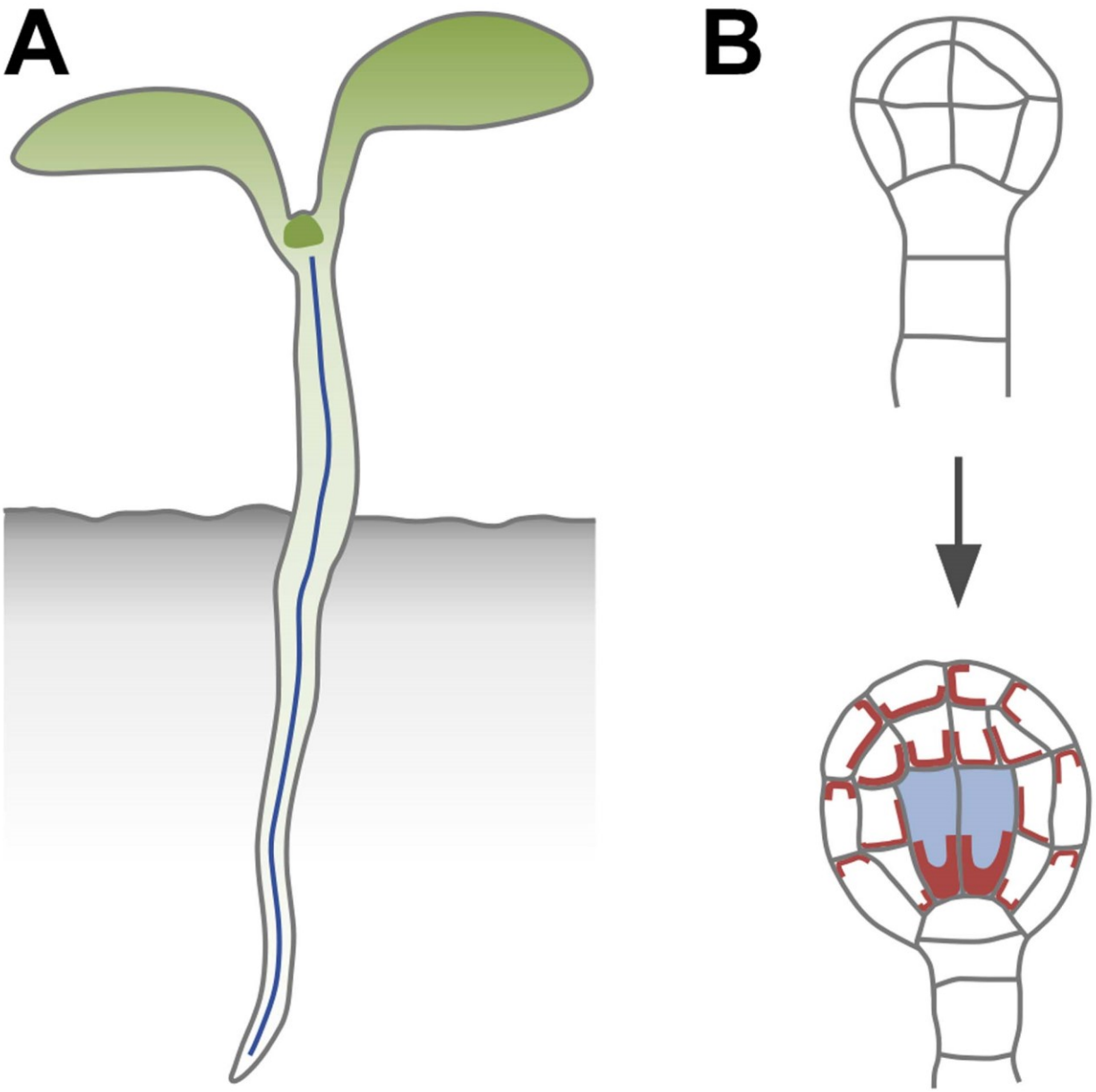

Figure 1.4. The first vascular strand and its formation. (A) Most of the seedling body is a cylinder with a central vascular strand (blue line). (B) The central vascular strand of the seedling derives from the division of the vascular cells (blue fill) of the globular embryo (bottom); these cells are characterized by strong, polarized expression of PIN1 (brown) and arise from the division of the inner cells of the dermatogen embryo (top), a division that is aligned along the future shoot-root axis of the embryo.

axis (Mansfield and Briarty 1991; Gillmor et al. 2010) (Figure 1.4B). The embryo axis first becomes evident from the division of the inner cells of the dermatogen-stage embryo (Figure 1.4B), a division that occurs along a single axis. The resulting globular embryo is no longer radially symmetrical but comprised of concentric cylinders, though its overall shape is still spherical (Figure 1.4B). At the molecular level, embryo axis formation in the globular embryo is associated with polar localization of PIN1 at the basal end of the inner cells (Steinmann et al. 1999) (Figure 1.4B). Consistent with predictions of the auxin canalization hypothesis, polarization of PIN1 localization is particularly pronounced in the first vascular cells (Figure 1.4B), which are thus molecularly polar. But these cells are also morphologically polar, as their apical end connects to the upper tier of cells and their basal end to the uppermost cell of the extra-embryonic suspensor—the hypophysis (Figure 1.4B). The following divisions will extend the individual cell files and elaborate the poles of the embryo axis, using this axis as a positional reference (Berleth 2001).

Available evidence suggests that the formation of the embryo axis and of the vascular strand in its center depend on polar auxin transport and signalling. Development of embryos in presence of auxin transport inhibitors occasionally results in nearly spherical, apparently apolar, embryos and seedlings (Schiavone and Cooke 1987; Hadfi et al. 1998). Similar defects seem to appear in the most extreme examples of mutants in multiple *PIN* genes (Friml et al. 2003) but can also be induced by mutation of a single gene of Arabidopsis: *EMBRYO DEFECTIVE30*/*GNOM* (*EMB30*/*GN*; *GN* hereafter) (Mayer et al. 1993). The GN protein is a guanine nucleotide exchange factor required to transport PIN proteins to their proper location at the plasma membrane (Steinmann et al. 1999; Geldner et al. 2003; Kleine-Vehn et al. 2008). However, only a small fraction of *gn* embryos develops into nearly spherical seedlings; most of them develop into seedlings in which the embryo axis is replaced by a conical structure composed of morphologically indistinct cells (Mayer et al. 1993), a defect that also appears in embryos treated with auxin antagonists and in mutants in auxin production, perception or response (Hadfi et al. 1998; Hardtke and Berleth 1998; Hamann et al. 2002; Dharmasiri et al. 2003; Hellmann et al. 2003; Dharmasiri et al. 2005; Cheng et al. 2007; Dharmasiri et al. 2007; Stepanova et al. 2008; Thomas et al. 2009). Among them, embryo axis defects are most pronounced in mutants of the *Arabidopsis* gene *MONOPTEROS*/*AUXIN RESPONSE FACTOR5* (*MP*/*ARF5*; *MP* hereafter),

which encodes a transcription factor that regulates auxin-responsive gene expression (Berleth and Jurgens 1993; Hardtke and Berleth 1998; Mattsson et al. 2003). Defects in *gn* and *mp* have been traced back to similar abnormal divisions in early embryogenesis (Mayer et al. 1993; Hamann et al. 1999), but these are likely to be consequence rather than cause of the embryo axis defects, as randomization of orientation of cell division does not lead to embryo axis defects [e.g., (Torres-Ruiz and Jurgens 1994; Lukowitz et al. 1996; Strompen et al. 2002)].

1.5 Formation of closed vascular networks

A cylindrical structure with a vascular strand in its center is not only the base unit of the embryo axis but of the whole body of early land plants (Fairon-Demaret and Li 1993). These leafless plants can in fact be described as two systems of branching cylindrical organs—one above and one below ground—with a vascular strand in the center of each cylinder (Figure 1.5A). Most extant plants bear flat organs such as leaves and thus deviate from the basic cylindrical structure; however, this basic structure can still be recognized at early stages of development of flat organs, when these organs appear as cylindrical primordia with a vascular strand in their center (Mattsson et al. 1999; Kang and Dengler 2004; Scarpella et al. 2004). The cylindrical shape is soon lost, and the organs acquire their distinctive flattened shape, a process which coincides with the formation of branching systems of vascular strands. These vascular networks are said to be "open", if each vascular strand ends freely at one end and contacts another strands at the other end, and "closed", if at least some vascular strands contact other strands at both ends (Roth-Nebelsick et al. 2001) (Figure 1.5B).

A unique shoot-to-root polarity can be assigned to all vascular strands in open networks, but in closed networks there are strands whose polarity is ambiguous (Sachs 1975) (Figure 1.5B). Thus closed networks seem incompatible with a control mechanism that relies on polar transport of auxin; however, the dynamics of PIN1 expression during the formation of closed vascular networks suggest that the incompatibility is only apparent (Scarpella et al. 2006; Wenzel et al. 2007; Sawchuk et al. 2013) (Chapter 2; Figure 1.5C). During formation of all vascular strands, weakly polar—or altogether apolar—PIN1 expression is initiated in broad domains in continuity

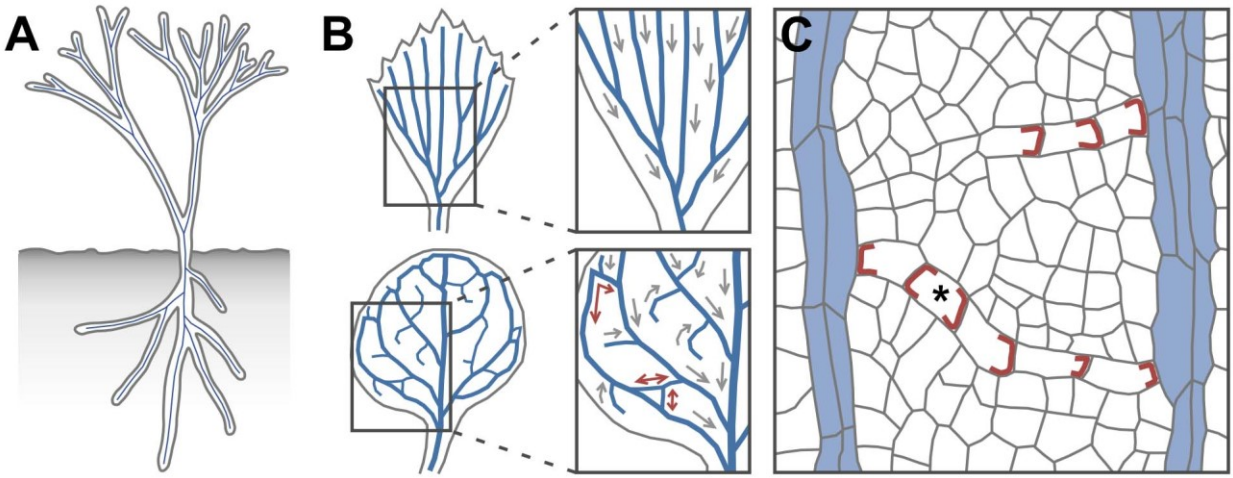

Figure 1.5. Networks of polar vascular strands. (A) The body of early, leafless plants was a system of branching cylinders with a vascular strand (blue line) in their center. (B) Extant plants bear leaves with open (top) or closed (bottom) networks of vascular strands. A unique shoot-to-root polarity (grey arrow) can be assigned to each vascular strand in open networks; attempts to assign shoot-to-root polarity to individual strands in closed networks lead to strands with ambiguous polarity (brown double-headed arrows). (C) Polar localization of PIN1 (brown) in files of vascular cells suggests auxin transport toward pre-existing vasculature (blue fill; for simplicity, PIN1 expression in pre-existing vasculature is not shown). Thus, in unilaterally connected vascular strands, a single auxin transport polarity exists; in bilaterally connected strands, the two opposite polarities are integrated by a cell with PIN1 at both ends (asterisk).

with pre-existing vasculature. Over time, the broad PIN1-expression domains narrow to sites of vascular strand formation, and PIN1 localization becomes polarized toward pre-existing vasculature; both processes initiate and proceed away from pre-existing vasculature. As a unilaterally connected PIN1 expression domain with uniform auxin-transport polarity toward pre-existing vasculature becomes connected at both ends, or merges with another unilaterally connected domain, a single cell in which PIN1 localizes at both ends—a "bipolar" cell—appears along the now bilaterally connected PIN1 expression domain; this bipolar cell bridges the two, opposite auxin-transport polarities—each toward pre-existing vasculature—that now exist in the bilaterally connected vascular strand.

As auxin application to other dividing tissues (Kirschner et al. 1971), auxin application to developing leaves induces formation of vascular strands in which cells are aligned along the axis of the strand (Scarpella et al. 2006; Sawchuk et al. 2007); however, this alignment is lost in wild-type leaves developed in presence of auxin transport inhibitors (Mattsson et al. 1999; Sieburth 1999) and in leaves of severe auxin-response mutants (Przemeck et al. 1996; Mattsson et al. 1999), suggesting that the orienting effect of auxin on cell alignment within vascular strands depends on both polar auxin signalling and the cell division capability of the tissue.

1.6 Continuous vascular differentiation

A control mechanism that relies on continuous, cell-to-cell transport of auxin predicts that vascular strands should form without interruptions; yet interruptions have been observed in vascular strands of wild-type and mutant leaves (Pray 1955b, a; Lersten 1965; Herbst 1971; Berleth and Jurgens 1993; Carland et al. 1999; Deyholos et al. 2000; Koizumi et al. 2000; Steynen and Schultz 2003; Sawa et al. 2005). Further scrutiny, however, suggests that some of these interrupted vascular strands are composed of stretches of mature vascular cells connected by stretches of immature vascular cells (Pray 1955b, a; Lersten 1965; Herbst 1972; Przemeck et al. 1996); because the identification of immature vascular cells can be problematic (Esau 1943), these strands have been interpreted as interrupted when they really are continuous, though only partly differentiated. By contrast, in other interrupted vascular strands, stretches of mature

vascular cells are separated by mature non-vascular tissue (Herbst 1972; Carland et al. 1999; Deyholos et al. 2000). However, these strands emerge as continuous files of immature vascular cells that over time break down into fragments (Herbst 1972; Scarpella et al. 2006; Naramoto et al. 2009); this is reflected in the breaking down of initially continuous PIN1 expression domains (Scarpella et al. 2006; Naramoto et al. 2009), suggesting that the interrupted strands are the outcome of defective maintenance of normally established, continuous auxin transport. All these "interrupted" strands are thus continuous, at least at formative stages and are thus compatible with an auxin-transport-dependent control mechanism. An observation that is instead more difficult to reconcile with such mechanism is the presence of seemingly isolated, randomly oriented, mature vascular cells in *gn* cotyledons (Mayer et al. 1993); however, it is unknown whether these cells are ever connected by immature vascular cells and, if so, what the axis of the resulting strand would be.

Continuity of vascular strands is a stringent requirement for a control mechanism that relies on continuous auxin transport but also for transport of water and nutrients, a complex function supported by the complex ultrastructure of vascular cells (Scott et al. 1960). Aspects of this ultrastructure are shared by isolated cells with no defined axis (Solereder 1908). Because these cells store—rather than transport—water and nutrients (Foster 1956), they cannot be considered vascular cells and are thus not an objection to a control mechanism that depends on continuous auxin transport; rather, they suggest that the same cellular differentiation pathway can be recruited to support different, though related, functions.

1.7 Conclusions

The discussion here focused on evidence in support of and objections against mechanisms proposed to control the formation of polar, continuous and aligned vascular strands. One such mechanism had been hypothesized to account for the polar and continuous—though not necessarily aligned—vascular strands that form in mature tissue in response to auxin application. However, the auxin canalization hypothesis and its predictions have turned out to be consistent also with the molecular genetics and cell biology of embryo axis formation and shoot organ

development. Objections to the hypothesis include claims of apolar or discontinuous vascular strands in callus and leaves; however, the evidence does not seem to support the claims, and thus the objections seem unjustified. Nevertheless, major questions remain unanswered.

The auxin canalization hypothesis seems to imply that cells can sense auxin flux—that is, the amount of auxin that flows through a cell over time. Though the positive effect of auxin on its own transport is experimentally well supported (Rayle et al. 1969; Paciorek et al. 2005), whether this effect is at the basis of an auxin-flux-sensing mechanism remains unclear. Alternatives to a "flux sensor" have been proposed (Mitchison 1981; Kramer 2009; Wabnik et al. 2010), but all of them make assumptions awaiting experimental support and reproduce only some aspects of vascular strand formation.

The auxin canalization hypothesis also predicts low amounts of auxin in vascular strands, which seems in conflict with experimental evidence (Mattsson et al. 2003); solutions to this conflict have been proposed (Kramer 2004; Feugier et al. 2005; Bayer et al. 2009; Kramer 2009; Wabnik et al. 2010), but whether the effects of experimentally interfering with the additional assumptions are consistent with the predicted outcomes remains unknown.

However successful the attempts to reconcile hypothesis and evidence may be, it would seem naïve to expect that a single mechanism can account for all the properties of a complex process such as vascular strand formation; instead, it would seem likely that at least some of these properties can be controlled by other, unidentified mechanisms. One of these properties seems to be vascular strand alignment: though necessary, polar auxin transport can in fact only promote the oriented divisions required for such alignment in tissue that has retained the capability to divide and can thus respond to the orienting signal.

In the end, however, the most surprising finding is perhaps that so few objections to the auxin canalization hypothesis have been raised. This may simply reflect the few, possibly exceptional, contexts in which the hypothesis has been tested, and as experimental evidence catches up with intuitive concepts we should expect many more inconsistencies to be exposed. Nevertheless, it seems justified to suggest that the consistencies outlined above will provide an entry point into dissecting the complexity of vascular strand formation.

1.8 Scope of the work and outline of the thesis

The evidence discussed above suggests a role for polar auxin transport in the formation of vascular strands. The scope of my Ph.D. thesis was to understand the contribution of auxin transport to the formation of networks of such vascular strands.

Networks of vascular strands are readily visible in the leaf, and the patterns of these "vein" networks are characterized by sets of reproducible features (e.g., (Nelson and Dengler 1997))—so reproducible that they are used as a taxonomic characteristic (e.g. (Klucking 1995)).

In Chapter 2, I explored the contribution of auxin transport mediated by the five plasma-membrane (PM)-localized (Chen et al. 1998; Galweiler et al. 1998; Luschnig et al. 1998; Muller et al. 1998; Friml et al. 2002a; Friml et al. 2002b; Friml et al. 2003; Petrasek et al. 2006) and the three endoplasmic-reticulum (ER)-localized members (Petrasek et al. 2006; Mravec et al. 2009; Bosco et al. 2012; Ding et al. 2012; Bender et al. 2013; Cazzonelli et al. 2013; Sawchuk et al. 2013) (Chapter 2) of the PIN family of Arabidopsis to vein patterning. I found that vein patterning is redundantly controlled by two distinct PIN-mediated auxin-transport pathways: one pathway, mediated by the PM-localized PIN1, transports auxin intercellularly; the other pathway, mediated by the ER-localized PIN5, PIN6 and PIN8, transports auxin intracellularly. Further, I found that *PIN1* is the only *PIN* gene with non-redundant functions in vein patterning, that *PIN6* functions redundantly with *PIN1* in vein patterning, and that *PIN8* functions redundantly with *PIN6* in *PIN1*-dependent vein patterning. Finally, *PIN1*, *PIN6* and *PIN8* redundantly inhibit the negative function of *PIN5* on vein patterning.

In contrast to the reproducible features of vein network patterns, features of vein networks such as the number of veins and the extent of their interconnectedness are variable.

In Chapter 3, I tested whether the relation between *PIN1*, *PIN5*, *PIN6* and *PIN8* in vein patterning persisted in vein network formation. I found that *PIN1* inhibits vein network formation, that *PIN6* functions redundantly with *PIN1* in inhibition of vein network formation, and that *PIN8* functions redundantly with *PIN6* in *PIN1*-dependent inhibition of vein network formation. Further, *PIN6* and *PIN8*, independently of *PIN1*, redundantly inhibit *PIN5*-dependent promotion of vein network formation. These results suggest that vein network formation and vein patterning are controlled by different—though overlapping—control mechanisms.

Though auxin transport seems to be required to define sites of vein formation (Sachs 1981), available evidence suggests that vascular differentiation depends on auxin signalling: mutants defective in auxin signalling have reduced vascular differentiation, and elevated levels of local auxin response precede vascular differentiation (Przemeck et al. 1996; Mattsson et al. 2003; Hardtke et al. 2004; Alonso-Peral et al. 2006; Candela et al. 2007; Strader et al. 2008; Donner and Scarpella 2009). Though the auxin signal can be transduced by different pathways (Leyser 2010), the best understood pathway relies on the function of the ARF family of transcription factors (Chapman and Estelle 2009), and the function of one ARF—ARF5/MP (Hardtke and Berleth 1998)—appears to be crucial for vascular differentiation (Przemeck et al. 1996; Hardtke et al. 2004). Thus analyses of vascular defects of *mp* mutants have advanced, and will continue to advance, our understanding of the role of auxin signalling in vascular differentiation. Unfortunately, an *mp* allelic series in the widely used Columbia wild-type background of Arabidopsis was lacking.

In Chapter 4, I extended the characterization of two known *mp* mutant alleles in the Columbia background of Arabidopsis. Further, I identified and characterized four new alleles of *mp* in the Columbia background. Among these four new *mp* mutant alleles, I found the first low-expression allele of *mp* and the strongest Columbia allele of *mp*.

The evidence discussed above suggests that the inductive effect of auxin on vein network formation is strictly mediated by PIN1 and possibly by other members of the PIN family.

In Chapter 5, I tested this hypothesis. I found that vein patterning still occurs in the absence of the function of PIN proteins or of any known intercellular auxin transporter. The vein patterning activity independent of carrier-mediated intercellular auxin-transport relies, at least in part, on the auxin signalling mediated by the TRANSPORT INHIBITOR RESPONSE1/AUXIN SIGNALLING F-BOX (TIR1/AFB) auxin receptors (Dharmasiri et al. 2005) and the MP auxin-responsive transcription factor (Hardtke and Berleth 1998). Further, my results—in combination with previous evidence—suggest that the GN guanine exchange factor for ADP rybosilation factor GTPases (Steinmann et al. 1999) promotes vein patterning upstream of both auxin transport and signalling.

Finally, in Chapter 6, I propose and discuss two non-mutually exclusive hypotheses of how intercellular and intracellular auxin transport might redundantly control vein patterning and

network formation.

CHAPTER 2: PATTERNING OF LEAF VEIN NETWORKS BY CONVERGENT AUXIN TRANSPORT PATHWAYS

2.1 Introduction

Branched structures pervade all levels of organization in living organisms, from molecules to organelles, cells, multicellular organs and entire organisms, and the principles that guide the formation of these branched structures have long been object of interest of biologists and mathematicians. However, few branched structures have historically captured more widespread attention than the vein networks of plant leaves. From a developmental standpoint, such attention seems justified as files of vein precursor cells are selected from within a population of seemingly identical cells (Foster 1952; Pray 1955a). Furthermore, in most species the product of this patterning process is both reproducible and variable: reproducible as vein networks supply all areas of the leaf; variable as the exact sites of vein formation are unpredictable (Sachs 1989). These observations argue against rigid specification of leaf vein patterns and suggest a self-organizing control mechanism that reconciles the plasticity of vein formation with the stringent requirement for organ vascularization (Berleth et al. 2000).

Though the identity of the molecules involved is largely unknown, varied evidence supports a decisive role for the polar, cell-to-cell transport of the plant signal auxin in leaf vein patterning: auxin application induces formation of new veins oriented towards pre-existing veins (Sachs 1989); the inductive and orienting effect of applied auxin on vein formation is suppressed by auxin transport inhibitors (Gersani 1987); and auxin transport inhibitors induce characteristic defects in vein patterns (Mattsson et al. 1999; Sieburth 1999). During leaf development, expression of the plasma-membrane (PM)-localized PIN-FORMED1 (PIN1) auxin transporter of *Arabidopsis thaliana* (Galweiler et al. 1998; Petrasek et al. 2006) is initiated in broad tissue domains and becomes gradually restricted to single files of vascular precursor cells (Scarpella et al. 2006; Wenzel et al. 2007). Narrowing of PIN1 expression domains is associated with polarization of PIN1 subcellular localization to the presumed auxin-efflux side of PIN1-expressing cells. Auxin levels define the initial size of PIN1 expression domains, and both

domain narrowing and PIN1 polarization are obstructed by auxin transport inhibitors. These observations agree with conceptual formulation (Sachs 1981, 1991a) and mathematical modeling (reviewed in (Smith and Bayer 2009; Garnett et al. 2010; Krupinski and Jonsson 2010; Santos et al. 2010; Wabnik et al. 2011a)) of progressive restriction of non-directional auxin transport across tissues to polar transport in single files of vascular precursor cells by positive feedback between auxin flow through a cell and the cell's auxin conductivity. However, in contrast to the severe vein-pattern defects induced by auxin transport inhibitors (Mattsson et al. 1999; Sieburth 1999), vein pattern defects in *pin1* mutant leaves are mild (Mattsson et al. 1999; Bilsborough et al. 2011; Guenot et al. 2012). PIN1 is member of a family comprising four other PM-localized PIN proteins and three, evolutionary older, endoplasmic reticulum (ER)-localized PIN proteins (Paponov et al. 2005; Krecek et al. 2009; Zazimalova et al. 2010; Viaene et al. 2012). Thus, the mild vein-pattern defects of *pin1* have been attributed to redundancy among PM-localized PIN proteins (e.g., (Mattsson et al. 1999; Clay and Nelson 2005; Scarpella et al. 2006; Bilsborough et al. 2011)), redundancy that has been shown to underlie, to different extents, many other developmental processes ((Fischer et al. 2006; Guenot et al. 2012; Sassi et al. 2012) and references therein).

Here we show that the vein network of the Arabidopsis leaf is patterned by two distinct and convergent auxin transport pathways: intercellular auxin transport mediated by PM-localized PIN1 and intracellular auxin transport mediated by ER-localized PIN6, PIN8 and PIN5. Our results suggest an ancestral auxin-transport-dependent mechanism to specify cell files to vascular function that predates evolution of PM-localized PIN proteins.

2.2 Results

2.2.1 Vein patterning functions of Arabidopsis *pin* genes

WT Arabidopsis grown under normal conditions forms separate leaves, whose vein patterns are defined by reproducible features (Nelson and Dengler 1997; Candela et al. 1999) (Figure 2.1A and 2.1B): a narrow, central midvein that runs the length of the leaf; lateral veins that branch from the midvein and join distal veins to form closed loops; minor veins that branch from

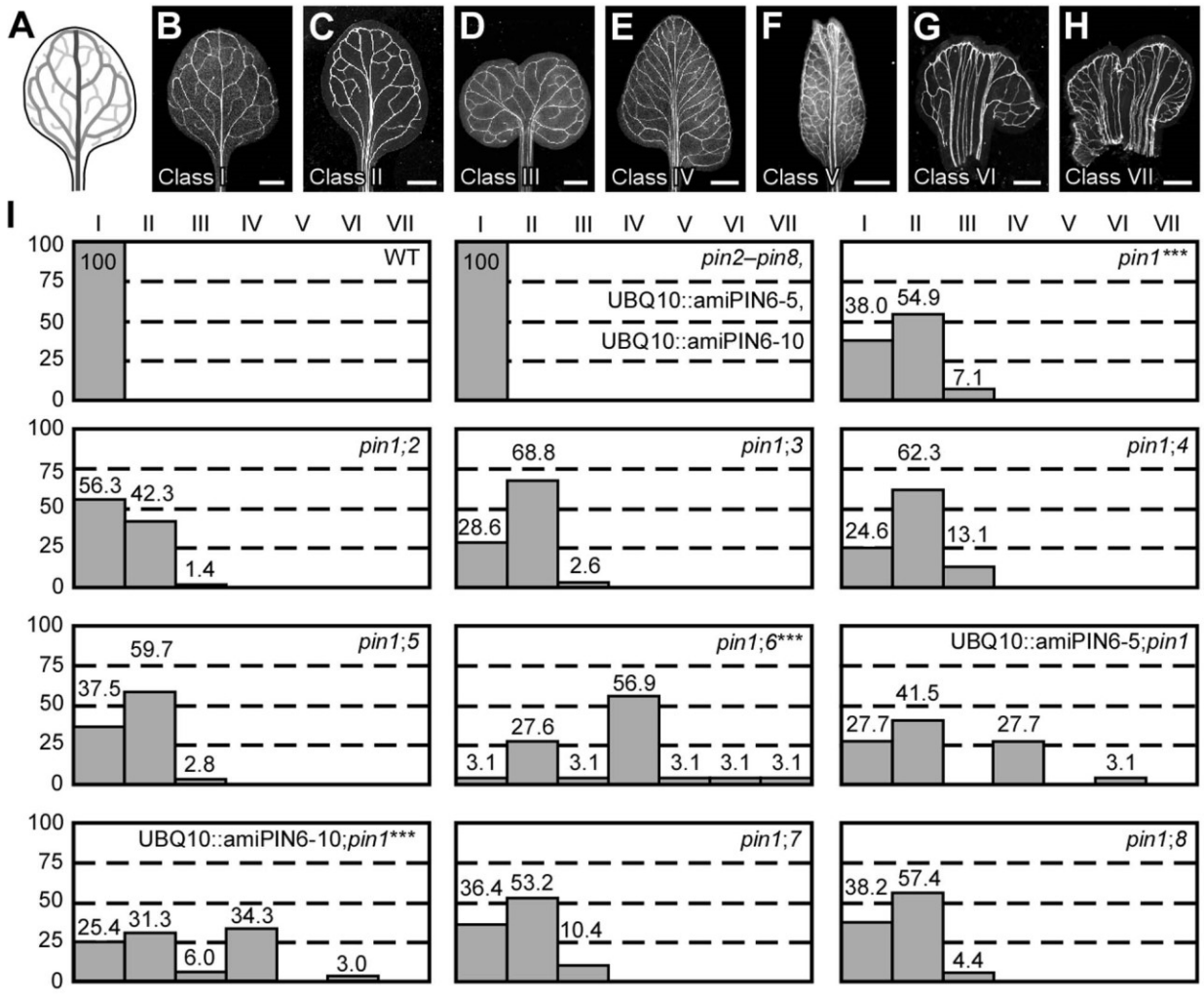

Figure 2.1. Vein patterning functions of Arabidopsis *PIN* genes. (A,B) Vein pattern of WT mature first leaf. In (A), dark grey, midvein; grey, loops; light grey, minor veins. (B-H) Dark-field illumination of cleared mature first leaves illustrating phenotype classes: unbranched, narrow midvein and scalloped vein-network outline (B); bifurcated midvein and scalloped vein-network outline (C); fused leaves with scalloped vein-network outline (D); conspicuous marginal vein (E); fused leaves with conspicuous marginal vein (F); wide midvein (G); fused leaves with wide midvein (H). (I) Percentages of leaves in phenotype classes. Difference between *pin1* and WT, between *pin1*;*6* and *pin1*, and between UBQ10::amiPIN6;*pin1* and *pin1* was significant at $P<0.001$ (***) by Kruskal-Wallis and Mann-Whitney test with Bonferroni correction. Sample population sizes: WT, 65; *pin2*, 68; *pin3*, 68; *pin4*, 68; *pin5*, 68; *pin6*, 68; UBQ10::amiPIN6-5, 65; UBQ10::amiPIN6-10, 65; *pin7*, 68; *pin8*, 68; *pin1*, 71; *pin1*;*2*, 71; *pin1*;*3*, 77; *pin1*;*4*, 69; *pin1*;*5*, 72; *pin1*;*6*, 65; UBQ10::amiPIN6-5;*pin1*, 65; UBQ10::amiPIN6-10;*pin1*, 67; *pin1*;*7*, 77; *pin1*;*8*, 68. Bars: (B-F) 1.5 mm; (G,H) 0.75 mm.

midvein and loops and either end freely or join other veins; and minor veins and loops that curve near the leaf margin, lending a scalloped outline to the vein network. By contrast, WT leaves developed in the presence of auxin transport inhibitors often show separation defects ('fused leaves'), and vein patterns of auxin-transport-inhibited leaves deviate from the norm in at least four respects (Mattsson et al. 1999; Sieburth 1999). First, the midvein bifurcates near the leaf tip. Second, the vein network consists of more lateral veins. Third, lateral veins do not join the midvein at the centre of the leaf but run parallelly to one another to form a wider midvein. Fourth, lateral veins end in a marginal vein that closely parallels the leaf margin, lending a smooth outline to the vein network. Mutation of *PIN1* (AT1G73590) approximates these defects, but vein patterns are only mildly affected in *pin1* (Mattsson et al. 1999; Bilsborough et al. 2011) (Figure 2.1). As *PIN1* is one of eight *PIN* genes (Paponov et al. 2005; Krecek et al. 2009; Zazimalova et al. 2010; Viaene et al. 2012) and other gene families have been implicated in auxin transport (Geisler and Murphy 2006; Barbez et al. 2012; Peret et al. 2012), the mild vein-pattern defects of *pin1* might reflect contribution of other auxin transporters to vein patterning; here we tested whether other *PIN* genes contribute to vein patterning.

We first explored this possibility by analyzing vein patterns of single mutants in *PIN2* (AT5G57090), *PIN3* (AT1G70940), *PIN4* (AT2G01420), *PIN5* (AT5G16530), *PIN6* (AT1G77110), *PIN7* (AT1G23080) and *PIN8* (AT5G15100). *pin2 – pin8* (Table 2.1) had WT vein patterns (Figure 2.1), limiting non-redundant vein-patterning functions to *PIN1*. Thus, to uncover potential vein-patterning functions of *PIN2 – PIN8*, we next analyzed vein patterns of double mutants between *pin1* and *pin2 – pin8*. Only mutation of the auxin-transporter-encoding *PIN6* (Petrasek et al. 2006) had a significant effect on *pin1* phenotype spectrum, with ~65% of *pin1pin6* (*pin1*;*6*) leaves belonging to new, stronger classes (Figure 2.1). *pin6* had a similar effect on *pin1* phenotype spectrum in seedlings (Figure 2.2): ~95% penetrance of cotyledon defects in *pin1*;*6* vs. ~35% in *pin1*, and appearance in *pin1*;*6* of a cup-shaped cotyledon phenotype resembling that of embryos developed in the presence of auxin transport inhibitors (Liu et al. 1993; Hadfi et al. 1998). In both leaves and seedlings, the *pin1*;*6* phenotype spectrum was mimicked by expressing an artificial microRNA targeting *PIN6* (UBQ10::amiPIN6) in the *pin1* background (Figures 2.1 and 2.2). We conclude that *PIN6* is the *PIN* gene that most contributes to auxin-transport-dependent vein patterning in the absence of *PIN1* function.

Table 2.1. Origin and nature of lines.

Line	Origin/Nature
pin1-1	(Goto 1987; Galweiler et al. 1998); WT at the *TTG1* (AT5G24520) locus
eir1-1 (pin2)	(Roman et al. 1995; Luschnig et al. 1998)
pin3-3	(Friml et al. 2002b)
pin4-2	(Friml et al. 2002a)
pin5-4	(Mravec et al. 2009)
pin6	SM_3_15050 (ABRC) (Tissier et al. 1999) containing a single dSpm transposable element at position +183 of *PIN6* (AT1G77110)
UBQ10::amiPIN6	Transcriptional fusion of *UBQ10* (AT4G05320; -1516 to –1; primers: 'UBQ10 HindIII Forw' and 'UBQ10 SmaI Rev') to an artificial microRNA (Schwab et al. 2006) targeting *PIN6* (AT1G77110; primers: 'PIN6 I miR-s', 'PIN6 II miR-a', 'PIN6 III miR*s', 'PIN6 IV miR*a', 'pRS300 A' and 'pRS300 B')
pin7^{En}	(Blilou et al. 2005)
pin8-1	(Bosco et al. 2012)
PIN6::PIN6:GFP	Translational fusion of *PIN6* (AT1G77110; -3784 to +4252; primers: 'PIN6 prom SmaI forw' and 'PIN6 2179 SphI rev', 'PIN6 2180 EcoRI forw' and 'PIN6 UTR XhoI rev') to EGFP (Clontech; insertion at +2179 of *PIN6*; primers: 'EGFP PstI SphI forw' and 'EGFP EcoRI rev'); reverts the cotyledon phenotype of *pin1*;*6* to that of *pin1*
PIN6::YFPnuc	Transcriptional fusion of *PIN6* (AT1G77110; -3747 to -6; primers: 'PIN6 transc forw' and 'PIN6 transc rev') to HTA6:EYFP (Zhang et al. 2005)
PIN1::PIN1:CFP	(Gordon et al. 2007)
35S::YFPer	(Nelson et al. 2007)
35S::RTNLB4:YFP	(Nziengui et al. 2007)
J1721::GFPer	(Haseloff 1999; Sawchuk et al. 2007)
ATHB8::GFPnuc	Transcriptional fusion of *ATHB8* (AT4G32880; -1997 to -1; primers: 'ATHB8 attB1F' and 'ATHB8 attB2R') to EGFP:nuc (Kubo et al. 2005)
35S::YFPpm	(Cutler et al. 2000)
PIN8::PIN8:GFP	Translation fusion of *PIN8* (AT5G15100; -1812 to +2443; primers: 'PIN8 prom BamHI forw' and 'PIN8 UTR SacI Rev') to EGFP (Clontech;

	insertion at +684 of *PIN8*; primers: 'EGFP BglII forw' and 'EGFP BglII rev'); reverts the cotyledon phenotype of *pin1*;*6*;*8* to that of *pin1*;*6*
PIN8::YFPnuc	Transcriptional fusion of *PIN8* (AT5G15100; -1812 to -1; primers: 'PIN8 transc forw' and 'PIN8 transc rev') to HTA6:EYFP (Zhang et al. 2005)
DR5rev::YFPnuc	(Heisler et al. 2005); transformed into Col-0
PIN1::PIN1:YFP	(Xu et al. 2006)
MP::PIN6	Transcriptional fusion of *MP* (AT1G18950; -3282 to -1; primers: 'MP SalI Fwd' and 'MP BamHI Rev') to *PIN6* coding sequence (AT1G77110; primers: 'PIN6OX SmaI forw' and 'PIN6OX Ecl136II rev')
MP::YFPnuc	Transcriptional fusion of *MP* (AT1G18950; -3281 to –1; primers: 'MP prom Gateway Fwd' and 'MP prom Gateway Rev') to HTA6:EYFP [12]
ATHB8::CFPnuc	(Sawchuk et al. 2007)
RPS5A::PIN6	Transcriptional fusion of *RPS5A* (AT3G11940; -2236 to –1; primers: 'RPS5A SmaI Forw' and 'RPS5A SmaI Rev') to *PIN6* coding sequence (AT1G77110; primers: 'PIN6OX SmaI forw' and 'PIN6OX Ecl136II rev')
MP::PIN8	Transcriptional fusion of *MP* (AT1G18950; -3282 to -1; primers: 'MP SalI Fwd' and 'MP BamHI Rev') to *PIN8* coding sequence (AT5G15100; primers: 'PIN8OX KpnI forw' and 'PIN8OX BamHI rev')
MP::PIN5	Transcriptional fusion of *MP* (AT1G18950; -3282 to -1; primers: 'MP SalI Fwd' and 'MP BamHI Rev') to *PIN5* coding sequence (AT5G16530; primers: 'PIN5OX SmaI forw' and 'PIN5OX BamHI rev 2')
PIN6::iaaL	Transcriptional fusion of *PIN6* (AT1G77110; -3784 to -1; primers: 'PIN6 prom SalI F' and 'PIN6 prom BamHI R') to iaaL coding sequence (Roberto et al. 1990) (primers: 'IAAL BamHI F' and 'IAAL KpnI R')

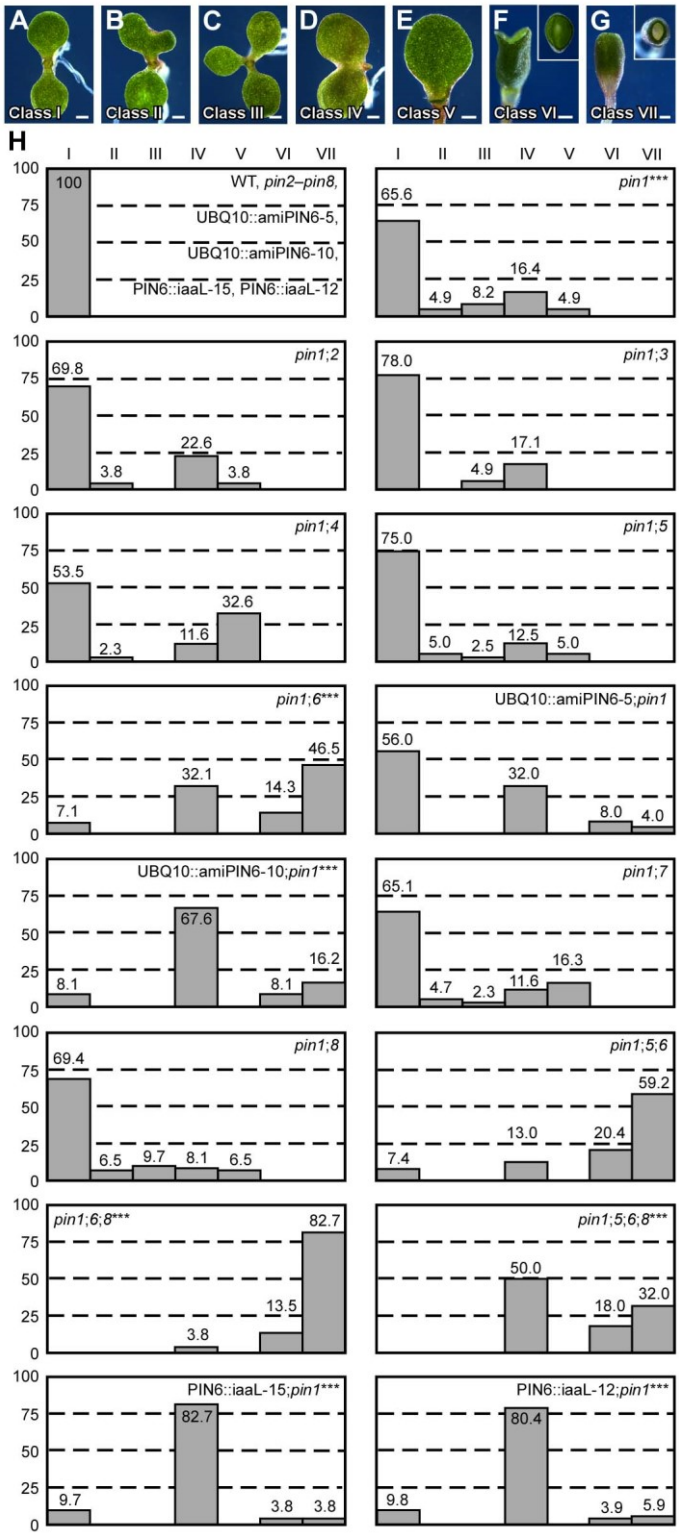

Figure 2.2. Cotyledon patterns of *pin* mutants. (A-G) Dark-field illumination of 4-day-old seedlings illustrating phenotype classes: two separate cotyledons (A); fused cotyledons and separate single cotyledon (B); three separate cotyledons (C); fused cotyledons (D); single

cotyledon (E); partially fused cup-shaped cotyledon, side view; inset: top view (F); completely fused cup-shaped cotyledon, side view; inset: top view (G). (H) Percentages of seedlings in phenotype classes. Difference between *pin1* and WT, between *pin1*;*6* and *pin1*, between UBQ10::amiPIN6-10;*pin1* and *pin1*, between *pin1*;*6*;*8* and *pin1*;*6*, and between *pin1;5;6;8* and *pin1;6;8*, and between PIN6::iaaL;*pin1* and *pin1* was significant at $P<0.001$ (***) by Kruskal-Wallis and Mann-Whitney test with Bonferroni correction. Sample population sizes: WT, 50; *pin2*, 50; *pin3*, 50; *pin4*, 50; *pin5*, 50; *pin6*, 50; UBQ10::amiPIN6-5, 50; UBQ10::amiPIN6-10, 50; *pin7*, 50; *pin8*, 50; PIN6::iaaL-15, 50; PIN6::iaaL-12, 50; *pin1*, 61; *pin1*;*2*, 53 *pin1*;*3*, 45; *pin1*;*4*, 49; *pin1*;*5*, 47; *pin1*;*6*, 56; UBQ10::amiPIN6-5;*pin1*, 50; UBQ10::amiPIN6-10;*pin1*, 74; *pin1*;*7*, 49; *pin1*;*8*, 62; *pin1*;*5*;*6*, 54; *pin1*;*6*;*8*, 52; *pin1*;*5*;*6*;*8*, 50; PIN6::iaaL-15;*pin1*, 53; PIN6::iaaL-12;*pin1*, 51. Bars: (A-C,E) 1 mm; (D,F) 0.4 mm; (G) 0.25 mm.

2.2.2 PIN6 expression in leaf development

Double-mutant analysis suggests functions for *PIN6* in vein patterning (Figure 2.1; see 2.3 Discussion). We thus asked whether *PIN6* was expressed during vein formation. To address this question, we imaged expression of a functional (Table 2.1) translational fusion of *PIN6* to GFP driven by the *PIN6* promoter (PIN6::PIN6:GFP). During leaf development, PIN6::PIN6:GFP expression was initiated in broad subepidermal domains that narrowed to sites of vein formation (Figure 2.3A-2.3H), suggesting PIN6 expression during vein formation. Expression of PIN6::PIN6:GFP was recapitulated by expression of a PIN6::YFPnuc transcriptional fusion (*PIN6* promoter driving expression of a nuclear YFP) (Figure 2.4A-2.4E), which overlapped with expression of PIN1::PIN1:CFP (Gordon et al. 2007) in leaf subepidermal tissues (Figure 2.3I). In *pin1*, PIN6::PIN6:GFP expression remained confined to subepidermal tissues, but expression was weaker (Figure 2.3J-2.3L).

A *PIN6* translational fusion localizes to the ER in tobacco suspension cells (Mravec et al. 2009). To determine PIN6 subcellular localization in Arabidopsis leaves, we quantified degree of colocalization between expression of PIN6::PIN6:GFP and expression of ER, or PM, markers. Expression of PIN6::PIN6:GFP correlated with expression of ER, but not PM, markers (Figure 2.3M-2.3T and Figure 2.5), suggesting ER-localization of PIN6 in vein development.

2.2.3 Genetic interaction between *PIN1*, *PIN5*, *PIN6* and *PIN8* in vein patterning

PIN6 belongs to a subfamily of proteins that includes the ER-localized PIN5 and PIN8 auxin transporters (Mravec et al. 2009; Ganguly et al. 2010; Bosco et al. 2012; Ding et al. 2012). Thus, we asked whether frequencies of vein pattern phenotypes in *pin1*;*6* were affected by additional mutation of *PIN5* or *PIN8*. While *pin8* shifted the distribution of *pin1*;*6* phenotypes towards stronger classes, *pin5* partially normalized *pin1*;*6*;*8* phenotype spectrum (Figure 2.6). *pin5* and *pin8* had similar effects in seedlings (Figure 2.2): (1) complete penetrance of cotyledon defects in *pin1*;*6*;*8* vs. ~95% in *pin1*;*6*; (2) ~95% penetrance of the cup-shaped cotyledon phenotype in *pin1*;*6*;*8* vs. ~60% in *pin1*;*6*; and (3) partial normalization of cotyledon defects of *pin1*;*6*;*8* by *pin5*.

2.2.4 PIN8 expression in leaf development

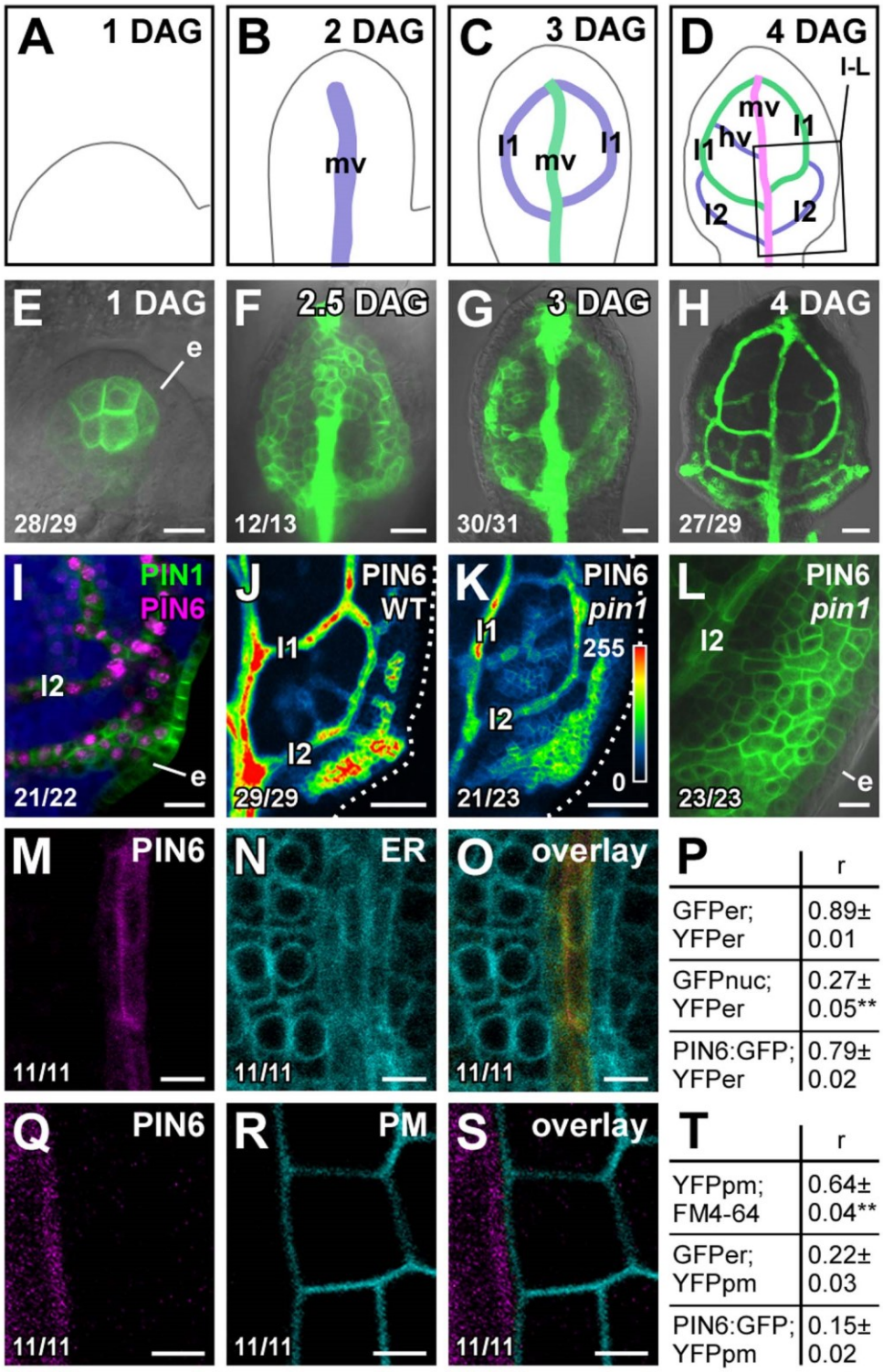

Figure 2.3. PIN6 expression in leaf development. (A-O,Q-S) Top right: leaf age in days after germination (DAG), marker and genotype. Bottom left: reproducibility index. First leaves. (A-D) Midvein, loops and minor veins differentiate progressively later in the same region of the

developing leaf, and loops and minor veins differentiate in a tip-to-base sequence during leaf development (Mattsson et al. 1999; Sieburth 1999; Scarpella et al. 2004); purple, green and magenta: successive stages of vein differentiation. Box in (D) illustrates position of close-ups in (I-L). (E-O,Q-S) Confocal laser scanning microscopy with (E-H,L) or without (I-K,M-O,Q-S) transmitted light. (E-H) PIN6::PIN6:GFP expression. (I) Expression of PIN6::YFPnuc and PIN1:PIN1:CFP at 4 DAG; blue: chlorophyll. (J-L) PIN6::PIN6:GFP expression in WT (J) and *pin1* (K,L) at 4 DAG. LUT (in K) visualizes expression levels. Dotted line: leaf outline. (M-O,Q-S) Expression of PIN6::PIN6:GFP (M,Q), 35S::YFPer (N), 35S::LTI6B:YFP (R) and respective overlays displayed with a dual-channel LUT (Demandolx and Davoust 1997) (O,S): prevalence of cyan over colocalized magenta signal is shown in green, opposite in red, and colocalized cyan and magenta signals of equal intensity in yellow. (P,T) Quantification of colocalized GFP and YFP signals (as mean ± SE of Manders' coefficient 'r') in populations (n=11) of positive controls: J1721::GFPer;35S::YFPer (P), 35S::YFPpm;FM4-64 (T); negative controls: ATHB8::GFPnuc;35S::YFPer (P), J1721::GFPer; 35S::YFPpm (T); and samples: PIN6::PIN6:GFP;35S::YFPer (P), PIN6::PIN6:GFP; 35S::YFPpm (T). (P) Difference between negative control and positive control, and between negative control and sample was significant at P<0.01 (**) by one-way ANOVA and Tukey's test. (T) Difference between positive control and negative control, and between positive control and sample was significant at P<0.01 (**) by one-way ANOVA and Tukey's test. e, epidermis; hv, minor vein; l1, first loop; l2, second loop; mv, midvein. Bars: (E,I,L) 10 µm; (F,G) 20 µm; (H,J,K) 50 µm; (M-O) 5 µm; (Q-S) 2.5 µm.

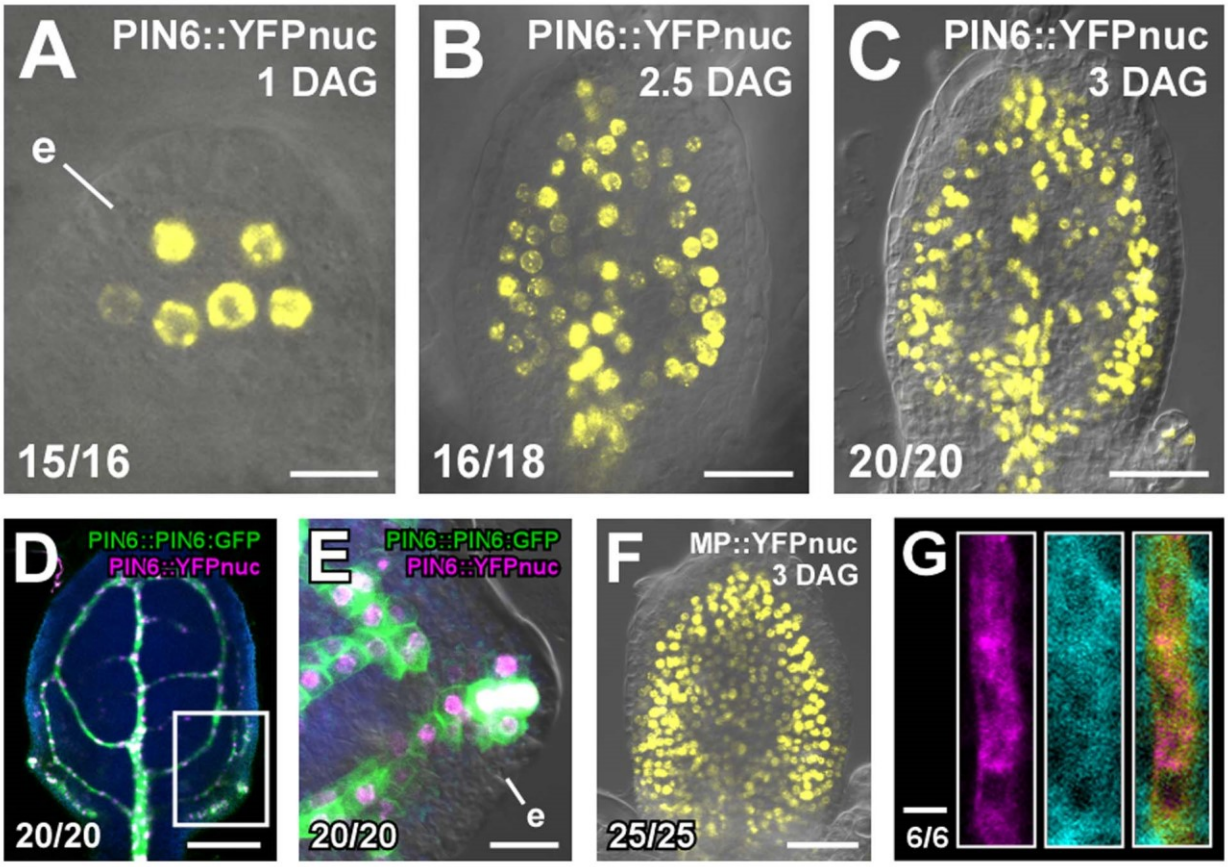

Figure 2.4. Expression of PIN6, PIN8 and *MP* in leaf development. (A-G) Confocal laser scanning microscopy with (A-C,E,F) or without (D,G) transmitted light. Top right: reporters and leaf age in days after germination (DAG). Bottom left: reproducibility index. First leaves. (D,E) Blue: chlorophyll. (E) Close-up of area as boxed in D. (G) Expression at 3.25 DAG of PIN8::PIN8:GFP (left), staining by ER-Tracker Blue-White DPX (centre) and their overlay displayed with a dual-channel LUT (defined in Figure 2.3) (right). e, epidermis. Bars: (A,B) 10 µm; (C,F) 50 µm; (D) 100 µm; (E) 20 µm; (G) 2 µm.

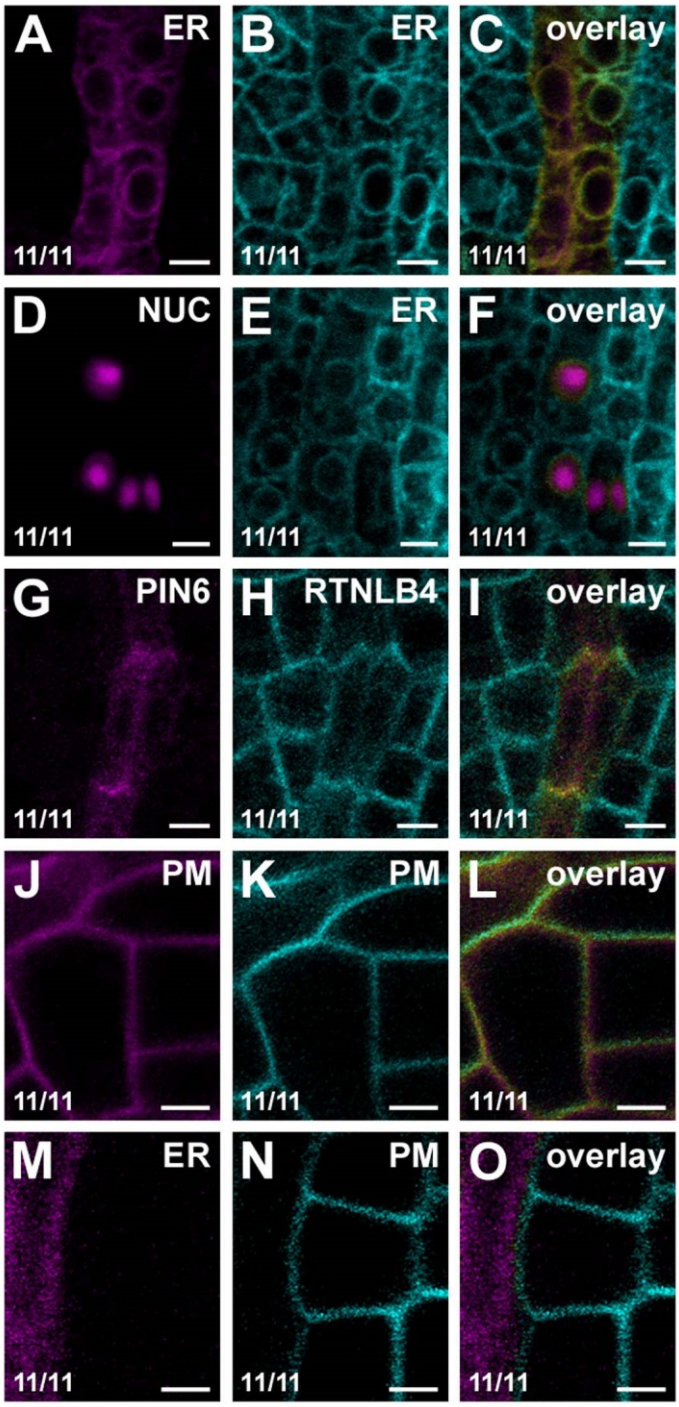

Figure 2.5. Colocalization analysis of PIN6 with endoplasmic-reticulum or plasma-membrane markers. (A-O) Top right: marker. Bottom left: reproducibility index. Confocal laser scanning microscopy. First leaves. Expression of J1721::GFPer (A,M), 35S::YFPer (B,E), ATHB8::GFPnuc (D), PIN6::PIN6:GFP (G), 35S::RTNLB4:YFP (H), 35S::YFPpm (J,N), FM4-64 (K) and respective overlays displayed with a dual-channel LUT (defined in Figure 2.3) (C,F,I,L,O). Bars: (A-L) 5 µm; (M-O) 2.5 µm.

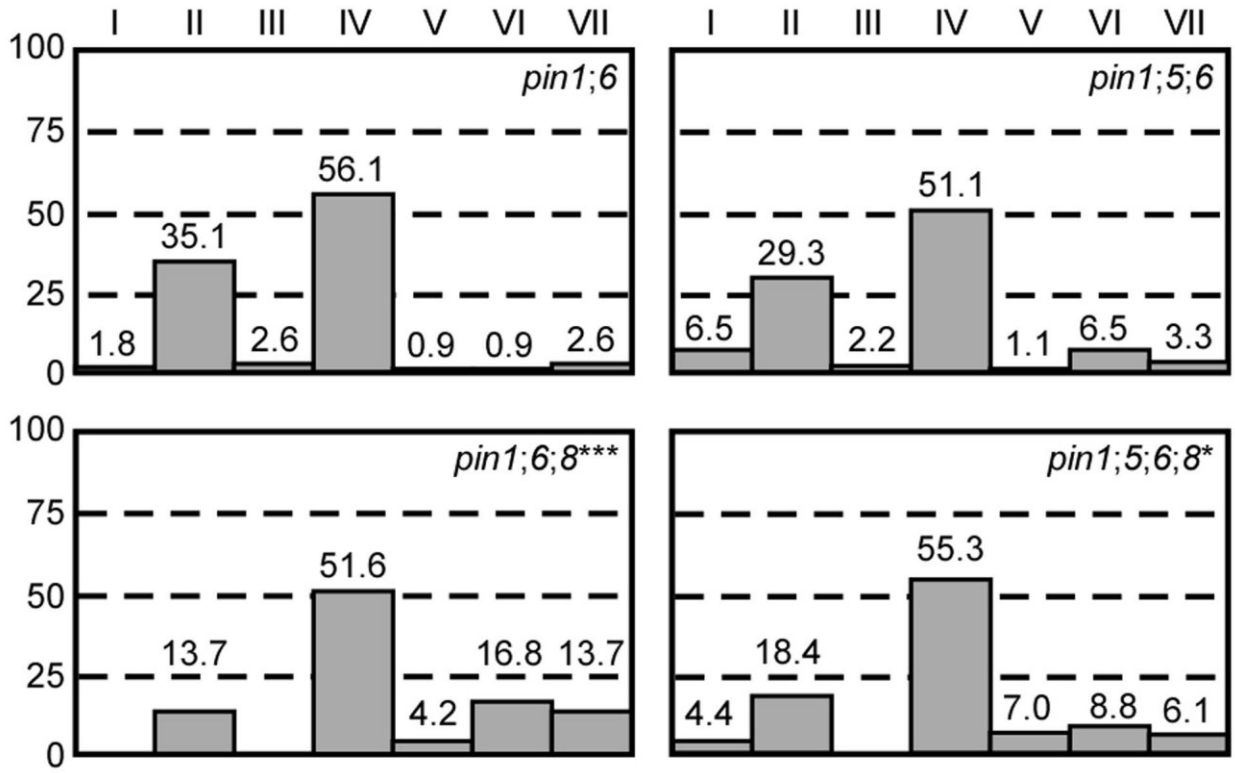

Figure 2.6. Genetic interaction between *PIN1*, *PIN5*, *PIN6* and *PIN8* in vein patterning. Percentages of leaves in phenotype classes (defined in Figure 2.1). Difference between *pin1*;*6*;*8* and *pin1*;*6*, and between *pin1*;*5*;*6*;*8* and *pin1*;*6*;*8* was significant at $P<0.05$ (*) or $P<0.001$ (***) by Kruskal-Wallis and Mann-Whitney test with Bonferroni correction. Sample population sizes: *pin1*;*6*, 114; *pin1*;*5*;*6*, 92; *pin1*;*6*;*8*, 95; *pin1*;*5*;*6*;*8*, 114.

Triple-mutant analysis suggests functions for *PIN8* in vein patterning (Figure 2.6; see 2.3 Discussion). We thus asked whether *PIN8* was expressed, as *PIN1* (Scarpella et al. 2006; Wenzel et al. 2007), *PIN5* (Mravec et al. 2009) and *PIN6* (Figure 2.3 and Figure 2.4A-2.42E), during vein development. To address this question, we imaged expression of a functional (Table 2.1) translational fusion of *PIN8* to GFP driven by the *PIN8* promoter (PIN8::PIN8:GFP). Expression of PIN8::PIN8:GFP was restricted to narrow sites of vein formation in both WT and *pin1*;*6* (Figure 2.7A-2.7E), suggesting PIN8 expression in vein development, a conclusion further supported by expression of a PIN8::YFPnuc transcriptional fusion (*PIN8* promoter driving expression of a nuclear YFP) (Figure 2.7H-2.7K).

In pollen, *PIN8* translational fusions localize to the ER (Bosco et al. 2012; Ding et al. 2012). To determine PIN8 subcellular localization in leaves, we quantified degree of colocalization between expression of PIN8::PIN8:GFP and staining by the glibenclamide-derived ER-Tracker Red dye, which selectively stains the ER (e.g., (Tan et al. 2006; Don et al. 2007; Yamasaki et al. 2007)). Expression of PIN8::PIN8:GFP correlated with staining by ER-Tracker Red (Figure 2.7F) (mean Manders' coefficient 'r' ± SE: 0.82 ± 0.03; *n*=10) and overlapped with staining by the dapoxyl-derived ER-Tracker Blue-White DPX dye (Cole et al. 2000) (Figure 2.4G), suggesting ER-localization of PIN8 in vein development.

2.2.5 Necessary functions of *PIN5*, *PIN6* and *PIN8* in vein network formation

Single mutation of *PIN5*, *PIN6* or *PIN8* had no effect on vein patterns (Figure 2.1). Thus, to test whether a function in vein patterning could be assigned to ER-localized PIN proteins in the presence of PIN1-mediated intercellular auxin-transport, we analyzed vein patterns of combinations of *pin5*, *pin6* and *pin8*. Double and triple mutants had WT vein patterns (sample population sizes: WT, 26; *pin5*;*6*, 22; *pin5*;*8*, 24; *pin6*;*8*, 39; *pin5*;*6*;*8*, 30), but *pin6*;*8* had a more complex vein network, a defect that was normalized by *pin5* (Figure 2.8A-2.8D).

We next asked whether *pin6*;*8* defects in vein network formation were associated with changes in auxin response levels. To address this question, we imaged expression of the DR5rev::YFPnuc auxin response reporter (Heisler et al. 2005). In subepidermal tissues of WT leaves, DR5rev::YFPnuc was strongly expressed at sites of vein formation (Figure 2.8E); in subepidermal tissues of *pin6*;*8* leaves, DR5rev::YFPnuc expression was weaker (Figure 2.8F), a

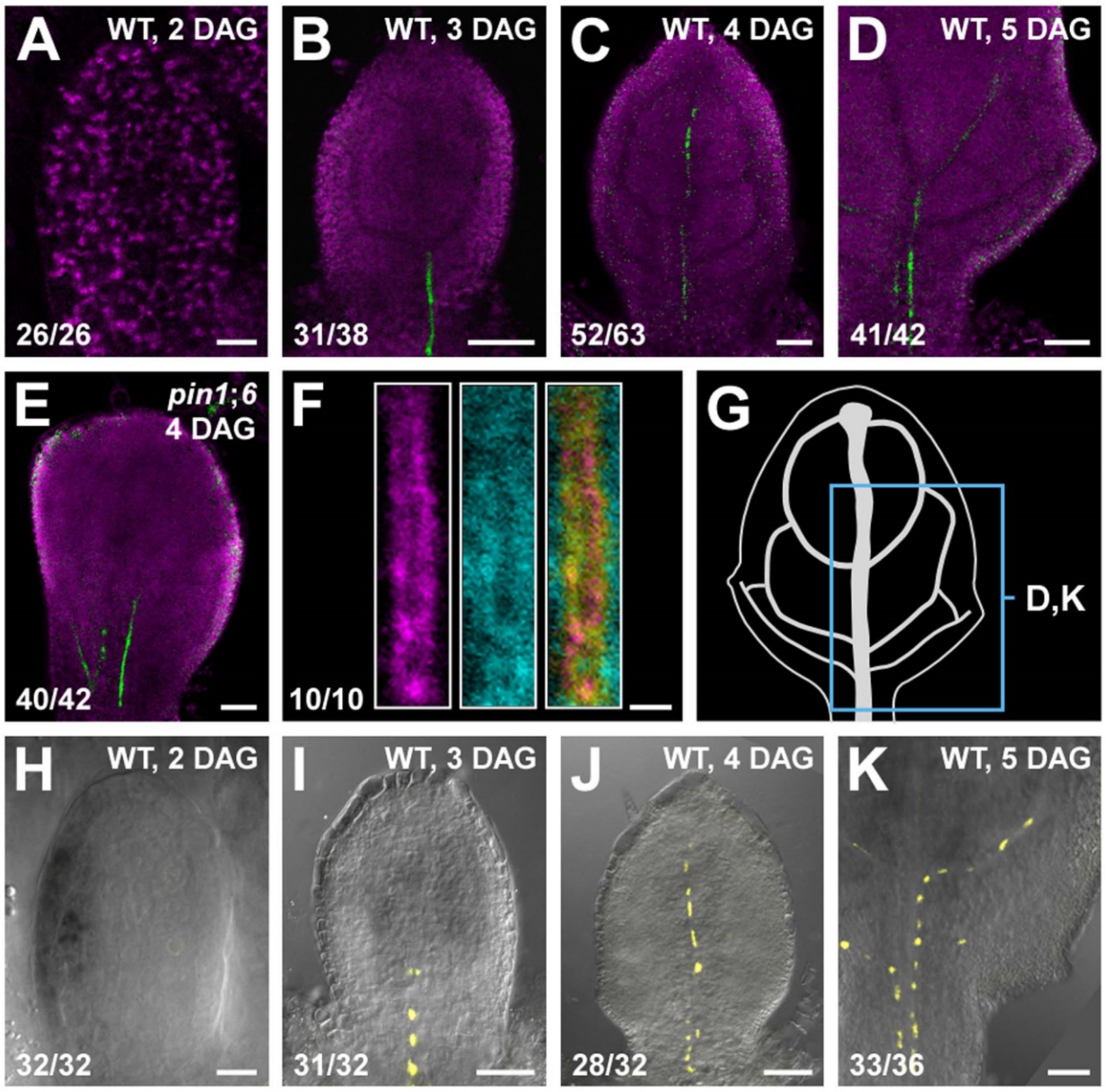

Figure 2.7. PIN8 expression in leaf development. (A-K) Top right: genotype, leaf age in days after germination (DAG). Bottom left: reproducibility index. Confocal laser scanning microscopy without (A-F) or with (H-K) transmitted light; first leaves. (A-E) Green: PIN8::PIN8:GFP expression; magenta: chlorophyll. (F) Expression at 3.25 DAG of PIN8::PIN8:GFP (left), staining by ER-Tracker Red (centre) and their overlay displayed with a dual-channel LUT (defined in Figure 2.3) (right). (G) 5-DAG first leaf illustrating positions of close-ups in (D) and (K). (H-K) PIN6::YFPnuc expression. Bars: (A,H) 10 μm; (B-E,I-K) 50 μm; (F) 2 μm.

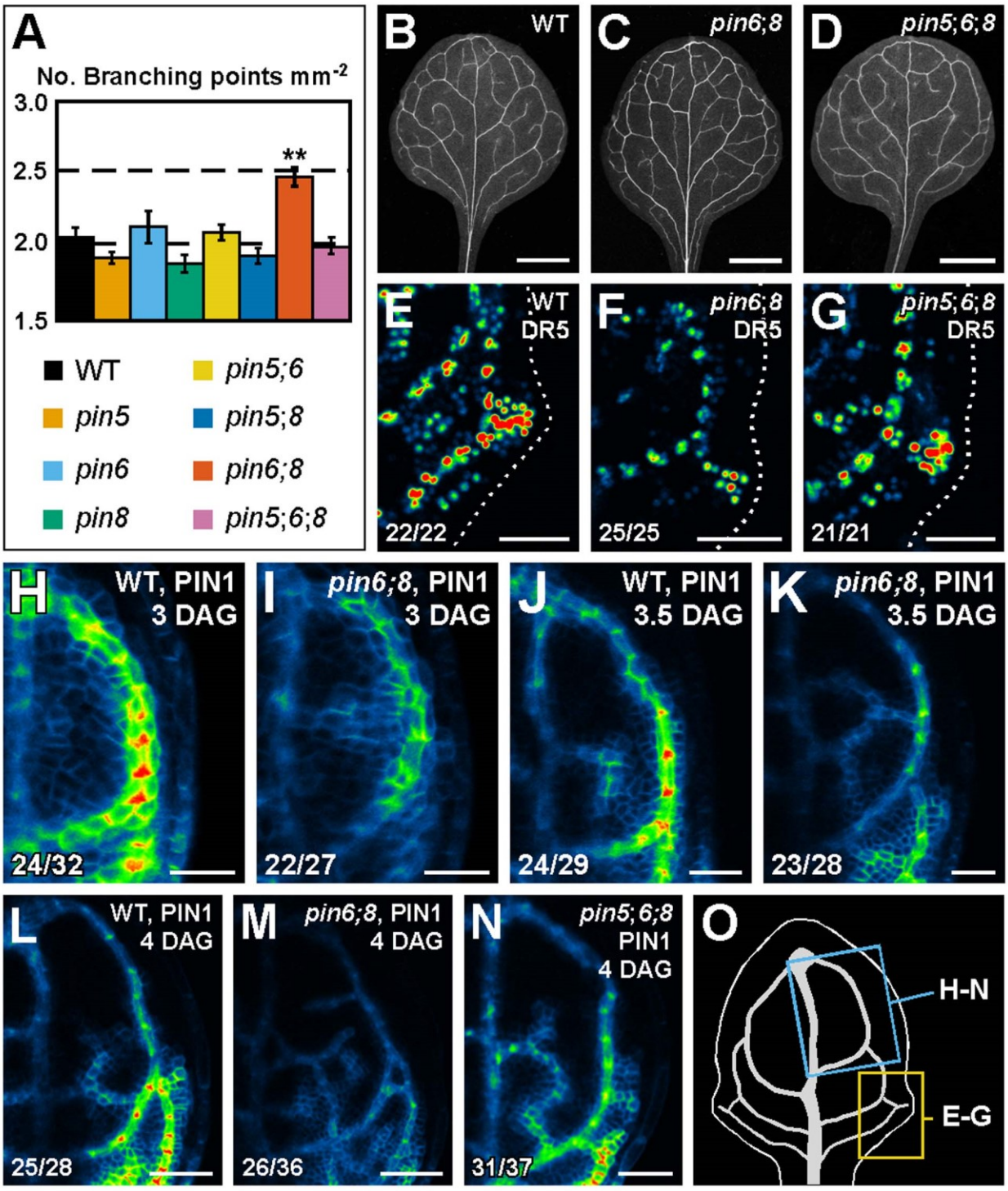

Figure 2.8. Necessity of *PIN5*, *PIN6* and *PIN8* for vein network formation. (A) Vein network complexity as mean ± SE number of vein branching points per first-leaf area unit in mm^2 (Candela et al. 1999). Difference between *pin6*;*8* and all other genotypes was significant at $P<0.01$ (**) by one-way ANOVA and Tukey's test. Sample population sizes: WT, 30; *pin5*, 30; *pin6*, 30; *pin8*, 27; *pin5*;*6*, 28; *pin5*;*8*, 28; *pin6*;*8*, 28; *pin5*;*6*;*8*, 28. (B-N) Top right: genotype,

markers and leaf age in days after germination (DAG). Bottom left: reproducibility index. (B-D) Dark-field illumination of cleared mature first leaves. (E-N) Confocal laser scanning microscopy; first leaves. LUT (in Figure 2.3K) visualizes expression levels. (E-G) DR5rev::YFPnuc expression, 4 DAG. Dotted line: leaf outline. (H-N) PIN1::PIN1:YFP expression. (O) 4-DAG first leaf illustrating positions of close-ups in (E-G) and (H-N). Bars: (B-D) 1.5 mm; (E-G,L-N) 50 μm; (H-K) 25 μm.

defect that was normalized by *pin5* (Figure 2.8G).

We then asked whether *pin6*;*8* defects in auxin response levels and vein network formation were associated with changes in auxin-responsive PIN1 expression (Heisler et al. 2005; Vieten et al. 2005; Nemhauser et al. 2006; Scarpella et al. 2006). To address this question, we imaged expression of PIN1::PIN1:YFP (Xu et al. 2006) in the leaf area enclosed by the first loop. In both WT and *pin6*;*8*, PIN1::PIN1:YFP expression was initiated in broad domains that narrowed to sites of vein formation (Figure 2.8H-2.8M). However, in *pin6*;*8* PIN1::PIN1:YFP expression was weaker (Figure 2.8H-2.8M), vein-associated domains of PIN1::PIN1:YFP expression became visible at earlier time-points (Figure 2.8H and 2.8I), and at each time point we observed more vein-associated domains of PIN1::PIN1:YFP expression (Figure 2.8H-2.8M). Defects in PIN1::PIN1:YFP expression levels of *pin6*;*8* were normalized by *pin5* (Figure 2.8N). In summary, *pin6*;*8* had defects in expression of DR5 and PIN1 and in formation of vein networks, and such defects were normalized by *pin5*.

2.2.6 Sufficient functions of *PIN5*, *PIN6* and *PIN8* in vein network formation

We next asked whether *PIN6* function was sufficient to control expression of DR5 and PIN1 and formation of vein networks. To address this question, we expressed the *PIN6* cDNA by the promoter of *RIBOSOMAL PROTEIN S5A* (AT3G11940) (RPS5A::PIN6) and by the promoter of *MONOPTEROS* (AT1G19850) (MP::PIN6), each highly active in developing leaves (Weijers et al. 2001) (Figure 2.4F). Expression of the auxin-responsive markers DR5rev::YFPnuc, ATHB8::CFPnuc (Donner et al. 2009) and PIN1::PIN1:YFP was stronger in leaves of RPS5A::PIN6 and MP::PIN6 (Figure 2.9A-2.9G). Furthermore, in both these backgrounds lateral domains of PIN1::PIN1:YFP expression often failed to join distal veins (Figure 2.9E-2.9G), defects that correlated with the simpler, open vein networks of the mature leaves (Figure 2.9I-2.9M).

We then asked whether ectopic expression of *PIN8* or *PIN5* had any effect on vein network formation. To address this question, we analyzed vein patterns of plants expressing the cDNA of *PIN8* or *PIN5* by the *MP* promoter (MP::PIN8 or MP::PIN5, respectively). We found that MP::PIN8 leaves had simpler, open vein networks and that MP::PIN5 leaves had a more complex vein network (Figure 2.9I and 2.9N-2.9Q).

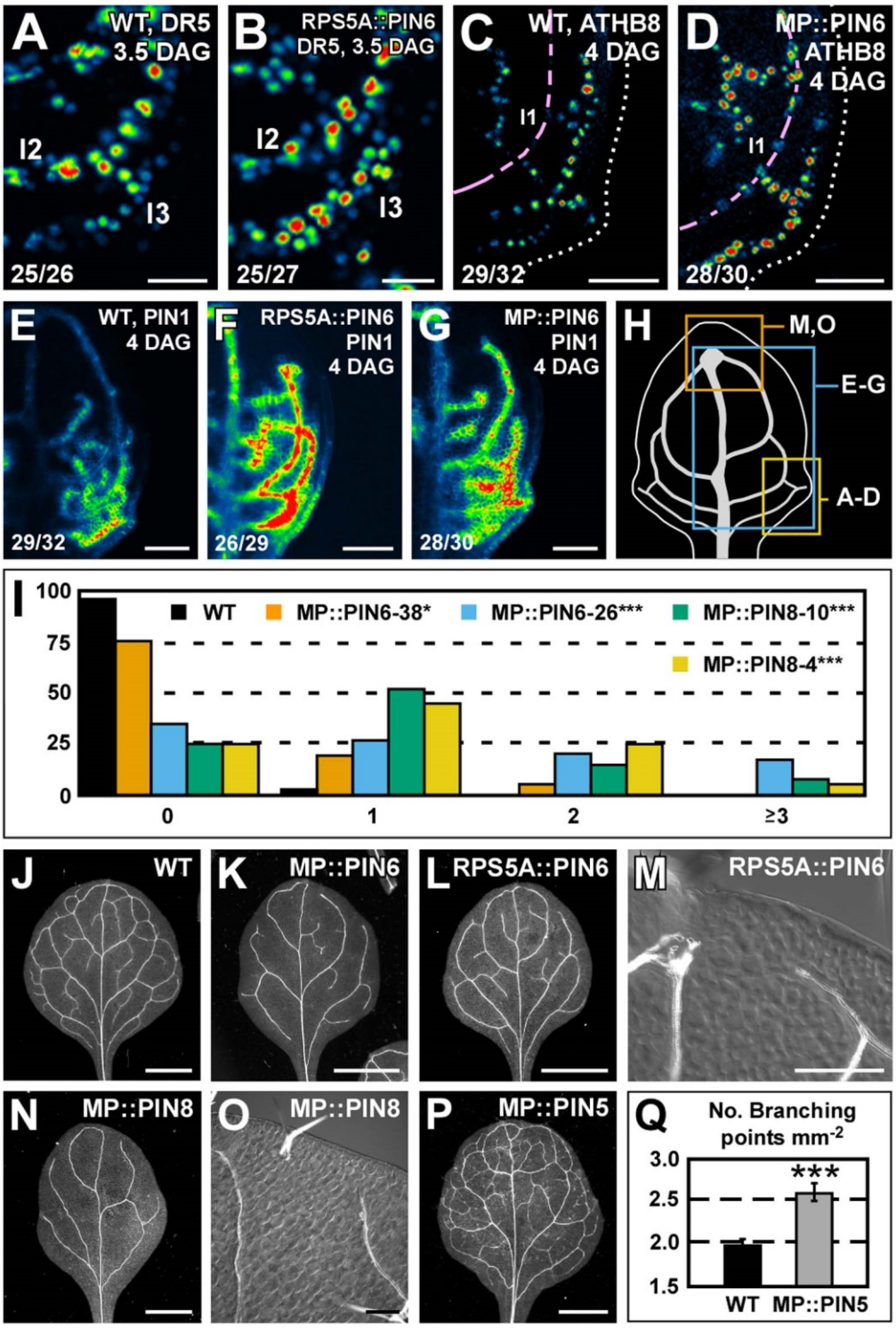

Figure 2.9. Sufficiency of *PIN5*, *PIN6* and *PIN8* for vein network formation. (A-G,J-P) Top right: genotype, markers and leaf age in days after germination (DAG). Bottom left: reproducibility index. (A-G) Confocal laser scanning microscopy; first leaves. LUT (in Figure

2.3K) visualizes expression levels. (J-P) Dark-field (J-L,N,P) or differential-interference-contrast (M,O) illumination of cleared mature first leaves. (A,B) DR5rev::YFPnuc expression. (C,D) ATHB8::CFPnuc expression. Magenta line connects nuclei in the first loop (l1). Dotted line: leaf outline. (E-G) PIN1::PIN1:YFP expression. (H) 4-DAG first leaf illustrating positions of close-ups in (A-D), (E-G) and (M,O). (I) Percentage of first leaves with 0, 1, 2 or ≥3 open loops. Difference between MP::PIN6 and WT, and between MP::PIN8 and WT was significant at $P<0.05$ (*) or $P<0.001$ (***) by Kruskal-Wallis and Mann-Whitney test with Bonferroni correction. Sample population sizes: WT, 43; MP::PIN6-38, 40; MP::PIN6-26, 42; MP::PIN8-10, 40; MP::PIN8-4, 40. (Q) Vein network complexity as mean ± SE number of vein branching points per first-leaf area unit in mm^2 (Candela et al. 1999). Difference between MP::PIN5 and WT was significant at $P<0.001$ (***) by unpaired, two-tailed *t*-test. Sample population sizes: WT, 28; MP::PIN5, 28. l1, first loop; l2, second loop; l3, third loop. Bars: (A,B) 25 μm; (C-G) 50 μm; (J-L,N,P) 1.5 mm; (M,O) 0.2 mm.

In summary, ectopic *PIN6* expression was sufficient to control expression of DR5 and PIN1. Furthermore, ectopic expression of *PIN6* or *PIN8*, on the one hand, and of *PIN5*, on the other, had opposite effects on vein network formation.

2.2.7 Simulation of *pin1*;*6* defects by reduction of auxin levels in *pin1*

Weaker expression of auxin responsive markers in *pin6*;*8* leaves and stronger expression of auxin responsive markers in leaves of RPS5A::PIN6 and MP::PIN6 suggest that PIN6-mediated auxin transport increases intracellular levels of biologically active auxin (see 2.3 Discussion). If this were the case, *pin1*;*6* phenotype spectrum might be mimicked by expressing in *pin1* the bacterial gene *iaaL*, which decreases levels of free auxin by its conjugation to lysine (Romano et al. 1991; Jensen et al. 1998). Expression of PIN6::iaaL (*PIN6* promoter driving expression of iaaL) in *pin1* mimicked the phenotype spectrum of *pin1*;*6* leaves (Figure 2.10) and cotyledons (Figure 2.2), a finding that is consistent with the hypothesis that PIN6-mediated intracellular auxin transport increases auxin levels.

2.3 Discussion

The mechanisms that control the patterning of vein networks of plant leaves have long fascinated biologists and mathematicians. Varied evidence has increasingly been accumulating that supports an inductive and orienting role for the transport of the plant signal auxin in leaf vein patterning (Sachs 1981; Gersani 1987; Sachs 1989, 1991a; Mattsson et al. 1999; Sieburth 1999; Scarpella et al. 2006; Wenzel et al. 2007), but molecular details have remained unclear. Here we show that the vein network of the Arabidopsis leaf is patterned by two distinct and convergent auxin-transport pathways: an intercellular pathway mediated at the plasma membrane (PM) by the PIN1 auxin transporter and an intracellular pathway mediated at the endoplasmic reticulum (ER) by the PIN6, PIN8 and PIN5 auxin transporters. While a role for other families of auxin transporters (Geisler and Murphy 2006; Barbez et al. 2012; Peret et al. 2012) in vein patterning is by no means precluded, our results suggest a new, unsuspected level of control of vein patterning by PIN-mediated auxin transport, one with repercussions on patterning of other plant features.

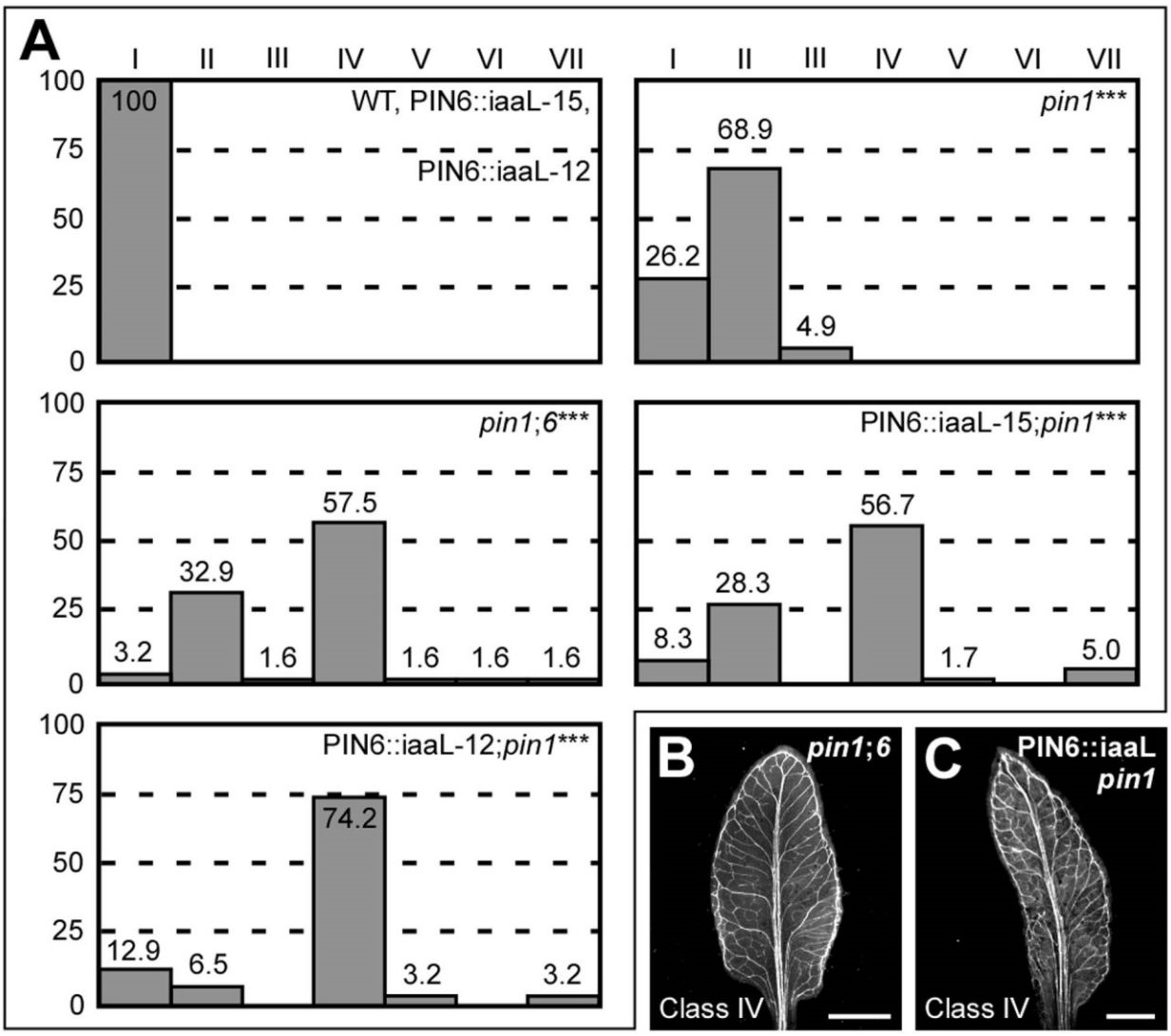

Figure 2.10. Control of *PIN1*-dependent vein patterning by intracellular auxin levels. (A) Percentages of leaves in phenotype classes (defined in Figure 2.1). Difference between *pin1* and WT, between *pin1*;*6* and *pin1*, and between PIN6::iaaL;*pin1* and *pin1* was significant at $P<0.001$ (***) by Kruskal-Wallis and Mann-Whitney test with Bonferroni correction. Sample population sizes: WT, 50; PIN6::iaaL-15, 50; PIN6::iaaL-12, 50; *pin1*, 61; *pin1*;*6*, 61; PIN6::iaaL-15;*pin1*, 60; PIN6::iaaL-12;*pin1*, 62. (B,C) Dark-field illumination of cleared mature first leaves. Top right: genotype. Bottom left: phenotype class. Bars: (B,C) 2 mm.

The localization of PIN1 to the PM (Galweiler et al. 1998) and of PIN6 to the ER together with the appearance in *pin1*;*6* of vein pattern defects that exceed the sum of the single-mutant defects suggest that *PIN1* and *PIN6* act in distinct auxin-transport pathways whose functions converge on vein patterning. By contrast, the overlapping subcellular localizations of PIN6 and PIN8 (Mravec et al. 2009; Ganguly et al. 2010; Bosco et al. 2012; Ding et al. 2012) together with the purely quantitative enhancement of *pin1*;*6* vein pattern defects by *pin8* suggest redundant function of *PIN6* and *PIN8* in *PIN1*-dependent vein patterning. Further, the overlapping subcellular localization of PIN8 (Mravec et al. 2009; Ganguly et al. 2010; Bosco et al. 2012; Ding et al. 2012) and PIN5 (Mravec et al. 2009; Ganguly et al. 2010; Ding et al. 2012) together with the partial normalization of *pin1*;*6*;*8* vein pattern defects by *pin5* suggest antagonistic functions of *PIN8* and *PIN5* in *PIN1*/*PIN6*-dependent vein patterning. The interaction between the intercellular auxin-transport pathway controlled by PIN1 and the intracellular auxin-transport pathway controlled by PIN6, PIN8 and PIN5 is relevant for at least two other patterning events, separation of cotyledons and of leaves, and might have implications for other developmental processes. The redundancy between *PIN6* and *PIN8* and the antagonism between *PIN8* and *PIN5* are, however, independent of PIN1-mediated intercellular auxin transport: in the presence of *PIN1* function, *PIN6* and *PIN8* redundantly control vein network formation, and such redundant functions are antagonized by *PIN5*. Redundant functions of *PIN6* and *PIN8* and antagonistic functions of *PIN5*, as inferred from loss-of-function data, are also consistent with gain-of-function evidence: ectopic *PIN8* expression induces vein pattern defects similar to those induced by ectopic *PIN6* expression and opposite to those of *pin6*;*8*, suggesting that *PIN8* can supply vein patterning functions similar to those of *PIN6*; and ectopic *PIN5* expression induces vein pattern defects opposite to those induced by ectopic expression of *PIN6* or *PIN8* and similar to those of *pin6*;*8*, suggesting that *PIN5* can supply vein patterning functions opposite to those of *PIN6* and *PIN8*. The internally consistent relation between the effects of loss of function of *PIN6*, *PIN8* and *PIN5* and the effects of gain of function of these genes is not limited to vein patterning but extends to auxin response: auxin response levels are decreased by simultaneous mutation of *PIN6* and *PIN8* and by ectopic expression of *PIN5* (Mravec et al. 2009) and increased by ectopic expression of *PIN6* or *PIN8* (Ding et al. 2012) and by mutation of *PIN5* (Mravec et al. 2009). Thus, the genetic interaction between *PIN5*, *PIN6* and *PIN8* might reflect general properties of

the mechanism with which these proteins function, a conclusion that is also supported by the antagonistic functions of *PIN8* and *PIN5* in a process unrelated to vein patterning such as pollen development (Ding et al. 2012). The most parsimonious explanation for the antagonistic interaction between PIN6/PIN8 and PIN5, which transports auxin from the cytoplasm to the ER lumen (Mravec et al. 2009), is that PIN6 and PIN8 transport auxin from the ER lumen to the cytoplasm or to the nucleus, whose envelope is continuous with the ER membrane (Graumann and Evans 2011; Oda and Fukuda 2011) (Figure 2.11C). This scenario is also supported by the observation that reducing auxin levels in *pin1* leads to *pin1*;*6* characteristic defects, and is consistent with higher levels of auxin measured in *PIN8* overexpressors (Bosco et al. 2012; Ding et al. 2012) and *pin5* mutants (Mravec et al. 2009). Alternatively, or in addition, PIN6, PIN8 and PIN5 could all transport in the same direction but have different affinities for auxins or auxin conjugates with different, even opposing, developmental functions (reviewed in (Ludwig-Muller 2012)) (Figure 2.11D).

Our data suggest that auxin transported by PIN6 and PIN8 increases levels of auxin-responsive PIN1 expression during vein formation (Figure 2.11A). In *pin6*;*8*, low auxin levels at sites of vein formation could accelerate formation of narrow vein-associated domains of PIN1 expression, thus resulting in high-complexity vein networks (Sachs 1981; Scarpella et al. 2004; Rolland-Lagan and Prusinkiewicz 2005; McKown and Dengler 2009; Wabnik et al. 2010). Conversely, in leaves ectopically expressing *PIN6*, high auxin levels at sites of vein formation could hinder or prevent formation and connection of vein-associated PIN1-expression domains, thus resulting in simple, open vein networks (Sachs 1970, 1981; Scarpella et al. 2004; Prusinkiewicz et al. 2009; Wabnik et al. 2010; Balla et al. 2011). Alternatively, PIN6/PIN8-mediated auxin transport could control vein network formation exclusively through PIN1-independent pathways; defects in auxin response or PIN1 expression would then be consequence, rather than cause, of defective vein-network formation (Figure 2.11B). In any case, the synthetic enhancement of *pin1* defects by *pin6* and *pin6*;*8*, as opposed to the epistasis of *pin6*;*8* to *pin1*, suggests vein patterning functions of PIN6/PIN8-mediated intracellular auxin transport beyond regulation of PIN1 expression or of intercellular auxin transport mediated by PM-localized PIN proteins (Figure 2.11A and 2.11B). We can probably exclude that such functions of PIN6 and PIN8 require physical interaction with PIN1 because PIN1 and PIN6/PIN8 localize to different

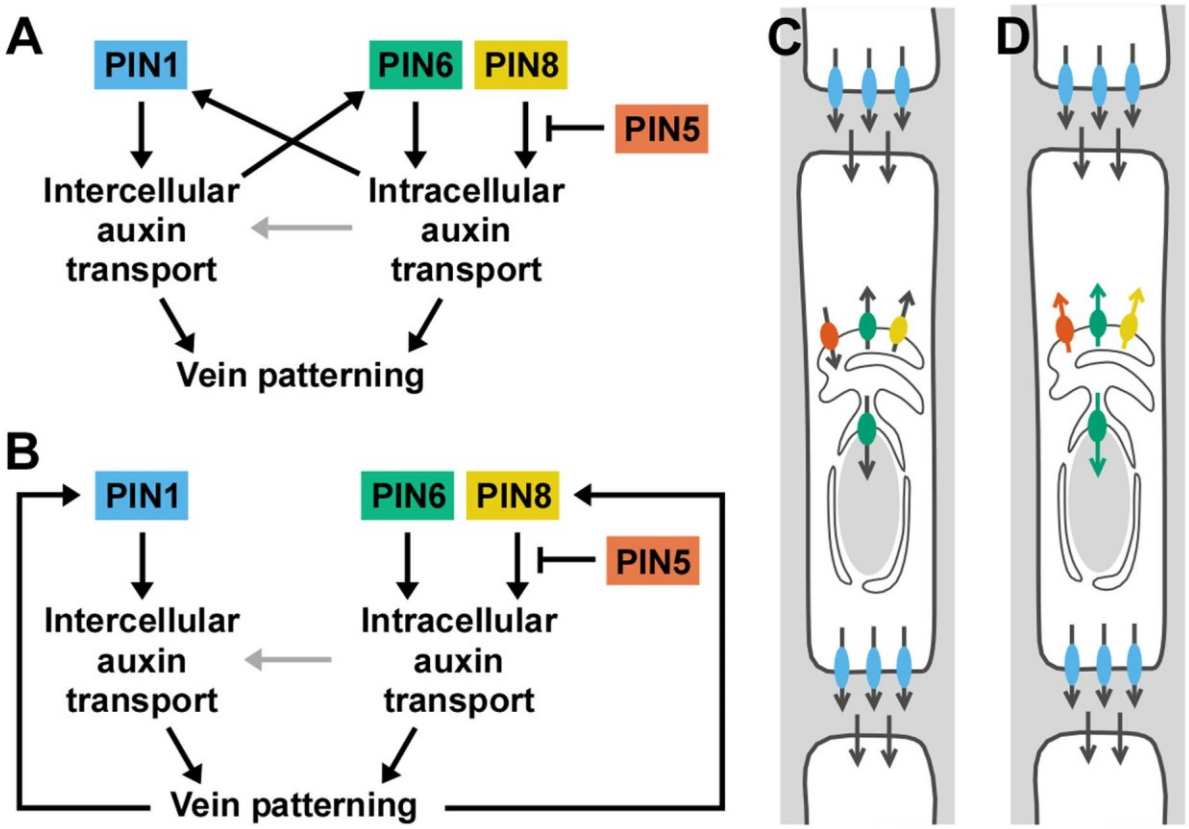

Figure 2.11. Summary and interpretation. (A,B) Two potential, non-mutually-exclusive regulatory circuits for *PIN1* and *PIN5*/*PIN6*/*PIN8* in vein patterning. Arrows indicate positive regulation; blunt-ended lines indicate negative regulation. Distinct functions of PIN1-mediated intercellular auxin transport and of PIN5/PIN6/PIN8-mediated intracellular auxin transport converge on vein patterning. Additionally, PIN1-mediated intercellular auxin transport could control vein patterning through regulation of PIN6 expression, and PIN5/PIN6/PIN8-mediated intracellular auxin transport could control vein patterning through regulation of PIN1 expression (A). Alternatively, vein patterning could feed back on expression of PIN1 and PIN6 (B). PIN1-independent functions of PIN5/PIN6/PIN8-mediated intracellular auxin transport in vein patterning could include intercellular auxin transport by a mechanism non-homologous to that used by PM-localized PIN proteins (Wabnik et al. 2011b) (grey arrows). (C,D) Localization of PIN1 (blue) at the basal plasma membrane and of PIN5 (orange), PIN6 (green) and PIN8 (yellow) at the endoplasmic reticulum/nuclear envelope (ER/NE) of vascular cells. For simplicity, PIN5, PIN6 and PIN8 are shown to be expressed in the same cell, only PIN6 is shown to be also localized at the NE, and localization of AUX/LAX (Peret et al. 2012), ABCB/PGP/MDR (Geisler and Murphy 2006) and PILS (Barbez et al. 2012) auxin transporters is not shown. Arrows indicate presumed directions of auxin transport. Antagonism between *pin5* and *pin6*;*8* in vein patterning could reflect opposite directions in which PIN5 and PIN6/PIN8 transport auxin (C), different abilities of PIN5 and PIN6/PIN8 to transport different auxins or auxin conjugates (orange, green and yellow arrows) (D; for simplicity, the mirror-image scenario, i.e. transport to the ER/NE lumen, is not shown), or varied combinations of the two. See text for additional details.

cellular compartments and because *PIN1*/*pin1*;*pin6*/*pin6* lacks defects in cotyledons and vein patterns (n>50), defects that would be expected for interacting proteins (reviewed in (Hawley and Gilliland 2006)). Because the localization of PIN6 and PIN8 is maintained in *pin1* backgrounds, it seems unlikely that these two proteins have auxin transport functions that are redundant and homologous with those of PIN1. Nevertheless, PIN6/PIN8/PIN5-mediated intracellular auxin-transport could contribute to intercellular auxin transport by a mechanism non-homologous to that used by PM-localized PIN proteins (Wabnik et al. 2011b) (Figure 2.11A and 2.11B), a function of ER-localized PIN proteins that would be particularly relevant in primitive land plants like mosses, which seem to lack PM-localized PIN proteins (Mravec et al. 2009) but do select cell files for vascular function (Ligrone et al. 2000).

2.4 Materials and Methods

2.4.1 Plants

Origin and nature of lines, genotyping strategies and oligonucleotide sequences are in Tables 2.1, 2.2, 2.3, respectively. Seeds were sterilized and germinated, and plants were grown and transformed as in (Sawchuk et al. 2008).

2.4.2 Imaging

For plasma-membrane stainings, seedlings were incubated in 10 μg ml^{-1} FM 4-64 (Invitrogen) for ~4 min under vacuum before mounting. For endoplasmic-reticulum stainings, dissected leaves were incubated in 10 μM ER-Tracker Red (Invitrogen/Life Technologies) or ER-Tracker Blue-White DPX (Invitrogen/Life Technologies) for ~30 min under vacuum before mounting. Leaf primordia were mounted in water under 0.17-mm-thick coverslips (Fischer Scientific) and imaged with the 20x/0.8 Plan-Apochromat or 40x/1.2 W C-Apochromat objective of an Axio Imager.M1/LSM 510 META confocal microscope (Carl Zeiss). 512x512-pixel frames were scanned unidirectionally at 8-bit depth with 1.6-μsec pixel dwell time and 8-fold averaging. Scanning zoom was adjusted to set pixel size to half the spacing of the features to be resolved, with minimum pixel size equal to half the objective lateral resolving power. Emission was

Table 2.2. Genotyping strategies.

Line	Strategy
pin1-1	'pin1-1 F' and 'pin1-1 R'; *Tat*I
eir1-1	'eir1-1 F' and 'eir1-1 R'; *Bse*LI
pin3-3	'pin3-3 F' and 'pin3-3 R'; *Sty*I
pin4-2	*PIN4*: 'PIN4 forw geno II' and 'PIN4en rev Ikram'; *pin4*: 'PIN4en rev Ikram' and 'en primer'
pin5-4	*PIN5*: 'SALK_042994 LP' and 'SALK_042994 RP'; *pin5*: 'SALK_042994 RP' and 'LBb1.3'
pin6	*PIN6*: 'PIN6 spm F' and 'PIN6 spm R'; *pin6*: 'PIN6 spm F' and 'Spm32'
$pin7^{En}$	*PIN7*: 'PIN7en forw Ikram' and 'PIN7en rev'; *pin7*: 'PIN7en rev Ikram II' and 'en primer'
pin8-1	*PIN8*: 'SALK_107965 LP' and 'SALK_107965 RP'; *pin8*: 'SALK_107965 RP' and 'LBb1.3'

Table 2.3. Oligonucleotide sequences.

Name	Sequence (5' to 3')
pin1-1 F	ATGATTACGGCGGCGGACTTCTA
pin1-1 R	TTCCGACCACCACCAGAAGCC
eir1-1 F	TTGTTGATCATTTTACCTGGGACA
eir1-1 R	GGTTGCAATGCCATAAATAGAC
pin3-3 F	GGAGCTCAAACGGGTCACCCG
pin3-3 R	GCTGGATGAGCTACAGCTATATTC
en primer	GAGCGTCGGTCCCCACACTTCTATAC
PIN4 forw geno II	GTCCGACTCCACGGCCTTC
PIN4en rev Ikram	ATCTTCTTCTTCACCTTCCACTCT
LBb1.3	ATTTTGCCGATTTCGGAAC
SALK_042994 LP	TGTGGTTGTGGGAGAGAAGTC
SALK_042994 RP	AAATTTGGACTTACGCTGTGC
Spm32	TACGAATAAGAGCGTCCATTTTAGAGTG
PIN6 spm F	CATAACGAAGCTAACTAAGGGGTAATCTC
PIN6 spm R	GGAGTTCAAAGAGGAATAGTAGCAGAG
UBQ10 HindIII Forw	CTCAAGCTTTCCCATGTTTCTCGTCTGTC
UBQ10 SmaI Rev	CGACCCGGGCTGTTAATCAGAAAAACTCAG
PIN6 I miR-s	GATTAAAGATACTATCATCCCACTCTCTCTTTTGTATTCC
PIN6 II miR-a	GAGTGGGATGATAGTATCTTTAATCAAAGAGAATCAATGA
PIN6 III miR*s	GAGTAGGATGATAGTTTCTTTATTCACAGGTCGTGATATG
PIN6 IV miR*a	GAATAAAGAAACTATCATCCTACTCTACATATATATTCCT
pRS300 A	CTGCAAGGCGATTAAGTTGGGTAAC
pRS300 B	GCGGATAACAATTTCACACAGGAAACAG
PIN7en forw Ikram	CCTAACGGTTTCCACACTCA
PIN7en rev	TAGCTCTTTAGGGTTTAGCTC
PIN7en rev Ikram II	GGTTTAGCTCTGCTGTGGAGTT
SALK_107965 LP	TGAAAGACATTTTGATGGCATC

SALK_107965 RP	CCAAATCAAGCTTTGCAAGAC
PIN6 prom SmaI forw	ATTCCCGGGGATGATTGTTTAAGATAAGTTGCAAAG
PIN6 2179 SphI rev	ATAGCATGCTTGCTTGCCAATCGCAGCCACC
PIN6 2180 EcoRI forw	ATGGAATTCGAAATGCCAAGTGCAATTGTAATGATG
PIN6 UTR XhoI rev	ATACTCGAGTCGAATGCTTTTGGTTTCGG
EGFP PstI SphI forw	TATCTGCAGGCATGCGCAGTGAGCAAGGGCGAGGAG CTG
EGFP EcoRI rev	TATGAATTCCTTGTACAGCTCGTCCATGCCG
PIN6 transc forw	GGGGACAAGTTTGTACAAAAAAGCAGGCTGCTCGGA TTATATTTATATG
PIN6 transc rev	GGGGACCACTTTGTACAAGAAAGCTGGGTTCTTTGCC TCTTCTTCTTC
ATHB8 attB1F	GGGGACAAGTTTGTACAAAAAAGCAGGCTGACGATA ATGATGATAACTAC
ATHB8 attB2R	GGGGACCACTTTGTACAAGAAAGCTGGGTCTTTGATC CTCTCCGATCTCTC
PIN8 prom BamHI forw	ATTGGATCCGAATTTTGTAAAATGTGAAGG
PIN8 UTR SacI Rev	ATAGAGCTCGGGAAGAAGAAAGGGTAAC
EGFP BglII forw	TATAGATCTGTGAGCAAGGGCGAGGAG
EGFP BglII rev	TATAGATCTCTTGTACAGCTCGTCCATGC
MP SalI Fwd	TATGTCGACCCCGGGTTAATCAGTATTATTAC
PIN8 transc forw	GGGGACAAGTTTGTACAAAAAAGCAGGCTGAATTTT GTAAAATGTGAAG
PIN8 transc rev	GGGGACCACTTTGTACAAGAAAGCTGGGTGTTTTTAT CAAATTGTACAATAC
MP BamHI Rev	TAGGGATCCACAGAGAGATTTTTCAATGTTCTG
PIN6OX SmaI forw	ATACCCGGGATGATAACGGGAAACGAATTCTAC
PIN6OX Ecl136II rev	ATTGAGCTCTCATAGGCCCAAGAGGACG
MP prom Gateway Fwd	GGGGACAAGTTTGTACAAAAAAGCAGGCTCCGGGTT AATCAGTATTATTAC
MP prom Gateway Rev	GGGGACCACTTTGTACAAGAAAGCTGGGTACAGAGA GATTTTTCAATGTTCTG
RPS5A SmaI Forw	ATACCCGGAGCAGGAGATCTATCAGTG

RPS5a SmaI Rev	ATACCCGGGGGCTGTGGTGAGAGAAAC
PIN8OX KpnI forw	TATGGTACCATGATCTCCTGGCTCGATATCTAC
PIN8OX BamHI rev	TATGGATCCTCATAGGTCCAATAGAAAATAATATGC
PIN5OX SmaI forw	ATACCCGGGATGATAAATTGTGGAGATGTTTAC
PIN5OX BamHI rev 2	AT GGATCCTCAATGAATAAACTCCAGAGC
PIN6 prom SalI F	GCGGTCGACTGATGATTGTTTAAGATAAG
PIN6 prom BamHI R	TCTGGATCCTCTTTGCCTCTTCTTCTTC
IAAL BamHI F	ATAGGATCCATGACTGCCTACGATATGGAAAAGG
IAAL BamHI R	TATGGTACCTCAGTTTCGGCGGTCGATGATG

collected from ~5-µm-thick (single-fluorophore imaging) or ~1-µm-thick (multi-fluorophore imaging) optical slices. Amplifier gain was set at 1; detector gain at ~50-60%. Laser transmission and offset value were adjusted to match signal to detector's input range. Marker-line-specific imaging parameters are in Tables 2.4 and 2.5. For multi-fluorophore imaging, sequential excitation and collection of emission were performed in line-by-line channel-switching mode, which did not result in signal crossover under our imaging conditions. Signal levels in images acquired at identical settings were visualized as in (Sawchuk et al. 2008). Signal colocalization was visualized as in (Demandolx and Davoust 1997) and quantified as in (Manders et al. 1993). Mature leaves were imaged as in (Donner et al. 2009). Images were analyzed and processed with ImageJ (National Institutes of Health), and figures were generated with Canvas (ACD Systems International Inc.).

Table 2.4. Imaging parameters: single-marker lines.

Line	Laser	Wavelength (nm)	Main dichroic beam splitter	First secondary dichroic beam splitter	Second secondary dichroic beam splitter	Emission filter (detector)
PIN6::PIN6:GFP	Ar	488	HFT 405/488/594	NFT 545	NFT 490	BP 505-530 (PMT3)
PIN6::YFPnuc	Ar	514	HFT 405/514/594	NFT 595	NFT 515	BP 520-555 IR (PMT3)
PIN8::PIN8:GFP	Ar	488	HFT 405/488/594			507-593 (META)
PIN8::YFPnuc	Ar	514	HFT 405/514/594	NFT 595	NFT 515	BP 520-555 IR (PMT3)
DR5rev::YFPnuc	Ar	514	HFT 405/514/594	NFT 595	NFT 515	BP 520-555 IR (PMT3)
PIN1::PIN1:YFP	Ar	514	HFT 405/514/594	NFT 595	NFT 515	BP 520-555 IR (PMT3)
MP::YFPnuc	Ar	514	HFT 405/514/594	NFT 595	NFT 515	BP 520-555 IR (PMT3)

Table 2.5. Imaging parameters: multi-marker lines.

Multi-marker lines	Single-marker lines	Laser	Wavelength (nm)	Main dichroic beam splitter	First secondary dichroic beam splitter	Second secondary dichroic beam splitter	Emission filter (detector)
PIN6::PIN6:GFP; PIN6::YFPnuc; chlorophyll	PIN6::PIN6:GFP	Ar	488	HFT 405/488/594	NFT 595	NFT 545	BP 505-530 (PMT2)
	PIN6::YFPnuc	Ar	514	HFT 405/515/594	NFT 595	NFT 515	BP 520-555 IR (PMT3)
	chlorophyll	Ar	488	HFT 405/488/594	NFT 595		604-700 (META)
PIN1::PIN1:CFP; PIN6::YFPnuc; chlorophyll	PIN1::PIN1:CFP	Ar	458	HFT 458/514	NFT 595	NFT 545	BP 470-500 (PMT2)
	PIN6::YFPnuc	Ar	514	HFT 458/514	NFT 595	NFT 545	BP 530-575 IR (PMT3)
	chlorophyll	Ar	458	HFT 458/514	NFT 595		604-700 (META)
PIN6::PIN6:GFP; 35S::YFPer	PIN6::PIN6:GFP	Ar	458	HFT 458/514	Mirror	NFT 515	BP 470-500 (PMT2)
	35S::YFPer	Ar	514	HFT 458/514	Mirror	NFT 515	BP 575-620 IR (PMT3)
PIN6::PIN6:GFP; 35S::RTNLB4:YFP	PIN6::PIN6:GFP	Ar	458	HFT 458/514	Mirror	NFT 545	BP 475-525 (PMT2)

	35S::RTNLB4:YFP	Ar	514	HFT 458/514	Mirror	NFT 515	BP 530-575 IR (PMT3)
J1721::GFPer; 35S::YFPer	J1721::GFPer	Ar	458	HFT 458/514	Mirror	NFT 515	BP 470-500 (PMT2)
	35S::YFPer	Ar	514	HFT 458/514	Mirror	NFT 515	BP 575-620 IR (PMT3)
ATHB8::GFPnuc; 35S::YFPer	ATHB8::GFPnuc	Ar	458	HFT 458/514	Mirror	NFT 515	BP 470-500 (PMT2)
	35S::YFPer	Ar	514	HFT 458/514	Mirror	NFT 515	BP 575-620 IR (PMT3)
PIN6::PIN6:GFP; 35S::YFPpm	PIN6::PIN6:GFP	Ar	458	HFT 458/514	Mirror	NFT 515	BP 470-500 (PMT2)
	35S::YFPpm	Ar	514	HFT 458/514	Mirror	NFT 515	BP 575-620 IR (PMT3)
J1721::GFPer; 35S::YFPpm	J1721::GFPer	Ar	458	HFT 458/514	Mirror	NFT 515	BP 470-500 (PMT2)
	35S::YFPpm	Ar	514	HFT 458/514	Mirror	NFT 515	BP 575-620 IR (PMT3)
35S::YFPpm; FM4-64	35S::YFPpm	Ar	488	HFT 488/543	Mirror	NFT 545	BP 505-530 (PMT2)
	FM4-64	HeNe	543	HFT 488/543	Mirror	NFT 545	BP 560-615 IR (PMT3)
PIN8::PIN8:GFP; ER-Tracker Red	PIN8::PIN8:GFP	Ar	488	HFT 488/543	Mirror	NFT 545	BP 505-530 (PMT2)
	ER-Tracker Red	HeNe	543	HFT 488/543	Mirror	NFT 545	BP 600-650 (PMT3)

ER-Tracker Blue-White DPX; PIN8::PIN8:GFP	ER-Tracker Blue-White DPX	Diode	405	HFT 405/488/543	Mirror	NFT 490	BP 420-480 (PMT2)
	PIN8::PIN8:GFP	Ar	488	HFT 405/488/543	Mirror	NFT 490	BP 505-530 (PMT3)
ATHB8::CFPnuc; PIN1::PIN1:YFP	ATHB8::CFPnuc	Ar	458	HFT 458/514	NFT 595	NFT 515	BP 470-500 (PMT2)
	PIN1::PIN1:YFP	Ar	514	HFT 458/514	NFT 595	NFT 515	BP 520-555 IR (PMT3)

CHAPTER 3: CONTROL OF ARABIDOPSIS VEIN-NETWORK FORMATION BY AUXIN TRANSPORT

3.1 Introduction

Most multicellular organisms form tissue networks for transport function. What controls the formation of tissue networks is thus a central question in biology. In animals, many of these networks are stereotyped, suggesting tight positional controls (Lu and Werb 2008). By contrast, the vein networks of plant leaves are both reproducible and variable: reproducible in their overall pattern features; variable in their fine spatial details (Sachs 1989). The coexisting reproducibility and variability of vein networks argue against a tight positional control and instead suggest an iterative, self-organizing vein-formation mechanism that integrates leaf growth with vein network formation (Sachs 1989).

Though genetic evidence is lacking, imaging and inhibitor studies suggest a role for cell-to-cell transport of the plant signal auxin in vein network formation. Expression of the PIN-FORMED1 (PIN1) auxin effluxer of *Arabidopsis thaliana* (Galweiler et al. 1998; Petrasek et al. 2006) is iteratively initiated in broad domains of leaf inner cells that become gradually restricted to files of vascular precursor cells in contact with pre-existing, narrow PIN1 expression domains (Scarpella et al. 2006; Wenzel et al. 2007). Within broad expression domains, PIN1 is localized isotropically—or nearly so—at the plasma membrane (PM) of leaf inner cells. As expression of PIN1 becomes gradually restricted to files of vascular precursor cells, PIN1 localization becomes polarized to the side of the PM facing the pre-existing, narrow PIN1 expression domains with which the narrowing domains are in contact. Initially, PIN1 expression domains are connected to pre-existing domains at one end only; the other end can eventually terminate freely in the leaf or become connected to other PIN1 expression domains. Inhibitors of cellular auxin efflux delay the restriction of PIN1 expression domains and the polarization of PIN1 localization (Scarpella et al. 2006; Wenzel et al. 2007), and induce the formation of more-complex vein networks characterized by more veins that are more frequently interconnected (Mattsson et al. 1999; Sieburth 1999).

By contrast, genetic evidence is available that suggests a role for intracellular auxin transport mediated by the endoplasmic-reticulum (ER)-localized PIN5, PIN6 and PIN8 (ER-PIN) auxin transporters of Arabidopsis (Petrasek et al. 2006; Mravec et al. 2009; Bosco et al. 2012; Ding et al. 2012; Bender et al. 2013; Cazzonelli et al. 2013; Sawchuk et al. 2013) (Chapter 2) in vein network formation: *pin6*;*pin8* double-mutant leaves have more-complex vein networks, a defect suppressed by *pin5* (Sawchuk et al. 2013) (Chapter 2); furthermore, overexpression of *PIN6* or *PIN8* results in less-complex vein networks, while overexpression of *PIN5* results in the opposite defect.

Here we asked whether PIN1-mediated intercellular auxin transport controlled vein network formation and—if so—whether it interacted with the control of vein network formation mediated by *ER-PIN*-dependent intracellular auxin transport. By a combination of cellular imaging and molecular genetic analysis, we find that: PIN1-mediated intercellular auxin transport inhibits vein network formation; *PIN6* acts redundantly with *PIN1* in inhibition of vein network formation; and *PIN8* acts redundantly with *PIN6* in *PIN1*-dependent inhibition of vein network formation—though *PIN8*'s function in this process is likely indirect and mediated by cell-cell interactions. We further show that, independently of PIN1-mediated intercellular auxin transport, *PIN5* promotes vein network formation—though likely indirectly and through cell-cell interactions—and that such function of *PIN5* is inhibited by *PIN6* and *PIN8*. We derive cellular expression and genetic interaction maps of *PIN1*, *PIN5*, *PIN6* and *PIN8* that can be used to generate predictions to test the evolutionary conservation of the function of *PIN* genes and PIN-mediated auxin transport in vein network formation.

3.2 Results and discussion

3.2.1 *PIN5* expression during leaf development

Veins are formed sequentially during leaf development: the formation of the centrally located vein ("midvein") is followed by the formation of the first loops of veins ("first loops"), which in turn is followed by the formation of the second loops and minor veins (Mattsson et al. 1999; Sieburth 1999; Kang and Dengler 2004; Scarpella et al. 2004) (Figure 3.1A,3.1E,3.1I).

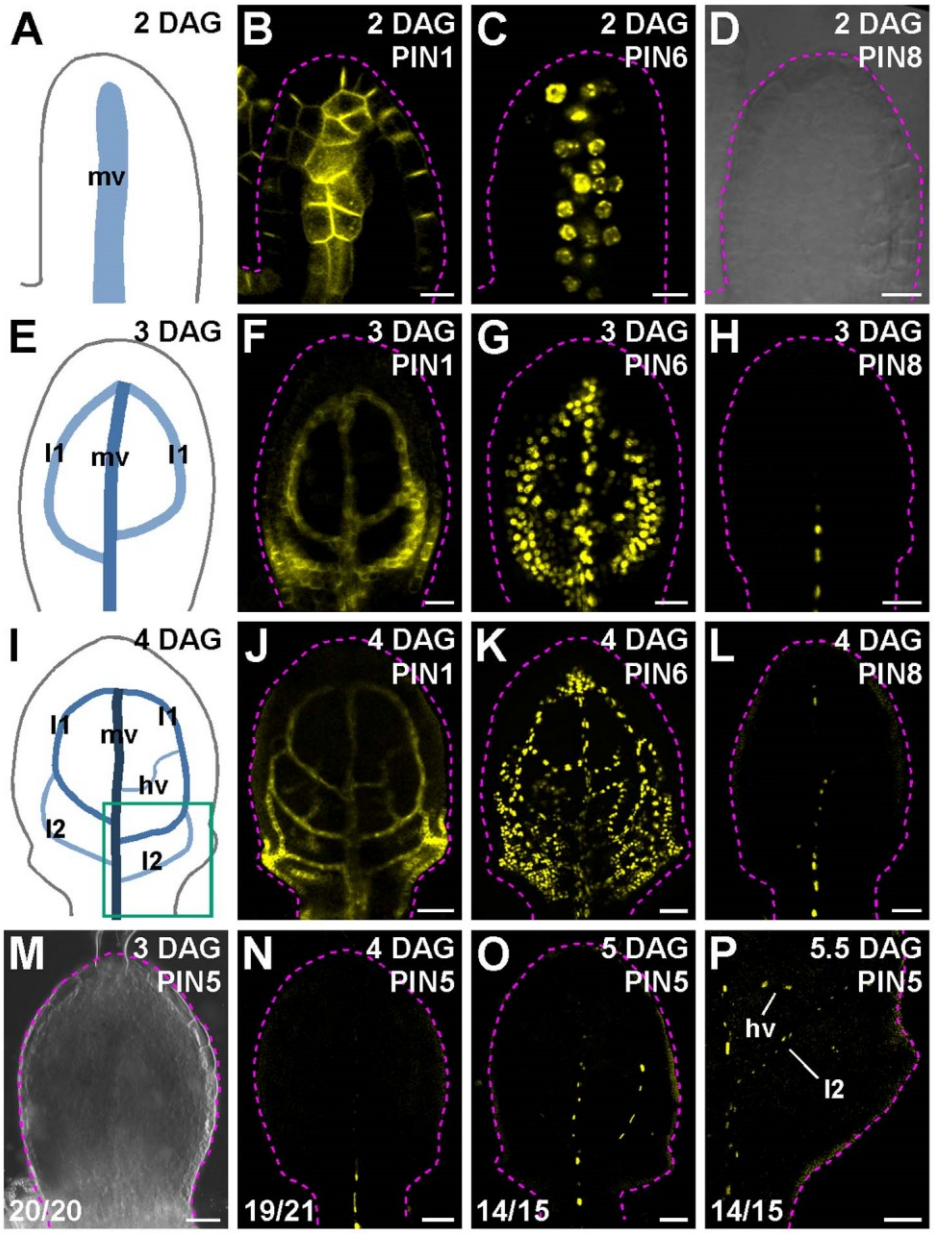

Figure 3.1. Expression of *PIN1*, *PIN5*, *PIN6* and *PIN8* of Arabidopsis in first leaf development. (A-P) Top right, leaf age in days after germination (DAG) and reported gene. (M-P) Bottom left, reproducibility index. (A,E,I) Midvein, loops and minor veins are formed sequentially in leaf development (Mattsson et al. 1999; Sieburth 1999; Kang and Dengler 2004; Scarpella et al. 2004); increasingly darker blue depicts progression through successive stages of vein development. Box in (I) illustrates position of close-up in (P). (B-D,F-H,J-P) Confocal laser scanning microscopy with (D,M) or without transmitted light (B,C,F-H,J-L,N-P), first leaves. (B,F,J) PIN1::PIN1:GFP expression. (C,G,K) PIN6::YFPnuc expression. (D,H,L) PIN8::YFPnuc expression. (M-P) PIN5::YFPnuc expression. Dashed magenta line delineates leaf primordium outline. hv, minor veins; l1, first loop; l2, second loop; mv, midvein. Bars: (B-D) 10 μm; (F-H,M) 25 μm; (J-L,N-P) 50 μm.

Two distinct auxin-transport pathways have overlapping functions in patterning of Arabidopsis vein networks (Sawchuk et al. 2013) (Chapter 2). One pathway—mediated by the plasma-membrane (PM)-localized PIN1 protein—transports auxin intercellularly (Galweiler et al. 1998; Petrasek et al. 2006); the other pathway—mediated by the endoplasmic-reticulum (ER)-localized PIN5, PIN6 and PIN8 proteins—transports auxin intracellularly (Petrasek et al. 2006; Mravec et al. 2009; Bosco et al. 2012; Ding et al. 2012; Bender et al. 2013; Cazzonelli et al. 2013; Sawchuk et al. 2013) (Chapter 2).

Consistent with their role in vein patterning, *PIN1*, *PIN6* and *PIN8* are expressed in developing veins, though with different dynamics: expression of *PIN1* and *PIN6* is initiated in broad domains of inner cells that over time become restricted to single files of vascular precursor cells, whereas *PIN8* expression is restricted from early on to single files of vascular cells and is initiated after the onset of expression of both *PIN1* and *PIN6* (Scarpella et al. 2006; Wenzel et al. 2007; Sawchuk et al. 2013) (Chapter 2; Figure 3.1B-D,3.1F-H,3.1J-L).

PIN5 is expressed in veins of mature leaves (Mravec et al. 2009; She et al. 2010), but its expression during leaf development is unknown. A *PIN5* transcriptional fusion (*PIN5* promoter driving expression of a reporter protein) and a *PIN5* translational fusion (*PIN5* promoter driving expression of a PIN5-reporter fusion protein) are expressed in similar domains (Mravec et al. 2009; She et al. 2010), suggesting that the *PIN5* promoter contains all the regulatory elements required for *PIN5* expression. Thus, to visualize *PIN5* expression during leaf development, we imaged expression of a transcriptional fusion of *PIN5* to a nuclear yellow fluorescent protein (PIN5::YFPnuc) in first leaves at 3, 4, 5 and 5.5 days after germination (DAG).

Expression of PIN5::YFPnuc was first detected in the midvein of 4-DAG leaves (Figure 3.1N); at 5 DAG, PIN5::YFPnuc was additionally expressed in the first loops (Figure 3.1O), and at 5.5 DAG PIN5::YFPnuc was additionally expressed in the second loops and minor veins (Figure 3.11P). *PIN5* expression is initiated after *PIN8* expression (Figure 3.1H and 3.1M), but—as *PIN8—PIN5* is expressed from early on in single files of vascular cells (Figure 3.1H,3.1L,3.1N-P).

3.2.2 Expression of *PIN1*, *PIN5*, *PIN6* and *PIN8* in leaf vascular cells

Because *PIN1*, *PIN5*, *PIN6* and *PIN8* are all expressed in developing veins (Figure 3.1), we asked whether these genes were expressed in the same vascular cells. To address this question, we imaged pairwise combinations of fluorescent reporters of *PIN1*, *PIN5*, *PIN6* and *PIN8* in midvein cells of 4-DAG first leaves—where these genes are expressed (Figure 3.1J-L and 3.1N)—and quantified reporter coexpression.

In none of the 20 analyzed leaves coexpressing PIN5::YFPnuc and PIN6::CFPnuc (*PIN6* promoter driving expression of a nuclear cyan fluorescent protein) or PIN8::YFPnuc and PIN6::CFPnuc, were cells expressing PIN5::YFPnuc or PIN8::YFPnuc ever on the same plane as cells expressing PIN6::CFPnuc: cells expressing PIN5::YFPnuc or PIN8::YFPnuc were located ventrally, while cells expressing PIN6::CFPnuc were located dorsally (Figure 3.2A-3.2F).

Though cells expressing PIN5::YFPnuc or PIN8::PIN8:GFP (*PIN8* promoter driving expression of a PIN8:GFP fusion protein) were both on the same ventral plane (Figure 3.2G-3.2I), only less than 3% of the cells expressing either reporter expressed both (Figure 3.2S).

Approximately 95% of PIN5::YFPnuc-expressing cells expressed PIN1::PIN1:GFP, but only ~25% of the PIN1::PIN1:GFP-expressing cells that were on the same ventral plane expressed PIN5::YFPnuc (Figure 3.2J-3.2L and 3.2S).

Approximately 90% of PIN8::YFPnuc-expressing cells expressed PIN1::PIN1:GFP, but only ~25% of the PIN1::PIN1:GFP-expressing cells that were on the same ventral plane expressed PIN8::YFPnuc (Figure 3.2M-3.2O and 3.2S).

Finally, in agreement with previous observations (Sawchuk et al. 2013) (Chapter 2), ~95% of PIN6::YFPnuc-expressing cells expressed PIN1::PIN1:GFP, and ~75% of the PIN1::PIN1:GFP-expressing cells that were on the same dorsal plane expressed PIN6::YFPnuc (Figure 3.2P-3.2S). Thus our results suggest that *PIN5*, *PIN6* and *PIN8* are expressed in mutually exclusive domains of vascular cells and that the *PIN1* cellular-expression domain overlaps with—but extends beyond—the *ER-PIN* cellular-expression domain (Figure 3.8A).

3.2.3 Unique and redundant functions of *PIN1*, *PIN6*, *PIN8* and *PIN5* in vein network formation

PIN1, *PIN5*, *PIN6* and *PIN8* control vein patterning (Mattsson et al. 1999; Bilsborough et al. 2011; Guenot et al. 2012; Sawchuk et al. 2013) (Chapter 2); we asked what their function is in

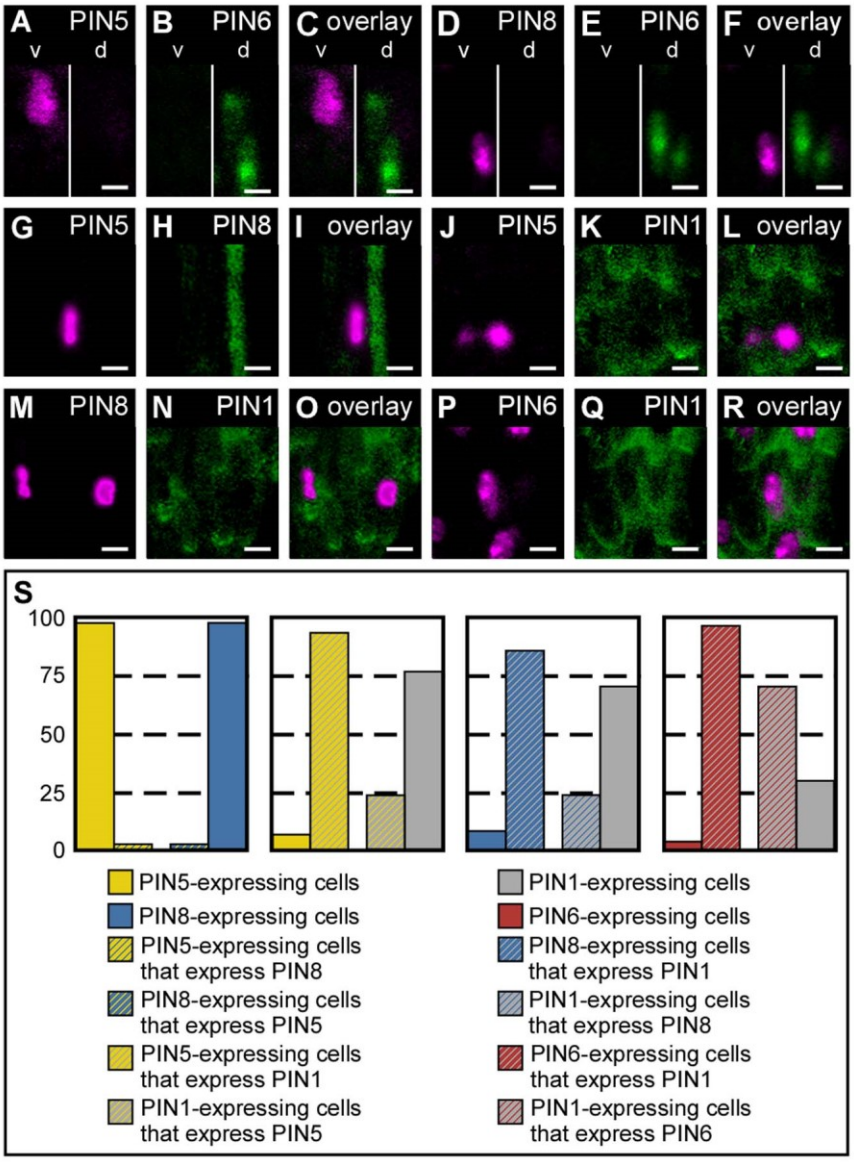

Figure 3.2. Expression of *PIN1*, *PIN5*, *PIN6* and *PIN8* in leaf vascular cells. (A-R) Top right, expression-reported gene. Confocal laser scanning microscopy, first leaves. (A-R) Expression of PIN5::YFPnuc (A,G,J), PIN6::CFPnuc (B,E), PIN8::YFPnuc (D,M), PIN8::PIN8:GFP (H), PIN1::PIN1:GFP (K,N,Q), PIN6::YFPnuc (P) and respective overlays (C,F,I,L,O,R). (S) Percentage of cells expressing fluorescent reporters in 25-μm-by-25-μm midvein regions of 4-day-old first leaves (1 region per midvein) in different pairwise combinations of reporters. Sample population sizes: PIN5::YFPnuc;PIN8::PIN8:GFP: 40 leaves (41 PIN5::YFPnuc-expressing cells, 39 PIN8::PIN8:GFP-expressing cells); PIN5::YFPnuc;PIN1::PIN1:GFP: 26 leaves (30 PIN5::YFPnuc-expressing cells, 119 PIN1::PIN1:GFP-expressing cells); PIN8::YFPnuc;PIN1::PIN1:GFP: 25 leaves (34 PIN8::YFPnuc-expressing cells, 122 PIN1::PIN1:GFP-expressing cells); PIN6::YFPnuc;PIN1::PIN1:GFP: 31 leaves (127 PIN6::YFPnuc-expressing cells, 174 PIN1::PIN1:GFP-expressing cells). d, dorsal focal plane; v, ventral focal plane. Bars: (A-R) 5 μm.

vein network formation. We used the number of vein branching points as a descriptor of vein network complexity, as this number is proportional to the number of veins and the extent of their interconnectedness.

As previously reported (Sawchuk et al. 2013) (Chapter 2), the vein network complexity of *pin5*, *pin6* or *pin8* was no different from that of WT (Figure 3.3); by contrast, the vein networks of *pin1* were more complex than those of WT (Figure 3.3), suggesting that *PIN1* inhibits vein network formation (Figure 3.8B and 3.8C).

We next asked whether *PIN5*, *PIN6* or *PIN8* acted redundantly with *PIN1* in inhibition of vein network formation. The vein network complexity of neither *pin1*;*pin5* (*pin1*;*5* hereafter) nor *pin1*;*8* differed from that of *pin1* (Figure 3.3); however, the vein networks of *pin1*;*6* were more complex than those of *pin1* (Figure 3.3), suggesting that *PIN6* acts redundantly with *PIN1* in inhibition of vein network formation (Figure 3.8B and 3.8C). As the vein network complexity of *pin6* is no different from that of WT (Sawchuk et al. 2013) (Chapter 2; Figure 3.3) but that of *pin1* is (Figure 3.3), the redundancy between *PIN1* and *PIN6* is unequal: whereas *PIN1* can provide all—or nearly all (see below)—the functions of *PIN6* in inhibition of vein network formation, *PIN6* cannot provide all the functions of *PIN1* in this process (Figure 3.8B and 3.8C).

Next, we asked whether *PIN5* or *PIN8* acted redundantly with *PIN6* in *PIN1*-dependent inhibition of vein network formation. The vein network complexity of *pin1*;*6*;*5* was no different from that of *pin1*;*6* (Figure 3.4), but the vein networks of *pin1*;*6*;*8* were more complex than those of *pin1*;*6* (Figure 3.4), suggesting that *PIN8* acts redundantly with *PIN6* in *PIN1*-dependent inhibition of vein network formation (Figure 3.8B and 3.8C). Because the vein network complexity of neither *pin6* nor *pin8* differ from that of WT (Sawchuk et al. 2013) (Chapter 2; Figure 3.3), but the vein networks of *pin6*;*8* are more complex than those of WT (Sawchuk et al. 2013) (Figure 3.3), *PIN6* and *PIN8* also have redundant functions in inhibition of vein network formation that are independent of *PIN1* (Figure 3.8.B and 3.8C). We finally asked whether *PIN5* acted redundantly with *PIN6* and *PIN8* in *PIN1*-dependent or *PIN1*-independent inhibition of vein network formation. The vein network complexity of *pin1*;*6*;*8*;*5* was no different from that of *pin1*;*6* (Figure 3.4), and that of *pin6*;*8*;*5* was no different from that of WT (Sawchuk et al. 2013) (Chapter 2; Figure 3.3), suggesting that *pin5* suppresses the effects of *pin6* and *pin8* on *PIN1*-independent inhibition of vein network formation. We conclude that *PIN5* promotes vein

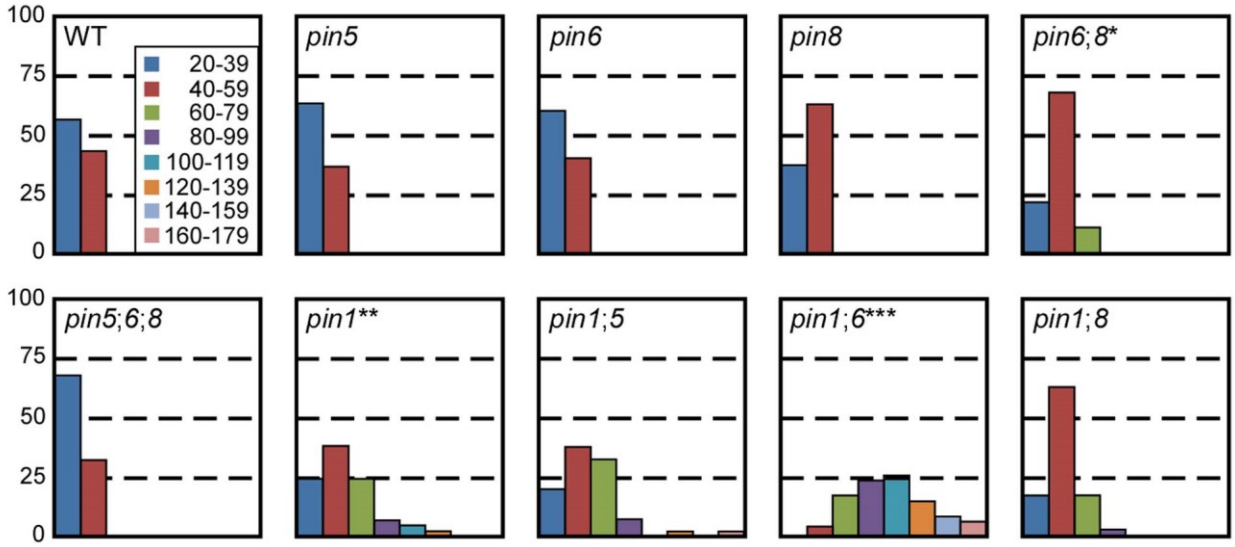

Figure 3.3. Functions of *PIN1*, *PIN5*, *PIN6* and *PIN8* in vein network formation. Percentage of first leaves in branching-point classes. Difference between *pin6*;*8* and WT, between *pin1* and WT, and between *pin1*;*6* and *pin1* was significant at $P<0.05$ (*), $P<0.01$ (**) or $P<0.001$ (***) by Kruskal-Wallis and Mann-Whitney test with Bonferroni correction. Sample population sizes: WT, 30; *pin5*, 30; *pin6*, 30; *pin8*, 27; *pin6*;*8*, 28; *pin5*;*6*;*8*, 28; *pin1*, 45; *pin1*;*5*, 56; *pin1*;*6*, 47; *pin1*;*8*, 35.

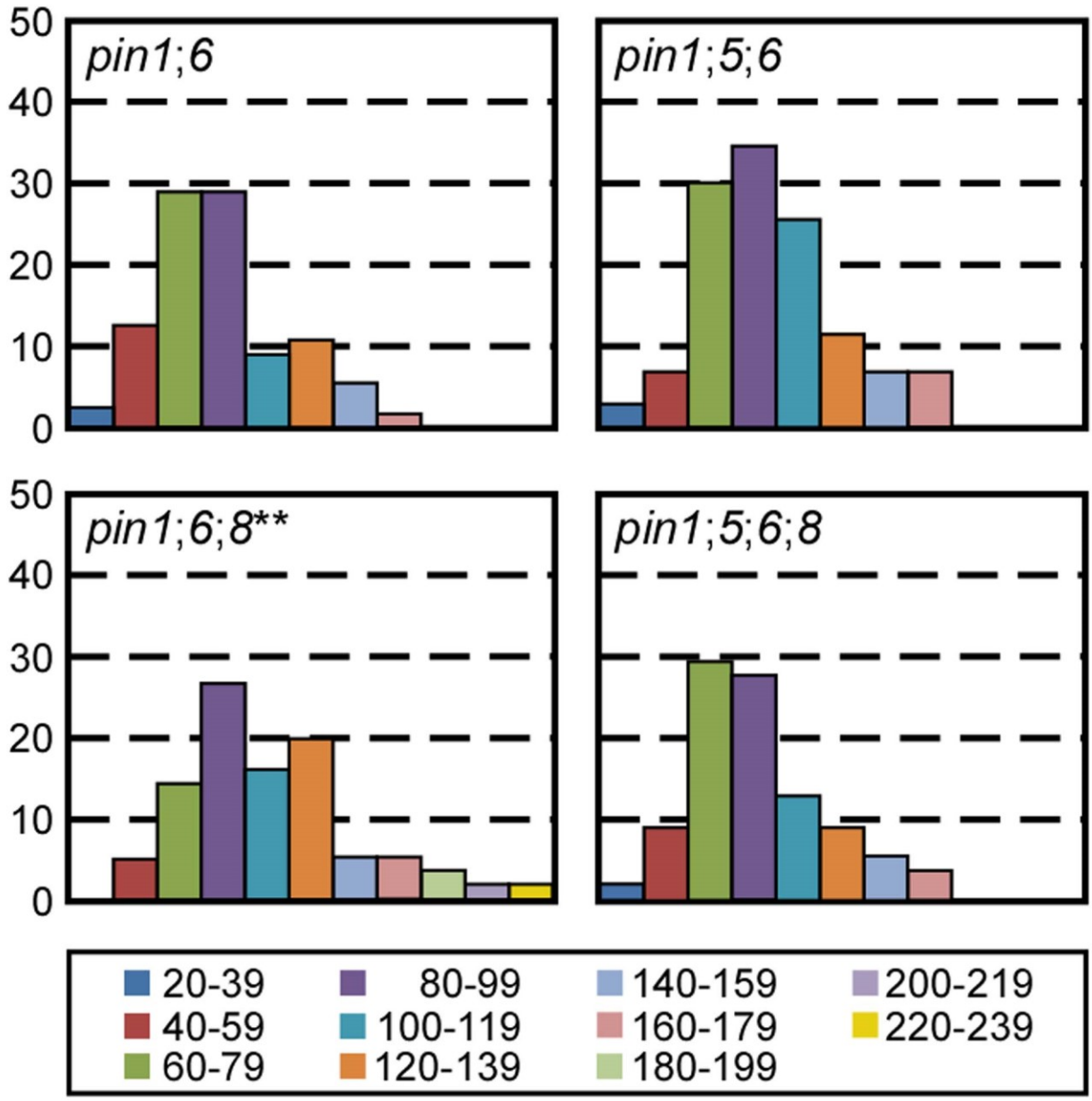

Figure 3.4. Functions of *PIN5* and *PIN8* in *PIN1*/*PIN6*-dependent vein-network formation. Percentage of class-IV first leaves (Figure 3.5D) in branching–point classes. Difference between *pin1*;*6*;*8* and *pin1*;*6* was significant at $P<0.01$ (**) by Kruskal-Wallis and Mann-Whitney test with Bonferroni correction. Sample population sizes: *pin1*;*6*, 55; *pin1*;*5*;*6*, 54; *pin1*;*6*;*8*, 56; *pin1*;*5*;*6*;*8*, 54.

network formation, that *PIN6* and *PIN8* redundantly inhibit *PIN5*-dependent promotion of vein network formation, and that these functions of *PIN5*, *PIN6* and *PIN8* are independent of *PIN1* (Figure 3.8B and 3.8C). Further, because expression of *PIN5* and *PIN8* is initiated at post-formative stages of vein development (Sawchuk et al. 2013) (Chapter 2; Figure 3.1), these genes most likely control vein network formation indirectly. Finally, because *PIN5*, *PIN6* and *PIN8* are expressed in non-overlapping sets of vascular cells (Figure 3.2), the interaction between *pin5*, *pin6* and *pin8* presumably reflects cell-cell interactions occurring in vein network formation.

3.2.4 Redundant functions of *PIN6* and *PIN8* in *PIN1*-dependent vein-network formation

PIN8 acts redundantly with *PIN6* in *PIN1*-dependent inhibition of vein network formation (Figure 3.3); however, the redundancy between *PIN6* and *PIN8* in *PIN1*-dependent inhibition of vein network formation is unequal: the vein network complexity of *pin1*;*8* is no different from that of *pin1*, but that of *pin1*;*6* is; thus *PIN6* can provide all the functions of *PIN8* in *PIN1*-dependent inhibition of vein network formation, but *PIN8* cannot provide all the functions of *PIN6* in this process (Figure 3.8B and 3.8C). Such unequal redundancy could be accounted for by the different expression of *PIN6* and *PIN8* during vein development (Sawchuk et al. 2013) (Chapter 2; Figures 3.1 and 3.2), but it could also reflect different functions of *PIN6* and *PIN8* in this process. We thus asked whether *PIN8* could provide functions similar to those of *PIN6*.

To address this question, we expressed the *PIN6* or the *PIN8* cDNAs by the *MONOPTEROS* (*MP*) promoter (MP::PIN6 or MP::PIN8)—which is highly active in developing organs (Sawchuk et al. 2013) (Chapter 2)—in the *pin1*;*6* background, and compared defects of MP::PIN6;*pin1*;*6* and MP::PIN8;*pin1*;*6* with those of *pin1*;*6* and *pin1*.

pin6 synthetically enhances the spectrum of vein pattern phenotypes of *pin1* (Sawchuk et al. 2013) (Chapter 2; Figure 3.5A-3.5H). We asked whether *PIN8* provided functions in *PIN1*-dependent vein patterning similar to those of *PIN6*. The spectrum of vein pattern phenotypes of MP::PIN6;*pin1*;*6* was no different from that of *pin1* (Figure 3.5H). The spectrum of vein pattern phenotypes of MP::PIN8;*pin1*;*6* was no different from that of MP::PIN6;*pin1*;*6* (Figure 3.5H), suggesting that *PIN8* can provide functions in *PIN1*-dependent vein patterning similar to those of *PIN6*.

We next asked whether *PIN8* provided functions in *PIN1*-dependent vein network formation

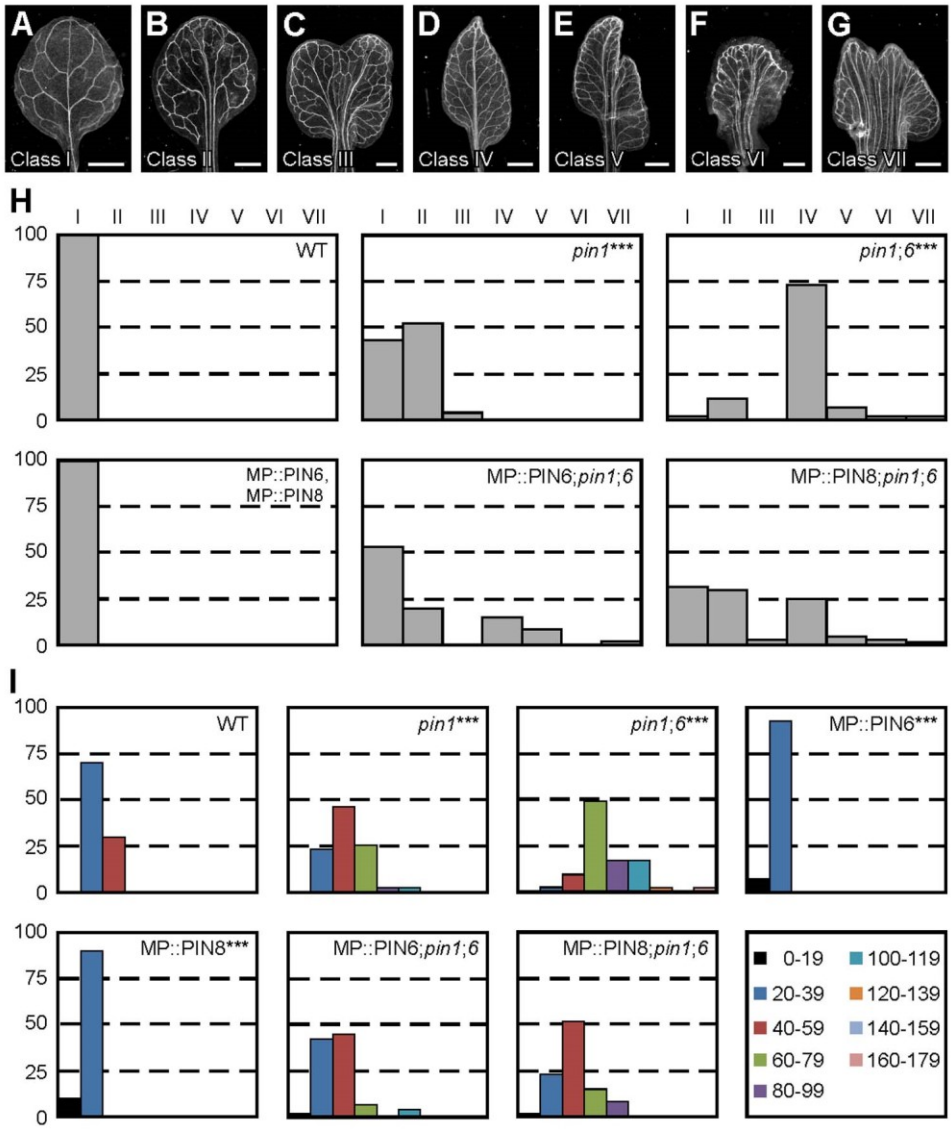

Figure 3.5. Functions of *PIN6* and *PIN8* in *PIN1*-dependent vein patterning and network formation. (A-G) Dark-field illumination of mature first leaves illustrating phenotype classes: unbranched, narrow midvein and scalloped vein-network outline (A); bifurcated midvein and scalloped vein-network outline (B); fused leaves with scalloped vein-network outline (C); conspicuous marginal vein (D); fused leaves with conspicuous marginal vein (E); wide midvein (F); fused leaves with wide midvein (G). (H) Percentages of leaves in phenotype classes. Difference between *pin1* and WT, and between *pin1*;*6* and *pin1* was significant at $P<0.001$ (***) by Kruskal-Wallis and Mann-Whitney test with Bonferroni correction. Sample population sizes: WT, 53; *pin1*, 46; *pin1*;*6*, 42; MP::PIN6, 54; MP::PIN8, 49; MP::PIN6;*pin1*;*6*, 45; MP::PIN8;*pin1*;*6*, 60. (I) Percentage of first leaves in branching-point classes. Difference between *pin1* and WT, between *pin1*;*6* and *pin1*, between MP::PIN6 and WT, and between MP::PIN8 and WT was significant at $P<0.001$ (***) by Kruskal-Wallis and Mann-Whitney test with Bonferroni correction. Sample population sizes as in H. Bars: (A-E,G) 1 mm; (F) 0.25 mm.

similar to those of *PIN6*. The vein networks of MP::PIN6 and MP::PIN8 were less complex than those of WT (Figure 3.5I). The vein network complexity of MP::PIN6;*pin1*;*6* was no different from that of *pin1* (Figure 3.5I). The vein network complexity of MP::PIN8;*pin1*;*6* was no different from that of MP::PIN6;*pin1*;*6* (Figure 3.4), suggesting that *PIN8* can provide functions in *PIN1*-dependent vein-network formation similar to those of *PIN6* (Figure 3.8B and 3.8C)

pin6 synthetically enhances the spectrum of cotyledon pattern phenotypes of *pin1* (Sawchuk et al. 2013) (Chapter2; Figure 3.6A-3.6H). We asked whether *PIN8* provided functions in *PIN1*-dependent cotyledon patterning similar to those of *PIN6*. MP::PIN6 shifted the spectrum of cotyledon pattern phenotypes of *pin1*;*6* toward that of *pin1* (Figure 3.6H). The spectrum of cotyledon pattern phenotypes of MP::PIN8;*pin1*;*6* was no different from that of MP::PIN6;*pin1*;*6* (Figure 3.6H), suggesting that *PIN8* can provide functions in *PIN1*-dependent cotyledon patterning similar to those of *PIN6*.

In summary, *PIN8* can provide functions similar to *PIN6* in *PIN1*-dependent cotyledon and vein development. Thus the unequal redundancy between *PIN6* and *PIN8* is unlikely the result of different functions of *PIN6* and *PIN8* and might instead be accounted for by their different expression.

3.2.5 Functions of *PIN5* in *PIN6*/*PIN8*-dependent vein-network formation

PIN6 is the only *ER-PIN* with functions in inhibition of vein network formation that are independent of *PIN5* (Figures 3.3; 3.4 and 3.8). We asked whether *PIN5* provided functions in vein network formation that are independent of *PIN6* or *PIN8*.

To address this question, we used plants expressing MP::PIN5 (*PIN5* cDNA driven by the *MP* promoter) because their vein networks are more complex than WT vein networks (Sawchuk et al. 2013) (Chapter 2; Figure 3.7). We reasoned that if *PIN5* provided functions that are independent of *PIN6* or *PIN8*, at least some of the effects of MP::PIN5 on vein network formation should persist in the MP::PIN6 or MP::PIN8 backgrounds. By contrast, if all *PIN5*'s functions depended on *PIN6* or *PIN8*, the effects of MP::PIN6 or MP::PIN8 on vein network formation should mask those of MP::PIN5. Because none of the vein network formation defects of MP::PIN5 persisted in the MP::PIN6 or MP::PIN8 backgrounds (Figure 3.7), we conclude that no function of *PIN5* escapes control by *PIN6* or *PIN8* (Figure 3.8B and 3.8C).

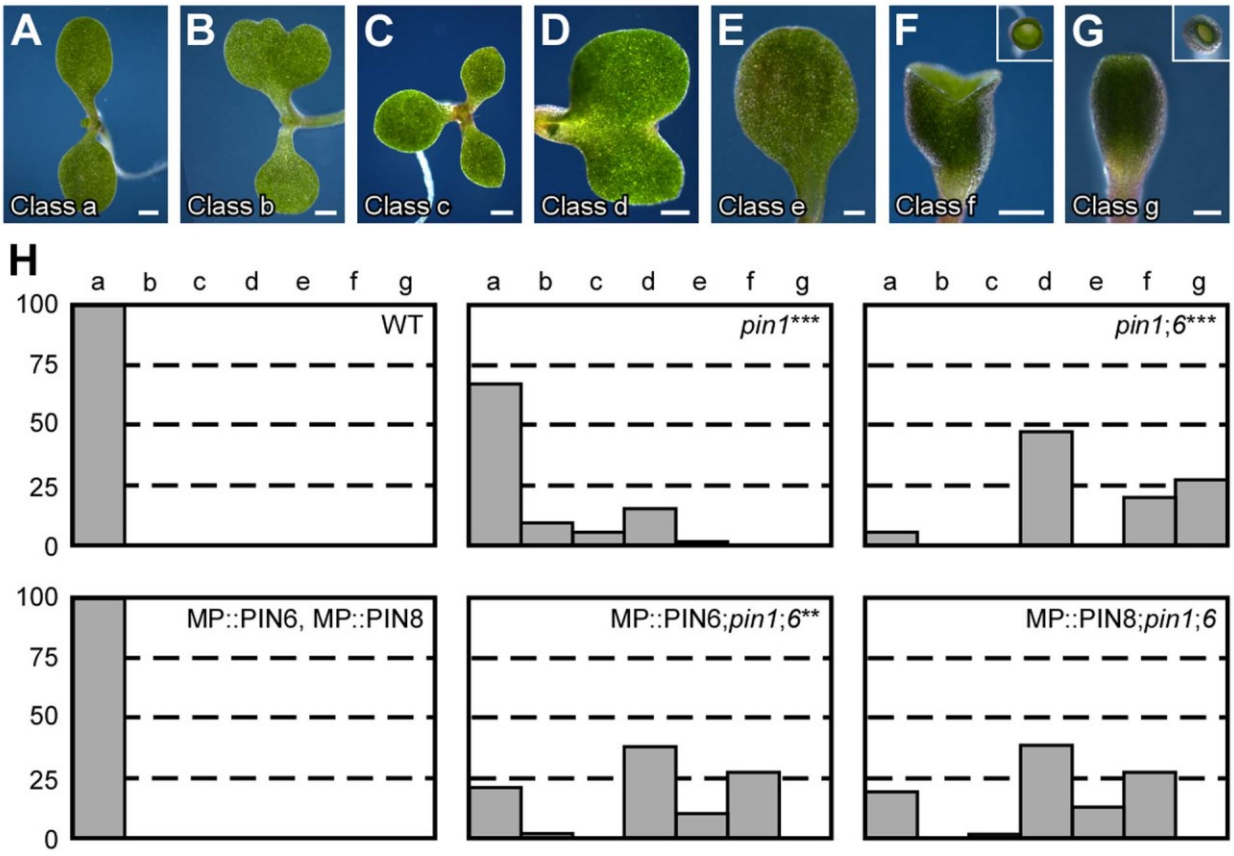

Figure 3.6. Functions of *PIN6* and *PIN8* in *PIN1*-dependent cotyledon patterning. (A-G) Dark-field illumination of 4-day old seedlings illustrating phenotype classes: two separate cotyledons (A); fused cotyledons and separate single cotyledon (B); three separate cotyledons (C); fused cotyledons (D); single cotyledon (E); partially fused cup-shaped cotyledons, side view; inset: top view (F); completely fused cup-shaped cotyledon, side view; inset: top view (G). (H) Percentages of seedlings in phenotype classes. Difference between *pin1* and WT, between *pin1*;*6* and *pin1*, between MP::PIN6;*pin1*;*6* and *pin1*;*6*, and between MP::PIN8;*pin1*;*6* and *pin1*;*6* was significant at $P<0.01$ (**) or $P<0.001$ (***) by Kruskal-Wallis and Mann-Whitney test with Bonferroni correction. Sample population sizes: WT, 53; *pin1*, 52; *pin1*;*6*, 55; MP::PIN6, 54; MP::PIN8, 49; MP::PIN6;*pin1*;*6*, 47; MP::PIN8;*pin1*;*6*, 62. Bars: (A-C) 1 mm; (D-F) 0.5 mm; (G) 0.25 mm.

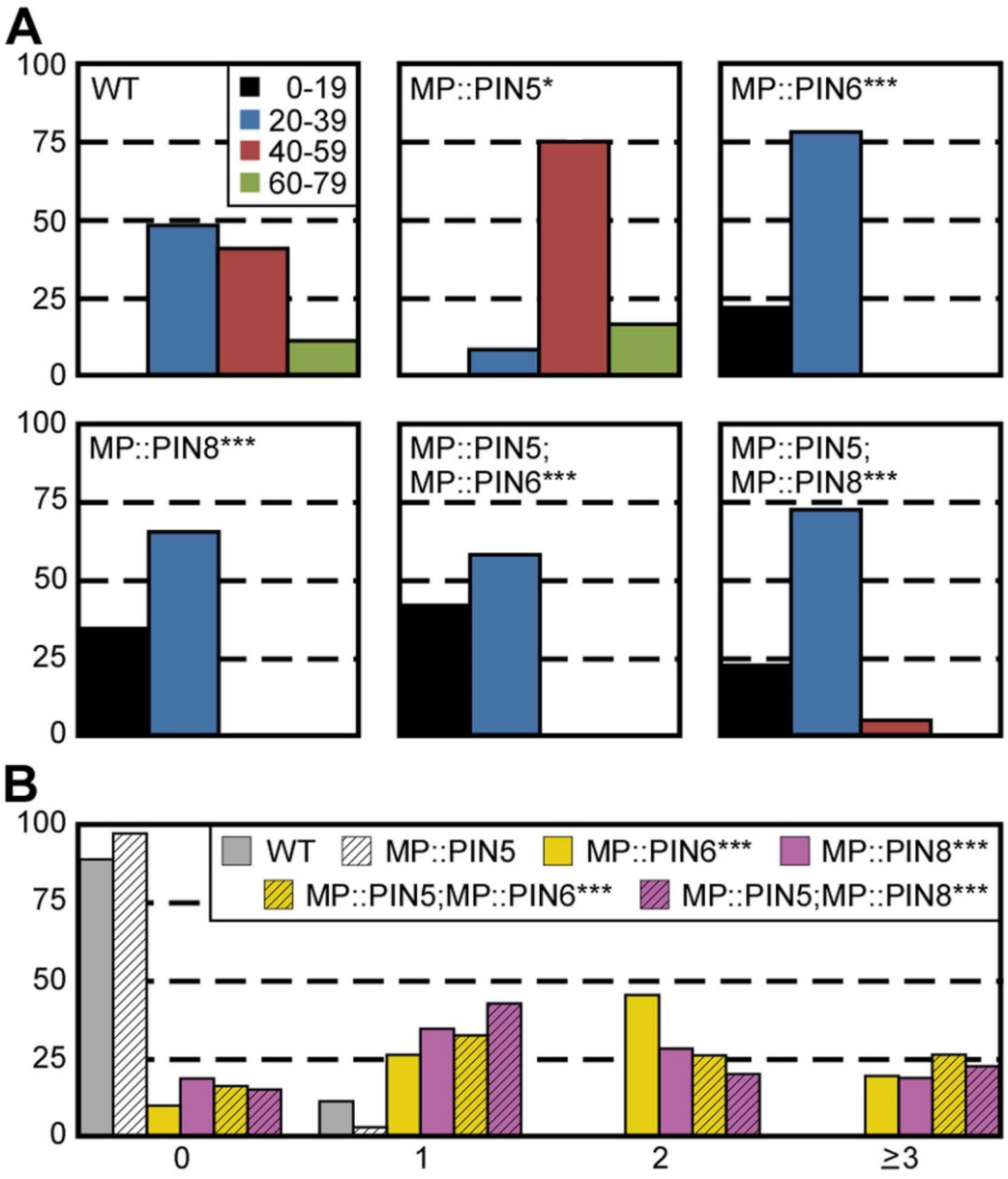

Figure 3.7. Functions of *PIN5* in *PIN6*/*PIN8*-dependent vein-network formation. (A) Percentages of first leaves in branching-point classes. Difference between MP::PIN5 and WT, between MP::PIN6 and WT, between MP::PIN8 and WT, between MP::PIN5;MP::PIN6 and MP::PIN5, and between MP::PIN5;MP::PIN8 and MP::PIN5 was significant at $P<0.05$ (*) or $P<0.001$ (***) by Kruskal-Wallis and Mann-Whitney test with Bonferroni correction. Sample population sizes: WT, 27; MP::PIN5, 36; MP::PIN6, 32; MP::PIN8, 32; MP::PIN5;MP::PIN6, 31; MP::PIN5;MP::PIN8, 40. (B) Percentage of first leaves with 0, 1, 2 or ≥3 open loops. Difference between MP::PIN6 and WT, between MP::PIN8 and WT, between MP::PIN5;MP::PIN6 and MP::PIN5, and between MP::PIN5;MP::PIN8 and MP::PIN5 was significant at $P<0.001$ (***) by Kruskal-Wallis and Mann-Whitney test with Bonferroni correction. Sample population sizes as in (A).

3.2.6 Control of vein network formation by auxin transport

One hypothesis to account for the functional overlap in vein network formation between PIN1-mediated intercellular auxin-transport and PIN6/PIN8-mediated intracellular auxin-transport the latter contributes to intercellular auxin transport—presumably by a mechanism non-homologous to that underlying PIN1-mediated intercellular auxin-transport; this hypothesis has been modeled assuming that expression of *ER-PIN* genes is restricted to sites of vein development (Wabnik et al. 2011b), an assumption supported by our data [(Sawchuk et al. 2013) (Chapter 2); this study].

One other, non-mutually exclusive hypothesis is that vein formation—the formation of efficient auxin transport canals—is promoted by prolonged exposure of incipient vascular cells to inductive auxin levels—a requirement consistent with available evidence (Mattsson et al. 2003; Wenzel et al. 2007)—and that such levels are, at least in part, the result of PIN1-mediated auxin transport toward sites of vein formation (Scarpella et al. 2006; Wenzel et al. 2007; Bayer et al. 2009) and of PIN6/PIN8-mediated increase in auxin levels within incipient vascular cells (Bosco et al. 2012; Ding et al. 2012; Bender et al. 2013; Cazzonelli et al. 2013; Sawchuk et al. 2013) (Chapter 2).

In either hypothesis, auxin would be inefficiently drained from developing leaves of *pin1* and *pin6*;*8*—an effect compounded in *pin1*;*6*;*8*—thus resulting in exposure of more leaf cells to inductive auxin levels for longer periods, thereby leading to formation of more veins that are more frequently interconnected and thus of more-complex vein networks.

Though it will be interesting to determine the basis for the functional overlap between PIN1-mediated intercellular auxin-transport and ER-PIN-mediated intracellular auxin-transport in vein network formation, it will be important to determine the level of evolutionary conservation of such functional overlap. However, mapping genetic interactions in non-model organisms requires predictive tools that allow reduction in the number of gene pairs to be tested experimentally, especially for genes—such as *PIN1*, *PIN5*, *PIN6* and *PIN8* [e.g., (Wang et al. 2009; Shen et al. 2010; Forestan et al. 2012; Pattison and Catala 2012; Roumeliotis et al. 2013; Wang et al. 2014)]—that have undergone duplication during evolution. In animals, conservation of genetic interactions is greater for genes expressed similarly (Zhong and Sternberg 2006; Lee et al. 2010). Thus our cellular expression map (Figure 3.8A) together with our experimentally defined genetic interactions (Figure 3.8C) provide a predictive—and thus testable—framework

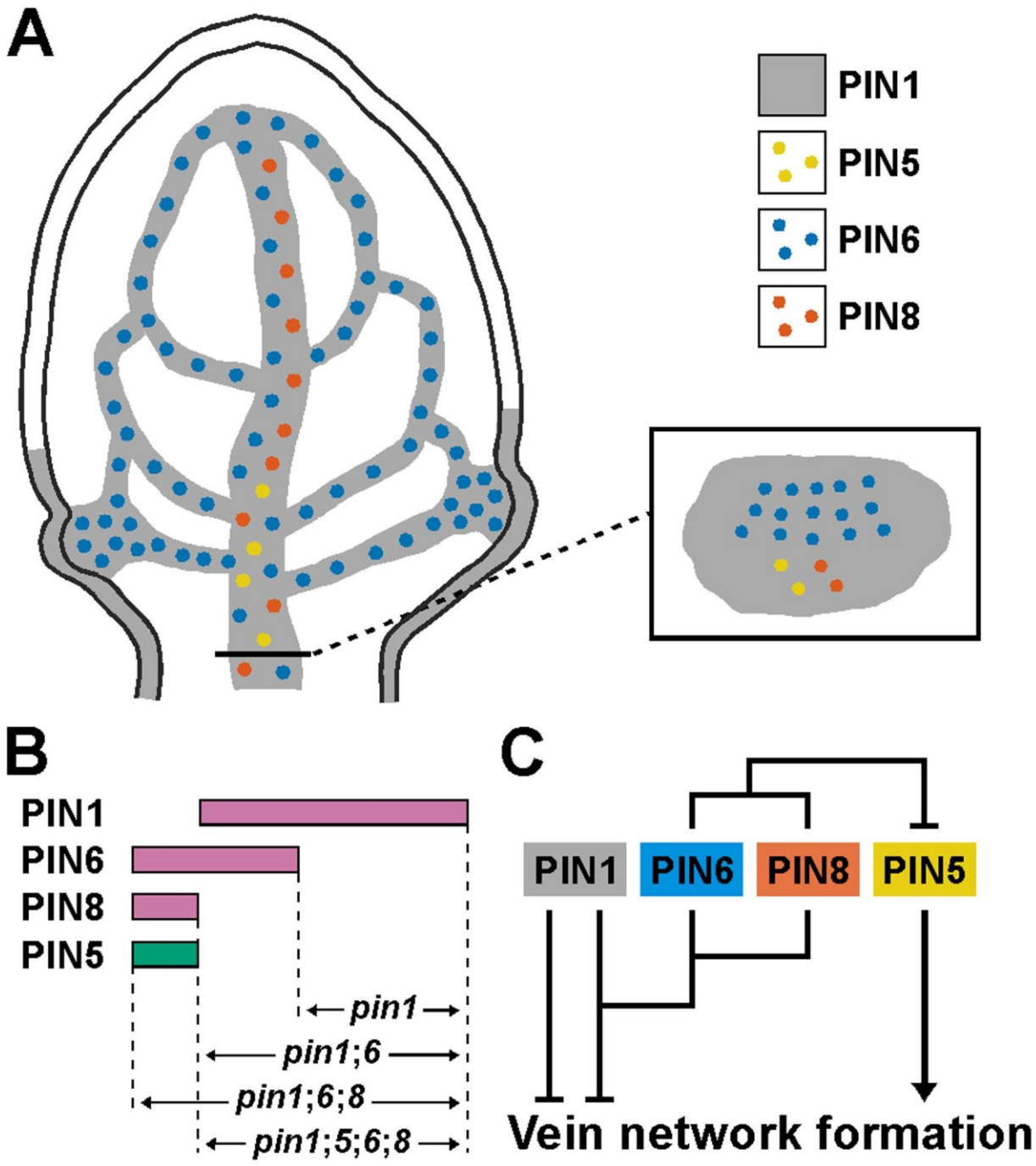

Figure 3.8. Summary and interpretations. (A) Cellular expression map of *PIN1*, *PIN5*, *PIN6* and *PIN8* in vein development. (B) Unique and redundant functions of *PIN1*, *PIN5*, *PIN6* and *PIN8* in vein network formation (pink, inhibiting functions; green, promoting functions) and derived mutant phenotypes. It is possible that *PIN8*'s functions overlap with *PIN6*'s in *PIN1*-dependent inhibition of vein network formation. (C) Genetic interaction network for *PIN1*, *PIN5*, *PIN6* and *PIN8* in vein network formation. Arrows indicate positive effects; blunt-ended lines indicate negative effects. See text for details.

to investigate functional conservation and repurposing of *PIN* genes and PIN-mediated auxin transport in vein network formation.

3.3 Materials and methods

3.3.1 Plants

Origin and nature of lines, genotyping strategies and oligonucleotide sequences are in Tables 3.1, 3.2, 3.3, respectively. Seeds were sterilized and germinated, and plants were grown and transformed as described in (Sawchuk et al. 2008).

3.3.2 Imaging

Developing leaves were mounted and imaged as in (Sawchuk et al. 2013) (Chapter 2). Marker-line-specific imaging parameters are in Tables 4 and 5. Mature leaves were fixed in 3:1 ethanol:acetic acid, rehydrated in 70% ethanol and water, cleared briefly (few seconds to few minutes) in 0.4 M sodium hydroxide, washed in water and mounted in 1:3:8 water:glycerol:chloral hydrate (Sigma-Aldrich Co. LLC.). Mounted leaves were imaged as in (Odat et al. 2014) (Chapter 4). Image brightness and contrast were adjusted by linear stretching of the histogram with ImageJ (National Institutes of Health). Images were cropped with Photoshop (Adobe Systems Inc.) and assembled into figures with Canvas (ACD Systems International Inc.).

Table 3.1. Origin and nature of lines.

Line	Origin/Nature
PIN1::PIN1:GFP	(Benkova et al. 2003)
PIN6::YFPnuc	(Sawchuk et al. 2013) (Chapter 2)
PIN8::YFPnuc	(Sawchuk et al. 2013) (Chapter 2)
PIN5::YFPnuc	Transcriptional fusion of *PIN5* (AT5G16530; -3279 to -3; primers: 'PIN5 SpeI KpnI transc forw' and 'PIN5 AgeI transc rev') to EYFP:3xNLS (Clontech Laboratories Inc.)
PIN6::CFPnuc	Transcriptional fusion of *PIN6* (AT1G77110; -3784 to -1; primers: 'PIN6 prom SalI F' and 'PIN6 prom BamHI R') to ECFP:3xNLS (Clontech Laboratories Inc.)
PIN8::PIN8:GFP	(Sawchuk et al. 2013) (Chapter 2)
pin1-1	(Goto 1987; Galweiler et al. 1998; Sawchuk et al. 2013); WT at the *TTG1* (AT5G24520) locus
pin5-4	(Mravec et al. 2009)
pin6	(Sawchuk et al. 2013)
pin8-1	(Bosco et al. 2012)
MP::PIN5	(Sawchuk et al. 2013) (Chapter 2)
MP::PIN6	(Sawchuk et al. 2013) (Chapter 2)
MP::PIN8	(Sawchuk et al. 2013) (Chapter 2)

Table 3.2. Genotyping strategies.

Line	Strategy
pin1-1	'pin1-1 F' and 'pin1-1 R'; *Tat*I
pin5-4	*PIN5*: 'SALK_042994 LP' and 'SALK_042994 RP'; *pin5*: 'SALK_042994 RP' and 'LBb1.3'
pin6	*PIN6*: 'PIN6 spm F' and 'PIN6 spm R'; *pin6*: 'PIN6 spm F' and 'Spm32'
pin8-1	*PIN8*: 'SALK_107965 LP' and 'SALK_107965 RP'; *pin8*: 'SALK_107965 RP' and 'LBb1.3'
MP::PIN5	'PIN5 ox SmaI forw' and 'PIN5 ox BamHI rev'
MP::PIN6	'PIN6 spm R' and 'WiscDsLox489-492C10 RP'
MP::PIN8	'SALK_107965 RP' and 'WiscDsLox489-492C10 RP'

Table 3.3. Oligonucleotide sequences.

Name	Sequence (5' to 3')
PIN5 SpeI KpnI transc forw	ATAACTAGTGGTACCGAGAGAGAGAGAGAGAGAC
PIN5 AgeI transc rev	CTCACCGGTTTTTATCAGAAAAATAGAAATGTTGCAG
PIN6 prom SalI F	GCGGTCGACTGATGATTGTTTAAGATAAG
PIN6 prom BamHI R	TCTGGATCCTCTTTGCCTCTTCTTCTTC
pin1-1 F	ATGATTACGGCGGCGGACTTCTA
pin1-1 R	TTCCGACCACCACCAGAAGCC
SALK_042994 LP	TGTGGTTGTGGGAGAGAAGTC
SALK_042994 RP	AAATTTGGACTTACGCTGTGC
LBb1.3	ATTTTGCCGATTTCGGAAC
PIN6 spm F	CATAACGAAGCTAACTAAGGGGTAATCTC
PIN6 spm R	GGAGTTCAAAGAGGAATAGTAGCAGAG
Spm32	TACGAATAAGAGCGTCCATTTTAGAGTG
SALK_107965 LP	TGAAAGACATTTTGATGGCATC
SALK_107965 RP	CCAAATCAAGCTTTGCAAGAC
PIN5 ox SmaI forw	ATACCCGGGATGATAAATTGTGGAGA
PIN5 ox BamHI rev	ATTGGATCCTTACGCTGTGCTTAGAA
WiscDsLox489-492C10 RP	TTGGAAAGGAAAAGAACACCC

Table 3.4. Imaging parameters: single-marker lines.

Line	Laser	Wavelength (nm)	Main dichroic beam splitter	First secondary dichroic beam splitter	Second secondary dichroic beam splitter	Emission filter (detector)
PIN1::PIN1:GFP	Ar	488	HFT 405/488/594	NFT 545	NFT 490	BP 505-530 (PMT3)
PIN6::YFPnuc	Ar	514	HFT 405/514/594	NFT 595	NFT 515	BP 520-555 IR (PMT3)
PIN8::YFPnuc	Ar	514	HFT 405/514/594	NFT 595	NFT 515	BP 520-555 IR (PMT3)
PIN5::YFPnuc	Ar	514	HFT 405/514/594	NFT 595	NFT 515	BP 520-555 IR (PMT3)

Table 3.5. Imaging parameters: double-marker lines.

Multi-marker lines	Single-marker lines	Laser	Wavelength (nm)	Main dichroic beam splitter	First secondary dichroic beam splitter	Second secondary dichroic beam splitter	Emission filter (detector)
PIN1::PIN1:GFP; PIN5::YFPnuc	PIN1::PIN1:GFP	Ar	488	HFT 405/488/594			507-593 (META)
	PIN5::YFPnuc	Ar	488	HFT 405/488/594			507-593 (META)
PIN1::PIN1:GFP; PIN6::YFPnuc	PIN1::PIN1:GFP	Ar	488	HFT 405/488/594			507-593 (META)
	PIN6::YFPnuc	Ar	488	HFT 405/488/594			507-593 (META)
PIN1::PIN1:GFP; PIN8::YFPnuc	PIN1::PIN1:GFP	Ar	488	HFT 405/488/594			507-593 (META)
	PIN8::YFPnuc	Ar	488	HFT 405/488/594			507-593 (META)
PIN6::CFPnuc; PIN5::YFPnuc	PIN6::CFPnuc	Ar	458	HFT 458/514	NFT 595	NFT 545	BP 475-525 (PMT2)
	PIN5::YFPnuc	Ar	514	HFT 458/514	NFT 595	NFT 515	BP 520-355 IR (PMT3)
PIN8::PIN8:GFP; PIN5::YFPnuc	PIN8::PIN8:GFP	Ar	488	HFT 405/488/594			507-593 (META)
	PIN5::YFPnuc	Ar	488	HFT 405/488/594			507-593 (META)

PIN6::CFPnuc; PIN8::YFPnuc	PIN6::CFPnuc	Ar	458	HFT 458/514	NFT 595	NFT 545	BP 475-525 (PMT2)
	PIN8::YFPnuc	Ar	514	HFT 458/514	NFT 595	NFT 515	BP 520-355 (PMT3)

CHAPTER 4: CHARACTERIZATION OF AN ALLELIC SERIES IN THE *MONOPTEROS* GENE OF ARABIDOPSIS

4.1 Introduction

Auxin is a central regulator of plant development: during embryogenesis, it controls patterning of the embryo parts; during post-embryonic development, it controls the patterned formation of lateral shoot organs and lateral roots, and of their tissues (De Smet and Jurgens 2007). The auxin signal is transduced by multiple pathways (Leyser 2010); best understood is that which ends with the transcriptional activation or repression of auxin-responsive genes by transcription factors of the AUXIN RESPONSE FACTOR (ARF) family (Chapman and Estelle 2009).

Of the 22 *ARF* genes in *Arabidopsis thaliana* (Guilfoyle and Hagen 2007), *MONOPTEROS* (*MP*)/*ARF5* is the only one whose mutation results in conspicuous patterning defects in embryos and seedlings (Okushima et al. 2005). In *mp* embryos and seedlings, hypocotyl and root are typically replaced by a conical structure with no apparent cellular organization ("basal peg"), but weak mutant alleles occasionally form a short hypocotyl (Berleth and Jurgens 1993) or both hypocotyl and root (Cole et al. 2009; Donner et al. 2009; Schlereth et al. 2010). In *mp*, the two cotyledons may be separate—as in wild-type (WT)—they may be fused to varying extents, or a single cotyledon may be formed (Berleth and Jurgens 1993). Invariably, however, the vein network of *mp* cotyledons is simplified (Berleth and Jurgens 1993). The severity of these defects has been shown to be inversely proportional to the amount of residual *MP* function and has thus been conventionally used as criterion to define allele strength (Berleth and Jurgens 1993; Hardtke and Berleth 1998; Cole et al. 2009; Donner et al. 2009; Schlereth et al. 2010).

Most *mp* alleles are in the Landsberg *erecta* background (Berleth and Jurgens 1993), and only seven, recessive *mp* alleles have been reported in the widely used Columbia (Col) background: two extensively characterized (mp^{G33} and mp^{S319}/*arf5-2*) and five only partially characterized (mp^{G12}, mp^{G25}, mp^{BS1354}, *arf5-1* and mp^{B4149}) (Przemeck et al. 1996; Hardtke and Berleth 1998; Okushima et al. 2005; Weijers et al. 2005; Cole et al. 2009; Donner et al. 2009; Schlereth et al. 2010). One of these five *mp* alleles (mp^{G25}) appears to be extinct and thus unavailable for

analysis. We show that two of the four remaining, partially characterized *mp* alleles reported to be in the Columbia background (mp^{BS1354} and mp^{B4149}) are in fact not in this background. We extend characterization of the remaining two Columbia alleles of *mp* (mp^{G12} and *arf5-1*), and we identify and characterize four new alleles of *mp* in the Columbia background (*mp-11*, *mp-12*, *mp-13* and *mp-14*), among which the first low-expression allele of *mp* (*mp-11*) and the strongest Columbia allele of *mp* (*mp-13*). These genetic resources provide the research community with new experimental opportunities for insight into the function of *MP*-dependent auxin signalling in plant development.

4.2 Results and discussion

We were unable to induce germination of seed stocks of mp^{G25}; it is therefore possible that this allele has to be considered extinct and thus unavailable for further analysis. Because WT-looking siblings of mp^{BS1354} and mp^{B4149} appeared different from Col plants (not shown), we characterized their background and found that mp^{BS1354} is in a Col/Wassilewskija mixed background (Figure 4.1B) and mp^{B4149} is in the Utrecht background (Figure 4.1C). We thus excluded these two alleles from further analysis.

The inviability of mp^{G25} seed stocks and the non-Col backgrounds of mp^{BS1354} and mp^{B4149} left only mp^{G12} and *arf5-1* as partially characterized *mp* alleles in the Col background. We thus surveyed available resources and identified seven additional, putative alleles of *mp* in the Col background: lines WiscDsLox489-492C10, SAIL_1265_F06, SALK_144183, SALK_149553, WiscDsLoxHs148_11H, WiscDsLoxHs148_12G and SALK_001058.

None of the 30 plants that grew from the seed stock of line SALK_144183 (predicted to have an insertion in the first intron of *MP*) or of the 60 plants that grew from the seed stock of line WiscDsLoxHs148_12G (predicted to have an insertion in the 10th exon of *MP*) had *mp*-like defects. Furthermore, we were unable to confirm the presence of insertion in *MP* in any of those plants. Finally, none of the progeny of those plants (~50 seedlings/plant) had *mp*-like defects. It is thus possible that lines SALK_144183 and WiscDsLoxHs148_12G are incorrectly annotated or that seeds that have inherited those insertions are extremely infrequent in the currently

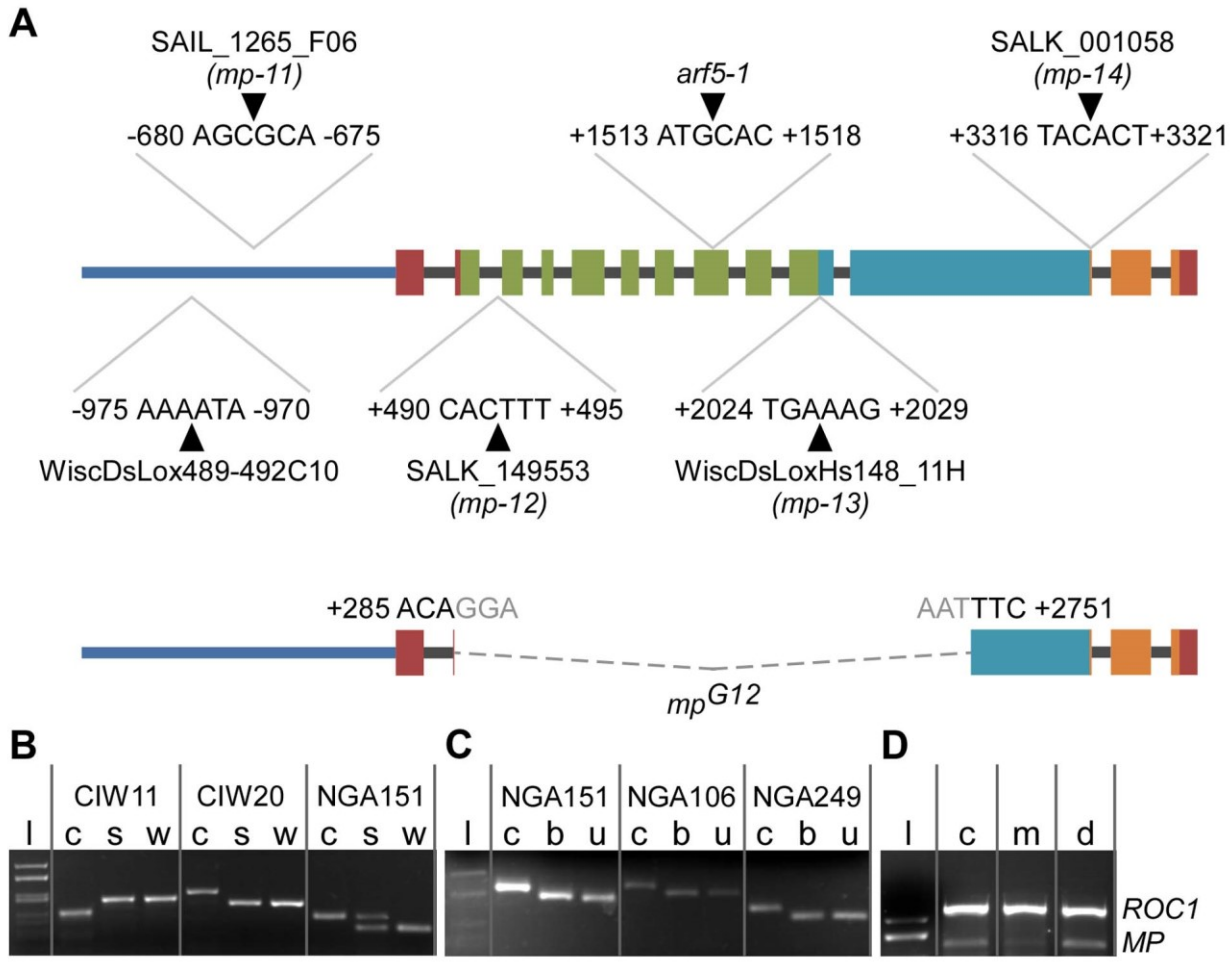

Figure 4.1. Mutations in the *MP* gene. (A) Schematic diagram of the *MP* gene indicating position of insertions (black triangles) in *mp* mutants (top) or nature of molecular lesion in mp^{G12} (bottom). Coordinates are in nucleotides relative to the first nucleotide of the start codon. Lines depict promoter (blue, -1500 to -1) or introns (grey). Boxes depict translated exons: brown, sequences with unclear function (+1 to +309 and +3744 to +3827); green, sequence encoding the DNA-binding domain (Ulmasov et al. 1999b) (+310 to +2018); teal, sequence encoding the activation domain (Tiwari et al. 2003) (+2019 to +3312); orange, sequence encoding the carboxyl-terminal dimerization domain (Guilfoyle and Hagen 2012) (+3313 to +3743). Dashed line depicts region of *MP* deleted in mp^{G12} and replaced with a sequence identical to sequences on all chromosomes (grey font, 5'-end of deletion) or with a sequence identical to gene AT1G16400 (grey font, 3'-end of deletion). See text for details. (B) Analysis of SSLP markers CIW11, CIW20, and NGA151 in Columbia (c), mp^{BS1354} (s), and Wassilewskija (w). l, molecular weight marker (*Hae*III-digested pBluescript II). (C) Analysis of SSLP markers NGA151, NGA106, and NGA249 in Columbia (c), mp^{B4149} (b), and Utrecht (u). l, molecular weight marker (*Hae*III-digested pBluescript II). (D) RT-PCR analysis of *MP* expression in 4-day-old seedlings of Columbia (c), SAIL_1265_F06/*mp-11* (m), and WiscDsLox489-492C10 (d). The nearly evenly expressed *ROC1* (Lippuner et al. 1994) was used as control. l, molecular weight marker (*Hae*III-digested pBluescript II).

available stocks.

We found a T-DNA insertion after nucleotide -973 of *MP*—nucleotide coordinates are relative to the first nucleotide of the start codon—in line WiscDsLox489-492C10 (Figure 4.1A), but seedlings homozygous for such insertion had no defects (not shown) or reduction in *MP* transcript (Figure 4.1D). We thus excluded line WiscDsLox489-492C10 from further analysis.

Here we extend the characterization of the Col alleles mp^{G12} and *arf5-1*, and we characterize four new alleles of *mp* in the Col background, including the first low-expression allele and the strongest Col allele.

We first determined the precise location of insertion in lines SAIL_1265_F06, SALK_149553, WiscDsLoxHs148_11H, and SALK_001058, and in *arf5-1*. We found a T-DNA insertion after nucleotide -678 of *MP* in line SAIL_1265_F06 (Figure 4.1A); seedlings homozygous for such insertion had lower levels of *MP* transcript (Figure 4.1D). Line SALK_149553 has a T-DNA insertion in the second intron of *MP* (Figure 4.1A). *arf5-1* has a T-DNA insertion in the eighth exon of *MP*, which encodes part of the DNA-binding domain (DBD) (Ulmasov et al. 1999b) (Figure 4.1A). Line WiscDsLoxHs148_11H has a T-DNA insertion in the 10^{th} exon of *MP*, at the beginning of the sequence encoding the activation domain (AD) (Ulmasov et al. 1999a; Tiwari et al. 2003) (Figure 4.1A). And line SALK_001058 has a T-DNA insertion in the 11^{th} exon of *MP*, at the beginning of the sequence encoding for the carboxyl-terminal domain (CTD), which mediates interaction with ARF proteins or with repressors of the AUX/IAA family (Guilfoyle and Hagen 2012) (Figure 4.1A). Next, we determined by PCR the nature of the *MP* lesion in mp^{G12} and found that in this allele part of the *MP* gene was missing (not shown). By Vectorette PCR, we found that the missing sequence extended from nucleotide +288 to nucleotide +2748 (Figure 4.1A). We isolated 435 bp of the sequence that preceded nucleotide +2748 of *MP* in mp^{G12} and found it to be identical to the sequence from nucleotide +2076 to nucleotide +1641 of gene AT1G16400. We also isolated 34 bp of the sequence that followed nucleotide +288 of *MP* in mp^{G12} and found it to be identical to a sequence present on all five chromosomes. Our results are thus consistent with those of RFLP mapping, suggesting that the mp^{G12} allele is the result of a large chromosomal defect (Hardtke and Berleth 1998).

We next analyzed the axis of seedlings homozygous for mp^{G12} or *arf5-1*, or for insertions SAIL_1265_F06, SALK_149553, WiscDsLoxHs148_11H, or SALK_001058. WT seedlings can

be formalized as a top-to-bottom sequence of pattern elements: shoot meristem, cotyledons, and seedling axis—composed of hypocotyl and root (Capron et al. 2009) (Figure 4.2A). In ~20-25% of the progeny of self-fertilized plants heterozygous for mp^{G12} (*n*=667) or *arf5-1* (*n*=626), or for insertions SAIL_1265_F06 (*n*=823), SALK_149553 (*n*=669), or WiscDsLoxHs148_11H (*n*=735), hypocotyl and root were replaced by a basal peg lacking the central vein typical of WT hypocotyl and root (Figure 4.2A,4.2B,4.2D,4.2E,4.2G). Approximately 22% (*n*=784) of the progeny of self-fertilized plants heterozygous for insertion SALK_001058 were rootless; the hypocotyl was missing from most rootless seedlings, but a short hypocotyl with its central vein was formed in small proportion (<1%) of them (Figure 4.2C and 4.2F). The proportion of rootless seedlings in the progeny of self-fertilized plants heterozygous for mp^{G12} or *arf5-1*, or for insertions SAIL_1265_F06, SALK_149553, WiscDsLoxHs148_11H, or SALK_001058, was not significantly different from that expected for a recessive phenotype associated with mutation in a single nuclear gene as tested by Chi-squared test (not shown). We renamed SAIL_1265_F06, SALK_149553, WiscDsLoxHs148_11H, and SALK_001058 as *mp-11*, *mp-12*, *mp-13*, and *mp-14*, respectively.

Next, we analyzed cotyledon patterns of seedlings homozygous for mp^{G12}, *arf5-1*, *mp-11*, *mp-12*, *mp-13*, or *mp-14*. WT seedlings had two separate cotyledons (Figure 4.3E). Nearly 75% of *mp-11* seedlings had two separate cotyledons, and all *mp-11* seedlings had at least one cotyledon (Figure 4.3E). Approximately 50% of mp^{G12} seedlings had two separate cotyledons, and all mp^{G12} seedlings had at least one cotyledon (Figure 4.3E). The spectrum of cotyledon pattern phenotypes of *arf5-1* seedlings was similar to that of *mp-12* seedlings: ~35-45% of seedlings had two separate cotyledons, and ~5% of seedlings had no cotyledons (Figure 4.3E). And the spectrum of cotyledon pattern phenotypes of *mp-13* seedlings was similar to that of *mp-14* seedlings: ~15-20% of seedlings had two separate cotyledons, and ~5% of seedlings had no cotyledons (Figure 4.3E).

Finally, we analyzed cotyledon vein patterns of seedlings homozygous for mp^{G12}, *arf5-1*, *mp-11*, *mp-12*, *mp-13*, or *mp-14*. Four days after germination, nearly 75% of WT cotyledons had a central midvein and at least four vein loops (phenotype class I); ~25% had a simpler vein pattern, with a central midvein and up to three loops (class II) (Figure 4.4A,4.4B,4.4F). Nearly 35% of *mp-11* cotyledons belonged to class I, ~45% belonged to class II, ~5% had no loops (class III),

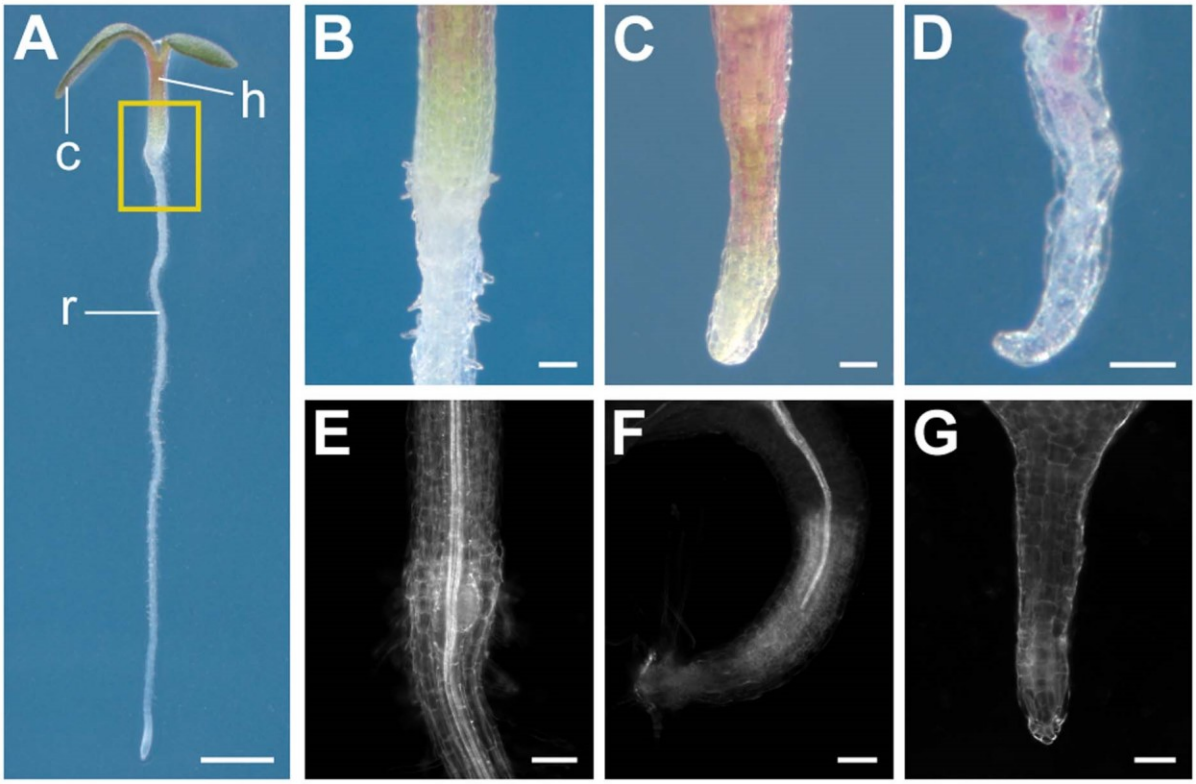

Figure 4.2. Seedling axis defects of *mp* alleles. (A-G) Dark-field illumination of seedlings 3 days after germination. (A,B,E) WT. c, cotyledon; h, hypocotyl; r, root. (C,D,F,G) *mp*. (A-D) Live. (E-G) Cleared; mature veins appear bright due to their refraction properties. (B,E) Hypocotyl-root transition zone. Detail of an area as boxed in (A). (C,F) Hypocotyl-basal peg transition zone. (D,G) Basal peg. Bars: (A) 1 mm; (B-G) 0.1 mm.

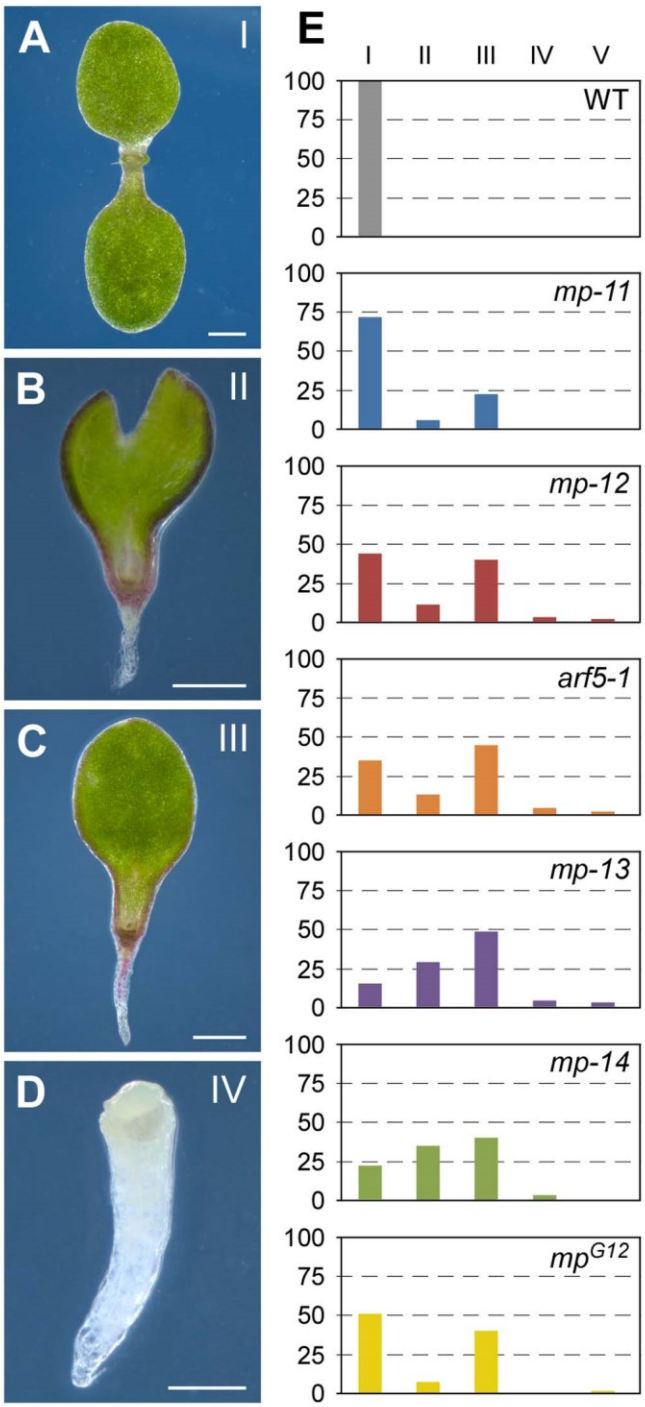

Figure 4.3. Cotyledon pattern defects of *mp* alleles. (A-D) Dark-field illumination of seedlings 4 days after germination illustrating phenotype classes: Class I, two separate cotyledons (A); Class II, fused cotyledons (B); Class III, single cotyledon (C); Class IV, no cotyledons (D). Other, infrequent cotyledon-pattern defects were grouped in Class V (not shown). (E) Percentage of seedlings in phenotype classes. Sample population sizes: WT, 191; *mp-11*, 168; *mp-12*, 188; *arf5-1*, 164; *mp-13*, 179; *mp-14*, 172; mp^{G12}, 207. Bars: (A-C) 0.5 mm; (D) 0.25 mm.

~10% had a vein pattern in which the midvein bifurcated near the cotyledon tip (class IV), and nearly 5% had no veins (class V) (Figure 4.4C-4.4F). Most (~55%) of *mp-14* cotyledons belonged to class II, and the remaining ~45% were nearly equally distributed among classes III-V (Figure 4.4F). The spectrum of vein pattern phenotypes of *mp-12* cotyledons was similar to that of *arf5-1* cotyledons and of mp^{G12} cotyledons: ~5-10% belonged to class II, ~65-70% to class III, and 25-35% to class V (Figure 4.4F). Approximately 45% of *mp-13* cotyledons belonged to class III, and ~50% belonged to class V (Figure 4.4F).

Our results suggest that *mp-11* is the weakest of the Col alleles characterized here and the first low-expression allele of *mp*. Insertion after nucleotide -973 of *MP* in line WiscDsLox489-492C10 results in WT-looking individuals with normal levels of *MP* transcript. By contrast, insertion after nucleotide -678 of *MP* in *mp-11* results in ~30% reduction in levels of *MP* transcript and defects in hypocotyl and root formation, cotyledon separation and vein patterning. This suggests that the 295-bp region of the *MP* promoter from nucleotide -972 to nucleotide -678—which contains putative binding sites for several transcription-factor families (Figure 4.5)—might be required for *MP* function in these processes. Though it will be interesting to determine whether any of the putative regulatory elements in this promoter region are required for functional *MP* expression, the low-expression allele *mp-11* could already be used to test the hypothesis that *MP* expression dynamics are dependent on *MP* levels (Lau et al. 2011).

Our results also suggest that *mp-13* is the strongest Col allele available. *mp-13* has an insertion at the beginning of the sequence that encodes MP's AD. It is difficult to explain how such mutation could result in stronger defects than those of mp^{G12}, in which the entire sequence encoding MP's DBD is missing. However, part of the sequence encoding MP's AD and the entire sequence encoding MP's CTD are present in mp^{G12}, and a similar *ARF* fragment has been shown to be sufficient to enhance auxin-responsive gene expression (Ulmasov et al. 1999a). Should the mp^{G12} allele be transcribed and translated, the resulting gene product might thus account for the weaker defects of mp^{G12} relative to those of *mp-13*. Alternatively, should the *mp-13* allele be transcribed and translated, the resulting protein—presumably lacking AD and CTD—might still be able to occupy MP binding sites in target promoters. Binding of such truncated protein might prevent binding of ARF proteins whose function is redundant to that of MP (e.g., (Hardtke et al. 2004)) and might thus account for the stronger defects of *mp-13* relative

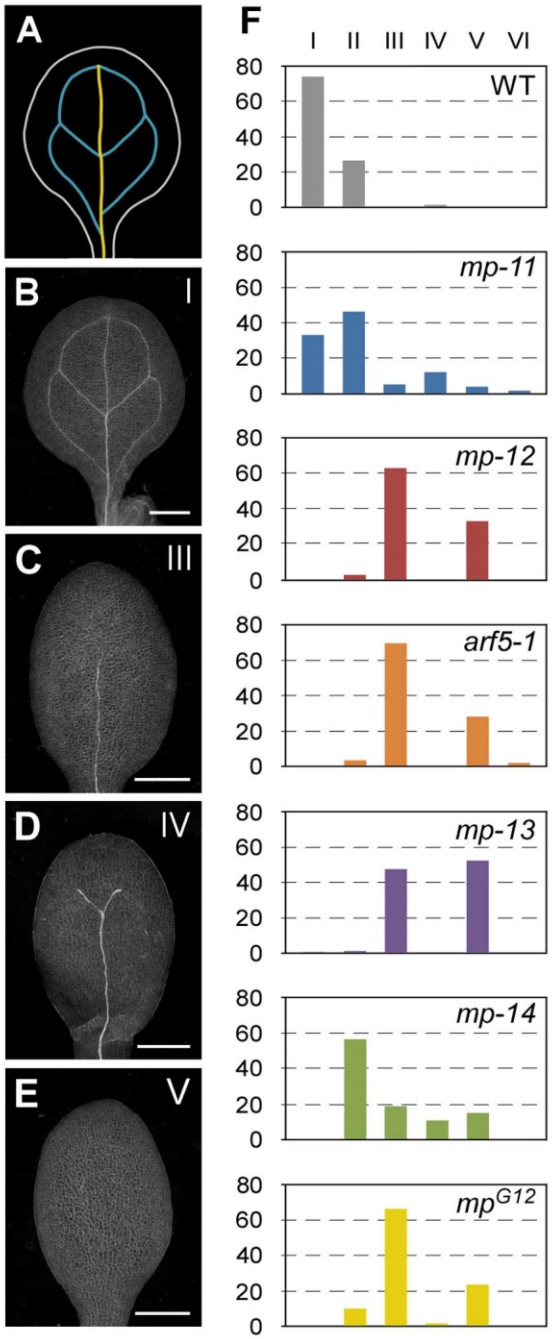

Figure 4.4. Vein pattern defects of *mp* alleles. (A,B) Vein pattern of WT mature cotyledon. In (A), yellow, midvein; blue, vein loops. (B-E) Dark-field illumination of cleared cotyledons 4 days after germination illustrating phenotype classes: Class I, unbranched midvein and four or more loops (B); Class III, solitary, unbranched midvein (C); Class IV, bifurcated midvein (D); Class V, no veins (E). Class II is defined by unbranched midvein and up to three loops (not shown). Other, infrequent vein-pattern defects were grouped in Class VI (not shown). (F) Percentage of cotyledons in phenotype classes. Samples population sizes: WT, 191; *mp-11*, 168; *mp-12*, 188; *arf5-1*, 164; *mp-13*, 179; *mp-14*, 172; mp^{G12}, 207. Bars: (B-E) 0.5 mm.

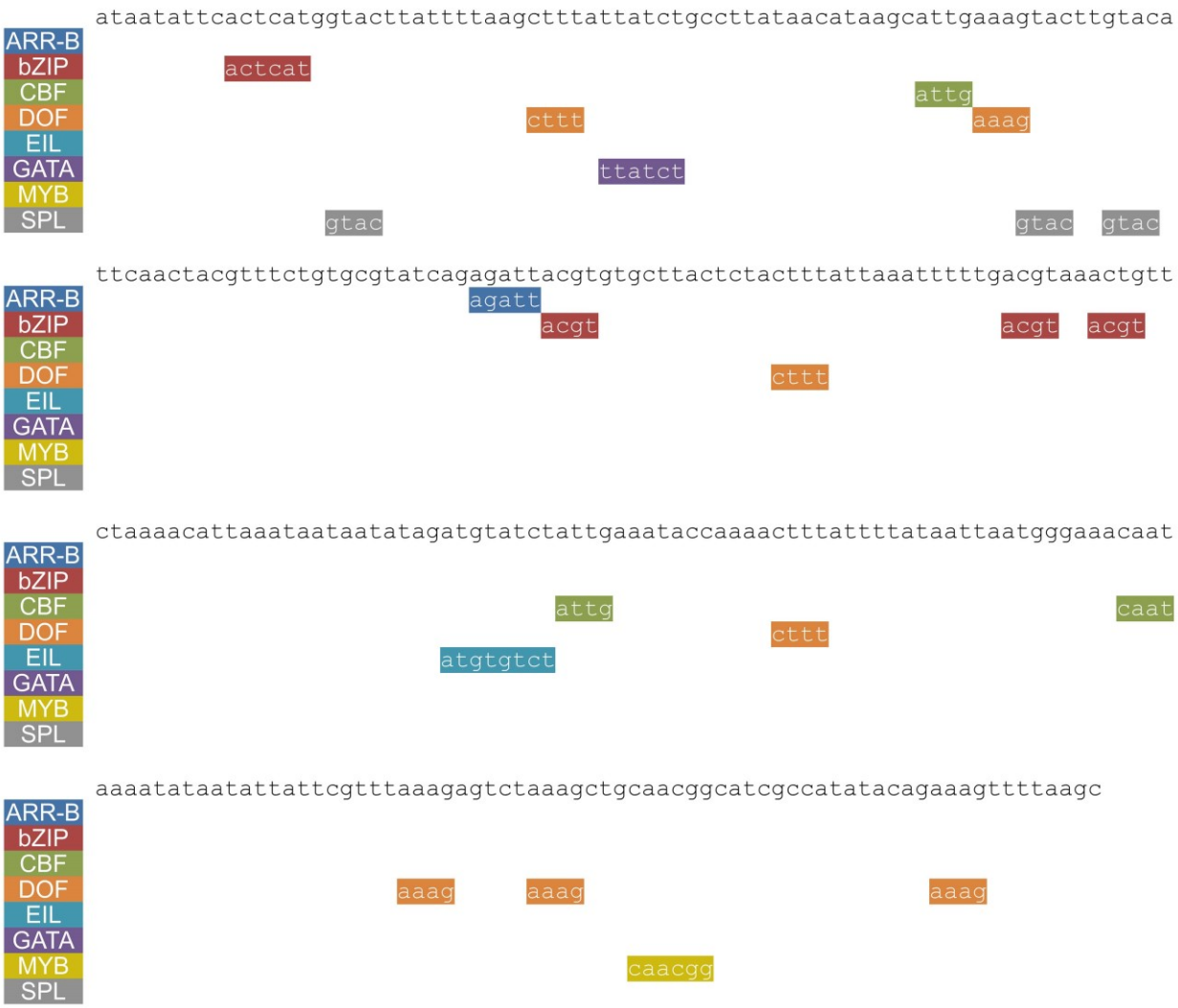

Figure 4.5. Putative transcription-factor binding sites in the 295-bp region of the *MP* promoter from nucleotide -972 to nucleotide -678. Putative binding sites for transcription factors of the ARR-B (Hosoda et al. 2002), bZIP (Jakoby et al. 2002; Satoh et al. 2004), CBF (Bezhani et al. 2001), DOF (Yanagisawa 2002), EIL (Kosugi and Ohashi 2000), GATA (Reyes et al. 2004), MYB (Prouse and Campbell 2012), and SPL (Birkenbihl et al. 2005) families are below sequence. Putative transcription-factor binding sites were identified as in (Donner and Scarpella 2012). Presence of intact core sequence for each bioinformatically identified transcription-factor binding site was manually confirmed.

to those of *mp*^{G12}. However, these and other possibilities remain to be tested experimentally.

Unlike the defects of all the other *mp* alleles characterized here, the defects of *mp-14* appeared more or less severe depending on the phenotype feature used to asses strength: as weak alleles in other backgrounds (Berleth and Jurgens 1993), *mp-14* seedlings occasionally form a short hypocotyl with a central vein; by contrast, cotyledon separation defects of *mp-14* are similar to those of *mp-13*, the strongest Col allele; and vein pattern defects of *mp-14* are intermediate between those of *mp-13* and those of *mp-11*, the weakest allele described here. *mp-14* has an insertion at the beginning of the sequence encoding for MP's CTD, which mediates interaction with ARF proteins or AUX/IAA repressors (Guilfoyle and Hagen 2012). The unusual behavior of *mp-14* might thus reflect the uneven contribution of these interactions to different developmental processes. This conclusion is consistent with the finding that *mp*^{S319}/*arf5-2*, which has an insertion only a few nucleotides downstream of the location of the *mp-14* insertion, has completely penetrant defects only in some of the developmental processes that depend on *MP* (Cole et al. 2009; Donner et al. 2009; Schlereth et al. 2010); it is also consistent with the finding that an MP protein lacking the entire CTD supplies semidominant functions only in a subset of *MP*-dependent developmental processes (Krogan et al. 2012).

In conclusion, by characterizing six mutant alleles of *MP* in the Col background—including four new alleles, among which the first low-expression allele and the strongest Col allele—we have provided the research community with new genetic resources to understand the role of *MP*-dependent auxin signalling in plant development.

4.3 Materials and methods

4.3.1 Plants

Origin of lines is in Table 4.1. Unless otherwise stated, seeds were sterilized and germinated as in the work by (Sawchuk et al. 2008). Genotyping strategies are in Table 4.2. Oligonucleotide sequences are in Table 4.3.

Table 4.1. Origin of lines.

Line Name	Origin
mp^{BS1354}	(Hardtke and Berleth 1998)
mp^{B4149}	(Weijers et al. 2005)
SALK_144183	ARBC; (Alonso et al. 2003)
WiscDsLoxHs148_12G	ARBC (CS914207); (Zhang et al. 2003; Nishal et al. 2005; Woody et al. 2007)
WiscDsLox489-492C10	ARBC (CS858306); (Woody et al. 2007)
mp^{G12}	(Hardtke and Berleth 1998)
arf5-1	(Okushima et al. 2005)
mp-11/SAIL_1265_F06	ARBC (CS879048); (Sessions et al. 2002)
mp-12/SALK_149553	ARBC; (Alonso et al. 2003)
mp-13 /WiscDsLoxHs148_11H	ARBC (CS914200); (Zhang et al. 2003; Nishal et al. 2005; Woody et al. 2007)
mp-14/SALK_001058	ARBC; (Alonso et al. 2003)

Table 4.2. Genotyping strategies.

Line	Strategy
SALK_144183	*MP*: 'SALK_144183 LP' and ' SALK_144183 RP '; *mp*.: 'SALK_144183 RP' and ' LBb1.3'
WiscDsLoxHs148_12G	*MP*: WiscDsLoxHs148_12G/148_11H LP ' and WiscDsLoxHs148_12G/149_11H RP '; *mp*: WiscDsLoxHs148_12G/149_11H RP ' and 'L4'
WiscDsLox489-492C10	*MP*: 'WiscDsLox489-492C10 LP' and 'WiscDsLox489-492C10 RP'; *mp*: 'WiscDsLox489-492C10 RP' and 'p745'
mp^{G12}	*MP*: 'BS1354-F' and 'BS1354-R'; *mp*: ' G12 inst 2 forw ' and ' MP vec2 Rev '
arf5-1	*MP*: 'SALK_023812 LP' and 'SALK_023812 RP' *mp*: ' MP2082-AS ' and 'LBb1.3';
mp-11/SAIL_1265_F06	*MP*: SAIL_1265_F06LP ' and ' SAIL_1265_F06RP '; *mp*: ' SAIL_1265_F06RP ' and 'LB3'
mp-12/SALK_149553	*MP*: 'SALK_149553 LP' and 'SALK_149553 RP'; *mp*: 'SALK_149553 RP' and 'LBb1.3'
mp-13/WiscDsLoxHs148_11H	*MP*: WiscDsLoxHs148_12G/148_11H LP ' and WiscDsLoxHs148_12G/149_11H RP '; *mp*: WiscDsLoxHs148_12G/149_11H RP ' and 'L4'
mp-14/SALK_001058	*MP*: 'SALK_001058 LP' and 'SALK_001058 RP'; *mp* 'SALK_001058 RP' and 'LBb1.3'

Table 4.3. Oligonucleotide sequences.

Primer Name	Sequence (5' to 3')
SALK_144183 LP	AGAAACCTCCATGTGTGCTTG
SALK_144183 RP	AATTCCTCTGGTTTGTCCTGG
LBb1.3	ATTTTGCCGATTTCGGAAC
WiscDsLoxHs148_12G/148_11H LP	TTTGTCCTTTGAAAATGTGCC
WiscDsLoxHs148_12G/149_11H RP	GTTAGCTTGTTTTGTGGCTGC
L4	TGATCCATGTAGATTTCCCGGACATGAAG
WiscDsLox489-492C10LP	GGCTCTTGCCTCTTCTCTTTC
WiscDsLox489-492C10RP	TTGGAAAGGAAAAGAACACCC
p745	AACGTCCGCAATGTGTTATTAAGTTGTC
BS1354-F	GAGATGGCCTGGTTCTAAGTGGC
BS1354-R	GCCAGTTCAACATCTCGGTTATCG
G12 inst 2 forw	GGATAAAGGTTTGATGCCAAGCGTG
MP vec2 Rev	CAAGAGACTGGAAGGAAGAGACTTGTG
SALK_023812 LP	GAGAGGAAGTAAGCACCCGAC
SALK_023812 RP	TCATTACATCCAGGCTCATCC
MP2082-AS	ATGGATGGAGCTGACGTTTGAGTTCGGACTCAAACGTCAGCTCCATCCA
SAIL_1265_F06LP	GCTTCATCTCTTCAAGCAAGG
SAIL_1265_F06RP	TCCCAAAGTCTCACCACTCAC
LB3	TAGCATCTGAATTTCATAACCAATCTCGATACAC
SALK_149553 LP	AATTCCTCTGGTTTGTCCTGG-
SALK_149553 RP	AGAAACCTCCATGTGTGCTTG
SALK_001058 LP	ATGGACTTGAGCAGTCAATGG
SALK_001058 RP	CCTTCTTCACTCATCTGCTGG
CIW11 Primer 1	CCCCGAGTTGAGGTATT
CIW11 Primer 2	GAAGAAATTCCTAAAGCATTC
CIW20 Primer 1	CATCGGCCTGAGTCAACT
CIW20 Primer 2	CACCATAGCTTCTTCCTTTCTT
NGA151 Primer 1	CAGTCTAAAAGCGAGAGTATGATG
NGA151 Primer 2	GTTTTGGGAAGTTTTGCTGG
NGA106 Primer 1	TGCCCCATTTTGTTCTTCTC
NGA106 Primer 2	GTTATGGAGTTTCTAGGGCACG
NGA249 Primer 1	GGATCCCTAACTGTAAAATCCC
NGA249 Primer 2	TACCGTCAATTTCATCGCC

V-PCR FORWARD	TACAGGAGAGGACGCTGTCTGTCGAAGGTAAGGA ACGGACGAGAGAAGGGAGAG
V-PCR rev	CTCTCCCTTCTCGAATCGTAACCGTTCGTACGAGA ATCGCTGTCCTCTCCTG
V3	ATCGTAACCGTTCGTACGAGAATCGC
MP pro1 forw	GAGAGAGAAAGAGAAGAGGCAAGAGC
MP vec1 Rev	CATCTTGAGCAAAGCTAGTGTTGTTG
V4	ACCGTTCGTACGAGAATCGCTGTC
MP pro3 forw	GCTAAAGCCTAGTTAGTGTTGAGTGTGG
MP 1993 geno	TCGGGTCAGTCCATGGGATATCG
ROC1 F	CAAACCTCTTCTTCAGTCTGATAGAGA
ROC1 R	GAGTGCTCATTCCTTATTTCTGGTAG

4.3.2 Vectorette PCR

About 500 ng of *mp*^{G12} DNA were digested with *Csp*6I for two hours and ligated to a vectorette unit generated by annealing the "V-PCR FORWARD" and "V-PCR rev" oligonucleotides (Table 4.3). The sequences flanking the ligated vectorette unit were amplified with Phusion High-Fidelity DNA Polymerase (Thermo Fisher Scientific inc., Waltham, MA) and the "V3" and "MP pro1 forw", or the "V3" and "MP vec1 Rev", oligonucleotides (Table 4.3). The resulting product was amplified with the "V4" and "MP pro3 forw", or the "V4" and "MP vec2 Rev", oligonucleotides (Table 4.3), and sequenced.

4.3.3 RT-PCR

Total RNA was extracted as in the work by (Chomczynski and Sacchi 1987) from 4-day-old seedlings grown in half-strength Murashige and Skoog salts (Caisson Laboratories, North Logan, UT), 15 g l^{-1} sucrose (BioShop Canada Inc., Burlington, Canada), 0.5 g l^{-1} MES (BioShop Canada Inc.), pH 5.7, at 25°C under continuous light (~65 µmol m^{-2} sec^{-1}) on a rotary shaker at 50 rpm. RT-PCR was performed on 100 ng of total RNA with the "MP 1993 geno" and "WiscDsLoxHs148_12G/149_11H RP" oligonucleotides (Table 4.3), and with the "ROC1 F" and "ROC1 R" oligonucleotides (Beeckman et al. 2002) (Table 4.3), using the Access RT-PCR System (Promega, Fitchburg, WI).

4.3.4 Imaging

Three-day-old seedlings were fixed, cleared, and mounted as in (Scarpella et al. 2004). Images were acquired with an Olympus SZ61TR (Olympus Corporation, Shinjuku, Japan) or an AxioImager.M1 (Carl Zeiss AG, Oberkochen, Germany) microscope equipped with an AxioCam HR camera (Carl Zeiss AG, Oberkochen, Germany) or a Hamamatsu ORCA-AG camera (Hamamatsu Photonics K.K., Hamamatsu, Japan), respectively. Brightness and contrast were adjusted by linear stretching of the histogram with ImageJ (Rasband 1997). Images were cropped with Adobe Photoshop 7.0 (Adobe Systems Inc., San Jose, CA) and assembled into figures with Canvas 8.0 (ACD Systems Inc., Victoria, Canada).

CHAPTER 5: A TISSUE CELL-POLARIZING SIGNAL UPSTREAM OF CARRIER-MEDIATED AUXIN TRANSPORT INDUCES VEIN FORMATION

5.1 Introduction

How cell polarity is coordinated across domains of cells is a central question in biology. In animals, such tissue cell polarization often involves extensive cell movements [e.g., (Ciruna et al. 2006; Yin et al. 2008)]. Cell movements are instead prevented in plants by a wall that holds cells in place; thus plants are a simplified system in which to address the question of tissue cell polarization. In both plants and animals, cell polarity can be coordinated within one-dimensional cell files [e.g., (Masucci and Schiefelbein 1994; Herwig et al. 2011)], two-dimensional cell sheets [e.g., (Piepho 1955; Heisler et al. 2005)] or three-dimensional cell blocks [e.g., (Steinmann et al. 1999; Boehm et al. 2010)].

The formation of veins in the inner tissue of plant leaves is an expression of three-dimensional tissue cell-polarization (Sachs 1991a; Sachs 2000; Boutte et al. 2007; Nakamura et al. 2012). Consider, for example, the formation of the midvein at the centre of the cylindrical leaf primordium. Initially, the plasma-membrane (PM)-localized PIN-FORMED1 (PIN1) auxin effluxer of *Arabidopsis thaliana* (Galweiler et al. 1998; Petrasek et al. 2006) is uniformly expressed in all the inner cells of the leaf primordium (Benkova et al. 2003; Reinhardt et al. 2003; Heisler et al. 2005; Scarpella et al. 2006; Wenzel et al. 2007; Bayer et al. 2009). Over time, however, PIN1 expression becomes gradually restricted to the file of cells that will form the midvein. PIN1 localization at the PM of the inner cells is initially isotropic—or nearly so—but, as PIN1 expression becomes restricted to the site of midvein formation, PIN1 localization becomes polarized: in the cells increasingly close to the developing midvein, PIN1 localization gradually changes from isotropic to medial—toward the developing midvein in the middle of the leaf primordium—to mediobasal; in the cells of the developing midvein, PIN1 becomes uniformly localized toward the base of the leaf primordium, where the midvein will connect to

the pre-existing vasculature. Both the restriction of PIN1 expression and the polarization of PIN1 localization initiate and proceed away from pre-existing vasculature, and are thus polar.

That vein formation is an expression of tissue cell polarization is also reflected in the relation between the parts of the mature vein and between the mature vein and the parts of the plant: vascular elements are elongated along the axis of the vein and connected to one another through their short sides (Esau 1942); as veins primarily connect shoot organs with roots (Dengler 2006), veins and their elements are unequal at their ends—one end connects with shoot tissues, the other with root tissues—and thus polar (Sachs 1975). Not all the mature veins in closed networks such as those of Arabidopsis leaves have unambiguous shoot-to-root polarity, but the vein networks themselves are polar (Sachs 1975).

The correlation between polar auxin transport—as expressed by the auxin-transport-polarity-defining localization of PIN1 (Wisniewska et al. 2006)—and polar vein formation is not coincidental. Auxin application to developing leaves induces the formation of broad expression domains of isotropically localized PIN1; such domains become restricted to the sites of auxin-induced vein formation, and PIN1 localization becomes polarized toward the pre-existing vasculature (Scarpella et al. 2006). Both the restriction of PIN1 expression and the polarization of PIN1 localization that occur during normal leaf development are slowed down by chemical inhibition of auxin transport (Scarpella et al. 2006; Wenzel et al. 2007), which induces vein-pattern defects similar to—though stronger than—those of *pin1* mutants (Mattsson et al. 1999; Sieburth 1999; Bilsborough et al. 2011; Guenot et al. 2012; Sawchuk et al. 2013) (Chapter 2). Thus available evidence suggests that auxin induces tissue cell polarization and derived polar vein formation, and that such inductive and orienting property of auxin strictly depends on the function of *PIN1* and possibly of other *PIN* genes.

Here we experimentally tested this hypothesis. Our results suggest that: (i) auxin-induced polar vein formation occurs in the absence of the function of PIN proteins or of any known intercellular auxin transporter; (ii) the vein patterning activity independent of carrier-mediated auxin transport relies, at least in part, on the auxin signal transduction mediated by the TRANSPORT INHIBITOR RESPONSE1/AUXIN SIGNALLING F-BOX (TIR1/AFB) auxin receptors and the MONOPTEROS (MP) auxin-responsive transcription factor; and (iii) a tissue cell-polarizing signal that depends on the function of the GNOM guanine-nucleotide exchange

factor for ADP-rybosilation-factor GTPases acts upstream of carrier-mediated auxin transport and—based on previous evidence (Mayer et al. 1993)—of TIR1/AFB/MP-mediated auxin signalling.

5.2 Results

5.2.1 Contribution of plasma-membrane-localized PIN proteins to vein patterning

In Arabidopsis, the PIN family of auxin transporters is composed of eight members (Paponov et al. 2005; Krecek et al. 2009; Viaene et al. 2012): PIN5, PIN6 and PIN8, which are localized to the endoplasmic reticulum (ER) (Mravec et al. 2009; Bosco et al. 2012; Ding et al. 2012; Sawchuk et al. 2013) (Chapter 2); and PIN1, PIN2, PIN3, PIN4 and PIN7, which are localized to the plasma membrane (PM) and catalyze cellular auxin efflux (Chen et al. 1998; Galweiler et al. 1998; Luschnig et al. 1998; Muller et al. 1998; Friml et al. 2002a; Friml et al. 2002b; Friml et al. 2003; Petrasek et al. 2006). Sequence analysis divides the PM-localized subfamily of PIN (PM-PIN) proteins into three groups: the PIN1 group, the PIN2 group and the PIN3 group, which also contains PIN4 and PIN7 (Krecek et al. 2009; Viaene et al. 2012).

Mutants of the *PM-PIN* gene *PIN1* are the only *pin* single mutants with vein pattern defects, and vein pattern defects of double mutants between *pin1*—on the one hand—and mutants of the *PM-PIN* genes *PIN2*, *PIN3*, *PIN4* or *PIN7*—on the other—are no different from vein pattern defects of *pin1* single mutants (Sawchuk et al. 2013) (Chapter 2), suggesting that either *PIN2*, *PIN3*, *PIN4* and *PIN7* have no function in *PIN1*-dependent vein patterning or their function in this process is redundant. To discriminate between these hypotheses, we first assessed the collective contribution to *PIN1*-dependent vein patterning of the *PM-PIN* genes of the *PIN3* group (*PIN3*, *PIN4* and *PIN7*), whose translational fusions to GFP (Zadnikova et al. 2010) (Table 5.1) are all expressed—as are translational fusions of *PIN1* to GFP (Benkova et al. 2003; Heisler et al. 2005; Scarpella et al. 2006; Wenzel et al. 2007)—in both epidermal and subepidermal cells of the developing leaf (Figure 5.1A and 5.1C-5.1E).

WT Arabidopsis grown under normal conditions forms separate leaves whose vein patterns are defined by at least four reproducible features (Nelson and Dengler 1997; Candela et al. 1999)

Table 5.1. Origin and nature of lines.

Line	Origin/Nature
PIN1::PIN1:GFP	(Benkova et al. 2003)
PIN2::PIN2:GFP	(Xu and Scheres 2005)
PIN3::PIN3:GFP	(Dello Ioio et al. 2007)
PIN4::PIN4:GFP	Translational fusion of *PIN4* (AT2G01420; -4598 to +3095; primers: 'PIN4 prom PstI forw' and 'PIN4 1032 SalI rev', 'PIN4 1033 SalI forw' and 'PIN4 UTR EcoRI rev') to EGFP (Clontech; insertion at +1032 of *PIN4*; primers: 'EGFP SalI Forw' and 'EGFP SalI Rev')
PIN7::PIN7:GFP	Translational fusion of *PIN7* (AT1G23080; -1537 to +2830; primers: 'PIN7 prom SalI forw' and 'PIN7 UTR KpnI rev') to EGFP (Clontech; insertion at +921 of *PIN7*; primers: 'EGFP SacI forw' and 'EGFP SacI rev')
pin1-1	ABRC; (Goto 1987; Galweiler et al. 1998; Sawchuk et al. 2013) (Chapter 2); WT at the *TTG1* (AT5G24520) locus
eir1-1 (*pin2*)	ABRC; (Roman et al. 1995; Luschnig et al. 1998)
pin3-3	(Friml et al. 2002b)
pin4-2	(Friml et al. 2002a)
pin6	ABRC; (Sawchuk et al. 2013) (Chapter 2)
$pin7^{En}$	(Blilou et al. 2005)
pin8-1	ABRC; (Bosco et al. 2012)
ACBC1::ACBC1:GFP	(Dhonukshe et al. 2008; Mravec et al. 2008)
ACBC19::ACBC19:GFP	(Dhonukshe et al. 2008; Mravec et al. 2008)
pgp1-100 (*abcb1*)	ABRC; (Lin and Wang 2005)
mdr1-101 (*abcb19*)	ABRC; (Lin and Wang 2005)
ucu2-4 (*twd1*)	ABRC; (Perez-Perez et al. 2004)
AUX1::AUX1:YFP	ABRC; (Peret et al. 2012)
LAX1::LAX1:YFP	(Peret et al. 2012)
LAX2::LAX2:YFP	(Peret et al. 2012)
LAX3::LAX3:YFP	(Peret et al. 2012)

aux1-21	ABRC; (Marchant and Bennett 1998)
lax1	(Bainbridge et al. 2008)
lax2	(Bainbridge et al. 2008)
lax3	(Bainbridge et al. 2008)
mp-11	ABRC; (Odat et al. 2014); (Chapter 4)
mp^{G12}	(Hardtke and Berleth 1998)
emb30-8 (*gn*)	ABRC; (Moriwaki et al. 2013)
gn-13	ABRC; (Alonso et al. 2003); SALK_045424
gn^{SALK_103014}	ABRC; (Okumura et al. 2013)
emb30-7 (*gn*)	(Koizumi et al. 2000); WT at the *ER* (AT2G26330) locus
gn^{R5}	(Geldner et al. 2004); WT at the *ER* (AT2G26330) locus
rbr1-3	ABRC; (Ebel et al. 2004)

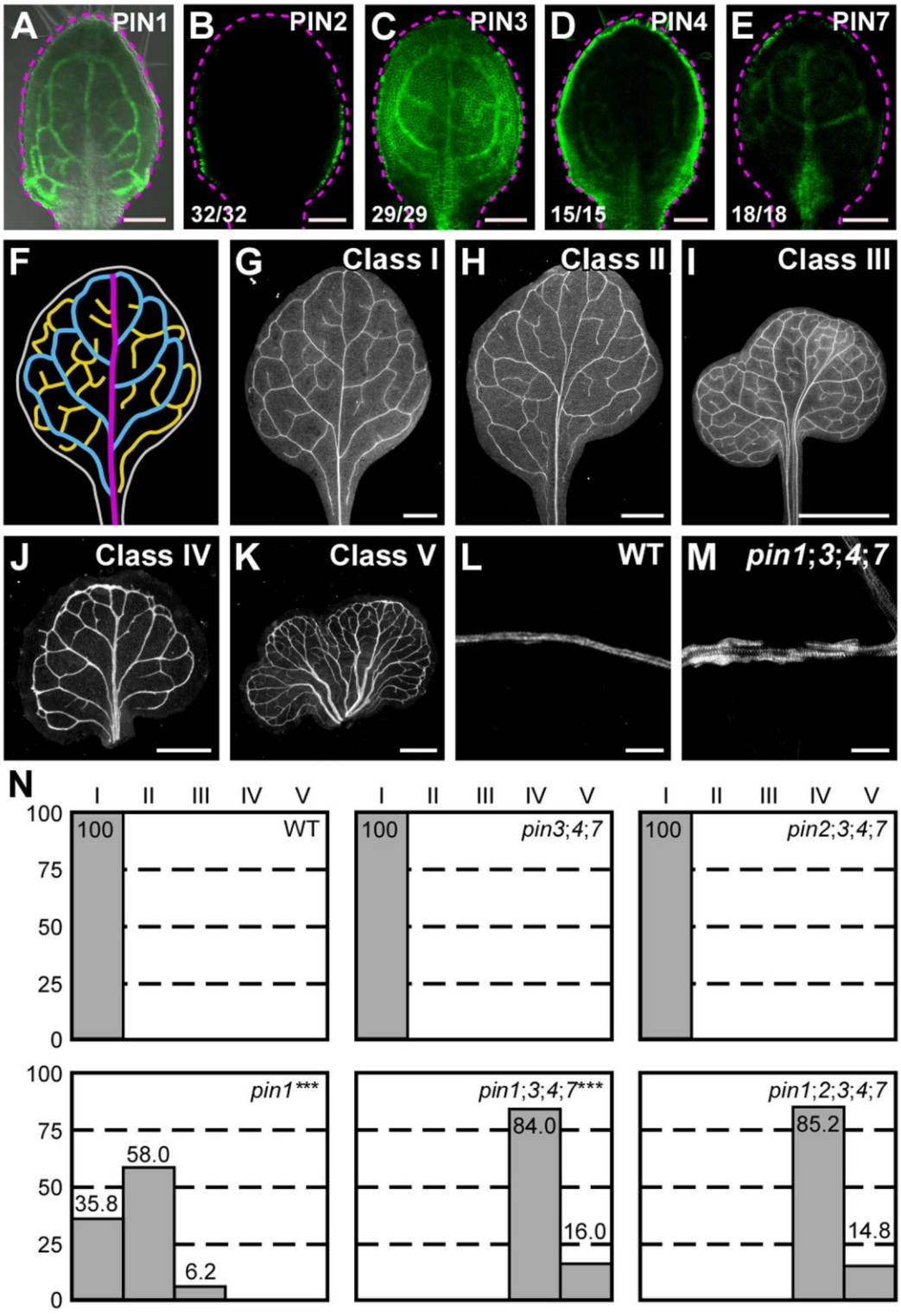

Figure 5.1. Contribution of plasma-membrane-localized PIN proteins of Arabidopsis to vein patterning. (A-E,G-M) Top right, expression-reported gene, phenotype class or genotype. (B-E) Bottom left, reproducibility index. (A-E) Confocal laser scanning microscopy with (A) and

without (B-E) transmitted light; 4-day-old first leaves. Dashed magenta line delineates leaf outline. (G-M) Dark-field illumination of mature first leaves. (A) PIN1::PIN1:GFP expression. (B) PIN2::PIN2:GFP expression. (C) PIN3::PIN3:GFP expression. (D) PIN4::PIN4:GFP expression. (E) PIN7::PIN7:GFP expression. (F,G) Vein pattern of WT mature first leaf. In (F), magenta, midvein; blue, loops; yellow, minor veins. (G-K) Phenotype classes: unbranched, narrow midvein and scalloped vein-network outline (G); bifurcated midvein and scalloped vein-network outline (H); fused leaves with scalloped vein-network outline (I); thick veins and scalloped vein-network outline (J); fused leaves with thick veins and scalloped vein-network outline (K). (L,M) Details of WT (L) or *pin1*;*3*;*4*;*7* (M) illustrating normal (Classes I-III) or thick (Classes IV and V) veins, respectively. (N) Percentages of leaves in phenotype classes. Difference between *pin1* and WT, and between *pin1*;*3*;*4*;*7* and *pin1* was significant at $P<0.001$ (***) by Kruskal-Wallis and Mann-Whitney test with Bonferroni correction. Sample population sizes: WT, 58; *pin2*;*3*;*4*;*7*, 55; *pin3*;*4*;*7*, 55; *pin1*, 81; *pin1*;*3*;*4*;*7*, 75; *pin1*;*2*;*3*;*4*;*7*, 54. Bars: (A-E,L,M) 0.1 mm; (G,H,J,K) 1 mm; (I) 5 mm.

(Figure 5.1F,5.1G,5.1L,5.1N): (1) a narrow, central midvein that runs the length of the leaf; (2) lateral veins that branch from the midvein and join distal veins to form closed loops; (3) minor veins that branch from midvein and loops, and either end freely or join other veins; (4) minor veins and loops that curve near the leaf margin, lending a scalloped outline to the vein network. Approximately 35% of *pin1* leaves have WT vein patterns, but in nearly 60% of *pin1* leaves the midvein bifurcates near the leaf tip ("bifurcated midvein"), and ~5% of *pin1* leaves have separation defects ("fused leaves") (Sawchuk et al. 2013) (Chapter 2; Figure 5.1G-5.1I and 5.1N). Vein patterns of *pin3pin4pin7* (*pin3*;*4*;*7* hereafter) were no different from those of WT (Figure 5.1N). *pin1*;*3*;*4*;*7* embryos were viable (Table 5.2) and developed into seedlings (Table 5.3) whose leaf separation and vein pattern defects were more severe than those of *pin1*: no *pin1*;*3*;*4*;*7* leaf had a WT vein pattern; *pin1*;*3*;*4*;*7* veins were thick—though unevenly so—and at vein thickenings single vascular elements or short stretches of them flanked continuous veins (Figure 5.1M); and ~15% of *pin1*;*3*;*4*;*7* leaves were fused (Figure 5.1J,5.1K,5.1M,5.1N). Cotyledon pattern defects of *pin1*;*3*;*4*;*7* were no different from those of *pin1* (Figure 5.2), but *pin1*;*3*;*4*;*7* seedlings were smaller than *pin1* seedlings (Figure 5.3).

Next, we asked whether mutation of *PIN2*—whose translational fusion to GFP (Xu and Scheres 2005) is only expressed in epidermal cells in the developing leaf (Figure 5.1B)—changed the spectrum of vein pattern defects of *pin1*;*3*;*4*;*7*. *pin2*;*3*;*4*;*7* embryos were viable and developed into seedlings (Table 5.4) whose vein patterns were no different from those of WT (Figure 5.1N). *pin1*;*2*;*3*;*4*;*7* embryos were viable (Table 5.2) and developed into seedlings (Table 5.3) whose vein pattern defects were no different from those of *pin1*;*3*;*4*;*7* (Figure 5.1N). Cotyledon pattern defects of *pin1*;*2*;*3*;*4*;*7* were no different from those of *pin1*;*3*;*4*;*7* (Figure 5.2), and size of *pin1*;*2*;*3*;*4*;*7* seedlings was similar to that of *pin1*;*3*;*4*;*7* seedlings (Figure 5.3).

In conclusion, the *PIN3* group of *PM-PIN* genes (*PIN3*, *PIN4* and *PIN7*) provides no non-redundant functions in vein patterning, but it contributes to *PIN1*-dependent vein patterning. Furthermore, *PIN1* and the *PIN3* group of *PM-PIN* genes redundantly restrict vascular differentiation to narrow zones. By contrast, *PIN2* seems to have no functions in these processes.

5.2.2 Contribution of *PIN* genes to vein patterning

Expression and genetic analyses suggest that the PM-PIN proteins PIN1, PIN3, PIN4 and PIN7 redundantly define a single intercellular auxin-transport pathway with vein patterning functions

Table 5.2. Embryo viability of *rbr1*, *mp*, *pin1*, *pin1*;*3*;*4*;*7*, *pin1*;*2*;*3*;*4*;*7* and *pin1*;*3*;*4*;*6*;*7*;*8*.

Genotype of self-fertilized parent	Proportion of viable embryos in siliques of self-fertilized parent (mean ± SD)	Sample population size (*n*)
RBR1/*rbr1-3*	0.61 ± 0.26**/***	186
MP/*mp*^{G12}	0.93 ± 0.10	133
PIN1/*pin1*	0.92 ± 0.05	217
PIN1/*pin1*;*pin3*/*pin3*;*pin4*/*pin4*;*pin7*/*pin7*	0.99 ± 0.02	209
PIN1/*pin1*;*pin2*/*pin2*;*pin3*/*pin3*;*pin4*/*pin4*;*pin7*/*pin7*	0.93 ± 0.11	238
PIN1/*pin1*;*pin3*/*pin3*;*pin4*/*pin4*;*pin6*/*pin6*;*pin7*/*pin7*;*pin8*/*pin8*	0.98 ± 0.04	280

Difference between positive control for embryo lethality (*rbr1*) and negative control for embryo lethality (*mp*^{G12}), and between positive control and *pin1*;*3*;*4*;*7*, *pin1*;*2*;*3*;*4*;*7* and *pin1*;*3*;*4*;*6*;*7*;*8* was significant at $P<0.001$ (***) by one-way ANOVA and Tukey's test. Difference between positive control and *pin1* was significant at $P<0.01$ (**) by one-way ANOVA and Tukey's test. Difference between negative control and *pin1*, *pin1*;*3*;*4*;*7*, *pin1*;*2*;*3*;*4*;*7* and *pin1*;*3*;*4*;*6*;*7*;*8* was not significant by one-way ANOVA.

Table 5.3. Embryo viability of *pin1*, *pin1*;*3*;*4*;*7*, *pin1*;*2*;*3*;*4*;*7* and *pin1*;*3*;*4*;*6*;*7*;*8*.

Genotype of self-fertilized parent	Proportion of homozygous mutants in progeny of self-fertilized parent (no. of homozygous seedlings/total no. of seedlings)	Percentage of homozygous mutants in progeny of self-fertilized parent
PIN1/*pin1*	66/239	27
PIN1/*pin1*;*pin3*/*pin3*;*pin4*/*pin4*;*pin7*/*pin7*	52/248	26
PIN1/*pin1*;*pin2*/*pin2*;*pin3*/*pin3*;*pin4*/*pin4*;*pin7*/*pin7*	61/236	26
PIN1/*pin1*;*pin3*/*pin3*;*pin4*/*pin4*;*pin6*/*pin6*;*pin7*/*pin7*;*pin8*/*pin8*	65/260	25

Difference between observed and theoretical frequency-distributions of embryo-viable homozygous mutants in the progeny of self-fertilized heterozygous parents was not significant by Pearson's chi-squared (χ^2) goodness-of-fit test (α=0.05, dF=1).

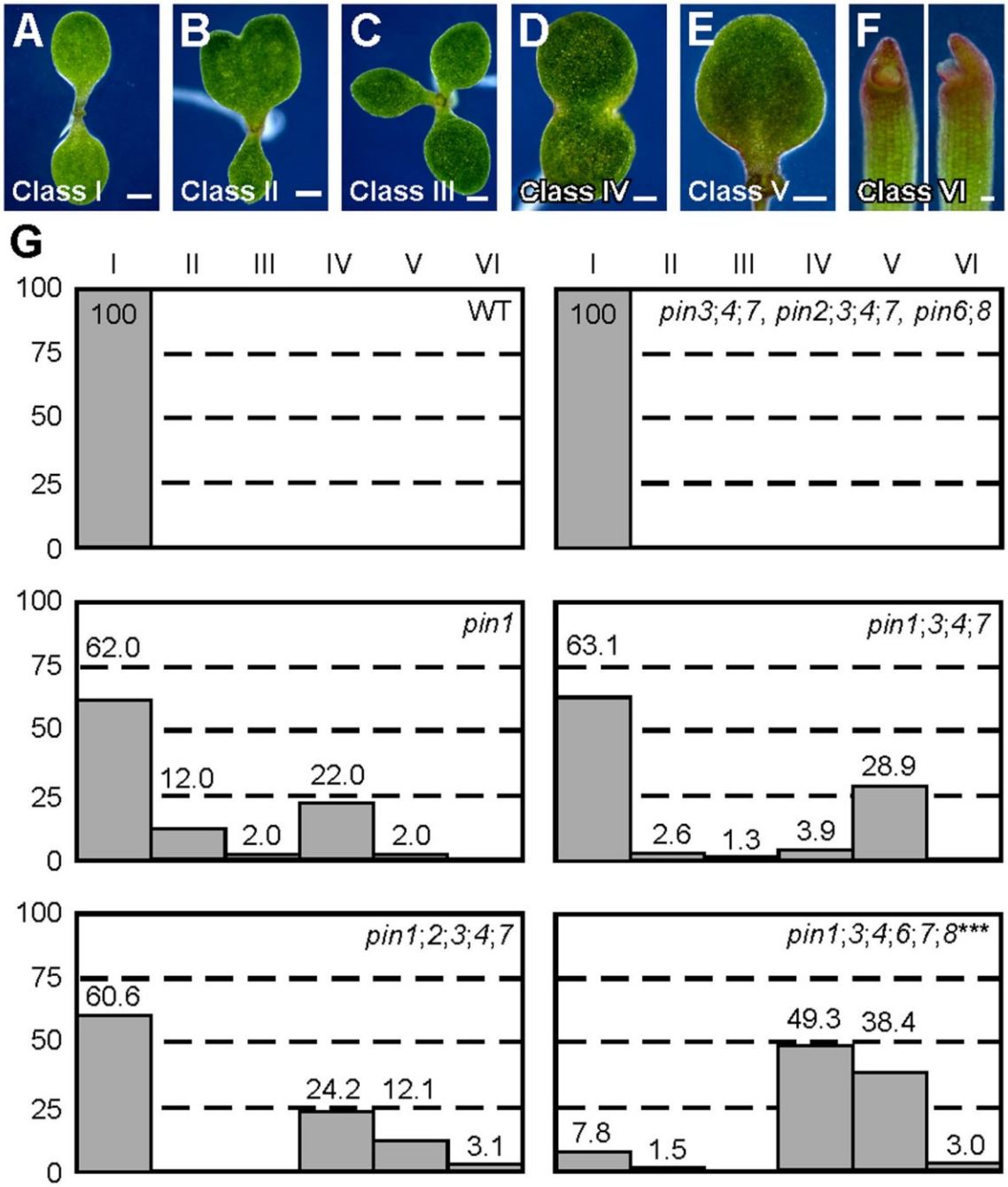

Figure 5.2. Cotyledon patterns of *pin* mutants. (A-F) Dark-field illumination of 4-day-old seedlings illustrating phenotype classes: two separate cotyledons (A), fused cotyledons and separate single cotyledon (B) three separate cotyledons (C), fused cotyledons (D), single cotyledon (E), small, hood-like cotyledon (F). (G) Percentages of seedlings in phenotype classes. Difference between *pin1* and WT, and between *pin1*;*3*;*4*;*6*;*7*;*8* and *pin1*was significant was significant at $P<0.001$ (***) by Kruskal-Wallis and Mann-Whitney test with Bonferroni correction. Sample population sizes: WT, 58; *pin3*;*4*;*7*, 55; *pin2*;*3*;*4*;*7*, 55; *pin6*;*8*, 50; *pin1*;*3*;*4*;*7*, 76; *pin1*;*2*;*3*;*4*;*7*, 80; *pin1*;*3*;*4*;*6*;*7*;*8*, 65. Bars: (A-E) 0.5 mm; (F) 0.25 mm.

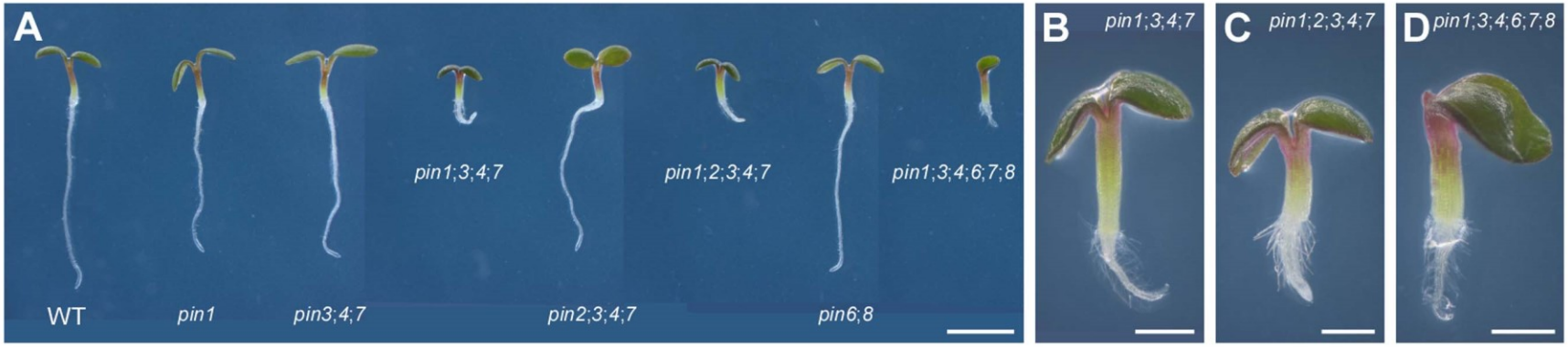

Figure 5.3. *pin* mutant seedlings. (A-D) Dark-field illumination composite of 3-day-old seedlings; genotypes below respective seedlings (A) or top right (B-D). (A) Overview. (B-D) Details. Bars: (A) 2 mm; (B-D) 0.5 mm.

Table 5.4. Embryo viability of WT, *pin3*;*4*;*7* and *pin2*;*3*;*4*;*7*.

Genotype of self-fertilized parent	**Proportion of viable embryos in siliques of self-fertilized parent (mean ± SD)**	**Sample population size (*n*)**
WT (Col-0)	0.99 ± 0.01	275
pin3/*pin3*;*pin4*/*pin4*;*pin7*/*pin7*	0.96 ± 0.04	272
pin2/*pin2*;*pin3*/*pin3*;*pin4*/*pin4*;*pin7*/*pin7*	0.92 ± 0.12	248

Difference between WT, *pin3*;*4*;*7* and *pin2*;*3*;*4*;*7* was not significant by one-way ANOVA.

(Figure 5.1; see 5.3 Discussion). The ER-localized PIN (ER-PIN) proteins PIN6 and PIN8 define a distinct, intracellular auxin-transport pathway with vein patterning functions that overlap with those of PIN1 (Sawchuk et al. 2013) (Chapter 2). We asked what the collective contribution of these two auxin-transport pathways is to vein patterning.

As previously reported (Sawchuk et al. 2013) (Chapter 2), vein patterns of *pin6*;*8* were no different from those of WT (Figure 5.4C). *pin1*;*3*;*4*;*6*;*7*;*8* embryos were viable (Table 5.2) and developed into seedlings (Table 5.3) the vein patterns of which differed from those of *pin1*;*3*;*4*;*7* in three respects: (1) the vein network comprised more lateral veins; (2) lateral veins failed to join the midvein but ran parallelly to it to form a wide "midvein"; (3) lateral veins ended in a marginal vein that—irrespectively of leaf shape—closely paralleled the leaf margin, lending a smooth outline to the vein network (Figure 5.4A-5.4C). Mutation of *PIN6* and *PIN8* in the *pin1*;*3*;*4*;*7* background shifted the distribution of *pin1*;*3*;*4*;*7* cotyledon pattern phenotypes towards stronger classes (Figure 5.2), but size of *pin1*;*3*;*4*;*6*;*7*;*8* seedlings was similar to that of *pin1*;*3*;*4*;*7* seedlings (Figure 5.3).

Because *pin6*;*8* synthetically enhanced vein pattern defects of *pin1*;*3*;*4*;*7*, we conclude that the intercellular auxin-transport pathway mediated by the PM-PIN proteins and the intracellular auxin-transport pathway mediated by the ER-PIN proteins provide overlapping functions in vein patterning (see 5.3 Discussion).

5.2.3 Genetic versus chemical interference of auxin transport

Cellular auxin efflux is inhibited by a class of structurally related compounds referred to as phytotropins, exemplified by 1-N-naphthylphthalamic acid (NPA) (Katekar and Geissler 1980; Sussman and Goldsmith 1981). Because PM-PIN proteins catalyze cellular auxin efflux (Chen et al. 1998; Petrasek et al. 2006), we asked whether defects resulting from simultaneous mutation of all the *PM-PIN* genes with vein patterning function were mimicked by growth of WT in the presence of NPA. To address this question, we compared defects of *pin1*;*3*;*4*;*7* to those induced in WT by germination and growth in the presence of 100 μM NPA, which is the highest concentration of NPA without toxic, auxin-efflux-unrelated effects (Petrasek et al. 2003; Dhonukshe et al. 2008). Because leaves develop more slowly at this concentration of NPA (Mattsson et al. 1999; Sieburth 1999), to ensure maximal vascular differentiation we allowed

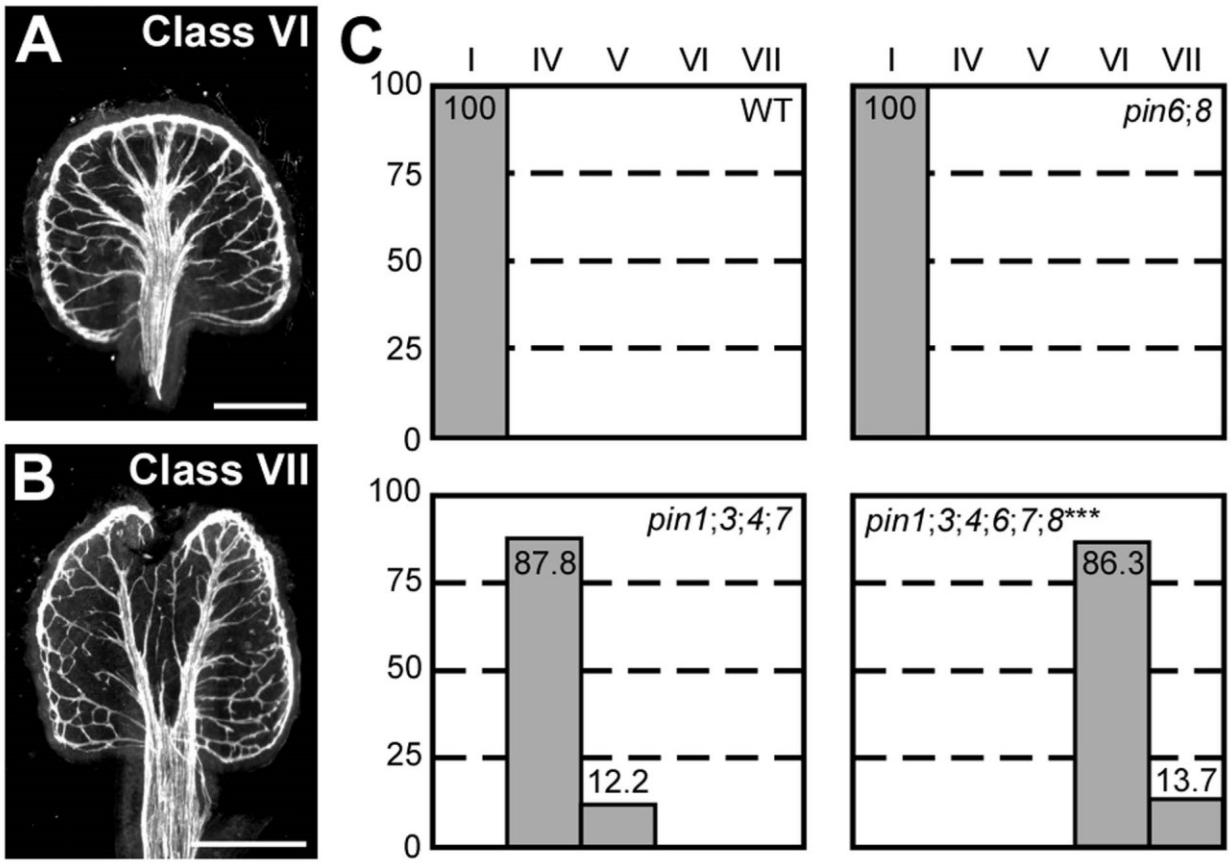

Figure 5.4. Contribution of *PIN* genes to vein patterning. (A,B) Dark-field illumination of mature first leaves illustrating phenotype classes: increased number of lateral veins, wide midvein and conspicuous marginal vein (A); fused leaves with increased number of lateral veins, wide midvein and conspicuous marginal vein (B). (C) Percentages of leaves in phenotype classes (Classes I, IV and V defined in Figure 5.1). Difference between *pin1*;*3*;*4*;*6*;*7*;*8* and *pin1*;*3*;*4*;*7* was significant at $P<0.001$ (***) by Kruskal-Wallis and Mann-Whitney test with Bonferroni correction. Sample population sizes: WT, 51; *pin6*;*8*, 47; *pin1*;*3*;*4*;*7*, 49; *pin1*;*3*;*4*;*6*;*7*;*8*, 73. Bars: (A,B) 0.5 mm.

them to grow for four weeks before analysis.

In agreement with previous reports (Mattsson et al. 1999; Sieburth 1999), high concentration of NPA only rarely induced leaf fusion in WT (see Figure 5.6G for one such rare occurrence) but reproducibly induced characteristic vein-pattern defects: (1) the vein network comprised more lateral veins; (2) lateral veins failed to join the midvein but ran parallelly to it to form a wide "midvein"; (3) lateral veins ended in a marginal vein that—irrespectively of leaf shape—closely paralleled the leaf margin, lending a smooth outline to the vein network (Figure 5.5D and 5.5G). Further, veins of NPA-grown WT were thick—though unevenly so—and at vein thickenings single vein elements or short stretches of them flanked continuous veins (Figure 5.5D and 5.5G).

By contrast, 20% of *pin1*;*3*;*4*;*7* leaves were fused, and though *pin1*;*3*;*4*;*7* veins were thick *pin1*;*3*;*4*;*7* vein patterns lacked the characteristic defects induced in WT by NPA (Figure 5.5B and 5.5G). However, such defects were induced in *pin1*;*3*;*4*;*7* by 100 μM NPA (Figure 5.5E and 5.5G), suggesting that this background has residual NPA-sensitive vein-patterning activity. The vein pattern defects induced in WT or *pin1*;*3*;*4*;*7* by NPA were no different from those of *pin1*;*3*;*4*;*6*;*7*;*8* (Figure 5.5C-5.5E,5.5G). Because no additional defects were induced in *pin1*;*3*;*4*;*6*;*7*;*8* by 100 μM NPA (Figure 5.5F and 5.5G), the residual NPA-sensitive vein-patterning activity of *pin1*;*3*;*4*;*7* is likely provided by *PIN6* and *PIN8*.

Thus our results suggest that in the absence of the function provided by *PIN1*, *PIN3*, *PIN4*, *PIN6*, *PIN7* and *PIN8* any residual NPA-sensitive vein-patterning activity—if existing—becomes inconsequential.

5.2.4 Contribution of *ABCB* genes to vein patterning

Cellular auxin efflux is catalyzed not only by PM-PIN proteins but by the PM-localized ATP-BINDING CASSETTE B1 (ABCB1) and ABCB19 proteins (Geisler et al. 2003; Geisler et al. 2005; Bouchard et al. 2006; Petrasek et al. 2006; Blakeslee et al. 2007; Wu et al. 2007), whose fusions to GFP (Dhonukshe et al. 2008; Mravec et al. 2008) are expressed at early stages of leaf development (Figure 5.6A and 5.6B). We asked whether ABCB1/19-mediated auxin efflux was required for vein patterning. Vein patterns of *abcb1*, *abcb19* and *abcb1*;*19* were no different from those of WT (Figure 5.6C,5.6D,5.6G; Figure 5.7), suggesting that ABCB1/19-mediated auxin efflux is dispensable for vein patterning.

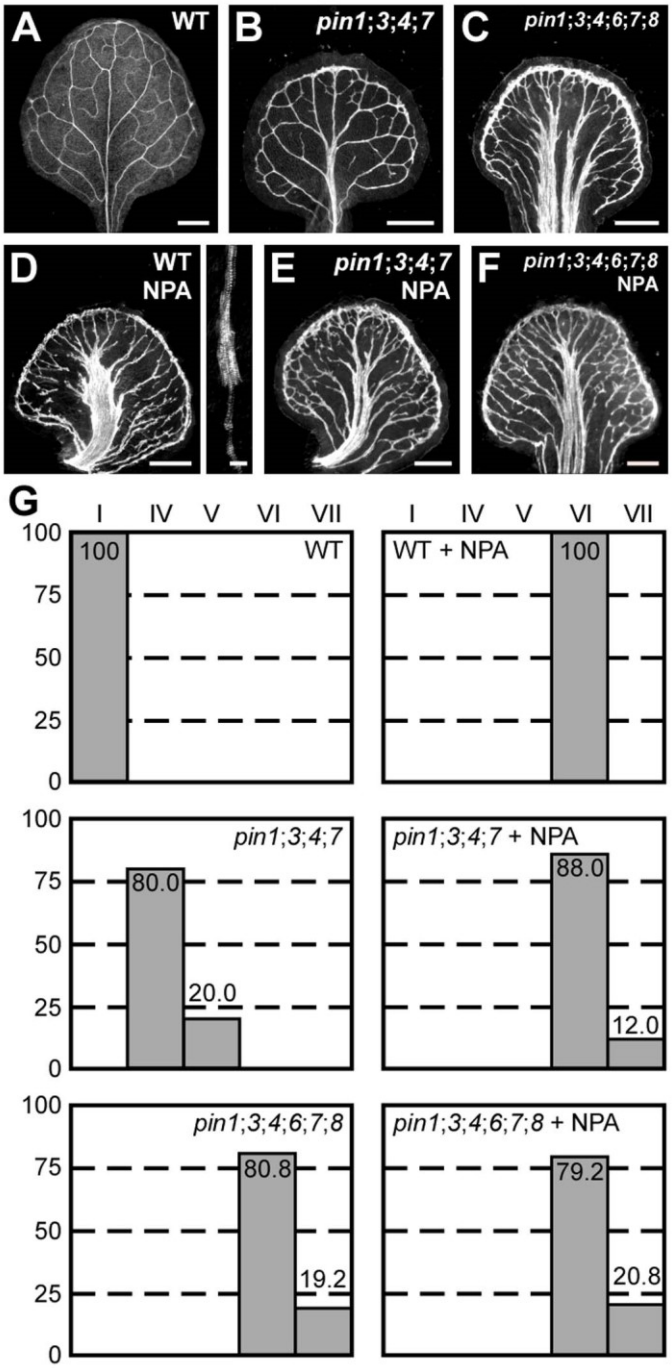

Figure 5.5. Genetic versus chemical interference of auxin transport. (A-F) Top right, genotype and treatment. (A-F) Dark-field illumination of mature first leaves. (A) WT. (B) *pin1*;*3*;*4*;*7*. (C) *pin1*;*3*;*4*;*6*;*7*;*8*. (D) NPA-grown WT; inset, detail illustrating thick veins in NPA-grown WT. (E) NPA-grown *pin1*;*3*;*4*;*7*. (F) NPA-grown *pin1*;*3*;*4*;*6*;*7*;*8*. (G) Percentages of leaves in phenotype classes (defined in Figures 5.1 and 5.4). Sample population sizes: WT, 38; *pin1*;*3*;*4*;*7*, 30; *pin1*;*3*;*4*;*6*;*7*;*8*, 73; NPA-grown WT, 41; NPA-grown *pin1*;*3*;*4*;*7*, 58; NPA-grown *pin1*;*3*;*4*;*6*;*7*;*8*, 48. Bars: (A-F) 0.5 mm, inset 80 μm.

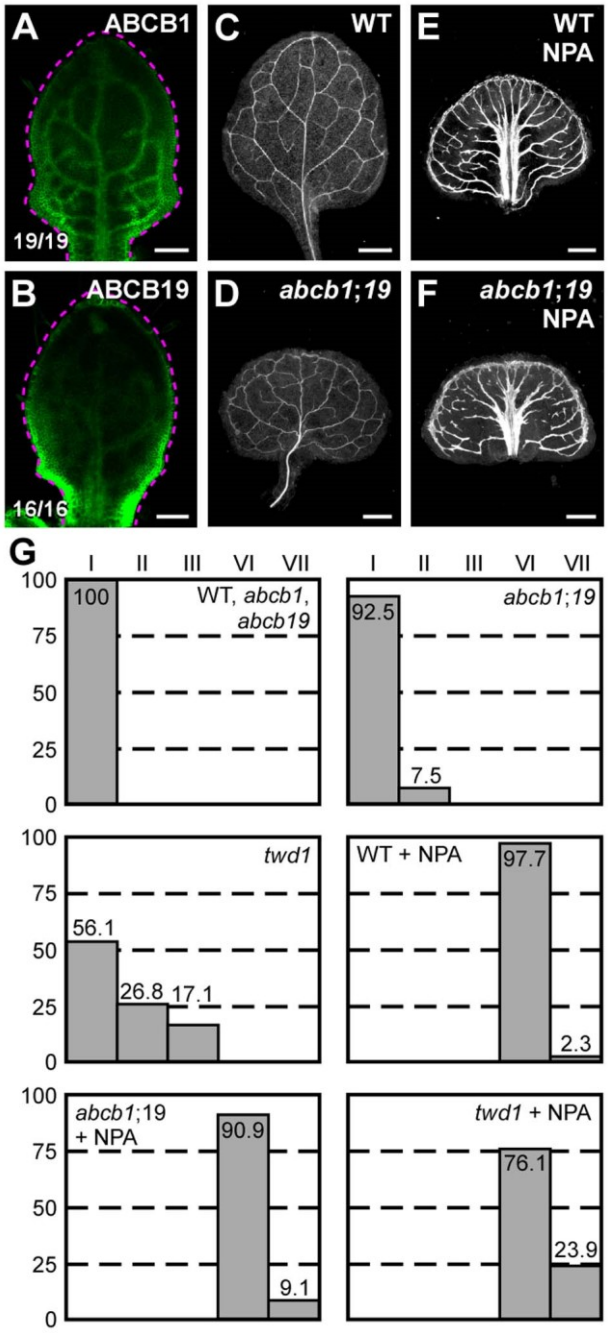

Figure 5.6. Contribution of *ABCB* genes to vein patterning. (A-F) Top right: expression-reported gene, genotype and treatment. (A-B) Bottom left: reproducibility index. (A-B) Confocal laser scanning microscopy without transmitted light; 4-day-old first leaves. Dashed magenta line delineates leaf outline. (C-F) Dark-field illumination of mature first leaves. (A) ABCB1::ABCB1:GFP expression. (B) ABCB19::ABCB19:GFP expression. (G) Percentages of leaves in phenotype classes (defined in Figures 5.1 and 5.4). Sample population sizes: WT, 41; *abcb1*, 53; *abcb19*, 49; *abcb1*;*19*, 40; *twd1*, 41; NPA-grown WT, 43; NPA-grown *abcb1*;*19*, 46; NPA-grown *twd1*, 46. Bars: (A-B) 100 μm; (C-F) 0.5 mm.

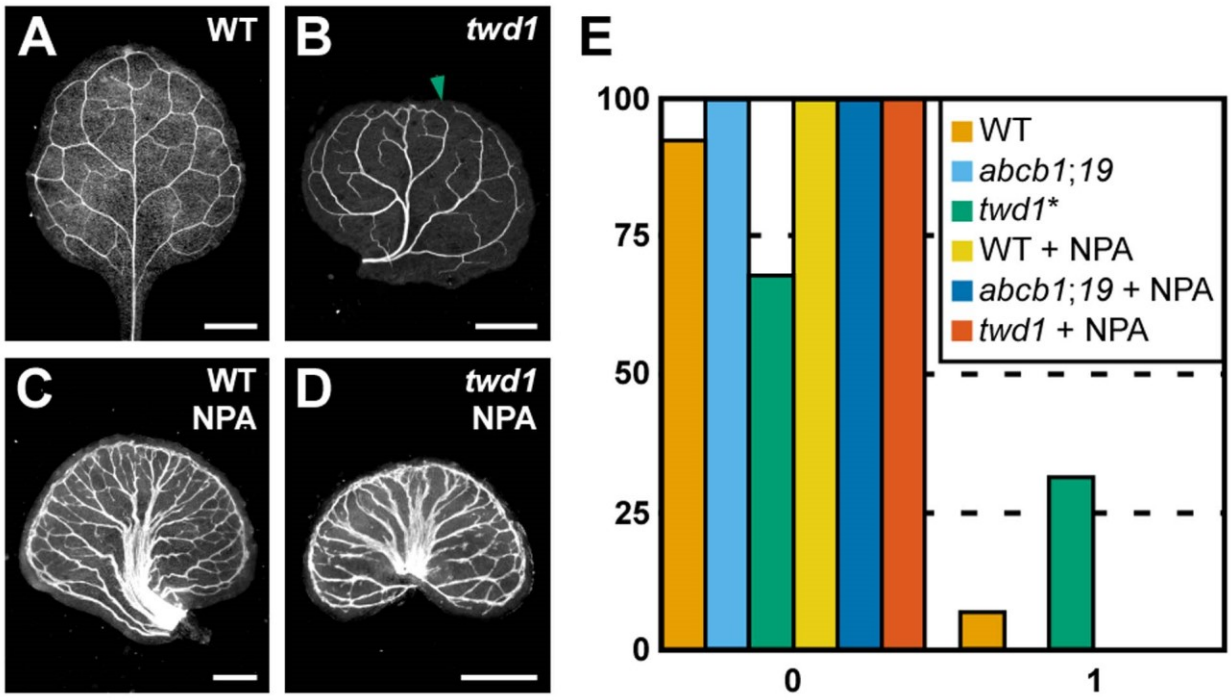

Figure 5.7. Contribution of *TWD1* to vein patterning. (A-D) Top right, genotype and treatment. Dark-field illumination of mature first leaves. In (B), arrowhead indicates open loop. (E) Percentage of first leaves with 0 or 1 open loops. Difference between *twd1* and WT was significant at $P<0.05$ (*) by Kruskal-Wallis and Mann-Whitney test with Bonferroni correction. Sample population sizes: WT, 41; *abcb1*;*19*, 36; *twd1*, 41; NPA-grown WT, 43; NPA-grown *abcb1*;*19*, 46; NPA-grown *twd1*, 46. Bars: (A-D) 1 mm.

Developmental functions of ABCB1/19-mediated auxin transport overlap with those of PIN mediated auxin transport (Blakeslee et al. 2007; Mravec et al. 2008). We thus asked whether vein pattern defects induced in WT by NPA—which phenocopies loss of *PIN*-dependent vein-patterning activity (Figure 5.5)—could be enhanced by mutation of *ABCB1* and *ABCB19*. Vein pattern defects induced in *abcb1*;*19* by 100 μM NPA were no different from those induced in WT by NPA (Figure 5.6E-G; Figure 5.7), suggesting no vein-patterning function of *ABCB1* and *ABCB19* in the NPA-induced vein-pattern phenocopy of *pin1*;*3*;*4*;*6*;*7*;*8*.

ABCB1 and ABCB19 are members of a large family (Geisler and Murphy 2006); vein patterning functions of ABCB1/19-mediated auxin efflux might thus be masked by redundant functions provided by other ABCB transporters. The TWISTED DWARF1/ULTRACURVATA2 (TWD1/UCU2; TWD1 hereafter) protein (Kamphausen et al. 2002; Perez-Perez et al. 2004) is a positive regulator of ABCB-mediated auxin transport (Geisler et al. 2003; Bouchard et al. 2006; Bailly et al. 2008; Wu et al. 2010; Wang et al. 2013). Consistent with this observation, defects of *twd1* are more severe than—though similar to—those of *abcb1*;*19* (Geisler et al. 2003; Bouchard et al. 2006; Bailly et al. 2008; Wu et al. 2010; Wang et al. 2013). We thus reasoned that analysis of *twd1* vein patterns might uncover vein patterning functions of ABCB-mediated auxin transport that could not be inferred from analysis of *abcb1*;*19*.

Approximately 25% of *twd1* leaves had bifurcated midveins, ~17% of *twd1* leaves were fused, and ~30% of *twd1* leaves had a discontinuous vein-network outline (Figure 5.6G; Figure 5.7), suggesting possible vein-patterning functions of *TWD1*-dependent ABCB-mediated auxin transport. However, vein pattern defects induced in *twd1* by 100 μM NPA were no different from those induced in WT or *abcb1*;*19* by NPA (Figure 5.6G; Figure 5.7), suggesting that vein patterning functions of *TWD1*-dependent ABCB-mediated auxin transport—if existing—become inconsequential in the NPA-induced vein-pattern phenocopy of *pin1*;*3*;*4*;*6*;*7*;*8*. By contrast, NPA enhanced leaf separation defects of *twd1* (Figure 5.6G), suggesting overlapping functions of *TWD1*-dependent ABCB-mediated auxin transport and NPA-sensitive auxin transport in leaf separation.

5.2.5 Contribution of *AUX1/LAX* genes to vein patterning

Auxin is predicted to enter the cell by diffusion and through an auxin influx carrier (Rubery and Sheldrake 1974; Raven 1975). In Arabidopsis, auxin influx activity is encoded by the *AUX1*, *LAX1*, *LAX2* and *LAX3* (*AUX1*/*LAX*) genes (Parry et al. 2001; Yang et al. 2006; Swarup et al. 2008; Peret et al. 2012), whose translational fusions to YFP (Peret et al. 2012) are all expressed at early stages of vein development (Figure 5.8A-5.8D). We thus asked whether AUX1/LAX-mediated auxin influx was required for vein patterning. Because vein patterns of *aux1*;*lax1*;*2*;*3* were no different from those of WT (Figure 5.8E,5.8G,5.8I), we conclude that *AUX1*/*LAX* function is dispensable for vein patterning.

We next asked whether contribution of *AUX1*/*LAX* genes to vein patterning only became apparent in conditions of extremely reduced auxin transport. To address this question, we germinated and grew *aux1*;*lax1*;*2*;*3* in presence of 100 μM NPA, which phenocopies mutation of all the *PIN* genes with vein patterning function (Figure 5.5). Vein pattern defects induced in *aux1*;*lax1*;*2*;*3* by NPA were no different from those induced in WT by NPA (Figure 5.8F,5.8H,5.8I), suggesting no vein-patterning function of *AUX1*/*LAX* genes in conditions of extremely reduced auxin transport. On the other hand, NPA induced leaf fusion in *aux1*;*lax1*;*2*;*3* but not in WT, suggesting that AUX1/LAX-mediated auxin influx and NPA-sensitive auxin transport have overlapping functions in leaf separation and that—consistent with previous observations (Reinhardt et al. 2003; Bainbridge et al. 2008; Kierzkowski et al. 2013)—AUX1/LAX-mediated auxin influx contributes to maintaining leaves separate in conditions of reduced auxin transport.

5.2.6 Response of *pin* leaves to auxin application

The uniform vein-pattern phenotype of *pin1*;*3*;*4*;*6*;*7*;*8* was mimicked by growth of WT in the presence of high concentration of NPA (Figures 5.4 and 5.5). Moreover, the vein-pattern phenotype of *pin1*;*3*;*4*;*6*;*7*;*8* was unchanged by NPA treatment, and the NPA-induced vein-pattern phenocopy of *pin1*;*3*;*4*;*6*;*7*;*8* was unchanged by mutation in any known intercellular auxin-transporter (Figures 5.5,5.6,5.8). These observations suggest that the function of known intercellular auxin-transporters in vein patterning is dispensable in the absence of the auxin transport activity of PIN1, PIN3, PIN4, PIN6, PIN7 and PIN8. Because auxin transport is thought to be essential for auxin-induced vascular-strand formation [reviewed in (Sachs 1981;

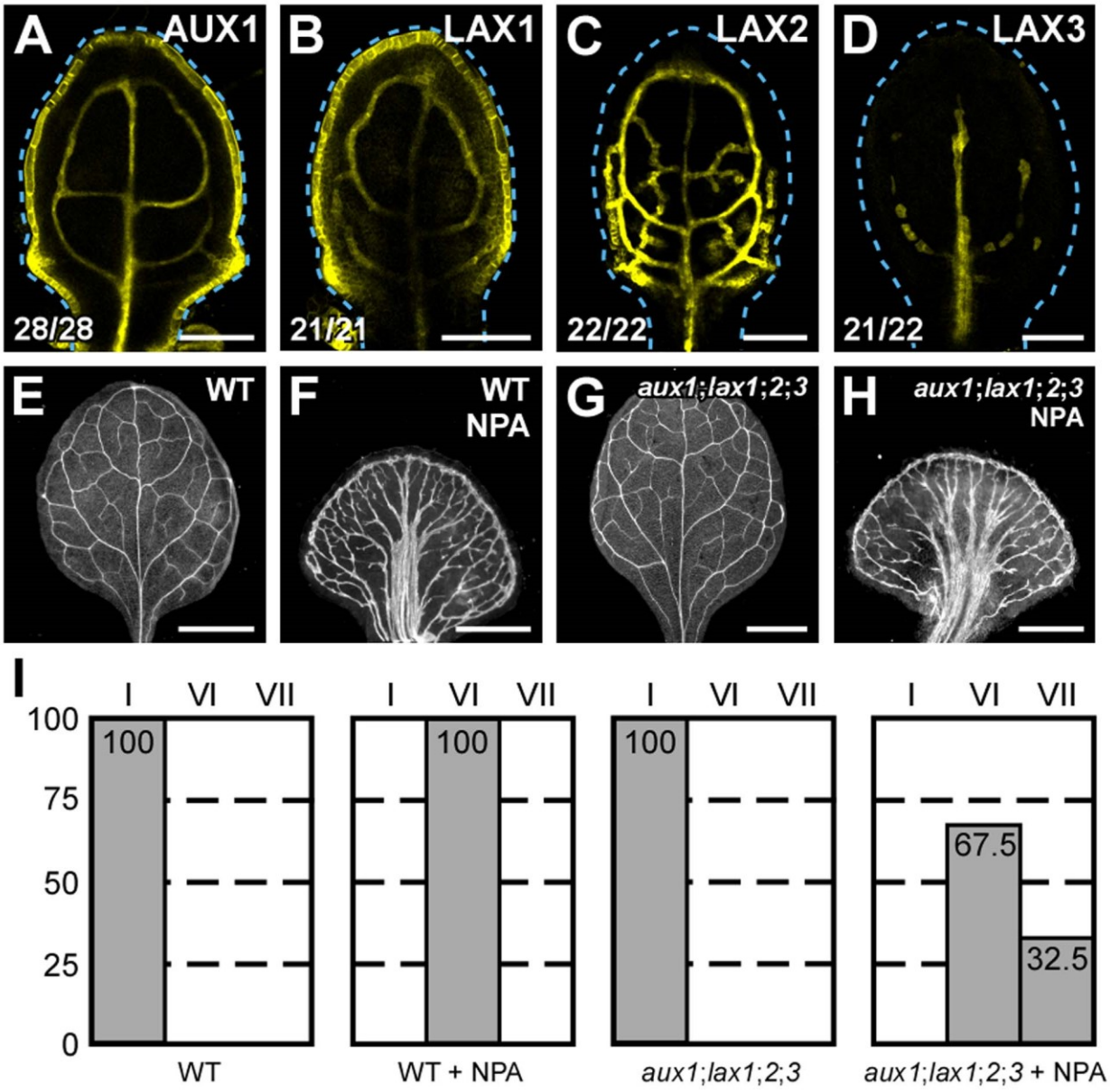

Figure 5.8. Contribution of *AUX1/LAX* genes to vein patterning. (A-H) Top right: expression-reported gene, genotype and treatment. (A-D) Bottom left: reproducibility index. (A-D) Confocal laser scanning microscopy without transmitted light; 4-day-old first leaves. Dashed cyan line delineates leaf outline. (E-H) Dark-field illumination of mature first leaves. (A) AUX1::AUX1:YFP expression. (B) LAX1::LAX1:YFP expression. (C) LAX2::LAX2:YFP expression. (D) LAX3::LAX3:YFP expression. (I) Percentages of leaves in phenotype classes (defined in Figures 5.1 and 5.4). Sample population sizes: WT, 54; *aux1*;*lax1*;*2*;*3*, 60; NPA-grown WT, 46; NPA-grown *aux1*;*lax1*;*2*;*3*, 40. Bars: (A-D) 100 μm; (E-H) 1 mm.

Berleth et al. 2000; Aloni 2010; Sawchuk and Scarpella 2013)] (Chapter 1), we asked whether auxin induced vascular strand formation in *pin1*;*3*;*4*;*6*;*7*;*8* and, consequently, whether vascular strands were formed by an auxin-dependent mechanism in *pin1*;*3*;*4*;*6*;*7*;*8*. To address this question, we applied lanolin paste containing 1% of the natural auxin indole-3-acetic acid (IAA) to one side of developing leaves of WT and *pin1*;*3*;*4*;*6*;*7*;*8* and recorded tissue response in mature leaves.

In agreement with previous reports (Kraus et al. 1936; Jost 1942; Sachs 1989; Scarpella et al. 2006; Sawchuk et al. 2007), IAA induced formation of extra veins in ~70% of WT leaves (27/38) (Figure 5.9A and 5.9B), while ~30% of WT leaves (9/38) failed to respond to IAA application.

The effects of IAA on *pin1*;*3*;*4*;*6*;*7*;*8* leaves were variable. In 40% of the leaves (28/70), IAA induced formation of extra veins (Figure 5.9C and 5.9D). In ~60% of the leaves in which IAA induced formation of extra veins (17/28), IAA also induced tissue outgrowth of varied shape (Figure 5.9E and 5.9F). In 30% of *pin1*;*3*;*4*;*6*;*7*;*8* leaves (21/70), IAA induced tissue outgrowth but failed to induce formation of extra veins in the leaf; however, in nearly 80% of the leaves in which IAA induced tissue outgrowth [30/(17+21)=30/38], IAA also induced formation of vascular strands in the outgrowth (Figure 5.9E and 5.9F). Finally, as in WT, 30% of *pin1*;*3*;*4*;*6*;*7*;*8* leaves (21/70) failed to respond to IAA application in any noticeable way.

We conclude that veins are formed by an auxin-dependent mechanism in the absence of PIN-mediated auxin transport.

5.2.7 Contribution of auxin signalling to vein patterning

Developing leaves of both WT and *pin1*;*3*;*4*;*6*;*7*;*8* responded to auxin application by forming extra veins (Figure 5.9), suggesting that *pin1*;*3*;*4*;*6*;*7*;*8* tissues can respond to vein-formation-inducing auxin signals. We thus asked what the contribution of auxin signalling is to vein formation in *pin1*;*3*;*4*;*6*;*7*;*8*.

The auxin signal is transduced by multiple pathways (Leyser 2010); the best understood is the pathway that is initiated by binding of auxin to receptors of the TRANSPORT INHIBITOR RESPONSE1/AUXIN SIGNALLING F-BOX (TIR1/AFB) family and terminates with activation of auxin-responsive gene expression by transcription factors of the AUXIN RESPONSIVE FACTOR (ARF) family (Chapman and Estelle 2009). Consistent with a requirement for auxin

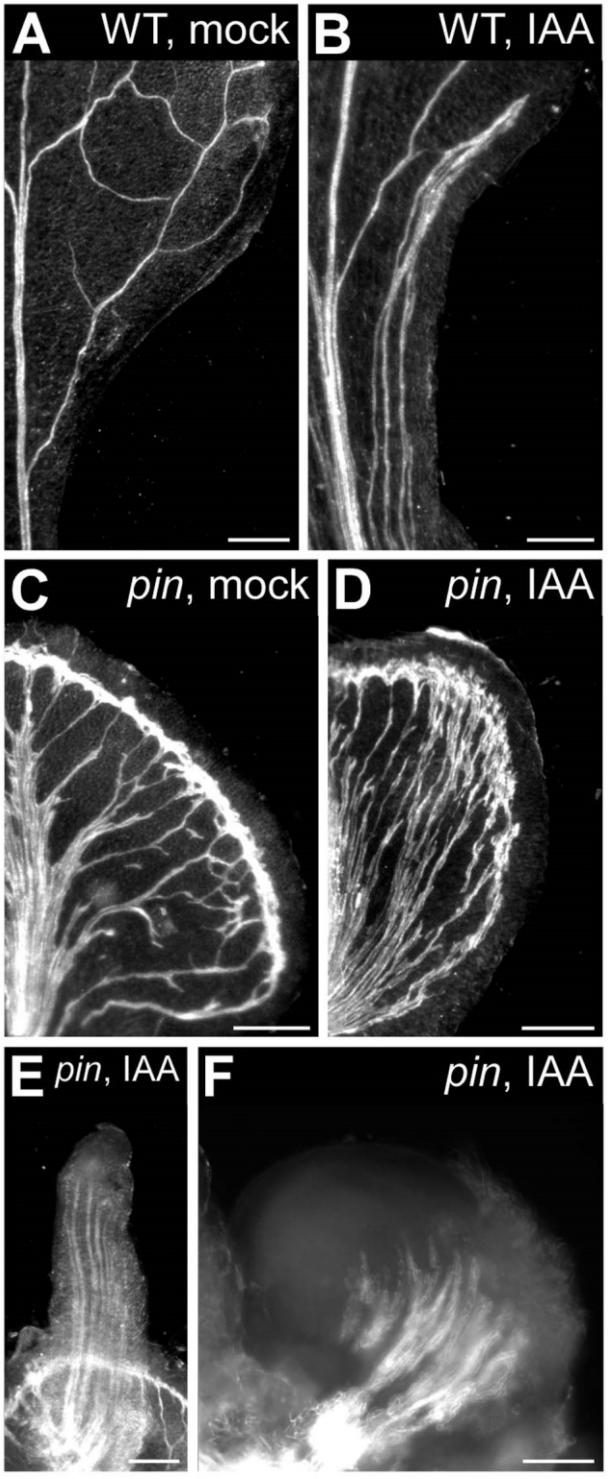

Figure 5.9. Response of *pin* leaves to auxin application. (A-F) Top right: genotype and treatment. Dark-field illumination of mature first leaves of WT (A,B) or *pin1*;*3*;*4*;*6*;*7*;*8* (C-F) at side of application of lanolin paste (A,C) or lanolin paste containing 1% IAA (B,D-F). Bars: (A) 0.5 mm; (B-E) 0.25 mm; (F) 0.1 mm.

signalling in vein formation, *tir1* mutants and mutants in the *ARF* gene *MONOPTEROS* (*ARF5*/*MP*; *MP* hereafter) have simplified vein networks (Berleth and Jurgens 1993; Przemeck et al. 1996; Hardtke and Berleth 1998; Strader et al. 2008; Donner et al. 2009).

To determine the contribution of auxin signalling to vein formation in *pin1*;*3*;*4*;*6*;*7*;*8*, we germinated and grew WT and *pin1*;*3*;*4*;*6*;*7*;*8* in the presence of the auxin antagonist auxinole, which competitively blocks binding of IAA to TIR1/AFB receptors and thus inhibits TIR1/AFB-mediated auxin responses, including *ARF*-dependent gene expression (Hayashi et al. 2012).

WT leaves formed in the presence of 50 μM auxinole were narrow and had simplified vein-networks that differentiated further away from the leaf margin than in control WT leaves (Figure 5.10A-5.10C), resembling *mp* leaves (Przemeck et al. 1996; Donner et al. 2009) (Figure 5.10M); in the most severe cases, auxinole-grown WT leaves were reduced to veinless filaments (Figure 5.10D), suggesting that TIR1/AFB-mediated auxin signalling is essential for vascular differentiation.

As in auxinole-grown WT, vascular differentiation was inhibited in *pin1*;*3*;*4*;*6*;*7*;*8* leaves formed in the presence of 50 μM auxinole, and vascular elements differentiated further away from the leaf margin in auxinole-grown *pin1*;*3*;*4*;*6*;*7*;*8* than in control *pin1*;*3*;*4*;*6*;*7*;*8* (Figure 5.10E,5.10G,5.10H,5.10J ,5.10K). These defects were particularly pronounced in more-severely affected leaves of auxinole-grown *pin1*;*3*;*4*;*6*;*7*;*8*, in which vascular differentiation was limited to a central region (Figure 5.10J and 5.10K). In this central region, vascular elements were organized in clusters that were shapeless or elongated along the proximodistal axis of the leaf (Figure 5.10J-5.10L). Vascular elements were oriented randomly at the distal side of the clusters and progressively more perpendicular to the leaf margin toward the proximal side of the clusters (Figure 5.10L). Vascular clusters were either isolated or connected laterally by short stretches of randomly oriented vascular elements (Figure 5.10J-5.10L). Occasionally, short stretches of vascular elements oriented perpendicularly to the leaf margin connected the proximal side of the clusters with the basal part of the leaf (Figure 5.10J-5.10L). In less-severely affected leaves of auxinole-grown *pin1*;*3*;*4*;*6*;*7*;*8*, the narrower vascular clusters were composed of elements that were uniformly oriented perpendicular to the leaf margin (Figure 5.10G-5.10I). Vascular clusters were frequently connected to one another by lateral stretches of vascular elements oriented parallelly to the leaf margin (Figure 5.10G-5.10I)—an orientation similar to that of the vascular

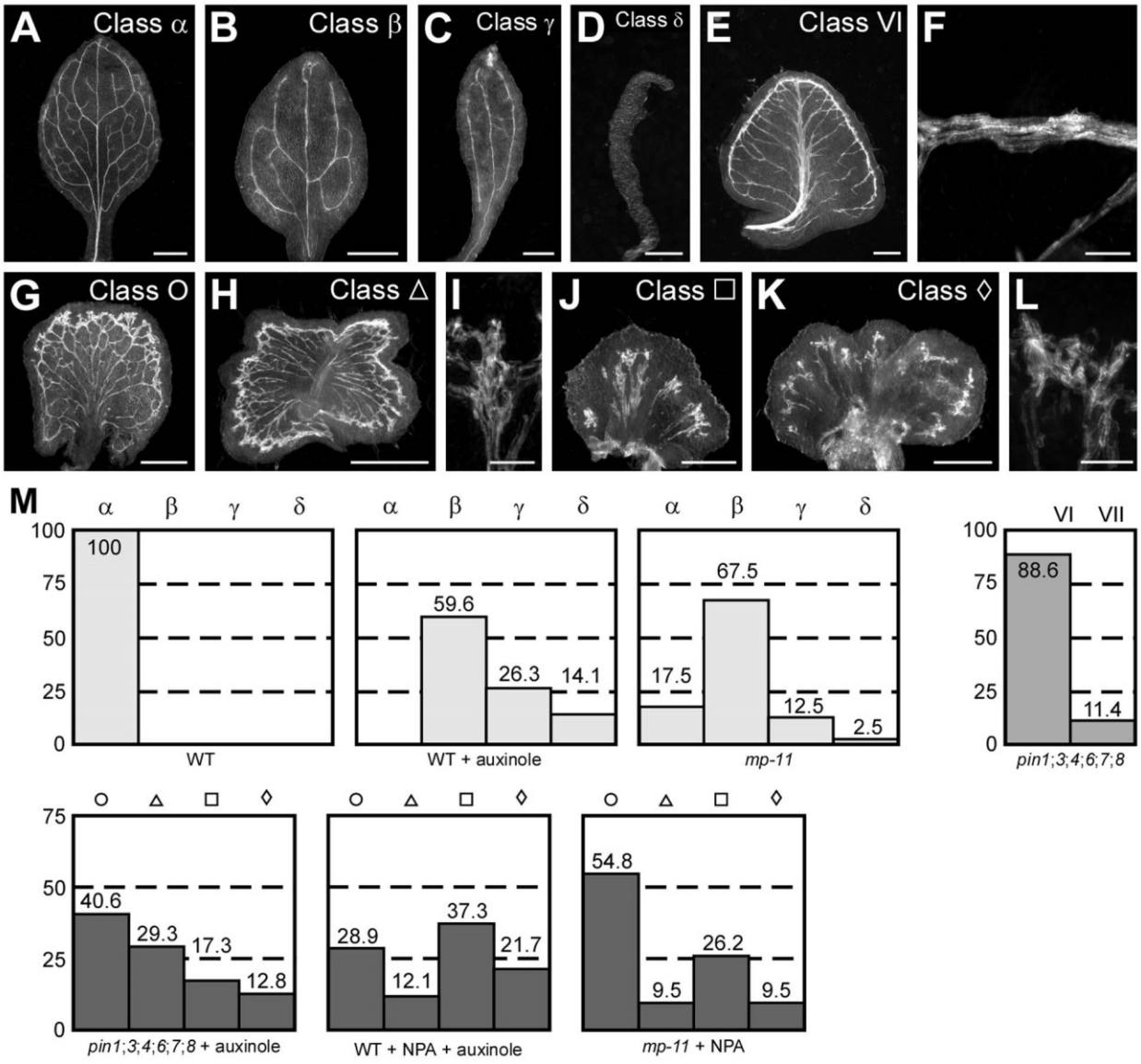

Figure 5.10. Contribution of auxin signalling to vein patterning. (A-L) Dark-field illumination of mature first leaves illustrating phenotype classes: midvein with five or six loops (A), midvein with three or four loops (B), midvein with one or two loops (C), midvein or no vascular differentiation (D), increased number of lateral veins, wide midvein and conspicuous marginal vein (E), detail of marginal vein (Classes VI and VII) illustrating vascular elements oriented parallelly to the leaf margin (F), jagged vein-network outline (G), fused leaves with jagged vein-network outline (H), detail of vascular cluster (Classes ○ and Δ) illustrating elements oriented perpendicularly to the leaf margin (I), vascular differentiation limited to clusters (J), fused leaves with vascular differentiation limited to clusters (K), detail of vascular cluster (Classes □ and ◊) illustrating random orientation of elements (L). (M) Percentages of leaves in phenotype classes. Sample population sizes: WT, 54; auxinole-grown WT, 57; *mp-11*, 40; *pin1*;*3*;*4*;*6*;*7*;*8*, 44; auxinole-grown *pin1*;*3*;*4*;*6*;*7*;*8*, 133; WT grown on auxinole and NPA, 83; NPA-grown *mp-11*, 42. Bars: (A-C,G,H) 1 mm; (D,E,J,K) 0.5 mm; (F,I,L) 0.1 mm.

elements of the marginal vein of control *pin1*;*3*;*4*;*6*;*7*;*8* leaves (Figure 5.10F); however, the vein network outline of less-severely affected leaves of auxinole-grown *pin1*;*3*;*4*;*6*;*7*;*8* was jagged, and not smooth like the vein network outline of control *pin1*;*3*;*4*;*6*;*7*;*8* leaves (Figure 5.10E,5.10G,5.10H). Finally, in less-severely affected leaves of auxinole-grown *pin1*;*3*;*4*;*6*;*7*;*8* veins oriented perpendicularly to the leaf margin (Figure 5.10G and 5.10H)—an orientation similar to that of the lateral veins of control *pin1*;*3*;*4*;*6*;*7*;*8* leaves (Figure 5.10E)—connected the vascular clusters with the middle and basal parts of the leaf, where vascular elements failed to differentiate (Figure 5.10G and 5.10H). We observed vascular defects similar to those induced in *pin1*;*3*;*4*;*6*;*7*;*8* by auxinole in WT germinated and grown on both NPA and auxinole (Figure 5.10M)

We next asked whether NPA could induce defects in the auxin-signalling mutant *mp* similar to those induced in *pin1*;*3*;*4*;*6*;*7*;*8* by auxinole and in WT by auxinole and NPA. To address this question, we used the weak allele *mp-11* (Odat et al. 2014) (Chapter 4), as NPA inhibits leaf formation in strong *mp* alleles because of their pre-existing shoot-apical-meristem defects (Schuetz et al. 2008). High concentrations of NPA inhibited leaf formation also in *mp-11*: only 16% (8/50) or 6% (3/50) of *mp-11* seedlings formed leaves in the presence of 50 or 100 μM NPA, respectively. We thus germinated and grew *mp-11* in the presence of 1 μM NPA, which allowed leaf formation in ~40% (38/94) of *mp-11* seedlings. Leaves of NPA-grown *mp-11* had vascular defects similar to those induced in *pin1*;*3*;*4*;*6*;*7*;*8* by auxinole and in WT by auxinole and NPA (Figure 5.10M).

In conclusion, our results suggest that the residual vein-patterning activity in *pin1*;*3*;*4*;*6*;*7*;*8* is provided, at least in part, by the auxin signalling mediated by the TIR1/AFB and MP proteins. Because inhibition or loss of TIR1/AFB/MP-mediated auxin signalling synthetically enhanced vein pattern defects resulting from inhibition or loss of PIN-mediated auxin transport, we conclude that TIR1/AFB/MP-mediated auxin signalling and PIN-mediated auxin transport provide overlapping functions in vein patterning. Moreover, simultaneous obstruction of TIR1/AFB/MP-mediated auxin signalling and PIN-mediated auxin transport interfered with the end-to-end juxtaposition of coherently aligned vascular-elements that defines a vein. Thus we also conclude that TIR1/AFB/MP-mediated auxin signalling and PIN-mediated auxin transport provide overlapping functions required for the very formation of veins.

5.2.8 Contribution of the *GNOM* gene to vein patterning

Vascular defects of leaves formed in conditions of simultaneously compromised TIR1/AFB/MP-mediated auxin signalling and PIN-mediated auxin transport resemble those reported for cotyledons of mutants of the *EMBRYO DEFECTIVE30*/*GNOM* (*GN* hereafter) gene, which encodes a guanine-nucleotide exchange factor for ADP-ribosylation factor GTPases (ARF GEF) that regulates vesicle formation in membrane trafficking (Mayer et al. 1991; Mayer et al. 1993; Shevell et al. 1994; Busch et al. 1996; Koizumi et al. 2000; Geldner et al. 2001; Geldner et al. 2003; Geldner et al. 2004; Sieburth et al. 2006). We asked whether leaves of a *gn* allelic series had similar vascular defects.

As leaves of control and auxinole-grown WT and of *mp-11* (Figure 5.10), ~95% of the leaves of gn^{R5} (Geldner et al. 2004) and gn^{van7} (Koizumi et al. 2000) had an unbranched midvein (Figure 5.11A and 5.11G); however—as in leaves of *pin1*;*3*;*4*;*7*, *pin1*;*3*;*4*;*6*;*7*;*8* and NPA-grown WT (Figure 5.1; Figure 5.4, Figure 5.5)—in leaves of gn^{R5} and gn^{van7}, lateral veins failed to join the midvein but ran parallelly to it to form a wide "midvein", and veins of gn^{R5} and gn^{van7} were thick (Figure 5.11A). Finally—as less-severely affected leaves of auxinole-grown *pin1*;*3*;*4*;*6*;*7*;*8*, NPA-grown *mp-11* and WT germinated and grown on both NPA and auxinole—leaves of gn^{R5} and gn^{van7} had a jagged vein-network outline with narrow vascular clusters that were composed of elements uniformly oriented perpendicular to the leaf margin and that were laterally connected by veins (Figure 5.11A,5.11D,5.11G). In ~60–75% of the leaves of gn^{SALK_103014} (Okumura et al. 2013), *emb30-8* (Moriwaki et al. 2013) and of the new allele *gn-13* (Table 5.1), a central, shapeless vascular cluster was connected with the basal part of the leaf by a wide "midvein" (Figure 5.11B,5.11G); vascular elements were oriented randomly at the distal side of the cluster and progressively more perpendicular to the leaf margin toward the proximal side of the clusters (Figure 5.11E). In ~15–30% of the leaves of gn^{SALK_103014}, *gn-13* and *emb30-8*, vascular differentiation was limited to a central, shapeless vascular cluster of randomly oriented elements (Figure 5.11C and 5.11F). Thus all the defects of leaves of gn^{SALK_103014}, *gn-13* and *emb30-8* were similar to—though more severe than—those of the more-severely affected leaves of auxinole-grown *pin1*;*3*;*4*;*6*;*7*;*8*, NPA-grown *mp-11* and WT germinated and grown on both NPA and auxinole (Figure 5.10).

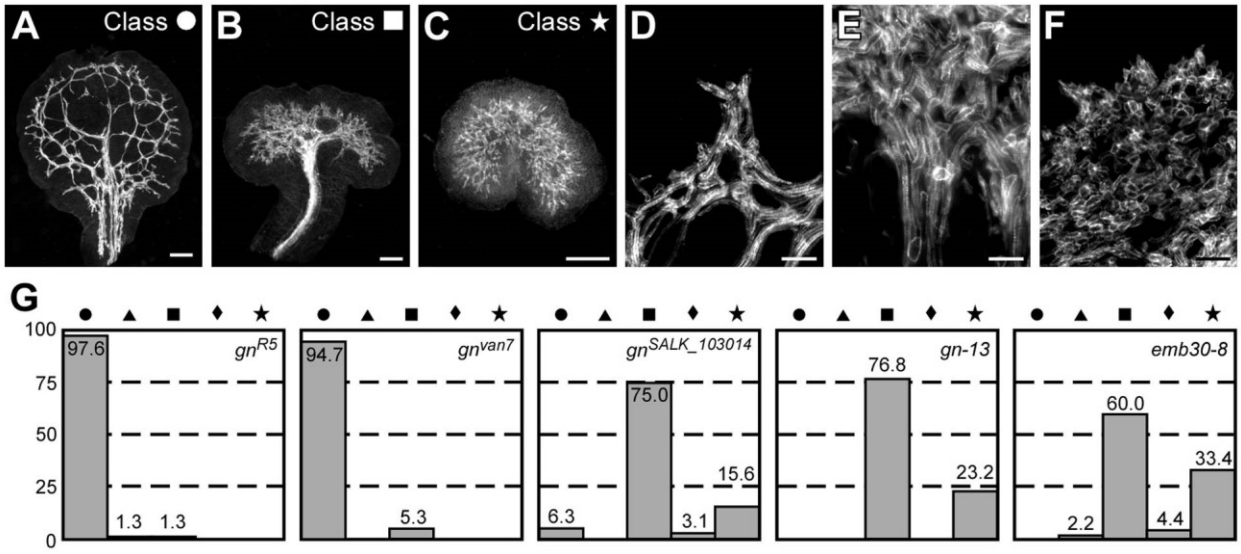

Figure 5.11. Contribution of the *GNOM* gene to vein patterning. (A-F) Dark-field illumination of mature first leaves illustrating phenotype classes: thick veins, wide midvein, jagged vein-network outline (A), shapeless vascular cluster with wide midvein (B), shapeless vascular cluster (C), detail of vascular cluster (Classes ● and ▲) illustrating elements oriented perpendicularly to the leaf margin (D), details of vascular cluster (Classes ■ and ♦) illustrating elements oriented randomly at the distal side of the cluster (top) and perpendicularly to the leaf margin at the proximal side of the cluster (bottom) (E), detail of vascular cluster (Class □) illustrating random orientation of elements (F). (G) Percentages of leaves in phenotype classes. Sample population sizes: gn^{R5}, 79; *van7*, 38; gn^{SALK_103014}, 32; *gn-13*, 56; *emb30-8*, 45. Bars: (A-C) 0.25 mm; (D-F) 50 μm.

We conclude that vascular defects of *gn* leaves resemble those of leaves formed in conditions of simultaneously compromised TIR1/AFB/MP-mediated auxin signalling and PIN-mediated auxin transport.

5.2.9 Genetic interaction between *GN* and *PIN* genes

Because vascular defects of *gn* resemble those resulting from simultaneous interference with TIR1/AFB/MP-mediated auxin signalling and PIN-mediated auxin transport (Figures 5.10 and 5.11), and because the *gn* phenotype is epistatic to the *mp* phenotype (Mayer et al. 1993), we asked whether *GN* genetically interacted with *PIN1*, *PIN3*, *PIN4* and *PIN6-PIN8*—the *PIN* genes with vein patterning function. Because the GN protein is required for coordinated polarization of PIN1 (Steinmann et al. 1999), we first asked whether *GN* genetically interacted with *PIN1*, *PIN3*, *PIN4* and *PIN7*—the *PM-PIN* genes with vein patterning function. To address this question, we used the strong allele *gn-13* (Figure 5.11).

Consistent with previous observations (Mayer et al. 1993; Shevell et al. 1994), in *gn* seedlings hypocotyl and root were replaced by a basal peg and the cotyledons were most frequently fused (70/85=~80%) (Figure 5.12A and 5.12C). *pin1*;*3*;*4*;*7* seedlings had hypocotyl, short root and two separate cotyledons (48/76=~60%) or a single cotyledon (22/76=~30%) (Figure 5.2; Figure 5.12A and 5.12B). A novel phenotype segregated in approximately one-sixteenth of the progeny of plants homozygous for *pin3*, *pin4* and *pin7* and heterozygous for *pin1* and *gn* (29/631)—no different from the one-sixteenth frequency expected for the *gn*;*pin1*;*3*;*4*;*7* homozygous mutants by Pearson's chi- squared (χ^2) goodness-of-fit test (α=0.05, dF=1). We genotyped three of the seedlings with the novel mutant phenotype and found they were *gn*;*pin1*;*3*;*4*;*7* homozygous mutants. *gn*;*pin1*;*3*;*4*;*7* seedlings had hypocotyl (Figure 5.12A and 5.12D)—suggesting that the *pin1*;*3*;*4*;*7* hypocotyl phenotype is epistatic to the *gn* hypocotyl phenotype—but had no root (Figure 5.12A and 5.12D)—suggesting that the *gn* root phenotype is epistatic to the *pin1*;*3*;*4*;*7* root phenotype. Further, *gn*;*pin1*;*3*;*4*;*7* seedlings had fused cotyledons (28/29=~97%) (Figure 5.12A and 5.12D); the absence of *gn*;*pin1*;*3*;*4*;*7* seedlings with two separate cotyledons or a single cotyledon— collectively characteristic of ~90% of *pin1*;*3*;*4*;*7* seedlings (Figure 5.2)—might be considered evidence of epistasis of the *gn* cotyledon phenotype to the *pin1*;*3*;*4*;*7* cotyledon phenotype.

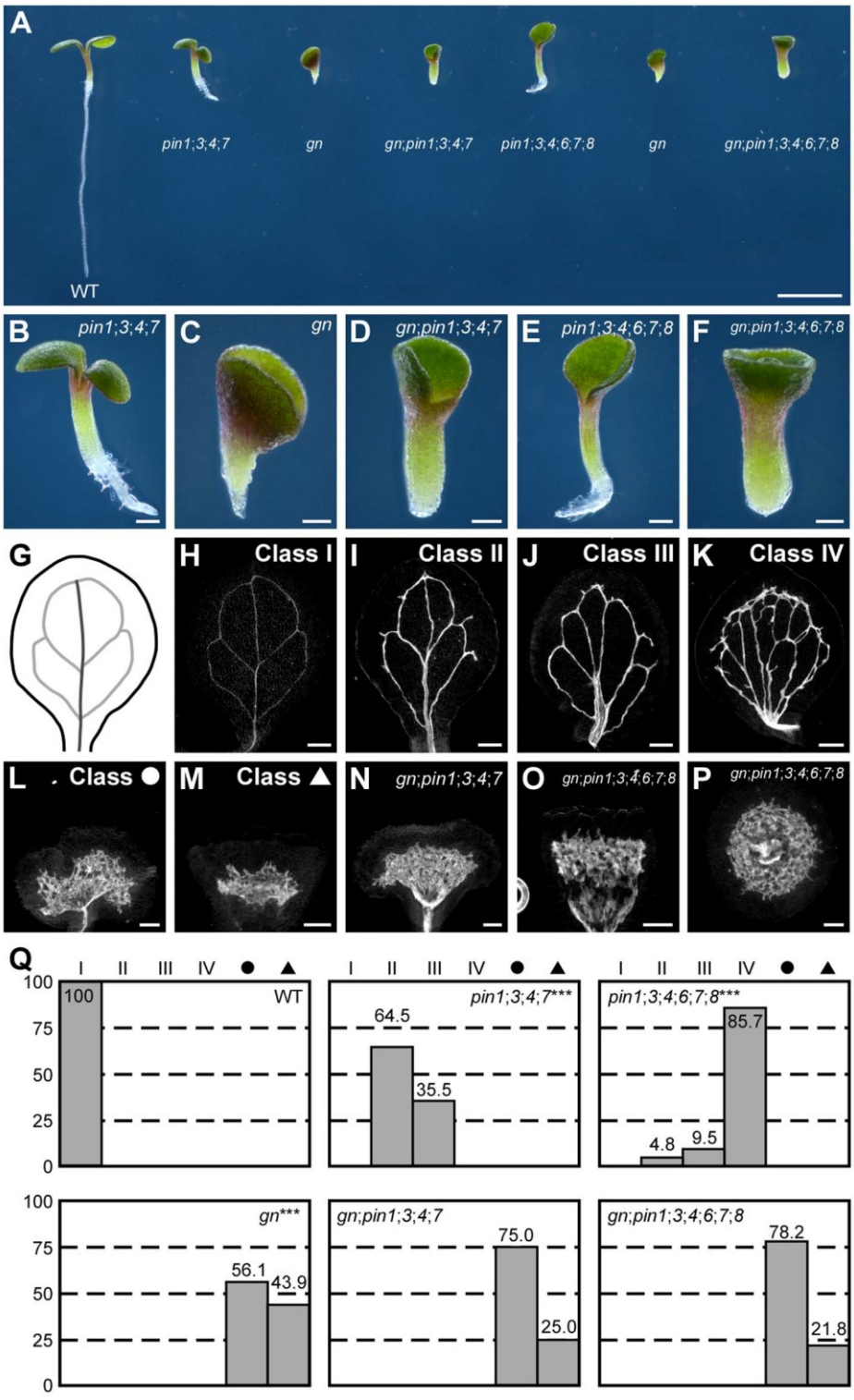

Figure 5.12. Genetic interaction between *GN* and *PIN* genes. (A-F) Dark-field illumination composites of 3-day-old seedlings. (A) Overview. (B-F) Details. Genotypes below respective seedlings (A) or top right (B-F). (G,H) Vein pattern of WT mature cotyledon. In (G), dark grey,

midvein; light grey, vein loops. (H-P) Dark-field illumination of mature cotyledons illustrating phenotype classes: unbranched midvein and three or four loops (H), thick veins, unbranched midvein, minor veins (I), thick veins, bifurcated midvein, minor veins (J), thick veins, loops joining midvein at base of cotyledon, thickening of top half of vein network outline (K), shapeless vascular cluster with short stretches of vascular elements connecting the cluster to base of cotyledon (L), shapeless vascular cluster (M). (N-P) Dark-field illumination of mature cotyledons of *gn*;*pin1*;*3*;*4*;*7* (Class V) (N) or *gn*;*pin1*;*3*;*4*;*6*;*7*;8 (Class V) (O, side view; P, top view). (Q) Percentages of cotyledons in phenotype classes. Difference between *pin1*;*3*;*4*;*7* and WT, difference between *pin1*;*3*;*4*;*6*;*7*;*8* and WT, and difference between *gn* and WT was significant at $P<0.001$ (***) by Kruskal-Wallis and Mann-Whitney test with Bonferroni correction. Sample population sizes: WT, 52; *pin1*;*3*;*4*;*7*, 31; *pin1*;*3*;*4*;*6*;*7*;*8*, 63; *gn*, 57; *gn*;*pin1*;*3*;*4*;*7*, 24; *gn*;*pin1*;*3*;*4*;*6*;*7*;*8*, 46. Bars: (A) 2mm; (B-F,H-P) 0.25 mm.

WT cotyledons had an unbranched midvein and three or four loops (Figure 5.12G,5.12H,5.12Q). All the veins of *pin1*;*3*;*4*;*7* cotyledons were thick, and all *pin1*;*3*;*4*;*7* cotyledons had three or four loops (Figure 5.12I,5.12J,5.12Q). In *pin1*;*3*;*4*;*7* cotyledons, the distal end of the first loops joined the midvein more proximally than in WT, and minor veins branched from midvein and loops (Figure 5.12I,5.12J,5.12Q). Approximately 65% of *pin1*;*3*;*4*;*7* cotyledons had an unbranched midvein, while the midvein bifurcated near the cotyledon tip in the remaining ~35% of *pin1*;*3*;*4*;*7* cotyledons (Figure 5.12J and 5.12Q). Consistent with previous observations (Mayer et al. 1993; Shevell et al. 1994), in ~55% of *gn* cotyledons short stretches of vascular elements connected the proximal side of a central, shapeless vascular cluster of randomly oriented elements with the basal part of the cotyledon, while vascular differentiation was limited to a central, shapeless vascular cluster in the remaining ~45% of *gn* cotyledons (Figure 5.12L,5.12M,5.12Q). Vascular defects of *gn*;*pin1*;*3*;*4*;*7* cotyledons were no different from those of *gn* cotyledons (Figure 5.12N and 5.12Q), suggesting that the *gn* vascular phenotype is epistatic to the *pin1*;*3*;*4*;*7* vascular phenotype.

We next asked whether *GN* also genetically interacted with all the *PIN* genes with vein patterning function.

pin1;*3*;*4*;*6*;*7*;*8* seedlings had hypocotyl, short root and fused cotyledons (32/65=~50%) or a single cotyledon (25/65=~40%) (Figure 5.2; Figure 5.12A and 5.12E). A phenotype similar to that of *gn*;*pin1*;*3*;*4*;*7* segregated in approximately one-sixteenth of the progeny of plants homozygous for *pin3*, *pin4*, *pin6*, *pin7* and *pin8* and heterozygous for *pin1* and *gn* (76/1074)—no different from the one-sixteenth frequency expected for the *gn*;*pin1*;*3*;*4*;*6*;*7*;*8* homozygous mutants by Pearson's χ^2 goodness-of-fit test (α=0.05, dF=1). We genotyped five of the seedlings with the novel mutant phenotype and found they were *gn*;*pin1*;*3*;*4*;*6*;*7*;*8* homozygous mutants. *gn*;*pin1*;*3*;*4*;*6*;*7*;*8* seedlings resembled *gn*;*pin1*;*3*;*4*;*7* seedlings: they had hypocotyl (Figure 5.12A and 5.12F)—suggesting that the *pin1*;*3*;*4*;*6*;*7*;*8* hypocotyl phenotype is epistatic to the *gn* hypocotyl phenotype—but had no root (Figure 5.12A and 5.12F)—suggesting that the *gn* root phenotype is epistatic to the *pin1*;*3*;*4*;*6*;*7*;*8* root phenotype. Unlike *gn*;*pin1*;*3*;*4*;*7* seedlings, however, ~90% (42/48) of *gn*;*pin1*;*3*;*4*;*6*;*7*;*8* seedlings had completely fused cup-shaped cotyledons (Figure 5.12A,5.12D,5.12F)—a phenotype not observed in *gn* (0/85) (Figure 5.12A and 5.12B) or *pin1*;*3*;*4*;*6*;*7*;*8* (0/65) (Figure 5.2; Figure 5.12A and 5.12B)—suggesting synthetic

enhancement of the *gn* cotyledon phenotype by the *pin1*;*3*;*4*;*6*;*7*;*8* cotyledon phenotype; because the *gn* cotyledon phenotype is epistatic to the *pin1*;*3*;*4*;*7* cotyledon phenotype, the synthetic enhancement is probably due to *pin6* and *pin8*.

Defects of *pin1*;*3*;*4*;*6*;*7*;*8* cotyledons were similar to those of *pin1*;*3*;*4*;*7* cotyledons, but in addition in ~85% of *pin1*;*3*;*4*;*6*;*7*;*8* cotyledons the loops joined the midvein at the base of the cotyledon and the top half of the vein network outline was thick (Figure 5.12I,5.12J,5.12K,5.12Q). Vascular defects of *gn*;*pin1*;*3*;*4*;*6*;*7*;*8* cotyledons were no different from those of *gn* cotyledons (Figure 5.12O-Q), suggesting that the *gn* vascular phenotype is epistatic to the *pin1*;*3*;*4*;*6*;*7*;*8* vascular phenotype.

Thus our results suggest that in vascular development *GN* acts upstream of the *PIN* genes with vein patterning function.

5.3 Discussion

5.3.1 Control of vein patterning by carrier-mediated auxin transport

Overwhelming experimental evidence places polar auxin transport at the core of the mechanism that defines sites of vein formation [reviewed in (Sachs 1981; Berleth et al. 2000; Sawchuk and Scarpella 2013)] (Chapter 1). The polarity of auxin transport is determined by the asymmetric localization of auxin effluxers of the PIN family at the plasma membrane (PM) of auxin-transporting cells (Wisniewska et al. 2006). Thus one might predict that loss of the function of all the PM-localized PIN (PM-PIN) proteins should lead to loss of reproducible vein-pattern features, or perhaps even—in the most extreme case—to the inability to form veins. Neither prediction is, however, supported by evidence: mutants in all the *PM-PIN* genes with vein patterning function—*PIN1*, *PIN3*, *PIN4* and *PIN7*—or in all the *PM-PIN* genes—*PIN1–PIN4* and *PIN7*—form veins, which are arranged in reproducible—though abnormal—patterns. The most parsimonious account for the discrepancy between the observed and expected mutants' defects is that vein patterning is controlled by additional, *PM-PIN*-independent auxin-transport pathways.

The existence of *PM-PIN*-independent auxin-transport pathways with vein patterning function can also be inferred from the discrepancy between the vein pattern defects resulting from simultaneous mutation in all the *PM-PIN* genes with vein patterning function, or in all the *PM-PIN* genes, and the vein pattern defects induced by NPA, which is thought to be a specific inhibitor of carrier-mediated cellular auxin-efflux (Rubery 1990; Dhonukshe et al. 2008). The vein pattern defects of WT grown in the presence of NPA are more severe than those of *pin1*;*3*;*4*;*7* or *pin1*;*2*;*3*;*4*;*7*, suggesting the existence of NPA-sensitive auxin-transport pathways with vein patterning function in addition to the *PM-PIN*-dependent pathway—a suggestion that is supported by the observation that growth in the presence of NPA enhances the *pin1*;*3*;*4*;*7* vein-pattern phenotype to match that of NPA-grown WT.

Such *PM-PIN*-independent NPA-sensitive auxin-transport pathway with vein patterning function depends on the activity of the endoplasmic-reticulum (ER)-localized PIN6 and PIN8 (Figure 5.13), as inferred from the identity of the vein pattern defects resulting from simultaneous mutation in *PIN1*, *PIN3*, *PIN4*, *PIN6*, *PIN7* and *PIN8* and those induced by NPA, and from the inability of NPA to induce further defects in *pin1*;*3*;*4*;*6*;*7*;*8*. Moreover, that NPA-grown WT phenocopies *pin1*;*3*;*4*;*6*;*7*;*8*, that no further defects can be induced in *pin1*;*3*;*4*;*6*;*7*;*8* by NPA, and that mutants and NPA-grown WT form veins arranged in reproducible patterns suggest no residual NPA-sensitive vein-patterning activity beyond that provided by *PIN1*, *PIN3*, *PIN4*, *PIN6*, *PIN7* and *PIN8*, and thus also the existence of NPA-insensitive vein-patterning pathways.

These NPA-insensitive vein-patterning pathways are unlikely to be mediated by known intercellular auxin transporters—the AUX1/LAX auxin influxers (Yang et al. 2006; Swarup et al. 2008; Peret et al. 2012) and the ABCB1 and ABCB19 auxin effluxers (Geisler et al. 2005; Bouchard et al. 2006; Petrasek et al. 2006)—as their mutation fails to enhance the vein pattern phenotype of the NPA-induced phenocopy of *pin1*;*3*;*4*;*6*;*7*;*8*. Though it remains undetermined whether the NPA-insensitive vein-patterning pathways depend on the function of unknown intercellular auxin transporters or other intracellular auxin transporters [e.g., (Barbez et al. 2012)], such pathways contribute to the polar propagation of the inductive auxin signal: as in WT, application of auxin to *pin1*;*3*;*4*;*6*;*7*;*8* developing leaves induces the formation of veins that connect the applied auxin to the pre-exiting vasculature basal to the site of auxin application.

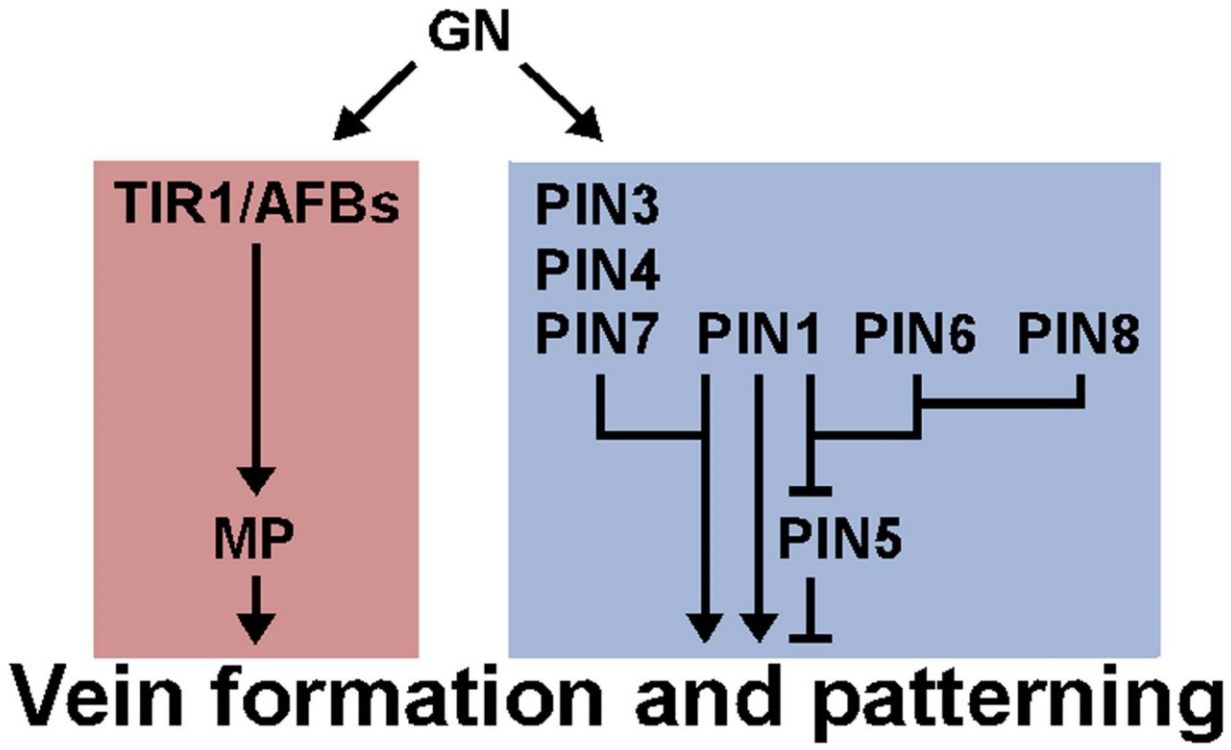

Figure 5.13. Genetic interaction network for GN, TIR1/AFB/MP-dependent auxin signalling and PIN-dependent auxin transport in vein formation and patterning. Arrows indicate positive effects; blunt-ended lines indicate negative effects. See text for details.

5.3.2 Control of vein patterning by auxin signal transduction

The residual NPA-insensitive auxin-dependent vein-patterning activity of *pin1*;*3*;*4*;*6*;*7*;*8* depends on, at least in part, the signal transduction mediated by the TIR1/AFB auxin receptors and the MP auxin-responsive transcription factor (Figure 5.13). Auxinole—a specific inhibitor of TIR1/AFB-mediated signalling (Hayashi et al. 2012) that in WT induces vascular differentiation defects characteristic of compromised auxin signalling—induces entirely new vein-patterning defects in *pin1*;*3*;*4*;*6*;*7*;*8*—defects observed in neither untreated *pin1*;*3*;*4*;*6*;*7*;*8* nor auxinole-grown WT: in the more-severely affected leaves of auxinole-grown *pin1*;*3*;*4*;*6*;*7*;*8*, vein formation is replaced by the differentiation of randomly oriented vascular elements organized in isolated, shapeless clusters. Not only are these defects observed in neither untreated *pin1*;*3*;*4*;*6*;*7*;*8* nor auxinole-grown WT, but they are more severe than the predicted sum of the defects of untreated *pin1*;*3*;*4*;*6*;*7*;*8* and auxinole-grown WT. A similar synthetic enhancement of vein pattern phenotypes is observed in WT grown in the presence of both auxinole and NPA and in NPA-grown *mp* mutants. These observations are especially interesting because genetic analysis of auxin signalling components had so far implicated auxin signalling only in the differentiation of normally patterned veins (Przemeck et al. 1996; Hardtke et al. 2004; Alonso-Peral et al. 2006; Candela et al. 2007). Instead, the mutual synthetic enhancement between the vein pattern phenotype of reduced auxin signalling and that of reduced auxin transport suggests non-homologous redundancy of auxin signalling and transport in vein patterning (Figure 5.13). Such redundancy is unequal, however: whereas auxin transport is required for vein patterning even in the presence of normal auxin signalling, the vein patterning activity of auxin signalling is only exposed in conditions of compromised auxin transport.

How auxin signalling—inherently non-directional—could propagate polar information is unclear. One possibility is that auxin diffuses through plasmodesmata (PD) intercellular channels—a possibility that had previously been suggested (Mitchison 1981) and that has recently found some experimental support (Han et al. 2014)—and that the size of the PD aperture or the proportion of PD in the transverse walls of incipient vascular cells are positively regulated by auxin signalling. Rapid, efficient PIN-mediated transport of auxin across the PM would normally limit or dominate the slow, inefficient diffusion of auxin through PD. But in the absence of PM-PIN-mediated transport, auxin would predominantly—or exclusively—move

through PD, thus exposing the relevance of such movement for vein patterning. Though PD aperture is greater at sites that seem to overlap with sites of maximum auxin signalling and vein formation (Mattsson et al. 2003; Kim et al. 2005), and though mathematical models of diffusion-mediated auxin transport successfully recapitulate aspects of vein formation (Mitchison 1981; Rolland-Lagan and Prusinkiewicz 2005), the possibility that auxin movement through PD controls vein patterning and alternative hypotheses remain to be experimentally tested.

5.3.3 A tissue-cell-polarizing signal upstream of auxin transport and signalling

The vascular defects of leaves in which both transport and transduction of the auxin signal are compromised are never observed in leaves in which either process is; yet those defects are not unprecedented: they are observed—though in more extreme form—in leaves and cotyledons of *gn* mutants, suggesting that *GN* might control both transport and transduction of the auxin signal (Figure 5.13).

Though it is unclear how the ARF GEF activity of GN might control auxin signalling, the suggestion is not unsupported: genetic analysis places *GN* upstream of *MP* in a linear pathway that controls the formation of the apical-basal polarity of the embryo (Mayer et al. 1993)—a process that depends on polar auxin signalling from the embryo vascular strand (Weijers et al. 2006).

Seemingly less surprising is the conclusion that *GN* controls PM-PIN-mediated auxin transport: the ARF GEF activity of GN is required for the coordinated polarization of PIN1 localization during embryogenesis (Steinmann et al. 1999). However, if failure to coordinate the polarization of the localization of PIN1—and possibly other PM-PIN proteins—were the cause of the *gn* vascular defects, one would predict these defects to be dependent on *PM-PIN* function and thus the *gn* vascular phenotype to be masked by the *pin1*;*3*;*4*;*7* vascular phenotype in the *gn*;*pin1*;*3*;*4*;*7* mutant. The epistasis of the *gn* vascular phenotype to the *pin1*;*3*;*4*;*7* vascular phenotype instead suggests that: (i) *gn* vascular defects are independent of *PM-PIN* function; (ii) *GN* acts upstream of *PM-PIN* genes in a linear pathway that controls formation and patterning of veins; (iii) the tissue-cell-polarizing function of *GN* entails more than the regulation of PM-PIN-mediated auxin transport and of the coordinated polarization of PM-PIN localization—a conclusion also suggested by the observation that vascular defects of *gn* are more severe than

those of auxinole-grown *pin1*;*3*;*4*;*6*;*7*;*8*, WT grown in the presence of both auxinole and NPA, and NPA-grown *mp*. Our observations and conclusions are also consistent with more-severe epidermal-cell-polarity defects in *gn* than in *pm-pin* mutants, defects that are associated with normal localization of PM-PIN proteins (Fischer et al. 2006).

Polarization of PIN1 localization and orientation of microtubule arrays during patterned formation of shoot lateral organs seem to be controlled by an upstream mechanical signal from the cell wall (Heisler et al. 2010). Because cell wall composition and properties are abnormal in *gn* (Shevell et al. 2000), it will be interesting to test whether *GN* contributes to the production of such mechanical signal with functions beyond polarization of PIN1 localization, and thus whether the functions of this mechanical signal overlap with those of the *GN*-dependent signal we have identified upstream of PM-PIN-mediated auxin transport.

Independently of a possible function of *GN* in mechanical signalling, one of the functions of *GN* beyond the regulation of PM-PIN-mediated auxin transport is the control of auxin transport mediated by the endoplasmic-reticulum (ER)-localized PIN6 and PIN8, a conclusion suggested by the epistasis of the *gn* vascular phenotype to the *pin1*;*3*;*4*;*6*;*7*;*8* vascular phenotype. Though it is unclear how *GN* could control ER-PIN-mediated auxin transport, it is possible that such control is indirect and mediated by *GN* function in ER–Golgi trafficking (Richter et al. 2007).

As in vein formation, the epistasis of the root phenotype of *gn* to that of *pin1*;*3*;*4*;*7* or *pin1*;*3*;*4*;*6*;*7*;*8* suggest that *GN* acts upstream of PIN-mediated auxin transport in root formation. By contrast, the epistasis of the hypocotyl phenotype of *pin1*;*3*;*4*;*7* or *pin1*;*3*;*4*;*6*;*7*;*8* to that of *gn* suggest that PIN-mediated auxin transport acts upstream of *GN* in hypocotyl formation. The genetic interaction between *GN* and *PIN* genes in cotyledon patterning is even more complex. The epistasis of the cotyledon phenotype of *gn* to that of *pin1*;*3*;*4*;*7* suggests that *GN* acts upstream of PM-PIN-mediated auxin transport in cotyledon patterning. On the other hand, *gn*;*pin1*;*3*;*4*;*6*;*7*;*8* mutant has defects that are more severe than the predicted sum of the defects of *gn*;*pin1*;*3*;*4*;*6*;*7*;*8* and *gn*;*pin1*;*3*;*4*;*6*;*7*;*8*. Because of the epistasis of the cotyledon phenotype of *gn* to that of *pin1*;*3*;*4*;*7*, the synthetic enhancement of the *gn* cotyledon phenotype by *pin1*;*3*;*4*;*6*;*7*;*8* is likely due to *pin6*;*8*. That the analysis of different phenotypes uncovered different functional relations between *GN* and *PIN* genes is consistent with the low level of conservation of genetic interactions between processes observed in animals (Horn et al. 2011).

As severe as they may be, the defects resulting from mutations in *PM-PIN* genes, *MP* or *GN* neither interfere with completion of embryogenesis nor obliterate embryo patterning or vein formation, suggesting that additional tissue-cell-polarizing signals exist beyond those provided by these genes. It will be focus of future research the identification of such signals.

5.4 Materials and Methods

5.4.1 Plants

Origin and nature of lines, genotyping strategies and oligonucleotide sequences are in Tables 5.1, 5.5 and 5.6, respectively. Seeds were sterilized as in (Sawchuk et al. 2008). For auxinole-related experiments, seeds were germinated and seedlings grown in half-strength Murashige and Skoog salts (Caisson Laboratories Inc.), 15 g l^{-1} sucrose (BioShop Canada Inc.), 0.5 g l^{-1} MES (BioShop Canada Inc.), pH 5.7], at 25°C under continuous light (~65 μmol m^{-2} s^{-1}) on a rotary shaker at 50 rpm. For all other experiments, seeds were germinated, and seedlings and plants were grown as in (Sawchuk et al. 2008).

5.4.2 Chemicals

1-N-naphthylphthalamic acid (NPA) (Chem Service Inc.) was dissolved in dimethyl sulfoxide; dissolved NPA was added to growth medium just before sowing. Indole-3-acetic acid (IAA) (Sigma-Aldrich Co. LLC.) was dissolved in melted (55°C) lanolin (Sigma-Aldrich Co. LLC.); the IAA-lanolin paste was applied to first leaves 4 days after germination and was reapplied weekly. The IAA-derivative auxinole (Hayashi et al. 2012) (a generous gift of Ken-ichiro Hayashi) was dissolved in dimethyl sulfoxide; dissolved auxinole was added to growth medium just before sowing and was replaced weekly.

5.4.3 Imaging

Leaves were mounted and imaged as in (Sawchuk et al. 2013) (Chapter 2). Fluorescent-protein-

Table 5.5. Genotyping strategies.

Line	Strategy
pin1-1	'pin1-1 F' and 'pin1-1 R'; *Tat*I
eir1-1	'eir1-1 F' and 'eir1-1 R'; *Bse*LI
pin3-3	'pin3-3 F' and 'pin3-3 R'; *Sty*I
pin4-2	*PIN4*: 'PIN4 forw geno II' and 'PIN4en rev Ikram'; *pin4*: 'PIN4en rev Ikram' and 'en primer'
pin6	*PIN6*: 'PIN6 spm F' and 'PIN6 spm R'; *pin6*: 'PIN6 spm F' and 'Spm32'
$pin7^{En}$	*PIN7*: 'PIN7en forw Ikram' and 'PIN7en rev'; *pin7*: 'PIN7en rev Ikram II' and 'en primer'
pin8-1	*PIN8*: 'SALK_107965 LP' and 'SALK_107965 RP'; *pin8*: 'SALK_107965 RP' and 'LBb1.3'
pgp1-100	*ABCB1*: 'SALK_083649 pgp1-100 LP' and 'SALK_083649 pgp1-100 RP'; *abcb1*: 'SALK_083649 pgp1-100 RP' and 'LBb1.3'
atmdr1-101	*ABCB19*: 'SALK_031406 atmdr1-101 LP' and 'SALK_031406 atmdr1-101 RP'; *abcb19*: 'SALK_031406 atmdr1-101 RP' and 'LBb1.3'
ucu2-4	*UCU2*: 'SALK_012836 twd1 LP' and 'SALK_012836 twd1 RP'; *ucu2*: 'SALK_012836 twd1 RP' and 'LBb1.3'
aux1-21	'aux1-21 fwd' and 'aux1-21 rev'; *Apa*LI
lax1	*LAX1*: 'lax1 fwd' and 'lax1 WT rev'; *lax1*: 'lax1 fwd' and 'lax123 mutant rev'
lax2	*LAX2*: 'lax2 fwd' and 'lax2 WT rev'; *lax3*: 'lax2 fwd' and 'lax123 mutant rev'
lax3	*LAX3*: 'lax3 fwd' and 'lax3 WT rev'; *lax3*: 'lax3 fwd' and 'dSpm5'
mp-11	*MP*: 'SAIL_1265_F06LP' and 'SAIL_1265_F06RP'; *mp*: 'SAIL_1265_F06RP' and 'LB3'
gn-13	*GN*: 'SALK_045424 gn LP' and 'SALK_045424 gn RP'; *gn*: 'SALK_045424 gn RP' and 'LBb1.3'

Table 5.6. Oligonucleotide sequences.

Name	Sequence (5' to 3')
PIN4 prom PstI forw	TCTCTGCAGTTTGTGTATCTTAATTATTTGAGTATG
PIN4 1032 SalI rev	TATGTCGACGTCATGGCTCGCTTTGCTATC
PIN4 1033 SalI forw	TATGTCGACGCTAAGGAGCTTCACATG
PIN4 UTR EcoRI rev	TACGAATTCCAGTATAAACCACTTAACTAGAAAC
EGFP SalI Forw	TATGTCGACGTGAGCAAGGGCGAGGAG
EGFP SalI Rev	TATGTCGACCTTGTACAGCTCGTCCATGC
PIN7 prom SalI forw	TAAGTCGACAAAAATAATATTTTATTTAAGATAA TTATG
PIN7 UTR KpnI rev	TATGGTACCCTTTCTCAAATAATCTC
EGFP SacI forw	TAAGAGCTCAGGTGAGCAAGGGCGAGGAG
EGFP SacI rev	TATGAGCTCCCTTGTACAGCTCGTCCATGC
pin1-1 F	ATGATTACGGCGGCGGACTTCTA
pin1-1 R	TTCCGACCACCACCAGAAGCC
eir1-1 F	TTGTTGATCATTTTACCTGGGACA
eir1-1 R	GGTTGCAATGCCATAAATAGAC
pin3-3 F	GGAGCTCAAACGGGTCACCCG
pin3-3 R	GCTGGATGAGCTACAGCTATATTC
en primer	GAGCGTCGGTCCCCACACTTCTATAC
PIN4 forw geno II	GTCCGACTCCACGGCCTTC
PIN4en rev Ikram	ATCTTCTTCTTCACCTTCCACTCT
Spm32	TACGAATAAGAGCGTCCATTTTAGAGTG
PIN6 spm F	CATAACGAAGCTAACTAAGGGGTAATCTC
PIN6 spm R	GGAGTTCAAAGAGGAATAGTAGCAGAG
PIN7en forw Ikram	CCTAACGGTTTCCACACTCA
PIN7en rev	TAGCTCTTTAGGGTTTAGCTC
PIN7en rev Ikram II	GGTTTAGCTCTGCTGTGGAGTT
LBb1.3	ATTTTGCCGATTTCGGAAC
SALK_107965 LP	TGAAAGACATTTTGATGGCATC
SALK_107965 RP	CCAAATCAAGCTTTGCAAGAC

SALK_083649 pgp1-100 LP	GAAGACTGCGACAAGGACAAG
SALK_083649 pgp1-100 RP	GCAAGAGCGATGTTGAAGAAC
SALK_031406 atmdr1-101 LP	GCAATTGCAATTCTCTGCTTC
SALK_031406 atmdr1-101 RP	CTCAGGCAATTGCTCAAGTTC
SALK_012836 twd1 LP	GTGAAGCTGAGGTCTTGGATG
SALK_012836 twd1 RP	TATGGCCTGAAACAGCAAAAC
aux1-21 fwd	CTGGAAAGCACTAGGACTCGC
aux1-21 rev	AAGCGGCGAAGAAACGATACAG
lax123 mutant rev	AAGCACGACGGCTGTAGAATAG
lax1 fwd	ATATGGTTGCAGGTGGCACA
lax1 WT rev	GTAACCGGCAAAAGCTGCA
lax2 fwd	ATGGAGAACGGTGAGAAAGCAGC
lax2 WT rev	CGCAGAAGGCAGCGTTAGCG
dSpm5	CGGGATCCGACACTCTTTAATTAACTGACACTC
lax3 fwd	TACTTCACCGGAGCCACCA
lax3 WT rev	TGATTGGTCCGAAAAAGG
LB3	TAGCATCTGAATTTCATAACCAATCTCGATACAC
SAIL_1265_F06LP	GCTTCATCTCTTCAAGCAAGG
SAIL_1265_F06RP	TCCCAAAGTCTCACCACTCAC
SALK_045424 gn LP	TGATCCAAATCACTGGGTTTC
SALK_045424 gn RP	AGCTGAAGATAGGGAATTCGC

specific imaging parameters are in Table 5.7. Mature leaves were fixed in 3:1 ethanol:acetic acid, rehydrated in 70% ethanol and water, cleared briefly (few seconds to few minutes) in 0.4 M sodium hydroxide, washed in water and mounted in 1:3:8 water:glycerol:chloral hydrate (Sigma-Aldrich Co. LLC.). Mounted leaves were imaged as in (Odat et al. 2014) (Chapter 4). Image brightness and contrast were adjusted by linear stretching of the histogram with ImageJ (National Institutes of Health). Images were cropped with Photoshop (Adobe Systems Inc.) and assembled into figures with Canvas (ACD Systems International Inc.).

Table 5.7. Fluorescent-protein-specific imaging parameters.

Fluorescent protein	Laser	Wavelength (nm)	Main dichroic beam splitter	First secondary dichroic beam splitter	Second secondary dichroic beam splitter	Emission filter (detector)
GFP	Ar	488	HFT 405/488/594	NFT 545	NFT 490	BP 505-530 (PMT3)
YFP	Ar	514	HFT 405/514/594	NFT 595	NFT 515	BP 520-555 IR (PMT3)

CHAPTER 6: DISCUSSION

6.1 Summary

The scope of my Ph.D. thesis was to understand the contribution of auxin transport to Arabidopsis vein patterning and network formation.

The patterns of veins within networks are characterized by sets of reproducible features—such as the propensity of lateral veins to join distal veins to form closed loops—features so reproducible that they are used to define plant species (e.g., (Klucking 1995)). However, other features of vein networks, such as their complexity—which depends on the number of veins and their extent of interconnectedness—are variable. As a result, the vein networks of two leaves may have the same pattern and complexity, the same vein pattern but different complexities, different patterns but the same complexity, or different patterns and complexities.

My results, in combination with previous evidence (Mayer et al. 1993), suggest that *EMBRYO DEFECTIVE30/GNOM* (*GN*) promotes vein patterning upstream of auxin signalling mediated by the TRANSPORT INHIBITOR RESPONSE1/AUXIN SIGNALLING F-BOX (TIR1/AFBs) auxin receptors and the MONOPTEROS (MP) auxin-responsive transcription factor (Chapter 5; Figure 6.1A). My results also suggest that *GN* promotes vein patterning upstream of auxin transport mediated by the PIN-FORMED (PIN) family of auxin transporters (Chapter 5; Figure 6.1A). The PIN family is composed of three endoplasmic reticulum-localized PIN proteins (PIN5, PIN6 and PIN8) (Petrasek et al. 2006; Mravec et al. 2009; Bosco et al. 2012; Ding et al. 2012; Bender et al. 2013; Cazzonelli et al. 2013; Sawchuk et al. 2013) (Chapter 2) and five plasma membrane-localized PIN proteins (PIN1-PIN4 and PIN7) (Chen et al. 1998; Galweiler et al. 1998; Luschnig et al. 1998; Muller et al. 1998; Friml et al. 2002a; Friml et al. 2002b; Friml et al. 2003). I found that *PIN1* is the only *PIN* gene with non-redundant functions in vein patterning (Sawchuk et al. 2013) (Chapter 2; Figure 6.1A), that *PIN3*, *PIN4* and *PIN7* act redundantly with *PIN1* in vein patterning (Chapter 5; Figure 6.1A), and that *PIN1*, *PIN6* and *PIN8* redundantly inhibit the negative function of *PIN5* in vein patterning (Sawchuk et al. 2013) (Chapter 2; Figure 6.1A).

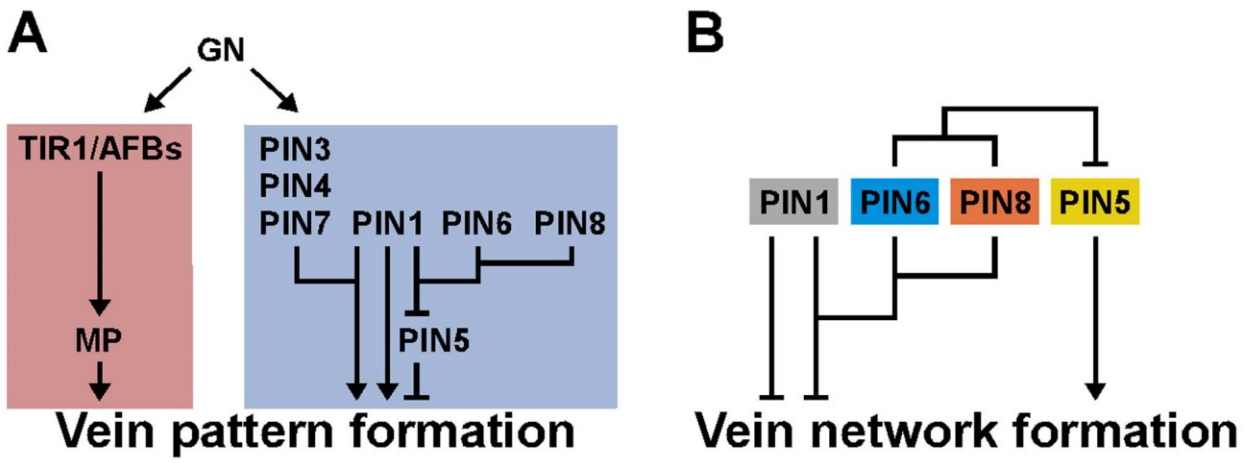

Figure 6.1. Summary. (A) Genetic interaction network for *GN*, *TIR1*/*AFB*/*MP*-dependent auxin signalling and *PIN*-dependent auxin transport in vein pattern formation. (B) Genetic interaction network for *PIN1*, *PIN5*, *PIN6* and *PIN8* in vein network formation. Arrows indicate positive effects; blunt-ended lines indicate negative effects.

Further, my results suggest that *PIN1* non-redundantly inhibits vein network formation, that *PIN6* acts redundantly with *PIN1* in inhibition of vein network formation, that *PIN8* acts redundantly with *PIN6* in *PIN1*-dependent inhibition of vein network formation, and that *PIN6* and *PIN8* redundantly inhibit— independently of *PIN1*—the positive function of *PIN5* in vein network formation (Chapter 3; Figure 6.1B). Thus my results suggest different genetic interaction networks for *PIN1*, *PIN5*, *PIN6* and *PIN8* in vein patterning and network formation (Figure 6.1).

In the Discussion section of the respective chapters, I provided an account of how I reached these conclusions from the experimental data, how these conclusions could be integrated with one another and with those in studies of others to advance our understanding of vascular development, and what the implications of such conclusions are for aspects of plant development beyond the formation of veins. Here I instead wish to attempt to account for an interaction whose mechanistic explanation is still eluding me; I am referring to the interaction in vein patterning and network formation between the intercellular auxin-transport pathway mediated by the plasma-membrane-localized PIN1 and the intracellular auxin-transport pathway mediated by the endoplasmic-reticulum-localized PIN6 and PIN8. The two non-mutually exclusive hypotheses I propose below should be understood as an attempt to develop a conceptual framework to guide future experimentation and not as an exhaustive mechanistic account. The specific observations my hypotheses try to account for are the following (Sawchuk et al. 2013) (Chapters 2 and 3):

(i) While in WT leaves lateral veins branch from the midvein and join distal veins to form closed loops (Nelson and Dengler 1997; Candela et al. 1999), in *pin1*;*6*;*8* leaves the many lateral veins end in a marginal vein that runs parallelly to the leaf margin. Further, the vein networks of *pin1*;*6*;*8* are more complex than those of WT and are the most complex among those of all the mutant and transgenic lines in my thesis.

(ii) *pin1* leaves lack a marginal vein and have fewer lateral veins, and the vein networks of *pin1* are less complex than those of *pin1*;*6*;*8* but more than those of *pin6*;*8*.

(iii) *pin6*;*8* leaves have WT vein pattern, and the vein networks of *pin6*;*8* are less complex than those of *pin1* but more than those of WT.

(iv) MP::PIN6 leaves have WT vein pattern, and the vein networks of MP::PIN6 are less complex than those of WT.

6.2 General assumptions of the hypotheses

(i) In the epidermis of the shoot apical meristem, PIN1 polarity converges on a single cell—an epidermal convergence-point of auxin transport polarity (Benkova et al. 2003; Reinhardt et al. 2003; Heisler et al. 2005; Scarpella et al. 2006; Wenzel et al. 2007). At the convergence point, auxin accumulates and induces the formation of a leaf primordium; from the convergence point in the epidermis, auxin is thought to be transported into the inner tissue, where it induces the formation of a broad domain of PIN1 expression that will narrow to the site of midvein formation and will transport auxin away from the convergence point toward the base of the leaf primordium (Benkova et al. 2003; Reinhardt et al. 2003; Heisler et al. 2005; Scarpella et al. 2006; Wenzel et al. 2007; Bayer et al. 2009).

As the primordium grows, new convergence points will form in the lateral epidermis; such lateral convergence points are thought to induce the formation of lateral veins by a mechanism similar to that by which they induce the formation of the leaf primordium and of the midvein—lateral veins that transport auxin away from the lateral convergence points toward the midvein, to which lateral veins connect (Hay et al. 2006; Scarpella et al. 2006; Wenzel et al. 2007).

(ii) Higher auxin levels reduce spacing of leaves and cotyledons, eventually resulting in organ fusion (Liu et al. 1993; Hadfi et al. 1998; Reinhardt et al. 2003), and reduce the spacing of lateral convergence points (Scarpella et al. 2006). Thus it is assumed that formation of convergence points and their spacing depend on auxin levels: higher auxin levels will induce more and more closely spaced convergence points, and vice versa.

(iii) Unlike formation of midvein and lateral veins, formation of minor veins is independent of convergence points (Scarpella et al. 2006; Wenzel et al. 2007). Instead, minor veins are thought to be formed within the growing leaf from PIN1 expression domains that are initiated in continuity with pre-existing veins. Such PIN1 expression domains—as those that are thought to

give rise to midvein and lateral veins—are initially broad but eventually narrow to sites of minor vein formation and transport auxin toward the pre-existing veins to which the minor veins connect.

(iv) After (Sachs 1989), it is assumed that during leaf development all dividing cells produce auxin.

6.3 Hypothesis I: Intracellular-auxin-transport-mediated intercellular auxin transport

After (Wabnik et al. 2011a), intracellular auxin transport mediated by PIN6 and PIN8 is assumed to contribute to intercellular auxin transport. It is further assumed, after (Sachs 1981), that auxin is the limiting inductive signal for vein formation; thus, vein formation is terminated in an area of the leaf that has been completely drained of auxin.

(i) *pin1*;*6*;*8*

Intercellular auxin transport mediated by PIN1, PIN6 and PIN8 is absent but that mediated by PIN3, PIN4 and PIN7 (Sawchuk et al. 2013) (Chapter 2) can partially compensate for the loss of PIN1 function in the epidermis, where PIN1, PIN3, PIN4 and PIN7 are expressed (Scarpella et al. 2006; Guenot et al. 2012) (Chapter 5). However, intercellular auxin transport mediated by PIN3, PIN4 and PIN7 is insufficient to compensate for the additional loss of function of PIN6 and PIN8 in the inner tissue, where all these PIN proteins are expressed (Sawchuk et al. 2013) (Chapters 2 and 5). Thus auxin is not efficiently transported in the inner tissue and accumulates near the leaf margin; there, auxin induces the formation of a marginal vein, and of more—and more closely spaced—convergence points and derived lateral veins.

(ii) *pin1*

Intercellular auxin transport mediated by PIN1 is absent but that mediated by PIN6 and PIN8 is present. Intercellular auxin transport mediated by PIN3, PIN4 and PIN7 can partially compensate for the sole loss of PIN1 function in both epidermis and inner tissue. Thus auxin is transported in the inner tissue more efficiently than in *pin1*;*6*;*8* and no longer accumulates near the margin. As

a result, no marginal vein is formed, and fewer convergence points and derived lateral veins than in *pin1*;*6*;*8* are formed.

(iii) *pin6*;*8*

Intercellular auxin transport mediated by PIN1 is present. Thus formation of convergence points and derived lateral veins is normal, resulting in WT vein patterns with fewer convergence points and derived lateral veins than in *pin1*. However, intercellular auxin transport mediated by PIN6 and PIN8 is absent. Thus intercellular auxin transport in the inner tissue is not as efficient as in WT. As a result, auxin remains longer in the inner tissue, inducing formation of more veins than in WT.

(iv) WT

Intercellular auxin transport mediated by PIN1 is present. Thus formation of convergence points and derived lateral veins is normal, resulting in WT vein patterns with fewer convergence points and derived lateral veins than in *pin6*;*8*. Intercellular auxin transport mediated by PIN6 and PIN8 is also present. Thus intercellular auxin transport in the inner tissue is more efficient than in *pin6*;*8*. As a result, auxin does not remain as long in the inner tissue, inducing the formation of fewer veins than in *pin6*;*8*.

(v) MP::PIN6

Intercellular auxin transport mediated by PIN1 is present. Thus formation of convergence points and derived lateral veins is normal, resulting in WT vein patterns. However, intercellular auxin transport mediated by PIN6 is increased in the inner tissue, where the *MP* promoter is active (Sawchuk et al. 2013) (Chapter 2). Thus intercellular auxin transport in the inner tissue is more efficient than in WT. As a result, auxin does not remain as long in the inner tissue, inducing the formation of fewer veins than in WT.

6.4 Hypothesis II: Intracellular-auxin-transport-mediated intracellular auxin level

Auxin levels in developing vascular cells are assumed to be increased by intracellular auxin transport mediated by PIN6 and PIN8 (Bender et al. 2013; Cazzonelli et al. 2013; Sawchuk et al. 2013) (Chaoter 2), and by intercellular auxin transport toward incipient veins mediated by PIN1 (Bayer et al. 2009). After (Sachs 1989; Mattsson et al. 2003), it is further assumed that a minimum auxin level is required to induce vein differentiation, which entails greater auxin transport capacity. After (Sachs 1989), it is finally assumed that auxin levels required for vein differentiation inhibit leaf growth. As a leaf area is drained of auxin by incipient veins, auxin levels fall below those which inhibit leaf growth; the area can thus resume growth and produce new auxin, allowing iteration of this process until—it is assumed after (Scarpella et al. 2004)—cessation of leaf growth by an auxin-independent mechanism.

(i) *pin1*;*6*;*8*

Intercellular auxin transport mediated by PIN1 is absent but that mediated by PIN3, PIN4 and PIN7 can partially compensate for loss of PIN1 function in epidermis and inner tissue. Intracellular auxin transport mediated by PIN6 and PIN8 is absent. Thus auxin levels in the inner tissue are initially below those required to induce vein differentiation. With no lateral veins initially being formed, auxin remains near the margin; there, it induces the formation of more—and more closely spaced—convergence points, resulting in further accumulation of auxin near the margin. Eventually enough auxin accumulates near the margin to induce differentiation of a marginal vein and of the many lateral veins derived from the many convergence points.

(ii) *pin1*

Intercellular auxin transport mediated by PIN1 is absent but that mediated by PIN3, PIN4 and PIN7 can partially compensate for loss of PIN1 function in epidermis and inner tissue. Intracellular auxin transport mediated by PIN6 and PIN8 is present; thus auxin levels in the inner tissue are higher than in *pin1*;*6*;*8* and above those required to induce vein differentiation, resulting in more efficient drainage of auxin. As a result, auxin does not remain as long near the margin, no marginal vein is formed, and fewer convergence points and derived lateral veins than in *pin1*;*6*;*8* are formed.

(iii) *pin6*;*8*

Intercellular auxin transport mediated by PIN1 is present. Thus formation of convergence points and derived lateral veins is normal, resulting in WT vein patterns with fewer convergence points and derived lateral veins than in *pin1*. Intracellular auxin transport mediated by PIN6 and PIN8 is absent. Thus auxin levels in the inner tissue are lower than in WT but above those required to induce vein differentiation. As a result, auxin is drained more efficiently than in WT, and growth and auxin production are resumed sooner than in WT; the additional auxin thus produced induces the formation of more veins than in WT before cessation of leaf growth by an auxin-independent mechanism.

(iv) WT

Intercellular auxin transport mediated by PIN1 is present. Thus formation of convergence points and derived lateral veins is normal, resulting in WT vein patterns with fewer convergence points and derived lateral veins than in *pin6*;*8*. Intracellular auxin transport mediated by PIN6 and PIN8 is also present. Thus auxin levels in the inner tissue are higher than in *pin6*;*8*. As a result, auxin is drained less efficiently than in *pin6*;*8*, and growth and auxin production are resumed later than in *pin6*;*8*. Thus fewer veins are formed in WT than in *pin6*;*8* before cessation of leaf growth by an auxin-independent mechanism.

(v) MP::PIN6

Intercellular auxin transport mediated by PIN1 is present. Thus formation of convergence points and derived lateral veins is normal, resulting in WT vein patterns. Intracellular auxin transport mediated by PIN6 is increased. Thus auxin levels in the inner tissue are higher than in WT—so high to overwhelm the intercellular auxin transport capacity of the tissue. Thus veins are formed more slowly—and auxin is drained less efficiently—in MP::PIN6 than in WT. As a result, growth and auxin production are resumed later—and fewer veins are formed—in MP::PIN6 than in WT before cessation of leaf growth by an auxin-independent mechanism.

6.5 Perspective

The hypotheses proposed above should not be interpreted as an attempt to provide an exact mechanistic account for the observed phenomena but as extremes of a spectrum of possible explanations—extremes that should be more easily discriminated than intermediate scenarios by experimental tests. However, because of the complexity of vein patterning and network formation, and because of the simultaneous presence of multiple variables in these hypotheses, it will be difficult—if not altogether impossible—to evaluate intuitively the ability of these hypotheses to recapitulate vein development in WT, mutant and transgenic lines. A more precise formulation—a mathematical one, one that can be simulated computationally—will be necessary. Should both of the hypotheses proposed above withstand testing by computational simulation, it should be possible to use such simulations to predict experimental conditions under which the hypothesis-generated models behave divergently, thus providing us with informative experimental tests to differentiate the ability of the hypotheses to describe plausibly vein patterning and network formation.

LITERATURE CITED

Aloni R (2010) The induction of vascular tissues by auxin. In: PJ D eds. *Plant hormones: biosynthesis, signal transduction, action.* Kluwer Academic Publishers, Dordrecht. pp. 485–506.
Aloni R, Pradel K, Ullrich C (1995) The three-dimensional structure of vascular tissues in Agrobacterium tumefaciens-induced crown galls and in the host stems of Ricinus communis L. *Planta* **196**, 597-605.
Alonso-Peral MM, Candela H, del Pozo JC, Martinez-Laborda A, Ponce MR, Micol JL (2006) The HVE/CAND1 gene is required for the early patterning of leaf venation in Arabidopsis. *Development* **133**, 3755-3766.
Alonso JM, Stepanova AN, Leisse TJ, Kim CJ, Chen H, Shinn P, Stevenson DK, Zimmerman J, Barajas P, Cheuk R, Gadrinab C, Heller C, Jeske A, Koesema E, Meyers CC, Parker H, Prednis L, Ansari Y, Choy N, Deen H, Geralt M, Hazari N, Hom E, Karnes M, Mulholland C, Ndubaku R, Schmidt I, Guzman P, Aguilar-Henonin L, Schmid M, Weigel D, Carter DE, Marchand T, Risseeuw E, Brogden D, Zeko A, Crosby WL, Berry CC, Ecker JR (2003) Genome-wide insertional mutagenesis of Arabidopsis thaliana. *Science* **301**, 653-657.
Avery GS, Jr. (1935) Differential Distribution of a Phytohormone in the Developing Leaf of Nicotiana, and Its Relation to Polarized Growth. *Bulletin of the Torrey Botanical Club* **62**, 313-330.
Bailly A, Sovero V, Vincenzetti V, Santelia D, Bartnik D, Koenig BW, Mancuso S, Martinoia E, Geisler M (2008) Modulation of P-glycoproteins by auxin transport inhibitors is mediated by interaction with immunophilins. *J Biol Chem* **283**, 21817-21826.
Bainbridge K, Guyomarc'h S, Bayer E, Swarup R, Bennett M, Mandel T, Kuhlemeier C (2008) Auxin influx carriers stabilize phyllotactic patterning. *Genes Dev* **22**, 810-823.
Balla J, Kalousek P, Reinohl V, Friml J, Prochazka S (2011) Competitive canalization of PIN-dependent auxin flow from axillary buds controls pea bud outgrowth. *Plant J* **65**, 571-577.
Barbez E, Kubes M, Rolcik J, Beziat C, Pencik A, Wang B, Rosquete MR, Zhu J, Dobrev PI, Lee Y, Zazimalova E, Petrasek J, Geisler M, Friml J, Kleine-Vehn J (2012) A novel putative auxin carrier family regulates intracellular auxin homeostasis in plants. *Nature* **485**, 119-122.
Bayer EM, Smith RS, Mandel T, Nakayama N, Sauer M, Prusinkiewicz P, Kuhlemeier C (2009) Integration of transport-based models for phyllotaxis and midvein formation. *Genes Dev* **23**, 373-384.
Beeckman T, Przemeck GK, Stamatiou G, Lau R, Terryn N, De Rycke R, Inze D, Berleth T (2002) Genetic complexity of cellulose synthase a gene function in Arabidopsis embryogenesis. *Plant Physiol* **130**, 1883-1893.
Bender RL, Fekete ML, Klinkenberg PM, Hampton M, Bauer B, Malecha M, Lindgren K, J AM, Perera MA, Nikolau BJ, Carter CJ (2013) PIN6 is required for nectary auxin response and short stamen development. *Plant J* **74**, 893-904.
Benkova E, Michniewicz M, Sauer M, Teichmann T, Seifertova D, Jurgens G, Friml J (2003) Local, efflux-dependent auxin gradients as a common module for plant organ formation. *Cell* **115**, 591-602.
Berleth T (2001) Top-Down and Inside-Out: Directionality of Signaling in Vascular and Embryo Development. *Journal of Plant Growth Regulation* **20**, 14-21.

Berleth T, Jurgens G (1993) The Role of the Monopteros Gene in Organizing the Basal Body Region of the Arabidopsis Embryo. *Development* **118**, 575-587.
Berleth T, Mattsson J, Hardtke CS (2000) Vascular continuity and auxin signals. *Trends Plant Sci* **5**, 387-393.
Bezhani S, Sherameti I, Pfannschmidt T, Oelmuller R (2001) A repressor with similarities to prokaryotic and eukaryotic DNA helicases controls the assembly of the CAAT box binding complex at a photosynthesis gene promoter. *J Biol Chem* **276**, 23785-23789.
Bilsborough GD, Runions A, Barkoulas M, Jenkins HW, Hasson A, Galinha C, Laufs P, Hay A, Prusinkiewicz P, Tsiantis M (2011) Model for the regulation of Arabidopsis thaliana leaf margin development. *Proc Natl Acad Sci U S A* **108**, 3424-3429.
Birkenbihl RP, Jach G, Saedler H, Huijser P (2005) Functional dissection of the plant-specific SBP-domain: overlap of the DNA-binding and nuclear localization domains. *J Mol Biol* **352**, 585-596.
Blakeslee JJ, Bandyopadhyay A, Lee OR, Mravec J, Titapiwatanakun B, Sauer M, Makam SN, Cheng Y, Bouchard R, Adamec J, Geisler M, Nagashima A, Sakai T, Martinoia E, Friml J, Peer WA, Murphy AS (2007) Interactions among PIN-FORMED and P-glycoprotein auxin transporters in Arabidopsis. *Plant Cell* **19**, 131-147.
Blilou I, Xu J, Wildwater M, Willemsen V, Paponov I, Friml J, Heidstra R, Aida M, Palme K, Scheres B (2005) The PIN auxin efflux facilitator network controls growth and patterning in Arabidopsis roots. *Nature* **433**, 39-44.
Boehm B, Westerberg H, Lesnicar-Pucko G, Raja S, Rautschka M, Cotterell J, Swoger J, Sharpe J (2010) The role of spatially controlled cell proliferation in limb bud morphogenesis. *PLoS Biol* **8**, e1000420.
Bosco CD, Dovzhenko A, Liu X, Woerner N, Rensch T, Eismann M, Eimer S, Hegermann J, Paponov IA, Ruperti B, Heberle-Bors E, Touraev A, Cohen JD, Palme K (2012) The endoplasmic reticulum localized PIN8 is a pollen specific auxin carrier involved in intracellular auxin homeostasis. *Plant J*.
Bouchard R, Bailly A, Blakeslee JJ, Oehring SC, Vincenzetti V, Lee OR, Paponov I, Palme K, Mancuso S, Murphy AS, Schulz B, Geisler M (2006) Immunophilin-like TWISTED DWARF1 modulates auxin efflux activities of Arabidopsis P-glycoproteins. *J Biol Chem* **281**, 30603-30612.
Boutte Y, Ikeda Y, Grebe M (2007) Mechanisms of auxin-dependent cell and tissue polarity. *Curr Opin Plant Biol* **10**, 616-623.
Busch M, Mayer U, Jurgens G (1996) Molecular analysis of the Arabidopsis pattern formation of gene GNOM: gene structure and intragenic complementation. *Mol Gen Genet* **250**, 681-691.
Candela H, Alonso-Peral MM, Ponce MR, Micol JL (2007) Role of HEMIVENATA and the Ubiquitin Pathway in Venation Pattern Formation. *Plant Signal Behav* **2**, 258-259.
Candela H, Martinez-Laborda A, Micol JL (1999) Venation pattern formation in Arabidopsis thaliana vegetative leaves. *Dev Biol* **205**, 205-216.
Capron A, Chatfield S, Provart N, Berleth T (2009) Embryogenesis: pattern formation from a single cell. *Arabidopsis Book* **7**, e0126.
Carland FM, Berg BL, FitzGerald JN, Jinamornphongs S, Nelson T, Keith B (1999) Genetic regulation of vascular tissue patterning in Arabidopsis. *Plant Cell* **11**, 2123-2137.
Cazzonelli CI, Vanstraelen M, Simon S, Yin K, Carron-Arthur A, Nisar N, Tarle G, Cuttriss AJ, Searle IR, Benkova E, Mathesius U, Masle J, Friml J, Pogson BJ (2013) Role

of the Arabidopsis PIN6 auxin transporter in auxin homeostasis and auxin-mediated development. *PLoS One* **8**, e70069.
Chapman EJ, Estelle M (2009) Mechanism of Auxin-Regulated Gene Expression in Plants. *Annual Review of Genetics* **43**, 265-285.
Chen R, Hilson P, Sedbrook J, Rosen E, Caspar T, Masson PH (1998) The arabidopsis thaliana AGRAVITROPIC 1 gene encodes a component of the polar-auxin-transport efflux carrier. *Proc Natl Acad Sci U S A* **95**, 15112-15117.
Cheng Y, Dai X, Zhao Y (2007) Auxin Synthesized by the YUCCA Flavin Monooxygenases Is Essential for Embryogenesis and Leaf Formation in Arabidopsis. *The Plant Cell Online* **19**, 2430-2439.
Chomczynski P, Sacchi N (1987) Single-step method of RNA isolation by acid guanidinium thiocyanate-phenol-chloroform extraction. *Anal Biochem* **162**, 156-159.
Ciruna B, Jenny A, Lee D, Mlodzik M, Schier AF (2006) Planar cell polarity signalling couples cell division and morphogenesis during neurulation. *Nature* **439**, 220-224.
Clay NK, Nelson T (2005) Arabidopsis thickvein mutation affects vein thickness and organ vascularization, and resides in a provascular cell-specific spermine synthase involved in vein definition and in polar auxin transport. *Plant Physiol* **138**, 767-777.
Cole L, Davies D, Hyde GJ, Ashford AE (2000) ER-Tracker dye and BODIPY-brefeldin A differentiate the endoplasmic reticulum and golgi bodies from the tubular-vacuole system in living hyphae of Pisolithus tinctorius. *J Microsc* **197**, 239-249.
Cole M, Chandler J, Weijers D, Jacobs B, Comelli P, Werr W (2009) DORNROSCHEN is a direct target of the auxin response factor MONOPTEROS in the Arabidopsis embryo. *Development* **136**, 1643-1651.
Cutler SR, Ehrhardt DW, Griffitts JS, Somerville CR (2000) Random GFP::cDNA fusions enable visualization of subcellular structures in cells of Arabidopsis at a high frequency. *Proc Natl Acad Sci U S A* **97**, 3718-3723.
Dalessandro G, Roberts LW (1971) Induction of Xylogenesis in Pith Parenchyma Explants of Lactuca. *American Journal of Botany* **58**, 378-385.
De Smet I, Jurgens G (2007) Patterning the axis in plants--auxin in control. *Curr Opin Genet Dev* **17**, 337-343.
Dello Ioio R, Linhares FS, Scacchi E, Casamitjana-Martinez E, Heidstra R, Costantino P, Sabatini S (2007) Cytokinins determine Arabidopsis root-meristem size by controlling cell differentiation. *Current Biology* **17**, 678-682.
Demandolx D, Davoust J (1997) Multicolour analysis and local image correlation in confocal microscopy. *Journal of Microscopy* **185**, 21-36.
Dengler NG (2006) The shoot apical meristem and development of vascular architecture. *Canadian Journal of Botany* **84**, 1660-1671.
Deyholos MK, Cordner G, Beebe D, Sieburth LE (2000) The SCARFACE gene is required for cotyledon and leaf vein patterning. *Development* **127**, 3205-3213.
Dharmasiri N, Dharmasiri S, Weijers D, Karunarathna N, Jurgens G, Estelle M (2007) AXL and AXR1 have redundant functions in RUB conjugation and growth and development in Arabidopsis. *The Plant Journal* **52**, 114-123.
Dharmasiri N, Dharmasiri S, Weijers D, Lechner E, Yamada M, Hobbie L, Ehrismann JS, Jurgens G, Estelle M (2005) Plant Development Is Regulated by a Family of Auxin Receptor F Box Proteins. *Developmental Cell* **9**, 109-119.

Dharmasiri S, Dharmasiri N, Hellmann H, Estelle M (2003) The RUB/Nedd8 conjugation pathway is required for early development in Arabidopsis. *EMBO J* **22**, 1762-1770.
Dhonukshe P, Grigoriev I, Fischer R, Tominaga M, Robinson DG, Hasek J, Paciorek T, Petrasek J, Seifertova D, Tejos R, Meisel LA, Zazimalova E, Gadella TW, Jr., Stierhof YD, Ueda T, Oiwa K, Akhmanova A, Brock R, Spang A, Friml J (2008) Auxin transport inhibitors impair vesicle motility and actin cytoskeleton dynamics in diverse eukaryotes. *Proc Natl Acad Sci U S A* **105**, 4489-4494.
Ding Z, Wang B, Moreno I, Duplakova N, Simon S, Carraro N, Reemmer J, Pencik A, Chen X, Tejos R, Skupa P, Pollmann S, Mravec J, Petrasek J, Zazimalova E, Honys D, Rolcik J, Murphy A, Orellana A, Geisler M, Friml J (2012) ER-localized auxin transporter PIN8 regulates auxin homeostasis and male gametophyte development in Arabidopsis. *Nat Commun* **3**, 941.
Don AS, Martinez-Lamenca C, Webb WR, Proia RL, Roberts E, Rosen H (2007) Essential requirement for sphingosine kinase 2 in a sphingolipid apoptosis pathway activated by FTY720 analogues. *J Biol Chem* **282**, 15833-15842.
Donner TJ, Scarpella E (2009) Auxin-transport-dependent leaf vein formation. *Botany-Botanique* **87**, 678-684.
Donner TJ, Scarpella E (2012) Transcriptional control of early vein expression of CYCA2;1 and CYCA2;4 in Arabidopsis leaves.
Donner TJ, Sherr I, Scarpella E (2009) Regulation of preprocambial cell state acquisition by auxin signaling in Arabidopsis leaves. *Development* **136**, 3235-3246.
Ebel C, Mariconti L, Gruissem W (2004) Plant retinoblastoma homologues control nuclear proliferation in the female gametophyte. *Nature* **429**, 776-780.
Esau K (1942) Vascular Differentiation in the Vegetative Shoot of Linum. I. The Procambium. *American Journal of Botany* **29**, 738-747.
Esau K (1943) Origin and development of primary vascular tissues in plants. *Botanical Review* **9**, 125-206.
Fairon-Demaret M, Li C-S (1993) Lorophyton goense gen. et sp. nov. from the Lower Givetian of Belgium and a discussion of the Middle Devonian Cladoxylopsida. *Review of Palaeobotany and Palynology* **77**, 1-22.
Feugier FG, Mochizuki A, Iwasa Y (2005) Self-organization of the vascular system in plant leaves: Inter-dependent dynamics of auxin flux and carrier proteins. *Journal of Theoretical Biology* **236**, 366-375.
Fischer U, Ikeda Y, Ljung K, Serralbo O, Singh M, Heidstra R, Palme K, Scheres B, Grebe M (2006) Vectorial information for Arabidopsis planar polarity is mediated by combined AUX1, EIN2, and GNOM activity. *Curr Biol* **16**, 2143-2149.
Forestan C, Farinati S, Varotto S (2012) The Maize PIN Gene Family of Auxin Transporters. *Front Plant Sci* **3**, 16.
Foster A (1956) Plant idioblasts: Remarkable examples of cell specialization. *Protoplasma* **46**, 184-193.
Foster AS (1952) Foliar Venation in Angiosperms from an Ontogenetic Standpoint. *American Journal of Botany* **39**, 752-766.
Friml J, Benkova E, Blilou I, Wisniewska J, Hamann T, Ljung K, Woody S, Sandberg G, Scheres B, Jurgens G, Palme K (2002a) AtPIN4 mediates sink-driven auxin gradients and root patterning in Arabidopsis. *Cell* **108**, 661-673.

Friml J, Vieten A, Sauer M, Weijers D, Schwarz H, Hamann T, Offringa R, Jurgens G (2003) Efflux-dependent auxin gradients establish the apical-basal axis of Arabidopsis. *Nature* **426**, 147-153.
Friml J, Wisniewska J, Benkova E, Mendgen K, Palme K (2002b) Lateral relocation of auxin efflux regulator PIN3 mediates tropism in Arabidopsis. *Nature* **415**, 806-809.
Galweiler L, Guan C, Muller A, Wisman E, Mendgen K, Yephremov A, Palme K (1998) Regulation of polar auxin transport by AtPIN1 in Arabidopsis vascular tissue. *Science* **282**, 2226-2230.
Ganguly A, Lee SH, Cho M, Lee OR, Yoo H, Cho HT (2010) Differential auxin-transporting activities of PIN-FORMED proteins in Arabidopsis root hair cells. *Plant Physiol* **153**, 1046-1061.
Garnett P, Steinacher A, Stepney S, Clayton R, Leyser O (2010) Computer simulation: the imaginary friend of auxin transport biology. *Bioessays* **32**, 828-835.
Gautheret R (1939) Sur la possibilité de réaliser la culture indéfinie des tissus de tubercules de carotte. *Comptes rendus Academi des Sciences* **208**, 118-130.
Geisler M, Blakeslee JJ, Bouchard R, Lee OR, Vincenzetti V, Bandyopadhyay A, Titapiwatanakun B, Peer WA, Bailly A, Richards EL, Ejendal KF, Smith AP, Baroux C, Grossniklaus U, Muller A, Hrycyna CA, Dudler R, Murphy AS, Martinoia E (2005) Cellular efflux of auxin catalyzed by the Arabidopsis MDR/PGP transporter AtPGP1. *Plant J* **44**, 179-194.
Geisler M, Kolukisaoglu HU, Bouchard R, Billion K, Berger J, Saal B, Frangne N, Koncz-Kalman Z, Koncz C, Dudler R, Blakeslee JJ, Murphy AS, Martinoia E, Schulz B (2003) TWISTED DWARF1, a unique plasma membrane-anchored immunophilin-like protein, interacts with Arabidopsis multidrug resistance-like transporters AtPGP1 and AtPGP19. *Mol Biol Cell* **14**, 4238-4249.
Geisler M, Murphy AS (2006) The ABC of auxin transport: the role of p-glycoproteins in plant development. *FEBS Lett* **580**, 1094-1102.
Geldner N, Anders N, Wolters H, Keicher J, Kornberger W, Muller P, Delbarre A, Ueda T, Nakano A, Jürgens G (2003) The Arabidopsis GNOM ARF-GEF Mediates Endosomal Recycling, Auxin Transport, and Auxin-Dependent Plant Growth. *Cell* **112**, 219-230.
Geldner N, Friml J, Stierhof YD, Jurgens G, Palme K (2001) Auxin transport inhibitors block PIN1 cycling and vesicle traficking. *Nature* **413**, 425-428.
Geldner N, Richter S, Vieten A, Marquardt S, Torres-Ruiz RA, Mayer U, Jurgens G (2004) Partial loss-of-function alleles reveal a role for GNOM in auxin transport-related, post-embryonic development of Arabidopsis. *Development* **131**, 389-400.
Gersani M (1987) The Induction of Differentiation of Organized Vessels in a Storage Organ. *Annals of Botany* **59**, 31-34.
Gillmor CS, Park MY, Smith MR, Pepitone R, Kerstetter RA, Poethig RS (2010) The MED12-MED13 module of Mediator regulates the timing of embryo patterning in Arabidopsis. *Development* **137**, 113-122.
Gordon SP, Heisler MG, Reddy GV, Ohno C, Das P, Meyerowitz EM (2007) Pattern formation during de novo assembly of the Arabidopsis shoot meristem. *Development* **134**, 3539-3548.
Goto N SM, Kranz AR (1987) Effect of gibberllins on flower development of the pin-formed mutant of Arabidopsis thaliana. *Arabidopsis Information Service* **23**, 66-71.

Graumann K, Evans DE (2011) Nuclear envelope dynamics during plant cell division suggest common mechanisms between kingdoms. *Biochem J* **435**, 661-667.
Groff P, Kaplan D (1988) The relation of root systems to shoot systems in vascular plants. *The Botanical Review* **54**, 387-422.
Guenot B, Bayer E, Kierzkowski D, Smith RS, Mandel T, Zadnikova P, Benkova E, Kuhlemeier C (2012) PIN1-Independent Leaf Initiation in Arabidopsis. *Plant Physiol* **159**, 1501-1510.
Guilfoyle TJ, Hagen G (2007) Auxin response factors. *Curr Opin Plant Biol* **10**, 453-460.
Guilfoyle TJ, Hagen G (2012) Getting a grasp on domain III/IV responsible for Auxin Response Factor-IAA protein interactions. *Plant Sci* **190**, 82-88.
Hadfi K, Speth V, Neuhaus G (1998) Auxin-induced developmental patterns in Brassica juncea embryos. *Development* **125**, 879-887.
Hamann T, Benkova E, Baurle I, Kientz M, Jurgens G (2002) The Arabidopsis BODENLOS gene encodes an auxin response protein inhibiting MONOPTEROS-mediated embryo patterning. *Genes & Development* **16**, 1610-1615.
Hamann T, Mayer U, Jurgens G (1999) The auxin-insensitive bodenlos mutation affects primary root formation and apical-basal patterning in the Arabidopsis embryo. *Development* **126**, 1387-1395.
Han X, Hyun TK, Zhang M, Kumar R, Koh EJ, Kang BH, Lucas WJ, Kim JY (2014) Auxin-callose-mediated plasmodesmal gating is essential for tropic auxin gradient formation and signaling. *Dev Cell* **28**, 132-146.
Hardtke CS, Berleth T (1998) The Arabidopsis gene MONOPTEROS encodes a transcription factor mediating embryo axis formation and vascular development. *Embo J* **17**, 1405-1411.
Hardtke CS, Ckurshumova W, Vidaurre DP, Singh SA, Stamatiou G, Tiwari SB, Hagen G, Guilfoyle TJ, Berleth T (2004) Overlapping and non-redundant functions of the Arabidopsis auxin response factors MONOPTEROS and NONPHOTOTROPIC HYPOCOTYL 4. *Development* **131**, 1089-1100.
Haseloff J (1999) GFP variants for multispectral imaging of living cells. *Methods Cell Biol* **58**, 139-151.
Hawley RS, Gilliland WD (2006) Sometimes the result is not the answer: the truths and the lies that come from using the complementation test. *Genetics* **174**, 5-15.
Hay A, Barkoulas M, Tsiantis M (2006) ASYMMETRIC LEAVES1 and auxin activities converge to repress BREVIPEDICELLUS expression and promote leaf development in Arabidopsis. *Development* **133**, 3955-3961.
Hayashi K, Neve J, Hirose M, Kuboki A, Shimada Y, Kepinski S, Nozaki H (2012) Rational Design of an Auxin Antagonist of the SCFTIR1 Auxin Receptor Complex. *Acs Chemical Biology* **7**, 590-598.
Heisler MG, Hamant O, Krupinski P, Uyttewaal M, Ohno C, Jonsson H, Traas J, Meyerowitz EM (2010) Alignment between PIN1 polarity and microtubule orientation in the shoot apical meristem reveals a tight coupling between morphogenesis and auxin transport. *PLoS Biol* **8**, e1000516.
Heisler MG, Ohno C, Das P, Sieber P, Reddy GV, Long JA, Meyerowitz EM (2005) Patterns of Auxin Transport and Gene Expression during Primordium Development Revealed by Live Imaging of the Arabidopsis Inflorescence Meristem. *Curr Biol* **15**, 1899-1911.

Hellmann H, Hobbie L, Chapman A, Dharmasiri S, Dharmasiri N, del Pozo C, Reinhardt D, Estelle M (2003) Arabidopsis AXR6 encodes CUL1 implicating SCF E3 ligases in auxin regulation of embryogenesis. *EMBO J* **22**, 3314-3325.
Henderson JHM, Bonner J (1952) Auxin Metabolism in Normal and Crown Gall Tissue of Sunflower. *American Journal of Botany* **39**, 444-451.
Herbst D (1971) Disjunct Foliar Veins in Hawaiian Euphorbias. *Science* **171**, 1247-1248.
Herbst D (1972) Ontogeny of Foliar Venation in Euphorbia forbesii. *American Journal of Botany* **59**, 843-850.
Herwig L, Blum Y, Krudewig A, Ellertsdottir E, Lenard A, Belting HG, Affolter M (2011) Distinct cellular mechanisms of blood vessel fusion in the zebrafish embryo. *Curr Biol* **21**, 1942-1948.
Horn T, Sandmann T, Fischer B, Axelsson E, Huber W, Boutros M (2011) Mapping of signaling networks through synthetic genetic interaction analysis by RNAi. *Nat Methods* **8**, 341-346.
Hosoda K, Imamura A, Katoh E, Hatta T, Tachiki M, Yamada H, Mizuno T, Yamazaki T (2002) Molecular structure of the GARP family of plant Myb-related DNA binding motifs of the Arabidopsis response regulators. *Plant Cell* **14**, 2015-2029.
Jacobs WP (1952) The role of auxin in differentiation of xylem around a wound *American Journal of Botany* **39**, 301-309.
Jakoby M, Weisshaar B, Droge-Laser W, Vicente-Carbajosa J, Tiedemann J, Kroj T, Parcy F (2002) bZIP transcription factors in Arabidopsis. *Trends Plant Sci* **7**, 106-111.
Jensen PJ, Hangarter RP, Estelle M (1998) Auxin transport is required for hypocotyl elongation in light-grown but not dark-grown Arabidopsis. *Plant Physiol* **116**, 455-462.
Jost L (1942) Über Gefässbrücken. *Zeitsch. Bot.* **38**, 161-215.
Kamphausen T, Fanghanel J, Neumann D, Schulz B, Rahfeld JU (2002) Characterization of Arabidopsis thaliana AtFKBP42 that is membrane-bound and interacts with Hsp90. *Plant J* **32**, 263-276.
Kang J, Dengler N (2004) Vein pattern development in adult leaves of Arabidopsis thaliana. *International Journal of Plant Sciences* **165**, 231-242.
Katekar GF, Geissler AE (1980) Auxin Transport Inhibitors: IV. EVIDENCE OF A COMMON MODE OF ACTION FOR A PROPOSED CLASS OF AUXIN TRANSPORT INHIBITORS: THE PHYTOTROPINS. *Plant Physiol* **66**, 1190-1195.
Kerk NM, Jiang K, Feldman LJ (2000) Auxin Metabolism in the Root Apical Meristem. *Plant Physiology* **122**, 925-932.
Kierzkowski D, Lenhard M, Smith R, Kuhlemeier C (2013) Interaction between meristem tissue layers controls phyllotaxis. *Dev Cell* **26**, 616-628.
Kim I, Cho E, Crawford K, Hempel FD, Zambryski PC (2005) Cell-to-cell movement of GFP during embryogenesis and early seedling development in Arabidopsis. *Proc Natl Acad Sci U S A* **102**, 2227-2231.
Kirschner H, Sachs T, Fahn A (1971) Secondary xylem reorientation as a special case of vascular tissue differentiation. *Israel Journal of Botany* **20**, 184-198.
Kleine-Vehn J, Dhonukshe P, Sauer M, Brewer PB, Wi, Paciorek T, Benková E, Friml J (2008) ARF GEF-Dependent Transcytosis and Polar Delivery of PIN Auxin Carriers in Arabidopsis. *Current biology* **18**, 526-531.
Klucking EP (1995) *Leaf Venation Patterns.* J. Cramer, Berlin.

Koizumi K, Sugiyama M, Fukuda H (2000) A series of novel mutants of Arabidopsis thaliana that are defective in the formation of continuous vascular network: calling the auxin signal flow canalization hypothesis into question. *Development* **127**, 3197-3204.
Kosugi S, Ohashi Y (2000) Cloning and DNA-binding properties of a tobacco Ethylene-Insensitive3 (EIN3) homolog. *Nucleic Acids Res* **28**, 960-967.
Kramer EM (2004) PIN and AUX/LAX proteins: their role in auxin accumulation. *Trends Plant Sci* **9**, 578-582.
Kramer EM (2009) Auxin-regulated cell polarity: an inside job? *Trends in Plant Science* **14**, 242-247.
Kraus EJ, Brown NA, Hamner KC (1936) Histological Reactions of Bean Plants to Indoleacetic Acid. *Botanical Gazette* **98**, 370-420.
Krecek P, Skupa P, Libus J, Naramoto S, Tejos R, Friml J, Zazimalova E (2009) The PIN-FORMED (PIN) protein family of auxin transporters. *Genome Biol* **10**, 249.
Krogan NT, Ckurshumova W, Marcos D, Caragea AE, Berleth T (2012) Deletion of MP/ARF5 domains III and IV reveals a requirement for Aux/IAA regulation in Arabidopsis leaf vascular patterning. *New Phytol*.
Krupinski P, Jonsson H (2010) Modeling auxin-regulated development. *Cold Spring Harb Perspect Biol* **2**, a001560. doi: 001510.001101/cshperspect.a001560.
Kubo M, Udagawa M, Nishikubo N, Horiguchi G, Yamaguchi M, Ito J, Mimura T, Fukuda H, Demura T (2005) Transcription switches for protoxylem and metaxylem vessel formation. *Genes Dev* **19**, 1855-1860.
Lau S, De Smet I, Kolb M, Meinhardt H, Jurgens G (2011) Auxin triggers a genetic switch. *Nat Cell Biol* **13**, 611-615.
Lee AY, Perreault R, Harel S, Boulier EL, Suderman M, Hallett M, Jenna S (2010) Searching for signaling balance through the identification of genetic interactors of the Rab guanine-nucleotide dissociation inhibitor gdi-1. *PLoS One* **5**, e10624.
Lersten N (1965) Histogenesis of Leaf Venation in Trifolium wormskioldii (Leguminosea). *American Journal of Botany* **52**, 767-774.
Leyser O (2010) The Power of Auxin in Plants. *Plant Physiology* **154**, 501-505.
Ligrone R, Duckett JG, Renzaglia KS (2000) Conducting tissues and phyletic relationships of bryophytes. *Philosophical Transactions of the Royal Society of London Series B-Biological Sciences* **355**, 795-813.
Lin R, Wang H (2005) Two homologous ATP-binding cassette transporter proteins, AtMDR1 and AtPGP1, regulate Arabidopsis photomorphogenesis and root development by mediating polar auxin transport. *Plant Physiol* **138**, 949-964.
Lippuner V, Chou IT, Scott SV, Ettinger WF, Theg SM, Gasser CS (1994) Cloning and characterization of chloroplast and cytosolic forms of cyclophilin from Arabidopsis thaliana. *J Biol Chem* **269**, 7863-7868.
Liu C, Xu Z, Chua NH (1993) Auxin Polar Transport Is Essential for the Establishment of Bilateral Symmetry during Early Plant Embryogenesis. *Plant Cell* **5**, 621-630.
Lu P, Werb Z (2008) Patterning mechanisms of branched organs. *Science* **322**, 1506-1509.
Ludwig-Muller J (2012) Auxin conjugates: their role for plant development and in the evolution of land plants. *J Exp Bot* **62**, 1757-1773.
Lukowitz W, Mayer U, JÃ¼rgens G (1996) Cytokinesis in the Arabidopsis Embryo Involves the Syntaxin-Related KNOLLE Gene Product. *Cell* **84**, 61-71.

Luschnig C, Gaxiola RA, Grisafi P, Fink GR (1998) EIR1, a root-specific protein involved in auxin transport, is required for gravitropism in Arabidopsis thaliana. *Genes Dev* **12**, 2175-2187.
Manders EMM, Verbeek FJ, Aten JA (1993) Measurement of Colocalization of Objects in Dual-Color Confocal Images. *Journal of Microscopy-Oxford* **169**, 375-382.
Mansfield SG, Briarty LG (1991) Early embryogenesis in Arabidopsis thaliana. II. The developing embryo. *Canadian Journal of Botany* **69**, 461-476.
Marchant A, Bennett MJ (1998) The Arabidopsis AUX1 gene: a model system to study mRNA processing in plants. *Plant Mol Biol* **36**, 463-471.
Masucci JD, Schiefelbein JW (1994) The rhd6 Mutation of Arabidopsis thaliana Alters Root-Hair Initiation through an Auxin- and Ethylene-Associated Process. *Plant Physiol* **106**, 1335-1346.
Mattsson J, Ckurshumova W, Berleth T (2003) Auxin signaling in Arabidopsis leaf vascular development. *Plant Physiol* **131**, 1327-1339.
Mattsson J, Sung ZR, Berleth T (1999) Responses of plant vascular systems to auxin transport inhibition. *Development* **126**, 2979-2991.
Mayer U, Buttner G, Jurgens G (1993) Apical-basal pattern formation in the Arabidopsis embryo: studies on the role of the gnom gene. *Development* **117**, 149-162.
Mayer U, Torres Ruiz RA, Berleth T, Miséra S, Jürgens G (1991) Mutations affecting body organization in the Arabidopsis embryo. *Nature* **353**, 402-407.
McKown AD, Dengler NG (2009) Shifts in leaf vein density through accelerated vein formation in C(4) Flaveria (Asteraceae). *Annals of Botany* **104**, 1085-1098.
Mitchison GJ (1980a) The Dynamics of Auxin Transport. *Proceedings of the Royal Society of London. Series B, Biological Sciences* **209**, 489-511.
Mitchison GJ (1980b) Model for Vein Formation in Higher-Plants. *Proceedings of the Royal Society of London Series B-Biological Sciences* **207**, 79-109.
Mitchison GJ (1981) The Polar Transport of Auxin and Vein Patterns in Plants. *Philosophical Transactions of the Royal Society of London Series B-Biological Sciences* **295**, 461-471.
Moriwaki T, Miyazawa Y, Fujii N, Takahashi H (2013) GNOM regulates root hydrotropism and phototropism independently of PIN-mediated auxin transport. *Plant Sci* **215-216**, 141-149.
Mravec J, Kubes M, Bielach A, Gaykova V, Petrasek J, Skupa P, Chand S, Benkova E, Zazimalova E, Friml J (2008) Interaction of PIN and PGP transport mechanisms in auxin distribution-dependent development. *Development* **135**, 3345-3354.
Mravec J, Skupa P, Bailly A, Hoyerova K, Krecek P, Bielach A, Petrasek J, Zhang J, Gaykova V, Stierhof YD, Dobrev PI, Schwarzerova K, Rolcik J, Seifertova D, Luschnig C, Benkova E, Zazimalova E, Geisler M, Friml J (2009) Subcellular homeostasis of phytohormone auxin is mediated by the ER-localized PIN5 transporter. *Nature* **459**, 1136-1140.
Muller A, Guan C, Galweiler L, Tanzler P, Huijser P, Marchant A, Parry G, Bennett M, Wisman E, Palme K (1998) AtPIN2 defines a locus of Arabidopsis for root gravitropism control. *Embo J* **17**, 6903-6911.
Nakamura M, Kiefer CS, Grebe M (2012) Planar polarity, tissue polarity and planar morphogenesis in plants. *Curr Opin Plant Biol* **15**, 593-600.
Naramoto S, Sawa S, Koizumi K, Uemura T, Ueda T, Friml J, Nakano A, Fukuda H (2009) Phosphoinositide-dependent regulation of VAN3 ARF-GAP localization and activity essential for vascular tissue continuity in plants. *Development* **136**, 1529-1538.

Neeff F (1914) Über Zellumlagerung. Ein Beitrag zur experimentellen anatomie. *Zeitsch. Bot* **6**, 465-547.
Nelson BK, Cai X, Nebenfuhr A (2007) A multicolored set of in vivo organelle markers for co-localization studies in Arabidopsis and other plants. *Plant J* **51**, 1126-1136.
Nelson T, Dengler N (1997) Leaf Vascular Pattern Formation. *Plant Cell* **9**, 1121-1135.
Nemhauser JL, Hong F, Chory J (2006) Different plant hormones regulate similar processes through largely nonoverlapping transcriptional responses. *Cell* **126**, 467-475.
Nishal B, Tantikanjana T, Sundaresan V (2005) An inducible targeted tagging system for localized saturation mutagenesis in Arabidopsis. *Plant Physiol* **137**, 3-12.
Nobécourt P (1939) Sur la pérennité et l'augmentation de volume des cultures de tissus végétaux. *C.R. Soc. Biol.* **130**, 1270-1271.
Nziengui H, Bouhidel K, Pillon D, Der C, Marty F, Schoefs B (2007) Reticulon-like proteins in Arabidopsis thaliana: structural organization and ER localization. *FEBS Lett* **581**, 3356-3362.
Oda Y, Fukuda H (2011) Dynamics of Arabidopsis SUN proteins during mitosis and their involvement in nuclear shaping. *Plant J* **66**, 629-641.
Odat O, Gardiner J, Sawchuk MG, Verna C, Donner TJ, Scarpella E (2014) Characterization of an allelic series in the MONOPTEROS gene of arabidopsis. *Genesis*.
Okumura K, Goh T, Toyokura K, Kasahara H, Takebayashi Y, Mimura T, Kamiya Y, Fukaki H (2013) GNOM/FEWER ROOTS is required for the establishment of an auxin response maximum for arabidopsis lateral root initiation. *Plant Cell Physiol* **54**, 406-417.
Okushima Y, Overvoorde PJ, Arima K, Alonso JM, Chan A, Chang C, Ecker JR, Hughes B, Lui A, Nguyen D, Onodera C, Quach H, Smith A, Yu G, Theologis A (2005) Functional genomic analysis of the AUXIN RESPONSE FACTOR gene family members in Arabidopsis thaliana: unique and overlapping functions of ARF7 and ARF19. *Plant Cell* **17**, 444-463.
Paciorek T, Zazimalova E, Ruthardt N, Petrasek J, Stierhof YD, Kleine-Vehn J, Morris DA, Emans N, Jurgens G, Geldner N, Friml J (2005) Auxin inhibits endocytosis and promotes its own efflux from cells. *Nature* **435**, 1251-1256.
Paponov IA, Teale WD, Trebar M, Blilou I, Palme K (2005) The PIN auxin efflux facilitators: evolutionary and functional perspectives. *Trends Plant Sci* **10**, 170-177.
Parry G, Marchant A, May S, Swarup R, Swarup K, James N, Graham N, Allen T, Martucci T, Yemm A, Napier R, Manning K, King G, Bennett M (2001) Quick on the uptake: Characterization of a family of plant auxin influx carriers. *Journal of Plant Growth Regulation* **20**, 217-225.
Pattison RJ, Catala C (2012) Evaluating auxin distribution in tomato (Solanum lycopersicum) through an analysis of the PIN and AUX/LAX gene families. *Plant J* **70**, 585-598.
Peret B, Swarup K, Ferguson A, Seth M, Yang YD, Dhondt S, James N, Casimiro I, Perry P, Syed A, Yang HB, Reemmer J, Venison E, Howells C, Perez-Amador MA, Yun JG, Alonso J, Beemster GTS, Laplaze L, Murphy A, Bennett MJ, Nielsen E, Swarup R (2012) AUX/LAX Genes Encode a Family of Auxin Influx Transporters That Perform Distinct Functions during Arabidopsis Development. *Plant Cell* **24**, 2874-2885.
Perez-Perez JM, Ponce MR, Micol JL (2004) The ULTRACURVATA2 gene of Arabidopsis encodes an FK506-binding protein involved in auxin and brassinosteroid signaling. *Plant Physiol* **134**, 101-117.
Petrasek J, Cerna A, Schwarzerova K, Elckner M, Morris DA, Zazimalova E (2003) Do phytotropins inhibit auxin efflux by impairing vesicle traffic? *Plant Physiol* **131**, 254-263.

Petrasek J, Mravec J, Bouchard R, Blakeslee JJ, Abas M, Seifertova D, Wisniewska J, Tadele Z, Kubes M, Covanova M, Dhonukshe P, Skupa P, Benkova E, Perry L, Krecek P, Lee OR, Fink GR, Geisler M, Murphy AS, Luschnig C, Zazimalova E, Friml J (2006) PIN proteins perform a rate-limiting function in cellular auxin efflux. *Science* **312**, 914-918.
Piepho H (1955) Uber die polaren Orientierung der Balge und Schuppen auf dem Schmetterlingsrumpf. *Biologisches Zentralblatt* **74**, 467-474.
Pray TR (1955a) Foliar venation in Angiosperms. II. Histogenesis of the venation of Liriodendron. *American Journal of Botany* **42**, 18-27.
Pray TR (1955b) Foliar venation of Angiosperms. IV. Histogenesis of the venation of Hosta. *American Journal of Botany* **42**, 698-706.
Prouse MB, Campbell MM (2012) The interaction between MYB proteins and their target DNA binding sites. *Biochim Biophys Acta* **1819**, 67-77.
Prusinkiewicz P, Crawford S, Smith RS, Ljung K, Bennett T, Ongaro V, Leyser O (2009) Control of bud activation by an auxin transport switch. *Proc Natl Acad Sci U S A* **106**, 17431-17436.
Przemeck GK, Mattsson J, Hardtke CS, Sung ZR, Berleth T (1996) Studies on the role of the Arabidopsis gene MONOPTEROS in vascular development and plant cell axialization. *Planta* **200**, 229-237.
Rasband WS (1997) ImageJ. U.S. National Institutes of Health, Bethesda, Maryland, USA, http://rsb.info.nih.gov/ij/.
Raven JA (1975) Transport of indole acetic acid in plant cells in relation to pH and electrical potential gradients, and its significance for polar IAA transport. *New Phytologist* **74**, 163-172.
Rayle DL, Ouitraku.R, Hertel R (1969) Effect of Auxins on Auxin Transport System in Coleoptiles. *Planta* **87**, 49-&.
Reinhardt D, Pesce ER, Stieger P, Mandel T, Baltensperger K, Bennett M, Traas J, Friml J, Kuhlemeier C (2003) Regulation of phyllotaxis by polar auxin transport. *Nature* **426**, 255-260.
Reyes JC, Muro-Pastor MI, Florencio FJ (2004) The GATA family of transcription factors in Arabidopsis and rice. *Plant Physiol* **134**, 1718-1732.
Richter S, Geldner N, Schrader J, Wolters H, Stierhof YD, Rios G, Koncz C, Robinson DG, Jurgens G (2007) Functional diversification of closely related ARF-GEFs in protein secretion and recycling. *Nature* **448**, 488-492.
Roberto FF, Klee H, White F, Nordeen R, Kosuge T (1990) Expression and fine structure of the gene encoding N epsilon-(indole-3-acetyl)-L-lysine synthetase from Pseudomonas savastanoi. *Proc Natl Acad Sci U S A* **87**, 5797-5801.
Roberts LW, Baba S (1968) IAA-induced xylem differentiation in the presence of colchicine. *Plant and Cell Physiology* **9**, 315-321.
Rolland-Lagan AG, Prusinkiewicz P (2005) Reviewing models of auxin canalization in the context of leaf vein pattern formation in Arabidopsis. *Plant J* **44**, 854-865.
Roman G, Lubarsky B, Kieber JJ, Rothenberg M, Ecker JR (1995) Genetic analysis of ethylene signal transduction in Arabidopsis thaliana: five novel mutant loci integrated into a stress response pathway. *Genetics* **139**, 1393-1409.
Romano CP, Hein MB, Klee HJ (1991) Inactivation of auxin in tobacco transformed with the indoleacetic acid-lysine synthetase gene of Pseudomonas savastanoi. *Genes Dev* **5**, 438-446.
Roth-Nebelsick A, Uhl D, Mosbrugger V, Kerp H (2001) Evolution and Function of Leaf Venation Architecture: A Review. *Annals of Botany* **87**, 553-566.

Roumeliotis E, Kloosterman B, Oortwijn M, Visser RG, Bachem CW (2013) The PIN family of proteins in potato and their putative role in tuberization. *Front Plant Sci* **4**, 524.
Rubery PH (1990) Phytotropins: receptors and endogenous ligands. *Symp Soc Exp Biol* **44**, 119-146.
Rubery PH, Sheldrake AR (1974) Carrier-Mediated Auxin Transport. *Planta* **118**, 101-121.
Sachs T (1968a) On determination of pattern of vascular tissues in peas. *Annals of Botany* **32**, 781-790.
Sachs T (1968b) The Role of the Root in the Induction of Xylem Differentiation in Peas. *Annals of Botany* **32**, 391-399.
Sachs T (1970) A control of bud growth by vascular tissue differentiation. *Israel Journal of Botany* **19**, 484-498.
Sachs T (1975) Control of Differentiation of Vascular Networks. *Annals of Botany* **39**, 197-204.
Sachs T (1981) The control of the patterned differentiation of vascular tissues. *Advances in Botanical Research* **9**, 151-262.
Sachs T (1989) The development of vascular networks during leaf development. *Current Topics in Plant Biochemistry and Physiology* **8**, 168-183.
Sachs T (1991a) Cell Polarity and Tissue Patterning in Plants. *Development* **Suppl 1**, 83-93.
Sachs T (1991b) *Pattern Formation in Plant Tissues.* Cambridge University Press, Cambridge.
Sachs T (2000) Integrating Cellular and Organismic Aspects of Vascular Differentiation. *Plant and Cell Physiology* **41**, 649-656.
Santos F, Teale W, Fleck C, Volpers M, Ruperti B, Palme K (2010) Modelling polar auxin transport in developmental patterning. *Plant Biol (Stuttg)* **12 Suppl 1**, 3-14.
Sassi M, Lu Y, Zhang Y, Wang J, Dhonukshe P, Blilou I, Dai M, Li J, Gong X, Jaillais Y, Yu X, Traas J, Ruberti I, Wang H, Scheres B, Vernoux T, Xu J (2012) COP1 mediates the coordination of root and shoot growth by light through modulation of PIN1- and PIN2-dependent auxin transport in Arabidopsis. *Development* **139**, 3402-3412.
Satoh R, Fujita Y, Nakashima K, Shinozaki K, Yamaguchi-Shinozaki K (2004) A novel subgroup of bZIP proteins functions as transcriptional activators in hypoosmolarity-responsive expression of the ProDH gene in Arabidopsis. *Plant Cell Physiol* **45**, 309-317.
Sauer M, Balla J, Luschnig C, Wisniewska J, Reinohl V, Friml J, Benkova E (2006) Canalization of auxin flow by Aux/IAA-ARF-dependent feedback regulation of PIN polarity. *Genes Dev* **20**, 2902-2911.
Sawa S, Koizumi K, Naramoto S, Demura T, Ueda T, Nakano A, Fukuda H (2005) DRP1A is responsible for vascular continuity synergistically working with VAN3 in Arabidopsis. *Plant Physiol* **138**, 819-826.
Sawchuk MG, Donner TJ, Head P, Scarpella E (2008) Unique and overlapping expression patterns among members of photosynthesis-associated nuclear gene families in Arabidopsis. *Plant Physiol* **148**, 1908-1924.
Sawchuk MG, Edgar A, Scarpella E (2013) Patterning of Leaf Vein Networks by Convergent Auxin Transport Pathways. *PLoS Genet* **9**, e1003294.
Sawchuk MG, Head P, Donner TJ, Scarpella E (2007) Time-lapse imaging of Arabidopsis leaf development shows dynamic patterns of procambium formation. *New Phytol* **176**, 560-571.
Sawchuk MG, Scarpella E (2013) Polarity, continuity, and alignment in plant vascular strands. *J Integr Plant Biol* **55**, 824-834.

Scarpella E, Francis P, Berleth T (2004) Stage-specific markers define early steps of procambium development in Arabidopsis leaves and correlate termination of vein formation with mesophyll differentiation. *Development* **131**, 3445-3455.
Scarpella E, Marcos D, Friml J, Berleth T (2006) Control of leaf vascular patterning by polar auxin transport. *Genes Dev* **20**, 1015-1027.
Schiavone FM, Cooke TJ (1987) Unusual patterns of somatic embryogenesis in the domesticated carrot: developmental effects of exogenous auxins and auxin transport inhibitors. *Cell Differentiation* **21**, 53-62.
Schlereth A, Moller B, Liu W, Kientz M, Flipse J, Rademacher EH, Schmid M, Jurgens G, Weijers D (2010) MONOPTEROS controls embryonic root initiation by regulating a mobile transcription factor. *Nature* **464**, 913-916.
Schuetz M, Berleth T, Mattsson J (2008) Multiple MONOPTEROS-dependent pathways are involved in leaf initiation. *Plant Physiol* **148**, 870-880.
Schwab R, Ossowski S, Riester M, Warthmann N, Weigel D (2006) Highly specific gene silencing by artificial microRNAs in Arabidopsis. *Plant Cell* **18**, 1121-1133.
Scott FM, Sjaholm V, Bowler E (1960) Light and Electron Microscope Studies of the Primary Xylem of Ricinus communis. *American Journal of Botany* **47**, 162-173.
Sessions A, Burke E, Presting G, Aux G, McElver J, Patton D, Dietrich B, Ho P, Bacwaden J, Ko C, Clarke JD, Cotton D, Bullis D, Snell J, Miguel T, Hutchison D, Kimmerly B, Mitzel T, Katagiri F, Glazebrook J, Law M, Goff SA (2002) A high-throughput Arabidopsis reverse genetics system. *Plant Cell* **14**, 2985-2994.
She W, Lin W, Zhu Y, Chen Y, Jin W, Yang Y, Han N, Bian H, Zhu M, Wang J (2010) The gypsy insulator of Drosophila melanogaster, together with its binding protein suppressor of Hairy-wing, facilitate high and precise expression of transgenes in Arabidopsis thaliana. *Genetics* **185**, 1141-1150.
Shen C, Bai Y, Wang S, Zhang S, Wu Y, Chen M, Jiang D, Qi Y (2010) Expression profile of PIN, AUX/LAX and PGP auxin transporter gene families in Sorghum bicolor under phytohormone and abiotic stress. *Febs J* **277**, 2954-2969.
Shevell DE, Kunkel T, Chua NH (2000) Cell wall alterations in the arabidopsis emb30 mutant. *Plant Cell* **12**, 2047-2060.
Shevell DE, Leu WM, Gillmor CS, Xia G, Feldmann KA, Chua NH (1994) EMB30 is essential for normal cell division, cell expansion, and cell adhesion in Arabidopsis and encodes a protein that has similarity to Sec7. *Cell* **77**, 1051-1062.
Sieburth LE (1999) Auxin is required for leaf vein pattern in Arabidopsis. *Plant Physiol* **121**, 1179-1190.
Sieburth LE, Muday GK, King EJ, Benton G, Kim S, Metcalf KE, Meyers L, Seamen E, Van Norman JM (2006) SCARFACE encodes an ARF-GAP that is required for normal auxin efflux and vein patterning in Arabidopsis. *Plant Cell* **18**, 1396-1411.
Simon SV (1908) Experimentelle Untersuchungen über die Differenzierungsvorgänge im Callusgewebe von Holzgewächsen. *Jahrbücher für wissenschaftliche botanik* **45**, 351-478.
Simon SV (1930) Transplantationsvercuche zwischen Solanum melongena und Iresine Lindeni. *Jahrbücher für wissenschaftliche botanik* **72**, 137-160.
Smith RS, Bayer EM (2009) Auxin transport-feedback models of patterning in plants. *Plant Cell Environ* **32**, 1258-1271.
Solereder H (1908) *Systematic Anatomy of the Dicotyledons.* Clarendon Press, Oxford.

Steinmann T, Geldner N, Grebe M, Mangold S, Jackson CL, Paris S, Galweiler L, Palme K, Jurgens G (1999) Coordinated polar localization of auxin efflux carrier PIN1 by GNOM ARF GEF. *Science* **286**, 316-318.
Stepanova AN, Robertson-Hoyt J, Yun J, Benavente LM, Xie D-Y, Dolezal K, Schlereth A, Jurgens G, Alonso JM (2008) TAA1-Mediated Auxin Biosynthesis Is Essential for Hormone Crosstalk and Plant Development. *Cell* **133**, 177-191.
Steynen QJ, Schultz EA (2003) The FORKED genes are essential for distal vein meeting in Arabidopsis. *Development* **130**, 4695-4708.
Strader LC, Monroe-Augustus M, Bartel B (2008) The IBR5 phosphatase promotes Arabidopsis auxin responses through a novel mechanism distinct from TIR1-mediated repressor degradation. *Bmc Plant Biology* **8**.
Strompen G, El Kasmi F, Richter S, Lukowitz W, Assaad FF, Jurgens G, Mayer U (2002) The Arabidopsis HINKEL gene encodes a kinesin-related protein involved in cytokinesis and is expressed in a cell cycle-dependent manner. *Curr Biol* **12**, 153-158.
Sugimoto K, Jiao Y, Meyerowitz EM (2010) Arabidopsis Regeneration from Multiple Tissues Occurs via a Root Development Pathway. *Developmental cell* **18**, 463-471.
Sussman MR, Goldsmith MH (1981) Auxin uptake and action of N-1-naphthylphthalamic acid in corn coleoptiles. *Planta* **151**, 15-25.
Swarup K, Benkova E, Swarup R, Casimiro I, Peret B, Yang Y, Parry G, Nielsen E, De Smet I, Vanneste S, Levesque MP, Carrier D, James N, Calvo V, Ljung K, Kramer E, Roberts R, Graham N, Marillonnet S, Patel K, Jones JDG, Taylor CG, Schachtman DP, May S, Sandberg G, Benfey P, Friml J, Kerr I, Beeckman T, Laplaze L, Bennett MJ (2008) The auxin influx carrier LAX3 promotes lateral root emergence. *Nature Cell Biology* **10**, 946-954.
Tan Y, Dourdin N, Wu C, De Veyra T, Elce JS, Greer PA (2006) Ubiquitous calpains promote caspase-12 and JNK activation during endoplasmic reticulum stress-induced apoptosis. *J Biol Chem* **281**, 16016-16024.
Thimann KV, Skoog F (1934) On the Inhibition of Bud Development and other Functions of Growth Substance in Vicia Faba. *Proceedings of the Royal Society of London. Series B, Containing Papers of a Biological Character* **114**, 317-339.
Thomas CL, Schmidt D, Bayer EM, Dreos R, Maule AJ (2009) Arabidopsis plant homeodomain finger proteins operate downstream of auxin accumulation in specifying the vasculature and primary root meristem. *Plant Journal* **59**, 426-436.
Tissier AF, Marillonnet S, Klimyuk V, Patel K, Torres MA, Murphy G, Jones JD (1999) Multiple independent defective suppressor-mutator transposon insertions in Arabidopsis: a tool for functional genomics. *Plant Cell* **11**, 1841-1852.
Tiwari SB, Hagen G, Guilfoyle T (2003) The roles of auxin response factor domains in auxin-responsive transcription. *Plant Cell* **15**, 533-543.
Torres-Ruiz RA, Jurgens G (1994) Mutations in the FASS gene uncouple pattern formation and morphogenesis in Arabidopsis development. *Development* **120**, 2967-2978.
Ulmasov T, Hagen G, Guilfoyle TJ (1999a) Activation and repression of transcription by auxin-response factors. *Proc Natl Acad Sci U S A* **96**, 5844-5849.
Ulmasov T, Hagen G, Guilfoyle TJ (1999b) Dimerization and DNA binding of auxin response factors. *Plant Journal* **19**, 309-319.

Viaene T, Delwiche CF, Rensing SA, Friml J (2012) Origin and evolution of PIN auxin transporters in the green lineage. *Trends Plant Sci*.
Vieten A, Vanneste S, Wisniewska J, Benkova E, Benjamins R, Beeckman T, Luschnig C, Friml J (2005) Functional redundancy of PIN proteins is accompanied by auxin-dependent cross-regulation of PIN expression. *Development* **132**, 4521-4531.
Wabnik K, Govaerts W, Friml J, Kleine-Vehn J (2011a) Feedback models for polarized auxin transport: an emerging trend. *Mol Biosyst* **7**, 2352-2359.
Wabnik K, Kleine-Vehn J, Balla J, Sauer M, Naramoto S, Reinohl V, Merks RM, Govaerts W, Friml J (2010) Emergence of tissue polarization from synergy of intracellular and extracellular auxin signaling. *Mol Syst Biol* **6**, 447.
Wabnik K, Kleine-Vehn J, Govaerts W, Friml J (2011b) Prototype cell-to-cell auxin transport mechanism by intracellular auxin compartmentalization. *Trends in Plant Science* **16**, 468-475.
Wang B, Bailly A, Zwiewka M, Henrichs S, Azzarello E, Mancuso S, Maeshima M, Friml J, Schulz A, Geisler M (2013) Arabidopsis TWISTED DWARF1 functionally interacts with auxin exporter ABCB1 on the root plasma membrane. *Plant Cell* **25**, 202-214.
Wang JR, Hu H, Wang GH, Li J, Chen JY, Wu P (2009) Expression of PIN genes in rice (Oryza sativa L.): tissue specificity and regulation by hormones. *Mol Plant* **2**, 823-831.
Wang P, Cheng T, Wu S, Zhao F, Wang G, Yang L, Lu M, Chen J, Shi J (2014) Phylogeny and Molecular Evolution Analysis of PIN-FORMED 1 in Angiosperm. *PLoS One* **9**, e89289.
Wangermann E (1974) The pathway of transport of applied indolyl-acetic acid through internode segments. *New Phytologist* **73**, 623-636.
Weijers D, Franke-van Dijk M, Vencken RJ, Quint A, Hooykaas P, Offringa R (2001) An Arabidopsis Minute-like phenotype caused by a semi-dominant mutation in a RIBOSOMAL PROTEIN S5 gene. *Development* **128**, 4289-4299.
Weijers D, Sauer M, Meurette O, Friml J, Ljung K, Sandberg G, Hooykaas P, Offringa R (2005) Maintenance of embryonic auxin distribution for apical-basal patterning by PIN-FORMED-dependent auxin transport in Arabidopsis. *Plant Cell* **17**, 2517-2526.
Weijers D, Schlereth A, Ehrismann JS, Schwank G, Kientz M, Jurgens G (2006) Auxin triggers transient local signaling for cell specification in Arabidopsis embryogenesis. *Developmental Cell* **10**, 265-270.
Went FW (1928) Wuchsstoff und Wachstum. *Recueil des travaux botaniques néerlandais* **25**, IV-116.
Wenzel CL, Schuetz M, Yu Q, Mattsson J (2007) Dynamics of MONOPTEROS and PIN-FORMED1 expression during leaf vein pattern formation in Arabidopsis thaliana. *Plant J* **49**, 387-398.
White PR (1939) Potentially Unlimited Growth of Excised Plant Callus in an Artificial Nutrient. *American Journal of Botany* **26**, 59-64.
Wisniewska J, Xu J, Seifertova D, Brewer PB, Ruzicka K, Blilou I, Rouquie D, Benkova E, Scheres B, Friml J (2006) Polar PIN localization directs auxin flow in plants. *Science* **312**, 883.
Woody ST, Austin-Phillips S, Amasino RM, Krysan PJ (2007) The WiscDsLox T-DNA collection: an arabidopsis community resource generated by using an improved high-throughput T-DNA sequencing pipeline. *J Plant Res* **120**, 157-165.
Wu G, Lewis DR, Spalding EP (2007) Mutations in Arabidopsis multidrug resistance-like ABC transporters separate the roles of acropetal and basipetal auxin transport in lateral root development. *Plant Cell* **19**, 1826-1837.

Wu G, Otegui MS, Spalding EP (2010) The ER-localized TWD1 immunophilin is necessary for localization of multidrug resistance-like proteins required for polar auxin transport in Arabidopsis roots. *Plant Cell* **22**, 3295-3304.
Xu J, Hofhuis H, Heidstra R, Sauer M, Friml J, Scheres B (2006) A molecular framework for plant regeneration. *Science* **311**, 385-388.
Xu J, Scheres B (2005) Dissection of Arabidopsis ADP-RIBOSYLATION FACTOR 1 function in epidermal cell polarity. *Plant Cell* **17**, 525-536.
Yamasaki S, Sakata-Sogawa K, Hasegawa A, Suzuki T, Kabu K, Sato E, Kurosaki T, Yamashita S, Tokunaga M, Nishida K, Hirano T (2007) Zinc is a novel intracellular second messenger. *J Cell Biol* **177**, 637-645.
Yanagisawa S (2002) The Dof family of plant transcription factors. *Trends Plant Sci* **7**, 555-560.
Yang Y, Hammes UZ, Taylor CG, Schachtman DP, Nielsen E (2006) High-affinity auxin transport by the AUX1 influx carrier protein. *Curr Biol* **16**, 1123-1127.
Yin C, Kiskowski M, Pouille PA, Farge E, Solnica-Krezel L (2008) Cooperation of polarized cell intercalations drives convergence and extension of presomitic mesoderm during zebrafish gastrulation. *J Cell Biol* **180**, 221-232.
Zadnikova P, Petrasek J, Marhavy P, Raz V, Vandenbussche F, Ding Z, Schwarzerova K, Morita MT, Tasaka M, Hejatko J, Van Der Straeten D, Friml J, Benkova E (2010) Role of PIN-mediated auxin efflux in apical hook development of Arabidopsis thaliana. *Development* **137**, 607-617.
Zazimalova E, Murphy AS, Yang H, Hoyerova K, Hosek P (2010) Auxin transporters--why so many? *Cold Spring Harb Perspect Biol* **2**, a001552.
Zhang C, Gong FC, Lambert GM, Galbraith DW (2005) Cell type-specific characterization of nuclear DNA contents within complex tissues and organs. *Plant Methods* **1**, 7.
Zhang S, Raina S, Li H, Li J, Dec E, Ma H, Huang H, Fedoroff NV (2003) Resources for targeted insertional and deletional mutagenesis in Arabidopsis. *Plant Mol Biol* **53**, 133-150.
Zhong W, Sternberg PW (2006) Genome-wide prediction of C. elegans genetic interactions. *Science* **311**, 1481-1484.